

NON-LINEAR FINITE ELEMENT ANALYSIS OF  
THIN-WALLED MEMBERS

by

Han-Ping Lee, B.E.S., M.Eng.

A thesis submitted to the Faculty of Graduate Studies  
and Research in partial fulfillment of the require-  
ments for the degree of Doctor of Philosophy

Department of Civil Engineering and Applied Mechanics  
McGill University  
Montreal, Canada

June 1977

ANALYSE NON LINEAIRE DE SECTIONS A PAROIS MINCES PAR LA  
METHODE DES ELEMENTS FINIS

Han-Ping Lee

Département de Génie Civil et  
de Mécanique Appliquée

Ph.D.  
Juin 1977

RESUME

Le comportement après flambage et la résistance ultime des éléments à parois minces de bâtiments est étudié à l'aide de la méthode des éléments finis. A l'aide des concepts de travail virtuel et d'énergie potentielle minimum, des formulations basées sur le principe des variations et sur le principe des variations par incréments sont développées. Les matériaux considérés sont élastiques et parfaitement plastiques, élastiques et subissant un écrouissement linéaire, et élastiques et subissant un écrouissement non-linéaire. Des matrices linéaires et non-linéaires sont dérivées de façon explicite jusqu'au niveau précédant l'intégration numérique. Des méthodes de solution du type de celle de Newton-Raphson par itération et du type graduel avec vérifications d'équilibre sont utilisées et comparées.

La formulation est d'abord utilisée pour étudier une variété de problèmes concernant des plaques. Les résultats se comparent de façon favorable avec des solutions théoriques et expérimentales déjà publiées dans la littérature technique. La méthode proposée est ensuite appliquée à un nombre de profilés à parois minces non plan. Les résultats de flexion, de contrainte et de plastification sont étudiés en détail. Des comparaisons avec les résistances ultimes obtenues d'autres sources sont effectuées lorsque possible.

NON-LINEAR FINITE ELEMENT ANALYSIS  
OF THIN-WALLED MEMBERS

Han-Ping Lee

Department of Civil Engineering  
and Applied Mechanics

Ph.D.  
June 1977

ABSTRACT

The post-buckling behaviour and the ultimate strength of thin-walled structural elements is studied using the finite element method. Formulations based on the variational principle and the incremental variational principle are developed using the approaches of virtual work and of minimum potential energy. Material treated as elastic-perfectly plastic, elastic-linear/strain hardening, and elastic-nonlinear strain hardening are considered. Linear and nonlinear matrices are derived explicitly up to the level prior to numerical integration. Solution procedures of the Newton-Raphson iterative technique and the step by step method with equilibrium check are employed and compared.

The formulation is first used to study a variety of plate problems. The results compare favourably with theoretical and experimental solutions already published in the technical literature. The proposed technique is then applied to a number of thin-walled non-planar structural sections with slope discontinuities. Results in terms of deflection, stress and plastification are studied in detail. Comparisons with ultimate strengths from other sources are also made whenever possible.

ACKNOWLEDGEMENTS

The author wishes to express his deepest gratitude to his research director, Professor P.J. Harris, for his guidance and advice throughout this research program.

The help and encouragement offered by the following persons and organizations is also gratefully acknowledged.

Professor G.R. Thomas who provided constant encouragement and valuable suggestions.

Professor W.D. Thorpe, Director of McGill University Computing Center, who provided computer funds when other sources were depleted.

Dr. J.G. Sutherland and Mr. R.B. Lidstone of the ALCAN Research Center in Kingston, Ont., who provided mechanical properties of certain aluminum alloys.

This study was sponsored by the National Research Council of Canada under Grant No. A-2737.



TABLE OF CONTENTS

	<u>Page</u>
Resume	ii
Abstract	iii
Acknowledgements	iv
Table of Contents	v
List of Tables	x
List of Figures	xi
List of Symbols	xv
Conversion Factors	xxi
 CHAPTER I: <u>Introduction</u>	 1
I.1 Thin-Walled Members	1
I.2 The Problem	3
I.3 Previous Work	6
I.3.1 Geometrical Nonlinearity - Elastic Plates and Thin-Walled Sections with Large Deflections	7
I.3.2 Material Nonlinearity - Elasto-Plastic Plates and Thin-Walled Sections	10
I.3.3 Ultimate Strength of Plates and Thin-Walled Sections	12
I.3.4 Overall Buckling of Thin-Walled Sections in the Post-Critical Range	17
I.4 Objective of Present Study	18
I.5 Proposed Approach	19
I.6 Scope of Present Study	19
 CHAPTER II. <u>Introduction to Nonlinear Finite Element Analysis</u>	 22
II.1 Some Notes on the Finite Element Method	22
II.2 Methods on Solving Nonlinear Problem	24

	<u>Page</u>
II.3 Formulations Based on Different Coordinate Systems	25
II.3.1 Convected Coordinate Formulation	25
II.3.2 Lagrangian Coordinate Formulation	27
II.3.3 Eulerian Coordinate Formulation	31
II.4 Solution Techniques Based on Differing Ways of Handling the Nonlinear Terms	32
II.4.1 Tangent Stiffness Approach	32
II.4.2 Pseudo-Force Approach	33
II.4.3 Combined Tangent Stiffness and Pseudo-Force Approach	34
II.5 Numerical Solution Procedures	35
II.5.1 Exact Solution Procedure - $\{f\} = 0$	35
II.5.2 Initial Value Procedure - $\{f\} = 0$	37
II.5.3 Self-Correcting Solution Procedures	39
II.6 Closure	41
CHAPTER III. <u>Mathematical Formulation of the Problem</u>	42
III.1 Principle of Variations	42
III.1.1 Principle of Virtual Work	42
III.1.2 Principle of Stationary Potential Energy	43
III.2 Incremental Variational Principle	45
III.2.1 Virtual Work Approach	45
III.2.2 Potential Energy Approach	47
III.3 Choice of Elements	48
III.4 Strain-Displacement Relations for Thin Plates	51
III.4.1 Total Strain-Displacement Relations	51
III.4.2 Incremental Strain-Displacement Relations	56

	<u>Page</u>
III.5 Incremental Theory of Plasticity	57
III.5.1 Yield Criterion	59
III.5.2 Hardening Rule	62
III.5.3 Formulas for Uniaxial Stress-Strain Relation	65
(III.5.4 Flow Rule	66
III.5.5 Incremental Total Stress-Strain Relation	68
III.6 Equilibrium Equations	70
III.6.1 Virtual Work Approach	70
III.6.2 Potential Energy Approach	71
III.7 Element Tangent Stiffness Matrix	72
III.8 Incremental Equilibrium Equations	74
III.8.1 Virtual Work Approach	74
III.8.2 Potential Energy Approach	76
III.9 Comments on Tangent Stiffness Matrix	77
III.10 Assemblage of Elements	80
III.11 Choice of Numerical Solution Procedure	81
III.12 Modified Cholesky Decomposition Technique	81
CHAPTER IV. <u>Test Examples</u>	86
IV.1 Restrained Simply Supported Beam, Elastic-Perfectly Plastic Material	87
IV.2 Simply Supported Square Plates Beyond the Buckling Load	91
IV.2.A Width-Thickness Ratio = 192, Elastic-Perfectly Plastic Material	92
IV.2.B Width-Thickness Ratio = 150	93
Case a: Elastic-Perfectly Plastic Material	93
Case b: Elastic-Linear Strain Hardening Material	95

	<u>Page</u>
IV.3 Restrained Simply Supported Square Plate Under Uniform Pressure, Elastic-Perfectly Plastic Material	95
IV.4 Simply Supported Rectangular Plates Beyond the Buckling Load	97
IV.4.A Aspect Ratio $(a/b) = 0.875$ , Width-Thickness Ratio $(b/t) = 80$ , Elastic-Perfectly Plastic Material	97
IV.4.B Aspect Ratio $(a/b) = 3.7$ , Width-Thickness Ratio $(b/t) = 49$ , Elastic-Linear Strain Hardening Material	99
IV.5 Discussion	102
CHAPTER V. <u>Application to Thin-Walled Sections</u>	110
V.1 A Cruciform Section Under Uniform Compression, Elastic-Nonlinear Strain Hardening Material	110
V.2 A Short Square Tube Column, Elastic-Perfectly Plastic Material	113
V.3 Hat-Sections Under Compression, Elastic-Linear Strain Hardening Material	116
V.4 Short Span Hat-Section Beam Under Local Loads on the Webs, Elastic-Linear Strain Hardening Material	118
V.4.A Hat-Section with Vertical Webs	119
V.4.B Hat-Section with Sloping Webs	125
V.5 A Channel-Section Beam Subjected to Combined Bending and Torsion, Elastic-Perfectly Plastic Material	128
V.6 A Z-Section Beam Under Uniform Vertical Load, Elastic-Perfectly Plastic Material	133
CHAPTER VI. <u>Summary and Conclusions</u>	137
VI.1 Summary	137
VI.2 General Conclusions	140
VI.3 Behaviour and Ultimate Strength of Thin-Walled Sections	142
VI.4 Recommendations for Future Work	144

	<u>Page</u>
VI.5 Discussion of Computing Cost on Non-Linear Analysis	145
Figures	147
References	207
Appendix A	227
Appendix B	238

LIST OF TABLES

<u>Title</u>	<u>Page</u>
1. Comparison of Computing Time	158
2. Computer Times per Increment	164

LIST OF FIGURES

	<u>Title</u>	Page
1.	Some Common Shapes of Thin-Walled Members	148
2.	Geometry of the Element and Degrees of Freedom	149
3.	Global and Local Coordinates	150
4.	Von Mises Yield Surface and Isotropic Hardening	150
5.	Uniaxial Stress-Strain and Stress-Plastic Strain Curves	151
6.	Numerical Solution Methods	152
7.	Elastic-Plastic Response of a Restrained Beam	153
8.	Progression of Elastic-Plastic Boundary in a Restrained Beam for Increasing Load	154
9.	Load-Deflection Curves of Simply Supported Square Plate with In-Plane Load ( $b/t = 192$ )	155
10.	Load-Deflection Curves of Simply Supported Square Plate with In-Plane Load ( $b/t = 150$ )	156
11.	Stress Distribution of Simply Supported Square Plate	157
12.	Lateral Deflection of Simply Supported Square Plate	158
13.	Extension of Plastic Area in Square Plate	159
14.	Response of Restrained Square Plates Under Uniform Pressure	160
15.	Restrained Plate Under Uniform Pressure, Elastic Membrane Stresses	161
16.	Restrained Plate Under Uniform Pressure, Elastic Extreme Fibre Bending Stresses	161
17.	Progression of Plastic Zone in a Restrained Plate	162
18.	Average Stress-Average Strain for Simply Supported Rectangular Plate ( $a/b = 0.875$ )	163
19.	Average Stress-Central Deflection for Simply Supported Plate	164
20.	Load-Shortening Curve for Simply Supported Rectangular Plate	165

	<u>Page</u>
21. Relation Between Ultimate Strength and Width-Thickness Ratio for Simply Supported Rectangular Plate	165
22. Load-Deflection Curves for Simply Supported Rectangular Plate	166
23. Deflection Profile Along the Longitudinal Center Line of Rectangular Plate	166
24. A Cruciform Section and Idealization	167
25. Material Properties of Cruciform	167
26. Average Stress-Average Strain for Cruciform Section	168
27. Shortening-Rotation of Cruciform Section	168
28. Strain and Stress Distribution Across a Flange of Cruciform	169
29. Idealization for Square Column	170
30. Stress-Strain Curve of Square Column	171
31. Out-of-Plane Deflection of Square Column	171
32. Deflection Profile Along the Longitudinal Center Line of a Plate Element of Square Column	172
33. Yielded Zone of Square Column at Ultimate Load	172
34. Curves of $\sigma_u/\sigma_{cr}$ versus $\sigma_{cr}/\sigma_y$ for Square Tube Columns and Plates	173
35. Idealization for Hat-Section Columns	174
36. Stress-Shortening of Hat-Section Under Concentric Load	175
37. Deflection Profile for a Concentric Loaded Hat-Section	175
38. Yielded Zones for a Concentrically Loaded Hat-Section	176
39. Stress-Shortening of Hat-Section Under Eccentric Load	177
40. Deflection Profile for an Eccentrically Loaded Hat-Section	177
41. Yielded Zones for an Eccentrically Loaded Hat-Section	178
42. Idealization for a Hat-Section Beam with Vertical Webs	179



43.	Transverse Deflection at Midspan of Hat-Section Beam with Vertical Webs	180
44.	Transverse Deflection at the End of Hat-Section Beam with Vertical Webs	180
45.	Deflection Profile at Midspan Cross-Section	181
46.	Deflection Profile at End Cross-Section	181
47.	Deflection Profile Along the Longitudinal Center Line of Top Flange of Hat-Section Beam with Vertical Webs	182
48.	Deflection Profile Along the Longitudinal Center Line of the Web of Hat-Section Beam with Vertical Webs	182
49.	Longitudinal Strain Distribution on Inner Face of Web Near Midspan	183
50.	Plastic Zone of Hat-Section Beam with Vertical Webs	183
51.	Distribution of Longitudinal Stress Along the Transverse Section of Hat-Section Beam with Vertical Webs	184
52.	Idealization for a Hat-Section Beam with Sloped Webs	185
53.	Transverse Deflection at Midspan and at the End of the Hat-Section Beam with Sloped Webs	186
54.	Deflection Profile at Midspan Cross-Section	187
55.	Deflection Profile at End Cross-Section	187
56.	Deflection Profile Along the Longitudinal Center Line of Top Flange of Hat-Section Beam with Sloped Webs	188
57.	Deflection Profile Along the Longitudinal Center Line of Web of Hat-Section Beam with Sloped Webs	188
58.	Plastic Zone of Hat-Section Beam with Sloped Webs	189
59.	Distribution of Longitudinal Stress Along the Transverse Section of Hat-Section Beam with Sloped Webs	190
60.	Idealization for Channel Section Beam	191
61.	Load/Torque-Angle of Twist Relation of Channel-Section	192
62.	Load-Deflection Relation of Channel-Section	192
63.	Distribution of Angle of Twist Along the Span of Channel-Section	193

	<u>Page</u>
64. Distortion of Channel-Section	194
65. Vertical Deflection Profile Along the Flange Tips of Channel-Section	195
66. Lateral Deflection Profile of Web of Channel-Section	195
67. Vertical Deflection Profile of Channel-Section	196
68. Longitudinal Stress Distribution Along the Transverse Section Sections of Channel-Section Beam	196
69. Distribution of Average Longitudinal Stress Along the Longitudinal Sections of Channel-Section Beam	198
70. Plastic Zone of Channel-Section at Ultimate Load	199
71. Idealization for a Z-Section Beam	200
72. Load-Angle of Twist Relation of Z-Section	201
73. Load-Deflection Relation of Z-Section	201
74. Distribution of Angle of Twist Along the Span of Z-Section	202
75. Distortion of Z-Section	203
76. Vertical Deflection Profile Along the Flange Tips of Z-Section	204
77. Lateral Deflection Profile of Web of Z-Section	204
78. Vertical Deflection Profile of Z-Section	205
79. Longitudinal Stress Distribution Along the Transverse Section of Z-Section Beam	205
80. Distribution of Longitudinal Stress Along the Longitudinal Sections of Z-Section Beam	206

LIST OF SYMBOLS

Symbols are generally defined in the text as they first appear.  
They are collected here for ready reference.

d.o.f.	Degree of freedom
A	Surface area of element
$\{A\}_i$	Transformation vectors relating nodal displacement gradients and linear part of strain
$\{A\}, \{B\}$	Constant vectors (Eq. 2.31)
$A_i, B_i$	Diagonal and off diagonal submatrix of stiffness matrix (Eq. 3.102)
a, b	Length of the sides of the plate; constants
$\{B^L\}_i$	Linear part of strain vectors (Eq. 3.30)
$\{B^{NL}\}_i$	Nonlinear part of strain vectors (Eq. 3.31)
$[B^L]$	Linear part of strain matrix
$[B^{NL}]$	Nonlinear part of strain matrix
c	Scalar (Eq. 2.30); yielding parameter (Eq. 3.43)
[D]	Transformation matrix relating nodal displacements and nodal displacement gradients; diagonal matrix (Eq. 3.98)
E	Young's modulus
$E_T$	Tangent modulus
[E]	Strain to stress transformation matrix
$[E_e]$	Strain to stress transformation matrix in elastic region
$[E_{ep}]$	Strain to stress transformation matrix in plastic region

$e_{ij}$	Green's strain tensor
$\{\Delta e\}$	Total incremental strain vector
$\{f\}$	Vector of unbalanced residual force
$f$	Yielding function; loading function
$F$	Function of plastic work
$\{G\}$	Vector of nodal displacement gradients
$g$	Positive scalar (Eq. 3.62)
$[H]_i$	Transformation matrices relating nodal displacement gradients and nonlinear part of strain
$H$	Function of equivalent plastic strain
$H'$	Slope of stress-plastic strain curve
$J_2$	Second invariant of the deviatoric stress tensor
$[K]$	Stiffness matrix
$[K_0]$	Conventional linear elastic stiffness matrix
$[K_1]$	Initial stress matrix (geometric matrix)
$[K_2]$	Initial displacement matrix
$[K^*]$	Nonlinear part of stiffness matrix in equilibrium equations
$[K_{NL}]$	Nonlinear part of stiffness matrix in incremental equilibrium equations
$[K_{NL(G)}]$	Geometrical nonlinear part of $[K_{NL}]$
$[K_{NL(\phi)}]$	Material nonlinear part of $[K_{NL}]$
$[K_T]$	Tangent stiffness matrix
$[\bar{R}_\sigma], [\hat{R}_\sigma]$	Matrices used to form initial stress matrix
$[\bar{R}_L], [\hat{R}_L]$	Matrices used to form conventional linear elastic stiffness matrix
$[\bar{R}_N], [\hat{R}_N]$	Matrices used to form initial displacement matrix

$[L]$	Lower triangular matrix (Eq. 3.98)
$L$	Length of structural member
$M_i$	Off diagonal submatrix (Eq. 3.103)
$m$	Ratio of tangent modulus to Young's modulus
$[N]$	Shape function matrix
$[N_1]$	First order incremental matrix
$[N_2]$	Second order incremental matrix
$n$	$n^{\text{th}}$ load increment; exponent; Euclidean norm
$\{P\}$	Vector of applied loads
$\{\bar{P}\}$	Vector of generalized loads
$p_i$	Body force per unit volume
$\{Q^{NL}\}$	Vector of pseudo forces to account for nonlinearity
$\{Q^{NL(p)}\}$	Material nonlinear part of $\{Q^{NL}\}$
$\{q\}$	Vector of nodal displacements
$q_i$	Components of $\{q\}$
$R_i$	Components of reaction force vector
$s$	Body surface; variable for load increment (Eq. 2.31)
$s_\sigma$	The portion of body surface prescribed by surface tractions
$s_u$	The portion of body surface prescribed by displacements
$T_i$	Surface traction forces per unit of surface area
$t$	Thickness of element
$U$	Strain energy
$u_i$	Displacement components

$u_{k,i}$	$\equiv \partial u_k / \partial u_i$
$V$	Potential energy due to external forces
$v$	Body volume
$u, v, w$	Components of displacement in x, y, z directions
$w^p$	Plastic work
$w_0$	Lateral initial imperfection
$x_i$	Rectangular cartesian coordinates of a point after deformation
$x_i$	Rectangular cartesian coordinates of a point in undeformed state
$\{Y\}$	Vector defined in Eq. 3.101
$x, y, z$	Rectangular cartesian coordinates of a point with respect to the local axes
$z$	Distance from the middle surface along the normal; amplification factor
$\{\Delta\}$	Vector of displacement changes, total displacements, unbalanced residual forces, or total applied loads
$\alpha$	Amplification factor
$\Delta$	Incremental designator
$\theta_x, \theta_y, \theta_z$	Components of rotation along x, y, z axes
$\{\Delta\theta\}$	Nonlinear part of $\{\Delta e\}$
$\{\epsilon\}$	Total strain vector
$\{\epsilon_p\}$	Membrane component of $\{\epsilon\}$
$\{\epsilon_b\}$	Bending component of $\{\epsilon\}$
$\epsilon_i, \epsilon_x, \epsilon_y, \epsilon_z$	Components of $\{\epsilon\}$
$\epsilon_i^L$	Linear part of $\epsilon_i$
$\epsilon_i^{NL}$	Nonlinear part of $\epsilon_i$
$\{\epsilon_0\}$	Initial strain vector

$\{\Delta\epsilon\}$	Linear part of $\{\Delta\epsilon\}$
$\Delta\epsilon_{ij}$	Linearized incremental strain components (Eq. 3.15)
$d\epsilon_{ij}^p$	Incremental plastic strain components
$\epsilon_e^p$	Equivalent plastic strain
$\epsilon_e$	Elastic strain
$\epsilon^p$	Plastic strain
$\epsilon$	Uniaxial strain
$\epsilon_u^p$	Plastic uniaxial strain at ultimate uniaxial stress
$\zeta, \eta$	Normalized coordinates
$\sigma$	Uniaxial stress
$\{\sigma\}$	Stress vector
$\sigma_{ij}$	Kirchhoff stress tensor
$\{\sigma_0\}$	Initial stress vector
$\sigma_x, \sigma_y, \tau_{xy}$	Stress components
$\sigma'_{ij}$	Deviatoric stress tensor
$\sigma_0$	Initial yield stress
$\bar{\sigma}$	Subsequent yield stress
$\sigma_e$	Equivalent stress
$\sigma_{0.7}$	Secant yield stress at 0.7E
$\sigma_2$	Specified 0.2 per cent proof stress
$\sigma_u$	Ultimate uniaxial stress
$\psi$	Potential function due to external force
$\psi_{xx}, \psi_{yy}, \psi_{xy}$	Components of curvature
$\lambda$	Scalar to denote the intensity of loading
$d\lambda$	Nonnegative constant (Eq. 3.61)

$\phi$	Total potential energy
$\phi_{NL}$	Part of total potential energy due to nonlinearity
$\omega$	Strain energy function
$\delta$	Variational operator
$\delta_{ij}$	Kronecker deltas
$\nu$	Poisson's ratio

>



## CONVERSION FACTORS

The following is a list of the conversion factors for all imperial units (English system) used throughout this thesis to the "Metric system" and the "S.I. system".

1 Foot	= 30.48 centimeters
1 ft <sup>2</sup>	= .09290304 meter <sup>2</sup>
1 Inch	= 2.54 cm
1 in. <sup>2</sup>	= 6.4516 cm <sup>2</sup>
1 in. <sup>3</sup>	= 16.387 cm <sup>3</sup>
1 in. <sup>4</sup>	= 41.623 cm <sup>4</sup>
1 kip-force	= 453.6 kilograms force = 4448.2 Newtons
1 kip/in <sup>2</sup> (ksi)	= 6.895 Mega-Pascal ( 1 Pascal = 1 Newton/m <sup>2</sup> )
1 Pound-force	= 453.5923 grams-force = 4.4482 Newtons
1 Pound-force/inch	= 178.5796 gr/cm
1 Pound-force in.	= 0.112985 Newton-meter
1 Pound-force foot	= 1.355818 Newton-meter
1 Pound-force/ft <sup>2</sup>	= 4.88242 kg/m <sup>2</sup>
1 Pound-force/in <sup>2</sup> (psi)	= 68947.6 Dynes/cm <sup>2</sup> = 6.895 Kilo-Pascal = 70.3069 gr/cm <sup>2</sup>

## CHAPTER I

### INTRODUCTION

#### I.1 Thin-Walled Members

Metallic thin-walled members are widely used in various industries. There is a long history involving the use of thin-walled members in ship building and aircraft manufacturing. In fact the investigation of thin-walled members was initiated in these industries and then extended to cover other applications. Thin-walled members are now used extensively in the construction of car bodies, railway coaches, water tanks, culverts, barriers, shell and tubular structures of many shapes, as well as various types of equipment.

Thin-walled members are fabricated by extrusion, cold-forming or by welding their component elements together. They are generally assemblages of curved or flat plates and their cross-sections can be either closed (tubular) or open (profile). Thin-walled members are distinguished from conventional compact members not simply because of the thinness of their walls but rather, more importantly, due to their different behaviour in areas which include local instability, post-buckling strength and torsional-warping. The classification as thin-walled members also depends on the loading configuration since external forces play an important role in governing the behaviour of the member.

The application of cold-formed thin-walled members in building construction is presently very popular. Standardized prefabricated buildings, entirely or partially constructed using cold-formed members, are already on the market. Shapes such as I-sections, hat sections,

channels, angles or any combination of these, with or without stiffening lips, are commonly used as roof purlins, wall girts or studs. Various sections are also used in open web steel joists and space frames. Although these members may be individually unstable due to their configuration and dimensions, their stability and hence their load-carrying capacity is greatly increased once they are connected to other parts of the structure such as roof decks, wall panels, etc.. Corrugated shapes are generally used as roof decking, floor decking, wall sheathing and siding. Thin-walled members are also used in the construction of folded plate and hyperbolic paraboloid roofs and may provide a pleasing appearance. In addition to carrying normal loads, these members may also form a diaphragm which resists inplane shear deformation, transfers lateral forces (wind and/or earthquake), and provides lateral bracing for individual members in a steel framed building.

The advantages of using cold-formed metal members are:

- (1) Economy: High strength-weight ratio, mass production and pre-fabrication, ease in transportation and erection, high durability and reusability, all contribute to substantial savings.
- (2) Multi-purpose applications: These members are often able to fulfill more than one purpose. For example, wall panels, while providing structural strength, may also be architecturally desirable. Floor decking, which creates a composite structural member in combination with concrete, serves as the form during construction and also provides utility conduits in the finished floor.

Today, various specifications and codes applying to thin-walled members are being used by designers and are under constant review in North America and Europe<sup>1-6</sup>. The analysis and design of such members have recently been the subject of books by several authors including Yu<sup>7</sup> and Walker<sup>8</sup>.

## I.2 The Problem

Thin-walled members ~~behave~~ nonlinearly, that is, the relationship between the applied loads and the resulting response of the members is nonlinear. Nonlinearities encountered are due to two effects:

### [1] Geometrical Nonlinearity:

When a member deflects significantly, the effect of changing geometry on equilibrium must be taken into account and the stretching of the middle plane of the plate must be included in the analysis. These effects lead to an increase in bending stiffness of the member, even though the stiffness of resistance to axial compression decreases. This type of nonlinearity is introduced by adding higher order terms in the strain-displacement relations and/or by updating the geometry of the member using a step-by-step approach.

[2] Material Nonlinearity:

At high load levels some portion of the member may yield, and based on its nonlinear constitutive relation, start to respond inelastically. This "softening" of the material due to plastification reduces the stiffness of the member and causes its final collapse. This type of nonlinearity is introduced through the stress-strain relation (plasticity).

These nonlinearities play an extremely important role in the behaviour of thin-walled members. It is well-known that the utilization of post-buckling strength is the prime advantage associated with thin-walled members. The investigation of behaviour above critical loads and the prediction of ultimate strength demand the inclusion of both of these two types of nonlinearity. These nonlinear characteristics of thin-walled members have not yet been thoroughly treated.

The analysis of thin-walled members is inherently difficult since it involves the problems of stability and warping. Furthermore, the inclusion of nonlinearities makes the analysis extremely complex and it cannot be solved in closed form. So far, attempts have been limited to simple problems such as plates or tubes under compression. Even in such simple cases an ad hoc approach was often adopted so that assumptions could be made to simplify the complex mathematics involved, although the final results still had to be obtained numerically. These earlier works have provided some important contributions towards solving the problem. However, they are by no means complete, exact or general, and hence their applications are limited.

Exact theoretical treatments of thin-walled flexural members are scarce. A recommended way for calculating the deflection of thin-walled beams, based on the effective section of the member, which is a function of the stress level and therefore varies along the span of the beam, is tedious. Further simplification by using only the least effective section (the location with the maximum moment) causes the calculated deflection to be conservative and approximate. Previous investigations involving more complicated problems such as thin-walled members under torsion or combined bending and torsion, with consideration of nonlinearities, are virtually nonexistent. This explains why the present codes and specifications, wherever nonlinearities must be taken into account, such as in post-buckling strength and web crippling, are based mainly on the results of experiments. In these experiments, obviously, limitations on the shape and dimensions of sections, loading configurations, boundary conditions and types of materials used, cannot be avoided. However, the results, in spite of the limitations, are applied for general use.

This evidence reflects the fact that theoretical work must be promoted, since the progress of theoretical work falls far behind experiments. Also, no matter how satisfactory the experimental work proves to be, ideally these results should be theoretically justified and a marriage of experimental and theoretical results should be set as the final goal. Further, even though experiments may provide answers to definite questions (e.g., ultimate load), a proper understanding of the behaviour of the member by a detailed study of stress distribution

patterns and the chronological spreading of plastic zones, which can be conveniently obtained by theoretical methods, is likely to be impractical by experiment. Using a theoretical study which includes nonlinearities, a better understanding of the behaviour and the strength of thin-walled members and further improvement of present specifications and codes are possible. This, in turn, promotes greater economy through lower margins of safety in the use of thin-walled members.

### 1.3 Previous Work

Classical treatments on the bending, torsion and buckling of thin-walled members follow small deformation theory and assume that the material is fully elastic. This type of treatment has been extensively studied and documented in numerous references in many well-known books<sup>10-13</sup>. This linear, elastic analysis is not the topic of the present study and hence a review on these works is not warranted. In this section, previous studies that considered only geometrical or material nonlinearity are presented first. Works considering combined nonlinearities follow. They are presented in chronological order. The object is to present a historical background and an up-to-date state-of-the-art review. Thin-walled sections with curved plates (shells) are excluded.

### I.3.1 Geometrical Nonlinearity - Elastic Plates and Thin-Walled Sections with Large Deflections

Even though the first treatment of plates with large deflections dates back to Kirchhoff (1877)<sup>9</sup>, it was Von Karman<sup>14</sup> who derived the present large deflection compatibility and equilibrium equations of plates in 1910. Timoshenko<sup>15</sup>, and Marguerre and Trefftz<sup>16</sup> were among the earliest in the nineteen thirties to investigate plates with large deflections where they used the energy method to obtain approximate solutions. Way<sup>17</sup> used the Ritz method to study a clamped rectangular plate under uniform lateral loads which was later studied by Wang<sup>18,19</sup> using finite differences, and by Chien and Yeh<sup>20</sup> using successive approximations. Levy<sup>21-23</sup> (1942) was able to reach an "exact" solution using double Fourier series for simply supported or clamped plates under uniform lateral load, in-plane load, or combined lateral and in-plane load. On the uniformly compressed, simply supported plate he constrained the unloaded edges to remain straight. This was extended by Hu, Lundquist and Batdorf<sup>24</sup> to include initial imperfection effects, by Coan<sup>25</sup> to consider unloaded edges free to move in its plane, and by Yamaki<sup>26</sup> to cover various boundary conditions. In his doctoral thesis of 1945, Koiter<sup>27</sup> initiated a perturbation technique to investigate immediate post-buckling behaviour and imperfection sensitivity of plates. Berger<sup>28</sup> proposed an approximate approach which simplified the nonlinear equations by neglecting the second invariant of the membrane strain. Post-buckling was later studied by Stein<sup>29</sup> using power series. Change of the buckling form of a plate was investigated by Stein<sup>30</sup>, Supple and Chilver<sup>31-33</sup>. For details on plates with large deflections, references 13, 34 and 125 can be consulted.



Recent work on plates is inclined towards numerical approaches due to the rapid growth of the storage capacity and speed of computers. Walker and others<sup>35-38</sup> studied the post-buckling of compressed plates using perturbation techniques. Alternatively, Rushton<sup>39-42</sup> used the method of dynamic relaxation. Rhodes and Harvey<sup>43-45</sup> used the Ritz method and solved Von Karman's compatibility equation "exactly". Finite difference methods were used by Chapman et al.<sup>46,47</sup> on plates under transverse load and under combined transverse and in-plane loads. A review on post-buckling by Hutchison and Koiter<sup>48</sup> and by Bieniek<sup>49</sup> also provided information on plates.

Studies of large deflection, elastic plate behaviour using finite elements are numerous. Early works mostly used a step-by-step method with the linear incremental equilibrium equation with inclusion of geometric stiffness being formulated and solved for a piecewise linear approximation of the true solution. Among them, Murray and Wilson<sup>50,51</sup> studied large deflection and post-buckling of plates with incremental equilibrium equations formulated using the principle of virtual work. The unbalanced residual forces are calculated and iteration is then performed within each increment. Lang and Hartz<sup>52</sup> later coupled a finite element formulation with a general energy perturbation approach to study post-buckling of plates. Roberts and Ashwell<sup>53</sup> proposed a (Newton-Raphson) corrector and (mid-increment stiffness) predictor solution procedure to investigate laterally loaded square plates and the post-buckling of an imperfect plate. Kawai and Yoshimura<sup>54</sup> employed energy formulations and reached a force-displacement relation where nonlinear terms are interpreted as additional nodal forces

which are functions of unknown nodal displacements and are solved iteratively. A sample problem of a clamped square plate under lateral loads using rectangular elements was given. Kawai<sup>55</sup> further combined the finite element method for the analysis of in-plane stress fields and Rayleigh-Ritz's procedure for plate bending problems to study bending and buckling of rectangular plates. Vos and Vann<sup>56</sup> studied buckling and post-buckling of plates utilizing a tensor formulation. Bergan<sup>57</sup> investigated bending and post-buckling of plates using the Marguerre shallow shell theory where equilibrium and incremental equations for general Rayleigh-Ritz type solution methods are derived from the Variational Principle of total potential energy. Yang<sup>58-62</sup> extended the incremental formulation initially introduced by Mallett and Marcal<sup>181</sup> to investigate rectangular flexure plate behaviour on an elastic foundation with support at the edges only being treated as a special case. The behaviour with initial deflection and the buckling and post-buckling problem was treated as well. Also, various types of boundary conditions were considered. Recently Bagchi and Rockety<sup>63</sup> used a rectangular plate element to investigate a web plate under partial edge loading. Works by Schmit et al.<sup>64</sup>, Brebbia and Connor<sup>65</sup>, Tezcan et al.<sup>66</sup>, Gallagher et al.<sup>67,68</sup>, Bergan and Clough<sup>69</sup>, and Gass and Tabarrok<sup>70</sup> also included applications to flat rectangular plates.

On thin-walled sections, Black<sup>71</sup> used Galerkin's method to study beams subjected to bending and torsion. Soltis and Christiano<sup>72</sup> employed finite difference and Newton-Raphson iterative methods to investigate sections under biaxial loading. Ghobarah and Tso<sup>73,74</sup> derived nonlinear differential equations using the minimum potential energy

principle for thin-walled beams and a perturbation process was carried out to obtain solutions for the beam problem with non-uniform torsion. Mikhail and Guralnick<sup>75</sup> also applied the minimum potential energy principle with a Rayleigh-Ritz method to a folded-plate type beam which was later studied by Khan and Harris<sup>76</sup> using finite elements. Rajasekaran and Murray<sup>77</sup> used finite elements and adopted "augmented stiffness" and "alpha constant" techniques to the solution of beams and beam-columns.

### I.3.2 Material Nonlinearity - Elasto-Plastic Plates and Thin-Walled Sections

Due to the difficulty in treating theoretically the elasto-plastic plate in bending, the extremum principle of plasticity<sup>78-81</sup> is generally applied to obtain upper and lower bounds for the true ultimate load. In this respect, the well-known limit analysis method is predominantly used. However, this simplified method assumes that the material is perfectly plastic and hence the strain hardening effect is neglected. Alternative approaches have been proposed by several investigators. Massonnet<sup>82</sup> and Cornelis<sup>83</sup> used a finite difference method with an incremental procedure for solving the plate bending problem. Ang and Lopez<sup>84</sup> attacked the problem by treating a plate as a grid system. A method using successive elastic approximations<sup>85</sup> was also attempted previously. Work on rectangular plate problems by Lin<sup>86,87</sup> who applied an analogy concept to reduce the analysis of a plate with plastic strain to the analysis of an identical plate with an additional set of lateral loads and edge moments, is worth noting.

Probably the approach most actively adopted in recent years is that using finite elements which not only provides a bounded value for the true solution, but also describes the stress distribution and the progress of plastification in the plate. Among previously published work on the initial strain method, Marcal and Mallett<sup>88</sup> investigated a centrally loaded and simply supported square plate using triangular elements, Armen et al.<sup>89,90</sup> employed both rectangular and triangular elements on various plates subjected to lateral loads and to combined lateral and in-plane loads, and Whang<sup>91</sup> adopted a shallow rectangular shell element to uniformly loaded clamped and simply supported square plates. For the tangent stiffness method, Bergan and Clough<sup>92</sup> studied uniformly loaded plates using refined quadrilateral elements, and Wegmuller<sup>93,94</sup> studied clamped square plates using a rectangular element. Using the initial stress method, Barnard and Sharman<sup>95</sup> recently adopted a hybrid plate-bending element to simply supported and clamped square plates under uniform loading.

Investigation of thin-walled sections considering only material nonlinearity is based on the assumption that the deflection is comparatively small and hence geometrical nonlinear effects can be neglected. This is unlikely to hold true for thin-walled members and studies under such assumptions are very rare. On the other hand, the limit analysis method (plastic design) for conventional compact sections has been well-established and is of little interest in the present study. However, it is worthwhile to point out that the finite element method has recently been applied by Rajaskaran and Murray<sup>96</sup> to investigate elasto-plastic plated-sections, and Lundgren<sup>97,98</sup> recently studied thin-walled beams under torsion assuming the material is nonlinear elastic or elastic-perfectly plastic.

### I.3.3 Ultimate Strength of Plates and Thin-Walled Sections

Investigation of the ultimate strength of plates and thin-walled sections requires the consideration of both geometrical and material nonlinearities as at this final stage of its loading history, the member has already deflected a significant amount and parts of the member have yielded. Because of its extreme mathematical complexity in theoretical treatment, closed-form solutions do not exist. There are two approaches most commonly used to predict the ultimate strength and both are semi-empirical in nature. The first approach is to propose a simplified formula where ultimate strength is expressed as a function of the member's critical stress and the yield stress of the material being used. The necessary factor term and exponent term in the formula is chosen by comparison with the experimental data. For the thin-walled section the ultimate strength is evaluated by summing the weighted strength of each plate element based on its cross-sectional area. The second approach is to use the effective width concept where post-buckling strength is considered to be uniformly carried by longitudinal strips along the stiffened edges of the plate so that the stress resultant of the plate remains the same. It simplifies the nonlinear stress distribution along the plate width to uniformly distributed stress blocks and the formula for effective width is generally based on experimental results. Consequently, the strength of thin-walled sections is evaluated using a reduced effective section.

Schuman and Back<sup>99</sup> tested rectangular plates under edge compression with unloaded edges supported in V grooves. They noticed that, because

the center part of the plate buckled most, the post-buckling load is mainly carried by strips along the unloaded but supported edges, and the capacity of the plate was not raised significantly by increasing the plate width. Von Karman<sup>100</sup> (1932) was the first to use the effective width concept and had derived an approximate formula for simply supported plates. Various expressions for the effective width were proposed by many researchers thereafter. Early works were conducted by Sechler<sup>101</sup> who tested steel plates and by Cox<sup>102,103</sup> and Marguerre et al.<sup>104,105</sup> who used the energy method and also included the effects due to initial imperfection. Stowell<sup>106</sup> used the deformation theory of plasticity to study rectangular plates with one unloaded edge simply supported and remaining straight, and the other unloaded edge totally free. This was simulated experimentally by testing cruciform columns where, due to symmetry, only torsional buckling occurs and the center line of the column (representing the supported edge of each flange) provides no restraint on rotation but remains straight. Good agreement between theoretical results and test data was obtained. Mayers and Budiansky<sup>107</sup> attempted an approximate theoretical solution using the energy method with the Rayleigh-Ritz procedure on simply supported square plates where unloaded edges remain straight. Deformation theory was adopted and the plate was treated as consisting of only two stress-carrying faces (sandwich-like). Results compared fairly well with experimental data but failed to show load shedding.

Heimerl<sup>108</sup> tested extruded sections and proposed semi-empirical formulas for ultimate stress. Applying the same formulation to formed

sections, Schuette<sup>109</sup> found consistent discrepancies and pointed out that the ultimate stress for formed sections depended on the width-thickness ratio. Later, Needham<sup>110</sup> proposed his ultimate stress formulas for formed sections to take this parameter into account. He further suggested that a formed member consisting of a series of flat plate elements can be treated as a series of angle sections by "cutting" through the center line of each stiffened plate element since that region is least rigid and hence less sensitive regarding the prediction of ultimate strength. After having reviewed previous investigations, Gerard<sup>111,112</sup> combined the formulas for extruded sections and formed sections into one and made further extensions to cover general shapes and stiffened panels. This work was mainly for the member whose effective slenderness ratio is small and hence the member fails due to local crippling rather than to overall column buckling.

Perhaps the most important work is due to Winter<sup>113,114</sup> who performed a series of tests on cold-formed steel sections. His results formed the basis for the main contents of the AISI<sup>4</sup> and other codes<sup>1,3,6</sup>. Chilver<sup>115</sup> has investigated lipped and unlipped channel sections of cold-formed steel. Work on post-buckling behaviour of plates was reviewed by Jombock and Clark<sup>116</sup>, and by European researchers<sup>117</sup>.

Research in the last ten years has been extensive. Dwight and Ractliffe<sup>118</sup> tested steel and aluminum alloy plates. Graves-Smith<sup>119-122</sup> used the Ritz method with a rigorous mathematical formulation to investigate rectangular tube columns and later square box beams. Massonnet<sup>123</sup> proposed a solution using the iterative finite difference method.

He employed the Prandtl-Reuss equations of plastic flow theory with the assumption that the plate performs a sudden transition from elastic to fully plastic behaviour once the plastic moment is reached. Reiss and Chilver<sup>124</sup> pointed out that, for some sections, the assumption that the ultimate strength of a compressed section is the linear summation of the individual strengths of the component plates assuming it is simply supported along the longitudinal edges, may be in error on the unsafe side. Bulson<sup>125</sup> summarized previous work. Abdel-Sayed<sup>126</sup> re-examined the effective width of plates within the elastic range including the case where unloaded edges are free to move in their planes. Rhodes et al.<sup>127,163,164</sup> used a semi-energy method on lipped channel beams subjected to end moments and on eccentrically loaded plates with initial imperfections. Sherbourne et al.<sup>128-130</sup> studied plates and tubes by using the energy method to formulate an elastic loading (post-buckling) line and a rigid-plastic unloading (mechanism) line. Their prediction for ultimate strength by considering the intersection of two lines overestimated the real capacity of the plate and may be considered as an upper bound. Wang<sup>131</sup> proposed a numerical method to predict post-buckling behaviour of thin-walled continuous beams where nonlinearities are accounted for by the nonlinear moment-curvature relations of a section derived with the aid of the effective width concept. Rockey et al.<sup>132-134</sup> investigated experimentally the ultimate strength of thin-walled members under patch loading and under combined patch loading and bending. They demonstrated that the method can be used to predict the failure loading of light gauge girders with a good degree of accuracy. Venkataramaiah<sup>135</sup> tested channel columns.



Equipped with reviews of formulas previously proposed for light gauge steel design and incorporated with the spirit of limit state design, Lind et al.<sup>136-138</sup> proposed a simple expression for effective width using a statistical approach. Lin et al.<sup>139</sup> studied plates using finite difference and special iteration techniques. Walker et al.<sup>140</sup> analysed plate mechanisms and predicted the unloading path of simply supported plates in compression.

Again, the finite element method has been employed to investigate the ultimate load of thin-walled members. Murray and Wilson<sup>141</sup> adopted triangular elements and developed an approximate formulation which was tested on plate bending problems. Marcal<sup>142</sup> used triangular elements to study a simply supported square plate under uniform pressure. Ohtsubo<sup>143</sup> also used triangular elements on square plates under uniform pressure or under edge compression. He adopted the Ritz procedure with the aid of the finite element method and had plastic analysis based on an initial strain concept. Crisfield<sup>144-148</sup> used the Ilyushin and the modified Ilyushin yield criterion with rectangular elements for the plate subjected to edge compression or to shear force. He later extended his work to cover eccentrically stiffened plates. Extensive stress analysis using finite elements has been performed by Armen et al.<sup>173</sup>. Arai<sup>149</sup> used refined triangular elements to study various problems where the theory of plasticity was not fully taken into account and hence his formulation can be considered as an approximation. Murray and Rajasekaran<sup>150</sup> presented a set of differential equilibrium equations for thin-walled open-section beams. Since the formulation was based on the principle of virtual work, the equations are valid for inelastic behaviour. However, the work is

limited to qualitative results. Stiffened plates have recently been investigated by Soreide, Bergan and Moan<sup>151,152</sup> where triangular elements were adopted. They have developed two computer programs based on the Lagrangian formulation and moving coordinate formulation respectively.

#### I.3.4 Overall Buckling of Thin-Walled Sections in the Post-Critical Range

Thin-walled columns with intermediate slenderness ratios may fail by overall buckling in the post-critical range. In this case the column may or may not yield depending upon its slenderness ratio. Study of this failure mode requires consideration of the interaction of post-buckling strength and the column deflection. Bijlaard and Fisher<sup>153</sup> reached approximate solutions using the energy method where formulations were derived specifically for H-sections and square tube columns. The possibility of generalization to other sections was claimed. Cherry<sup>154</sup> has analysed and tested I- and T-section beams which failed by lateral buckling after the compression flange had buckled locally. Jombock and Clark<sup>116,155</sup> used the effective width concept to account for post-buckling nonlinear effects. Graves-Smith<sup>119-122</sup> performed a rigorous mathematical derivation including plasticity effects for rectangular tube sections and obtained good agreement with tests on aluminum tubes. Bulson<sup>156</sup> suggested an empirically derived interaction equation to treat this problem. Ghobarah and Tso<sup>157</sup> investigated channel columns. Sharp<sup>158</sup> provided a simple empirical formula. Wang<sup>159</sup> proposed a numerical method and adopted effective width concepts to the investigation of rectangular

tube columns. Recently, Winter et al.<sup>160-162</sup> presented a semi-empirical effective width approach incorporated with the tangent modulus of the material to account for inelastic effects. This work was extended by De Wolf<sup>161</sup> to the case of overall torsional column buckling.

#### I.4 Objective of Present Study

The literature review reveals that most previous work has been limited to plates and tubes which are generally treated as plates. Work on other sections is almost all limited to loading cases of axial compression and the analysis is either empirical or semi-empirical. There is very little theoretical work on non-planar thin-walled open sections. This work, which includes only one type of nonlinearity, cannot be considered complete. Without geometrical nonlinearity, the behaviour cannot be investigated correctly and without material nonlinearity, the ultimate strength cannot be accurately predicted. Previous nonlinear analysis of three-dimensional, thin-walled members such as those shown in Fig. 1 with various loading and boundary conditions, to the writer's knowledge, is virtually non-existent. The aim of the present study is therefore to perform complete nonlinear investigations of this type of thin-walled member under various conditions of loading, boundary constraint and material. It is hoped that, by tracing the load history and response from initial loading to final collapse, a better understanding of nonlinear behaviour can be achieved. It is the aim of the present study to make a significant advance in the theoretical treatment of thin-walled members.

### I.5 Proposed Approach

Since obtaining a closed-form solution is practically impossible, a numerical approach is suggested. Among the many different methods, it is due to its simplicity and versatility that the finite element method appears to be the most appealing. A finite element displacement method using the tangent stiffness is proposed. Strain displacement relations (geometrical nonlinearity) are established by adopting the Lagrangian formulation and stress-strain relations (material nonlinearity) by the flow theory of plasticity. The Prandtl-Reuss relation and its associated Von Mises yield criterion is used and subsequent yielding is governed by an isotropic hardening rule. Solution of the equilibrium equations is based on the modified Cholesky decomposition procedure.

### I.6 Scope of Present Study

The present study only investigates thin-walled members which are composed of flat plates but the members can be of any shape and dimension. Even though the member behaves with large displacements, the strain remains small. The problem of large displacements and large strains is beyond the scope of the present study. No limitations on loading configuration and boundary conditions are required except that they must be consistent with the degrees of freedom used in the present finite element analysis. The material can be treated as elastic-perfectly plastic, elastic-linear hardening, and elastic-nonlinear hardening. Members are presumed to be initially stress free and the strain hardening of material due to cold

forming is not considered. Also, members are subjected to static conservative loads only. However, unloading and reloading in the post-yielding stage is allowed.

It is the intent of Chapter II to present the "state of the art" of nonlinear analysis using the finite element method. The general technique of attacking nonlinear problems is reviewed from two different perspectives. The first is to consider the formulation based on different coordinate systems. The second is to discuss the different ways of treating nonlinear terms in the governing equations. One important feature of nonlinear analysis is the solution procedure. There are quite a number of available solution procedures which are briefly described as the final part of this chapter.

Chapter III is devoted to the detailed mathematical formulation. The variational principle is introduced first. This is followed by a description of the element selected for the present study. Geometrical and material nonlinearity are treated separately at the beginning, and incorporated with strain-displacement equations and stress-strain equations in matrix notation. With the application of the variational principle, nonlinearities are subsequently combined and the tangent stiffness matrix is formed. The method of generating the tangent stiffness matrix, which vitally affects the computing cost is extremely important in nonlinear finite element analysis, is considered to be efficient. The Chapter is ended by introducing the modified Cholesky method of solving simultaneous linear equations.

In Chapter IV the computer program developed, based on the mathematical formulation of Chapter III, is described. Investigations primarily on square and rectangular plates which represent the early part of the study, are presented. Test examples cover various loading configurations, boundary conditions and material properties. Results are compared against the published values conducted by other researchers using either the finite element method or other means. Problems such as convergence, step size, and other miscellaneous items are also discussed.

Applications to three-dimensional (non-coplanar) thin-walled members are presented in Chapter V. On the basis of one test for each different shape, most types of commonly used sections are considered. Again, different types of loading configurations, boundary conditions, and material properties are involved. Behaviour is investigated in detail and comparison of results with experimental values and with present Canadian Standards is made wherever possible.

The work is concluded in Chapter VI. Recommendations are made for possible future work using the present program. The issue of computing costs which is a key obstacle to nonlinear analysis is also discussed.

## CHAPTER II

### INTRODUCTION TO NONLINEAR FINITE ELEMENT ANALYSIS

In this chapter it is intended to present a brief, but overall, look at the possible methods of attacking the nonlinear problem. No thorough derivations on each particular method are attempted. The purpose is to provide a philosophical view, in qualitative terms, and to present the current "state of the art" of nonlinear finite element methods.

#### II.1 Some Notes on the Finite Element Method

Two approaches are generally employed to formulate structural engineering problems<sup>166</sup>. The first approach is to form differential equations which govern the behaviour of a typical, infinitesimal region of the structure. The differential equations are solved using methods such as finite differences in a discrete manner. The second approach is to apply the principle of variations to minimize a functional (e.g. the potential energy of the structure) which is defined by suitable integration of the unknown quantities over the whole domain of the structure. The variational approach using the finite element method, which is now recognized as a variant of the Ritz process, has the structure "physically" discretized prior to the mathematic formulation. The derivation based on assumed displacement functions (or stress functions or a combination of two types of functions) for the "elements" leads finally to the solution of a set of algebraic equations. Actually the two approaches are essentially equivalent as they can be transformed from one form to the other through

the calculus of variations. The difference really lies in the solution procedures. A method of combining the two approaches by adopting a finite element formulation and a finite difference solution technique is possible and appealing<sup>197</sup>.

Alternatively, the finite element method can be formulated directly from differential equations without referring to the variational principles. This is the well known method of weighted residuals<sup>166,167</sup> where the integral of the residuals throughout the region of the structure due to the introduction of trial functions into the governing differential equations are minimized. This method has certain advantages particularly for nonstructural problems when a functional cannot be formed. Within the range of this method the Galerkin process of having the shape functions of the element play the role of weighting functions is commonly used.

Even within the domain of the finite element method, there are many possible ways to solve the same structural problem as several variational principles<sup>168,169</sup> are available to follow. The basis of the variational formulation is the principle of virtual work (principle of virtual displacement) which is based on the variation of strain and displacement. There also exists another important variational principle, the principle of complementary virtual work (principle of virtual force) which is based on the variation of stress and force. From these two basic principles, several other variational principles can be derived; such as the principle of stationary potential energy, the principle of stationary complementary energy, the Hellinger-Reissner variational principle and the very general Hu-Washizu variational principle. Among



these principles the principle of virtual work, including its subsequently derived principle of stationary potential energy (generally referred to as the displacement method), represents the main-stream of the various formulations in finite element analysis and is employed in the present study. Hence only this variational principle will be further referred to, investigated and discussed.

## II.2 Methods on Solving Nonlinear Problem

When nonlinearity is encountered, the problem is basically solved using iterations and/or increments of loading where each iteration or each increment is a linear process. This was pointed out in the first nonlinear (geometrical) finite element analysis by Turner et al<sup>170</sup>. The methods of treating the nonlinear problem can probably be classified separately from two different points of view. For each point of view, there are three distinct methods available:

The first view is generally relevant to the first stage of the analysis of the problem (i.e. derivation and formulation of governing equations). The different possible methods of formulation is due to the occurrence of geometrical nonlinearity. The three methods of formulation<sup>49</sup> are respectively based on a convected coordinate system, a Lagrangian (material) coordinate system, and an Eulerian (spatial) coordinate system.

Another view has more connection with the second stage of the analysis of the problem (i.e. solving governing equations). The different methods were initially developed for treating the problem of material

nonlinearity. However, the concepts of handling nonlinear terms are also applicable to the problem of geometrical nonlinearity and of combined nonlinearities. These may be best explained by using solution procedures as examples. The three methods are respectively the method of tangent stiffness, the method of pseudo force, and the method of combining tangent stiffnesses and pseudo forces.

These methods are discussed in the following sections.

### II.3 Formulation Based on Different Coordinate Systems

#### II.3.1 Convected Coordinate Formulation

The convected coordinate formulation was overwhelmingly used at an early stage of the development of geometrical nonlinear analysis<sup>170-172</sup> and is still employed by researchers<sup>173-175</sup> at the present time for combined nonlinear problems, even though it is becoming less favoured. In this formulation<sup>176</sup>, the problem is solved, using a step by step technique, by incrementing the total loads. The coordinate system is updated for the changed geometry after each load increment. Suppose it is desired to solve the problem for load increment  $n+1$ . The coordinate system after load increment  $n$  is considered as the "undeformed" position for, and only for, load increment  $n+1$ , remembering that the position of load increment  $n$  may be substantially different from its real initial configuration of load increment zero. Later the position of load increment  $n+1$  is used for increment  $n+2$  etc.. It is seen that within each increment the formulation is a Lagrangian one. The incremental stresses and strains are, respectively, the Kirchhoff stresses (2nd Piola-Kirchhoff stresses) increment and Green strains increment. However, the total stresses at the end of each

increment, which provide the initial stresses for the next increment, must be retained and transformed at each increment due to the moving of coordinates and are, therefore, the Eulerian stresses<sup>168</sup>. For the same reason as the updating of the coordinate system, the revision of the transformation matrix of local-global coordinates at each step is necessary. The formulation based on a convected coordinate system has also been named the incremental moving coordinate formulation or incremental combined Eulerian and Lagrangian formulation and is only valid for small strains.

The variational principles may now be applied in order to obtain the governing equations. Nonlinear terms in the strain-displacement relations are initially included. However, the higher order terms in the energy expression or in the incremental strain expression, which introduce nonlinearity into the stiffness matrix of the system, are deleted. This is justifiable since the geometry is kept updated. The final incremental linear equilibrium equations can be expressed symbolically at the  $(n+1)^{th}$  increment as

$$([K_0] + [K_1]_n)\{\Delta q\}_{n+1} = \{\Delta p\}_{n+1} + \{f\}_n \quad (2.1)$$

where  $\{\Delta q\}$  are the incremental displacements and  $\{\Delta p\}$  are the incremental applied loads.  $[K_0]$  is the conventional linear elastic stiffness matrix of the system.  $[K_1]$  is a function of the existing stress level of the system at the end of the  $n^{th}$  increment and is considered as the initial stress for the  $(n+1)^{th}$  increment. Also the merging of the  $[K_1]$  matrix is due to the

geometrical effect, as the individual terms of this matrix can be expressed in terms of geometrical parameters. Hence, it is often called the initial stress matrix<sup>170-172</sup> or geometric matrix<sup>177,178</sup>.  $\{f\}$  is the unbalanced residual forces at the end of the  $n^{\text{th}}$  increment and is added to improve the results. To continuously solve Eq. 2.1, a piecewise linear approximation of the true solution is obtained. Further iterations can be performed within each increment to reduce the unbalanced forces to within any limit of tolerance, and in this case the  $[K_1]$  matrix can either be retained or dropped<sup>150,51</sup>. The inclusion of the  $[K_1]$  matrix is essential and often sufficient for solving the stability problem<sup>167,179,216</sup>.

### II.3.2 Lagrangian Coordinate Formulation

The Lagrangian coordinate formulation is a more popular method today. It is often called the Total Lagrangian coordinate formulation to emphasize its difference from the previously discussed convected coordinate formulation. As its name implies, this formulation is totally based on the initial coordinate system of an undeformed configuration at load increment zero. Hence, no transformation of stresses, updating of geometry, and revision of the local-global coordinate transformation matrix is required. This formulation is valid for small strains as well as large. Further improvement is possible by accounting for changes in the direction of the loads during incremental changes in the deformation<sup>180</sup>. This can be done by transformation from deformed to global directions, whereas, it is inconsistent with the total Lagrangian formulation<sup>176</sup>.

By applying the variational principle and retaining all the higher order terms, the final nonlinear equilibrium equations can be expressed symbolically as

$$([K_0] + [K^*]) \{q\} = \{p\} \quad (2.2)$$

where  $[K^*]$  is a nonlinear stiffness matrix to account for the nonlinear effects.  $\{q\}$  and  $\{p\}$  are displacements and applied loads respectively.

Eq. 2.2 can be converted into an initial value problem by taking the total derivative of the equations with respect to a load parameter,  $\lambda$ , which is a scalar to denote the intensity of loading (i.e. let  $\{p\} = \lambda\{\bar{p}\}$ ), resulting in:

$$([K_0] + [K_{NL}]) \{\dot{q}\} = \{\bar{p}\} \quad (2.3)$$

where  $\{\dot{q}\}$  is the derivative with respect to  $\lambda$  and  $\{\bar{p}\}$  are the generalized loads.

The incremental linear equilibrium equations can be generated in many ways such as using a first order Taylor's series expansion of Eq. 2.2, taking a simple Euler forward difference of Eq. 2.3, or formulating directly through the incremental variational principle<sup>168</sup>. It can be written as

$$([K_0] + [K_{NL}]_n) \{\Delta q\}_{n+1} = \{\Delta p\}_{n+1} + \{f\}_n \quad (2.4)$$

where  $[K_{NL}]$  is the incremental nonlinear stiffness matrix evaluated using the known values of displacements, stresses and strains at the end of the  $n^{\text{th}}$  increment.

When only geometrical nonlinearity is involved (this represents the stage of initial loading up to, and just prior to, first yielding

of the structure), the nonlinear stiffness matrix is only a function of displacements. Formulations are often derived by minimizing the total potential energy of the system. Mallett and Marcal<sup>181</sup> presented an appealing formulation which is expressed as:

in total potential energy:

$$\phi = \{q\}^T \left( \frac{1}{2} [K_0] + \frac{1}{6} [N_1] + \frac{1}{12} [N_2] \right) - \{q\}^T \{p\} \quad (2.5)$$

in equilibrium equations:

$$([K_0] + \frac{1}{2} [N_1] + \frac{1}{3} [N_2]) \{q\} = \{p\} \quad (2.6)$$

in incremental equations:

$$([K_0] + [N_1]_n + [N_2]_n) \{\Delta q\}_{n+1} = \{\Delta p\}_{n+1} \quad (2.7)$$

where  $[N_1]$  includes all the first order nonlinear terms (first order geometrical matrix) and  $[N_2]$  the second order nonlinear terms (second order geometrical matrix). Either of the three equations can be used to solve nonlinear problems. Eq. 2.5 is solved by a direct search for the minimum potential energy<sup>64,182</sup>. Eq. 2.6 can be solved iteratively using either the direct iteration method, the Newton-Raphson method, or the modified Newton-Raphson method. Further explanation will be given later. Solving Eq. 2.7 using a step-by-step technique is straightforward.

Alternate formulations also based on the Lagrangian reference frame can be typified by the work by Stricklin et al<sup>183</sup>. This formulation is essentially the same as the previous one except it differs in the form of expression. Following the same routine of decomposing the strains into linear and nonlinear parts and applying the variational principle,

the equilibrium equations can be written as

$$[K_0] \{q\} + \left\{ \frac{\partial \phi_{NL}}{\partial q} \right\} = \{p\} \quad (2.8)$$

and in incremental form

$$([K_0] + \left[ \frac{\partial \phi_{NL}}{\partial q_i \partial q_j} \right]_n) \{\Delta q\}_{n+1} = \{\Delta p\}_{n+1} + \{f\}_n \quad (2.9)$$

where  $\phi_{NL}$  represents the part of the potential energy due to nonlinear terms.

The above mentioned incremental equilibrium equations have often been written in an alternate form as:

$$([K_0] + [K_1]_n + [K_2]_n) \{\Delta q\}_{n+1} = \{\Delta p\}_{n+1} + \{f\}_n \quad (2.10)$$

where  $[K_1]$  is the aforementioned initial stress matrix and  $[K_2]$  is referred to as the initial displacement matrix and covers all other nonlinear terms which were dropped in the convected coordinate formulation.

When material nonlinearity has to be included (this represents the loading stage of post-yielding), no strain energy function exists, which is uniquely defined by the current displacements in the flow theory of plasticity. Such a function would depend on previous loads and the deformation history. A formulation based on the incremental variational principle derived by using virtual work is, therefore, preferred. This is because the virtual work formulation is more general and does not involve the stress-strain relation; hence, it is independent of material properties. The loads, of course, have to be applied in increments in this case. The incremental equilibrium equation can now be written in

another form, by explicitly separating the geometrical and material nonlinear parts:

$$([K_0] + [K_{NL(G)}]_n + [K_{NL(P)}]_n) \{\Delta q\}_{n+1} = \{\Delta p\}_{n+1} + \{f\}_n \quad (2.11)$$

where subscripts G and P represent the terms due to geometrical nonlinearity and material nonlinearity, respectively.

Despite the difference in appearance due to the different ways of arranging the nonlinear terms, these equations are essentially the same if the same order of displacement functions were used. In any case the incremental equilibrium equations can be written in short as

$$[K_T]_n \{\Delta q\}_{n+1} = \{\Delta p\}_{n+1} + \{f\}_n \quad (2.12)$$

where  $[K_T]$  is called the tangent stiffness matrix or incremental stiffness matrix. The tangent stiffness matrix is originally referred to in the Newton-Raphson iteration solution procedure. However, the tangent stiffness matrix and the incremental stiffness matrix are really the same. This can be seen, for example, by noting that both the Newton-Raphson iteration and the generation of incremental equilibrium equations employ the first order Taylor's series expansion of the basic nonlinear equilibrium equations. Eq. 2.12 is the well-known incremental method with a one step Newton-Raphson iteration.

### II.3.3 Eulerian Coordinate Formulation

The formulation based on the Euler coordinate system has very limited application because of its disadvantages in formulation and computation. It is therefore not discussed here. References 49, 184 and 185 can be consulted for details.



## II.4 Solution Techniques Based on Differing Ways of Handling the Nonlinear Terms

We initiate our discussion by considering the material nonlinear problem, remembering that the loads are now applied in increments due to the consideration of the flow theory of plasticity. Write the stress-strain relation in a very general form<sup>166</sup>,

$$\{\sigma\} = [E] (\{\epsilon\} - \{\epsilon_0\}) + \{\sigma_0\} \quad (2.13)$$

where the parameters

$[E]$  = a matrix defining the constitutive relation for a multi-stress field

$\{\epsilon_0\}$  = initial strain in the system

$\{\sigma_0\}$  = initial stress in the system

By adjusting one or more of these parameters to satisfy the previously discussed equilibrium equations, a solution can then be found.

### II.4.1 Tangent Stiffness Approach

When parameter  $[E]$  is adjusted in Eq. 2.13, the nonlinearity due to plasticity is introduced directly into the stiffness matrix. This approach is called the tangent-modulus method<sup>186-190</sup> in finite element elasto-plastic analysis. It is seen that in this method the stiffness matrix is revised at each load increment and hence varies.

When this approach is applied to the problem of geometrical nonlinearity, or of combined nonlinearities by retaining the nonlinear terms within the stiffness matrix on the left hand side of the governing equations, it is called the tangent stiffness method. The stiffness matrix (or at least the nonlinear part of the matrix) is recalculated continuously to take

into account the latest nonlinear effects. The extra computing cost of evaluating and inverting the stiffness matrix is paid back by faster convergency and usually better accuracy. All equations given in Section II.3 were presented in forms representing the tangent stiffness approach.

#### II.4.2 Pseudo-Force Approach

We refer again to Eq. 2.13 for the problem of material nonlinearity. If the plastic part of the strains is interpreted as initial strain,  $\{\epsilon_0\}$ , which is kept adjusted and treated as external pseudo-forces, it is called the initial strain method<sup>177,191-194</sup>. An alternative is to find the difference between the stresses, based on elastic analysis and the subsequent stresses after relaxation due to plastification. This stress difference is considered as an initial stress,  $\{\sigma_0\}$ , and is also treated as pseudo-forces. It is called the initial stress method<sup>195</sup>.

It may be seen that either the initial strain method or the initial stress method retain the original constant (elastic) stiffness matrix but convert the nonlinear effects into external pseudo-forces. An iterative process is then applied until the pseudo-forces vanish.

This pseudo-force approach can be generalized to cover geometrical nonlinearity and combined nonlinearities by having the nonlinear terms formulated in the form of a force vector and transferred to the right hand side of the governing equations. In this case, the updating and inverting of the stiffness matrix is avoided. This advantage, however, is compensated for by the slower convergence<sup>196</sup> and possible numerical instability in certain cases. The pseudo-force method can be written

in a typical form as

$$[K_0] \{q\} = \{p\} + \{Q^{NL}\} \quad (2.14)$$

where  $\{Q^{NL}\}$  are the pseudo-forces to account for geometrical nonlinearity, or material nonlinearity, or both.

#### II.4.3. Combined Tangent Stiffness and Pseudo-Force Approach

On the problem of combined nonlinearities, the nonlinear tangent stiffness matrix consists of two parts, the geometrical nonlinear part and the material nonlinear part, which can be explicitly separated<sup>197</sup>. Similarly, the pseudo-force due to nonlinearity can also be decomposed into two parts. However, the pseudo-force approach in the incremental form is less appealing, since the pseudo-force of the geometrical nonlinear part may cause numerical instability<sup>200,202</sup>.

The alternate is to include geometrical nonlinearity within the tangent stiffness matrix but treat material nonlinearity as a pseudo-force. This can be written in incremental form as

$$([K_0] + [K_{NL(G)}]_n) \{\Delta q\}_{n+1} = \{\Delta p\}_{n+1} + \{\Delta Q^{NL(P)}\}_n + \{f\}_n \quad (2.15)$$

Armen et al<sup>173-175</sup> have used this approach by employing a convected coordinate system so that the initial stress matrix,  $[K_1]$ , has been used to replace  $[K_{NL(G)}]$ .

## II.5 Numerical Solution Procedures

A number of solution procedures have been tried and reported in the literature. Detailed descriptions and discussions of the merits and shortcomings of most of these procedures are available in some excellent papers such as those by Gallagher<sup>210</sup> and by Stricklin et al<sup>197-202</sup>. In this section, only the main feature of each solution procedure is presented and briefly discussed. The presentation follows the works by Stricklin et al, hence their terminologies are used as much as possible. The procedures will be described in both the form using the tangent stiffness and the form using pseudo-forces to further demonstrate the difference and the applicability of the two approaches.

We rewrite the fundamental nonlinear equilibrium equations for the tangent stiffness method and pseudo-force method respectively as

$$\{f(\lambda, q)\} = \lambda\{\bar{p}\} - ([K_0] + [K^*])\{q\} \quad (2.16)$$

$$\{f(\lambda, q)\} = \lambda\{\bar{p}\} + \{Q^{NL}\} - [K_0]\{q\} \quad (2.17)$$

all terms in these equations have been previously defined. The classification of solution procedures into three categories by Stricklin et al will be employed in the following demonstration.

### II.5.1 Exact Solution Procedure - $\{f\} = 0$

In this class, an exact solution is sought through iterations to reduce the force unbalance,  $\{f\}$ , to zero. At a given load,  $\lambda\{\bar{p}\}$ , and based upon some initial estimate of  $\{q\}_n$ , a first order Taylor's series

expansion of the force unbalance about point  $\{q\}_n$  and setting  $f(\lambda, q_n + \Delta q)$  of Eq. 2.16 to zero, yields the well known Newton-Raphson method

$$([K_0] + [K_{NL}]_n) \{\Delta q\}_{n+1} = \{f\}_n \quad (2.18)$$

The correction,  $\{\Delta q\}_{n+1}$ , is added to the approximate root,  $\{q\}_n$ , to obtain a more nearly correct  $\{q\}_{n+1}$  approximation. Eq. 2.18 clearly shows that the Newton-Raphson method is a tangent stiffness approach. Convergency difficulties have previously been reported by using the Newton-Raphson method on problems involving material nonlinearity<sup>202</sup>.

If  $[K_{NL}]$  in Eq. 2.18 were kept constant by avoiding further updating, after first iteration or after the first several iterations, the so called modified Newton-Raphson method is obtained. An advantage is gained by elimination of further re-evaluation of the tangent stiffness matrix. Of course, the convergency rate becomes slower as a consequence.

If  $[K_{NL}]$  is set to zero, a recurrence formula can be obtained from Eq. 2.16 and 2.17 by setting  $\{f\} = 0$ .

$$[K_0] \{q\}_{n+1} = \lambda \{\bar{p}\} - [K^*]_n \{q\}_n = \lambda \{\bar{p}\} + \{Q^{NL}\}_n \quad (2.19)$$

This is the direct iteration (successive approximation) method and is a pseudo-force approach. It can be seen that the iterative process of each increment for the aforementioned initial strain method and initial stress method is essentially Eq. 2.19. The initial strain method may encounter numerical instability for perfect-plastic material<sup>196</sup>.

In this class, even though the solution can be accomplished in a one-step operation for a full load on occasion for less severe geometrical

nonlinearity, it is possible that a non-unique solution may arise and the physically unimportant one may be obtained. Hence, it is generally better to proceed by incrementing the load and obtaining the solution for each increment as for material nonlinearity. The size of increments is important as the increment can be comparatively large for geometrical nonlinear problems, whereas it has to be kept small when material nonlinearity is involved.

#### II.5.2 Initial Value Procedure - $\{\dot{f}\} = 0$

This class is based on the assumption that the first derivative of the force unbalance with respect to load parameter,  $\lambda$ , is zero. It leads to the type of solution procedure which moves along the load-displacement path incrementally without iterations. Both the tangent stiffness method and the pseudo-force method are applicable. Differentiating Eq. 2.16 and 2.17 with respect to  $\lambda$  and setting to zero, we may obtain, with the aid of chain rule:

$$([K_0] + [K_{NL}]) \{\dot{q}\} = \{\dot{p}\} \quad (2.20)$$

$$[K_0] \{\dot{q}\} = \{\dot{p}\} + \{\dot{Q}^{NL}\} \quad (2.21)$$

Eq. 2.20 and 2.21, which are first order differential equations, together with the initial condition,  $\{q(\lambda=0)\} = 0$ , may be solved by various numerical procedures such as the Runge-Kutta method, open and closed integration formulas, and the direct substitution of difference approximations for the derivatives.

Using an Euler forward difference expression for  $\{\dot{q}\}$  and a backward difference formula for  $\{\dot{Q}^{NL}\}$ , Eq. 2.20 and 2.21 become the conventional incremental forms:

$$([K_o] + [K_{NL}]_n) \{\Delta q\}_{n+1} = \Delta \lambda \{\bar{p}\} \quad (2.22)$$

$$[K_o] \{\Delta q\}_{n+1} = \Delta \lambda \{\bar{p}\} + \{\Delta Q^{NL}\}_n \quad (2.23)$$

Another solution procedure which is included in this class is the well-known perturbation technique<sup>203-206</sup>. At a known equilibrium point on the load displacement path, the derivatives of this path may be used to predict a further point. Expanding the displacements in a Taylor series about some known load-displacement state  $(q, \lambda)$  yields

$$\begin{aligned} q_i(\lambda + \Delta \lambda) = & q_i(\lambda) + \dot{q}_i(\lambda) \Delta \lambda + \frac{1}{2} \ddot{q}_i(\lambda) (\Delta \lambda)^2 \\ & + \frac{1}{6} \ddot{\ddot{q}}_i(\lambda) (\Delta \lambda)^3 + \dots \end{aligned} \quad (2.24)$$

where  $i$  refers to the degree of freedom. Solve Eq. 2.20 or 2.21 for  $\dot{q}_i$ . Further differentiation of these equations repeatedly will yield similar sets of simultaneous equations which may be solved sequentially for  $\dot{q}_i$ ,  $\ddot{q}_i$ , etc.. Substituting the known value of  $q_i$  and of derivatives into Eq. 2.24, the displacement at  $(\lambda + \Delta \lambda)$  is then obtained.

The method is limited to problems with a moderate degree of nonlinearity such as the study of initial post-buckling response, but may not be suitable for extension far into the post-buckling range since the Taylor's series expansion employed is strictly valid only in an asymptotic sense at the bifurcation point. The solution then tends to drift away from the true equilibrium load path due to the accumulation of

errors at succeeding load steps. Also, a considerable amount of mathematical manipulation is required if a significant number of path derivatives must be calculated at each load step. To overcome these limitations, the method is often used in conjunction with other techniques. It involves the use of the perturbation method to yield a higher order predictor formula, and the employment of an iterative formula, such as the Newton-Raphson formula, as a corrector<sup>204</sup>. In this manner the perturbation technique may be extended for use on highly nonlinear portions of load-displacement curves. Recently the method has been used for solving the combined nonlinear problem<sup>207</sup>.

It has been reported that the pseudo-force approach under the class of  $\{f\} = 0$  may encounter numerical instability in geometrical nonlinear problems<sup>200,202</sup>.

### II.5.3 Self-Correcting Solution Procedures

This class of solution procedure is a natural extension of previous classes. Its main function is to provide a suitable correcting term to prevent the incremental approximate solution from drifting away from the true load-displacement path, as often occurs in the aforementioned second class solution procedure. This class is composed of two sub-classes.

- (a) The first order self-correcting solution procedure is characterized by

$$\{f\} + z \{f\} = 0 \quad (2.25)$$

where  $z$  is an amplification factor. Substituting Eq. 2.16 and 2.17



and their first derivatives with respect to load parameter,  $\lambda$ , into Eq. 2.25, yields the self-correcting first order differential equations:

$$([K_0] + [K_{NL}])\{\dot{q}\} + z([K_0] + [K^*])\{q\} = (1+z\lambda)\{\bar{p}\} \quad (2.26)$$

$$[K_0]\{\dot{q}\} + z\{q\} = (1+z\lambda)\{\bar{p}\} + z\{Q^{NL}\} + \{\dot{Q}^{NL}\} \quad (2.27)$$

Applying an Euler forward difference for  $\{\dot{q}\}_n$  and a backwards difference formula for  $\{\dot{Q}^{NL}\}_n$ , the equations result in incremental equilibrium equations with correcting term:

$$([K_0] + [K_{NL}]_n)\{\Delta q\}_{n+1} = \Delta\lambda\{\bar{p}\} + z(\Delta\lambda)\{f\}_n \quad (2.28)$$

$$[K_0]\{\Delta q\}_{n+1} = \Delta\lambda\{\bar{p}\} + \{\Delta Q^{NL}\}_n + z(\Delta\lambda)\{f\}_n \quad (2.29)$$

If we set  $z(\Delta\lambda)=1$ , the equations become the incremental solution procedure with a one step Newton-Raphson correction which is currently actively employed by researchers.

(b) Second order self-correcting solution procedure characterized by

$$\{\ddot{f}\} + c\{\dot{f}\} + z\{f\} = 0 \quad (2.30)$$

where  $c$  is also an arbitrary scalar quantity. Eq. 2.30 is identical to a simple harmonic motion. The variable  $c$  is analogous to the damping factor and the square root of  $z$  represents the undamped natural frequency of the system. This simulation provides some insight into the selection of these quantities. Solving Eq. 2.30 by employing exact integration:

$$\{f(s)\} = e^{+cs/2} \left[ \{A\} \cos \frac{\sqrt{4z-c^2}}{2} s + \{B\} \sin \frac{\sqrt{4z-c^2}}{2} s \right] \quad (2.31)$$

where  $s$  is a variable for the load increment such that at the beginning of each load step,  $s$  is set equal to zero, and at the end of the step  $s$  is equal to  $\Delta\lambda$ .  $\{A\}$  and  $\{B\}$  are constant vectors to be determined using the "initial" value of  $\{f(0)\}$  and  $\{\dot{f}(0)\}$ . The displacement vector at the end of the increment is then obtained. By rearranging Eq. 2.16 and 2.17, the expressions defining the force unbalance, yields

$$([K_0] + [K^*]_n) \{q\}_{n+1} = \lambda_{n+1} \{\bar{p}\} - \{f\}_{n+1} \quad (2.32)$$

$$[K_0] \{q\}_{n+1} = \lambda_{n+1} \{\bar{p}\} + \{Q^{NL}\}_n - \{f\}_{n+1} \quad (2.33)$$

where  $\{f\}_{n+1}$  is obtained from Eq. 2.31. The second order self-correcting procedure has not been widely accepted because of its high dependence on the analyst's familiarity and experience in choosing the step size as well as the parameters within the formula.

## II.6 Closure

A survey of finite element nonlinear analysis has been conducted by many researchers<sup>176,180,208-211</sup>. Most of the recently published finite element books<sup>166,212-214</sup> also cover, more or less, the fundamental treatment of nonlinearities. Qden<sup>215</sup> has devoted an entire book to this subject and has a wide range of nonlinear applications to physical problems. These references can be consulted for further details. The formulation and the solution procedure of the present study is based on the total Lagrangian coordinate system and the tangent stiffness method. Only these methods will be further investigated. The convected coordinate formulations and pseudo-force solutions are excluded.

## CHAPTER III

### MATHEMATICAL FORMULATION OF THE PROBLEM

#### III.1 Principle of Variations

##### III.1.1 Principle of Virtual Work

The following derivation employs the Lagrangian description and the reference coordinate system to be used is rectangular cartesian.

Let  $x_i$  be the coordinates of an arbitrary point of a continuous body in its initial undeformed state and let  $X_i$  be the coordinates of that material point after deformation. The equation of equilibrium can be expressed as<sup>217</sup>

$$(\sigma_{jk} \frac{\partial X_i}{\partial x_j})_{,k} + p_i = 0 \quad (3.1)$$

where  $\sigma_{jk}$  is Kirchhoff stress tensor (2nd Piola-Kirchhoff stress tensor) and is symmetric.  $p_i$  is the body force per unit volume of the initial configuration. The acceleration term in Eq. 3.1 is dropped because only static equilibrium will be considered in this study.

To derive the principle of virtual work, we integrate the product of the equilibrium equations and the corresponding displacements,  $\delta u_i$ , over the initial volume of the body<sup>168</sup>

$$\int_V [(\sigma_{jk} \frac{\partial X_i}{\partial x_j})_{,k} \delta u_i + p_i \delta u_i] dv = 0 \quad (3.2)$$

$\delta u_i$  is an arbitrary, infinitesimal, and kinematically admissible virtual displacement field. For simplicity, the body force term is now dropped. Applying integration by parts on Eq. 3.2, results in:

$$\int_V \left( \sigma_{jk} \frac{\partial X_i}{\partial x_j} \delta u_i \right)_{,k} dv - \int_V \left( \sigma_{jk} \frac{\partial X_i}{\partial x_j} \delta u_{i,k} \right) dv = 0 \quad (3.3)$$

Employing Gauss' divergence theorem to convert the volumetric integration to a surface integration, the first term of Eq. 3.3 can be written as

$$\int_V \left( \sigma_{jk} \frac{\partial X_i}{\partial x_j} \delta u_i \right)_{,k} dv = \int_S T_i \delta u_i ds = \int_{S_\sigma} T_i \delta u_i ds \quad (3.4)$$

where  $S$  represents the body surface which can be considered as consisting of two parts;  $S_\sigma$  where the surface tractions are prescribed and  $S_u$  where displacements are prescribed.  $T_i$  are the prescribed surface traction forces per unit of surface area. Eq. 3.4 denotes the external virtual work and is non-zero only in the  $S_\sigma$  part.

The second term of Eq. 3.3, after manipulations (which can be done, for example, by explicitly writing down all terms, regrouping them and then applying the strain-displacement relations), represents the internal virtual work of the body and is written as

$$\int_V \left( \sigma_{jk} \frac{\partial X_i}{\partial x_j} \delta u_{i,k} \right) dv = \int_V \sigma_{ij} \delta e_{ij} dv \quad (3.5)$$

where  $e_{ij}$  is the Green strain tensor.

Substituting Eq. 3.4 and 3.5 into Eq. 3.3, we obtain the well-known equation for virtual work:

$$\int_V \sigma_{ij} \delta e_{ij} dv - \int_{S_\sigma} T_i \delta u_i ds = 0 \quad (3.6)$$

### III.1.2 Principle of Stationary Potential Energy

When the body remains elastic, there exists a state function  $\omega(e_{ij})$  which does not depend on the loading path but only on final strains.

This function is perfectly differentiable such that<sup>168</sup>

$$\frac{\partial \omega}{\partial e_{ij}} = \sigma_{ij} \quad (3.7)$$

The state function,  $\omega$ , is called the strain energy function defined per unit volume of the reference body. Substituting the strain energy function into the first term of Eq. 3.6, the principle of virtual work is then specialized to the principle of stationary potential energy as:

$$\delta \int_V \omega(u_i) dv - \int_{S_\sigma} T_i \delta u_i ds = 0 \quad (3.8)$$

where the strain function  $\omega(u_i)$  is written in terms of  $u_i$ , by the use of the strain-displacement relations. Eq. 3.8 is very useful in application to elasticity problems in which external forces are not derivable from potential functions. If the applied external forces are constant or conservative, that is they are derivable from potential functions,  $\psi(u_i)$ , such that

$$\delta \psi = - T_i \delta u_i \quad (3.9)$$

substituting Eq. 3.9 into the second term of Eq. 3.8, we obtain:

$$\delta \left( \int_V \omega dv + \int_{S_\sigma} \psi ds \right) = 0 \quad (3.10)$$

or, in short:

$$\delta(U + V) = \delta(\phi) = 0 \quad (3.11)$$

where  $U$ ,  $V$  and  $\phi$  are respectively the strain energy, the potential energy due to external forces, and the total potential energy within the domain of the body under consideration.

The above equations of the principle of the stationary potential energy state that, for equilibrium to be ensured, the total potential energy,  $\phi$ , must be stationary for variations of admissible displacements. Limiting the principle to small displacements only, it can be shown that the stationary state is a minimum potential energy state. However, in large displacement theory, the energy does not necessarily attain a minimum for the stationary condition<sup>255</sup>.

### III.2 Incremental Variational Principle

#### III.2.1 Virtual Work Approach

A Lagrangian reference frame is again employed in the following derivation. The formulation of the incremental theories<sup>233</sup> begins by dividing the loading path of the solid body problem into a number of equilibrium states. It is assumed that all the state variables such as stress, strain and displacement together with the loading history, are known up to the  $n^{\text{th}}$  state. Our problem, then, is to formulate an incremental theory for determining all state variables in the  $(n+1)^{\text{th}}$  state, under the assumption that the  $(n+1)^{\text{th}}$  state is incrementally close to the  $n^{\text{th}}$  state and all the governing equations may be linearized with respect to the incremental quantities. We denote the stress, strain, displacements, and external forces acting on  $s_0$  in the  $n^{\text{th}}$  and  $(n+1)^{\text{th}}$  states respectively by

$$\begin{array}{cccc} \sigma_{ij}, & e_{ij}, & u_i, & T_i \\ \text{and} & (\sigma_{ij} + \Delta\sigma_{ij}), & (e_{ij} + \Delta e_{ij}), & (u_i + \Delta u_i), \quad (T_i + \Delta T_i) \end{array}$$

It is known that the Green strain tensors at the  $n^{\text{th}}$  and  $(n+1)^{\text{th}}$  states are respectively defined by<sup>168,218,219</sup>

$$e_{ij} = \frac{1}{2} (u_{i,j} + u_{j,i} + u_{k,i} u_{k,j}) \quad (3.12)$$

and

$$\begin{aligned} (\tilde{e}_{ij} + \Delta \tilde{e}_{ij}) = \frac{1}{2} [(u_i + \Delta u_i)_{,j} + (u_j + \Delta u_j)_{,i} \\ + (u_k + \Delta u_k)_{,i} (u_k + \Delta u_k)_{,j}] \end{aligned} \quad (3.13)$$

We readily obtain from Eq. 3.12 and 3.13 that

$$\begin{aligned} \Delta e_{ij} = \frac{1}{2} [(\delta_{kj} + u_{k,j}) \Delta u_{k,i} + (\delta_{ki} + u_{k,i}) \Delta u_{k,j} \\ + \Delta u_{k,i} \Delta u_{k,j}] \end{aligned} \quad (3.14)$$

If  $\Delta e_{ij}$  is linearized with respect to  $\Delta u_k$ , then

$$\Delta e_{ij} = \frac{1}{2} [(\delta_{kj} + u_{k,j}) \Delta u_{k,i} + (\delta_{ki} + u_{k,i}) \Delta u_{k,j}] \quad (3.15)$$

The principle of virtual work for the  $(n+1)^{\text{th}}$  state is now expressed by

$$\int_V (\sigma_{ij} + \Delta \sigma_{ij}) \delta (e_{ij} + \Delta e_{ij}) dv - \int_{S_0} (T_i + \Delta T_i) \delta (u_i + \Delta u_i) ds = 0 \quad (3.16)$$

Applying the relations given by Eqs. 3.12 through 3.15 to the above equation and noting that the variation is taken with respect to  $\Delta u_i$ , Eq. 3.16 (after some manipulations and neglecting the higher order terms) can be written as<sup>168</sup>

$$\begin{aligned} \int_V [\Delta \sigma_{ij} \delta \Delta e_{ij} + \sigma_{ij} \delta (\frac{1}{2} \Delta u_{k,i} \Delta u_{k,j})] dv - \int_{S_0} \Delta T_i \delta \Delta u_i ds \\ + (\int_V \sigma_{ij} \delta \Delta e_{ij} dv - \int_{S_0} T_i \delta \Delta u_i ds) = 0 \end{aligned} \quad (3.17)$$

The last part, which is enclosed by parentheses, in the above equation represents the unbalanced residual forces in the  $n^{\text{th}}$  state. It will vanish if equilibrium is achieved. However, the  $n^{\text{th}}$  state may not be in complete equilibrium in this kind of incremental theory due to neglect of the higher order terms and computational inaccuracies. Consequently these force unbalances are retained in Eq. 3.17 for an equilibrium check.

### III.2.2 Potential Energy Approach

Similar to the last section, the incremental governing equations can be formulated using the minimization of the incremental potential energy of the system ( $\Delta\phi$ ).

$$\delta(\Delta\phi) = 0 \quad (3.18)$$

where

$$\Delta\phi = \phi(u_i + \Delta u_i) - \phi(u_i) \quad (3.19)$$

The variation of  $\Delta\phi$  is mathematically equivalent to the variation of  $\phi(u_i + \Delta u_i)$  with respect to  $\Delta u_i$  since  $\phi(u_i)$  is independent of  $\Delta u_i$ . It can be found that the derivation, using the potential energy approach to obtain the governing equations, is likely the same procedure as that from Eq. 3.16 to Eq. 3.17 in the virtual work approach. The details are left to section III.8.2 where the explicit formulation is demonstrated in matrix notation.



### III.3 Choice of Elements

A simple non-conforming (discontinuity in the normal slope between two adjacent elements) flat rectangular element with six degrees of freedom (d.o.f.) at each node is used in this study. The definition of axes and d.o.f. are shown in Fig. 2 where  $x$ - $y$  represent local coordinates and  $\xi$ - $\eta$  normalized coordinates.  $u$  and  $v$  are in plane displacements and  $w$  is the transverse displacement.

The choice of the element geometry is largely influenced by the shape of the structure to be analysed and the rectangular element is found perfectly suitable and sufficient for the purpose of the present study. Comparison with other shapes such as triangular elements, the rectangular element generally produces better results with less effort on input data. There is also a corresponding reduction in the total number of degrees of freedom in the structure and hence a reduction in computer time required for solving the system of equations.

The use of a curved element is obviously unnecessary as most curved elements require the shell to possess continuous curvature or at least continuous slopes. The type of structures considered in this study (see Fig. 1) does not admit either of these conditions. Furthermore, the present formulation and solution is based on the undeformed configuration of the elements which were initially plane and has demonstrated that the use of a curved element is unnecessary. For the case where large initial imperfections are introduced through nodal coordinates, the four nodes of a rectangular element do not remain coplanar. A transformation matrix for each node, which was derived with respect to a plane passing through that node, and the two most adjacent ones, may be employed for better accuracy.

The choice of a "simple" or a "refined" element is again a matter of judgement. The refined elements<sup>221,222</sup> may eliminate the problem of nonconformity and produce comparable accuracy. However, this is traded off by generating higher order d.o.f. for which the corresponding force terms lack physical interpretation and/or by using other techniques such as static condensation which increase the time of calculation. Even though the refined elements have been used in nonlinear analysis<sup>57,149</sup>, it is generally agreed, particularly for the case of combined nonlinearities, that the simple element is preferred<sup>223,224</sup> due to its economy in computing cost.

One attractive conforming rectangular bending element is that developed by Bogner et al<sup>220</sup> and it has been used by others<sup>89,90</sup> in non-linear analysis. This element requires one more d.o.f. than the one employed in this study. At first glance, it would seem that adding one more d.o.f. at each node is not a big increase. However, when this is applied to a three dimensional structural member where quite a number of elements are required, the increase becomes very significant. Further, this additional d.o.f. ( $\frac{\partial^2 w}{\partial x \partial y}$ ), although it does not give difficulty in the present case, may prove awkward when a coordinate transformation is needed for more general structures thus preventing the possible extension of the current approach in future. Hence, even though the element by Bogner et al provides the merit of conformity, it was not adopted.

The proposed element has three components of translation ( $u, v, w$ ) and three of rotation ( $\theta_x, \theta_y, \theta_z$ ). These d.o.f.'s are first order tensor quantities and obey the simple law of vector transformation. The polynomial terms corresponding to each displacement function are

$$u: 1, x, y, xy$$

$$v: 1, x, y, x^2, xy, x^3, x^2y, x^3y$$

$$w: 1, x, y, x^2, xy, y^2, x^3, x^2y, xy^2, y^3, x^3y, xy^3$$

It can be seen that the bending part of the element is actually the ACM element<sup>225,226</sup>. Even though non-conforming, it has shown good convergency in practice in linear<sup>226-228</sup> and nonlinear<sup>144,229</sup> analysis. Note that for the membrane part, the  $v$  displacement varies linearly in the  $y$  direction but cubically in the  $x$  direction to achieve the same degree as the  $w$  displacement and it has also been previously employed<sup>230</sup>. This is due to the compatibility requirement between  $v$  and  $w$  for the neighbouring elements which are joined at non-zero angles along their common axis (see Fig. 3). This causes a preferential orientation by setting the  $x$ -axes of both the global and local coordinate systems parallel to the longitudinal direction of the member. However, in practice, this disadvantage does not create any inconvenience at all. On the contrary, advantages have been gained by using these higher order polynomial terms in the  $v$  displacement function. It improves the accuracy of the results which is reduced in the case of a large aspect ratio for an element which often has to be used for reasons of economy. The sixth d.o.f. ( $\theta_z$ ), which is created because of introducing higher order terms, also serves another purpose which is to provide in-plane rotational stiffness to avoid a singular matrix when neighbouring elements connecting to a node are all coplanar. Hence, the employment of a fictitious set of self-equilibrated moments<sup>166</sup> or any other means are not required.

The displacements at any point within the element can be expressed in terms of nodal displacements as:

$$\{u\} = [N] \{q\} \quad (3.20)$$

or in incremental form

$$\{\Delta u\} = [N] \{\Delta q\} \quad (3.21)$$

The explicit form of the shape function,  $[N]$ , and of Eq. 3.20 is shown in Appendix A-1 and A-2. The explicit form of Eq. 3.21 is similar to that of Eq. 3.20.

### III.4 Strain-Displacement Relations for Thin Plates

#### III.4.1 Total Strain-Displacement Relations

Let  $x_i$  be a set of rectangular cartesian coordinate axes and let  $u_i$  be the components of the displacement vector along these axes. The Green's strain tensor  $e_{ij}$  is defined in the Lagrangian frame by Eq. 3.12.

For plates, it is common to replace the tensor subscript notation by the more familiar notation  $x, y, z$  for  $x_1, x_2, x_3$  and  $u, v, w$  for  $u_1, u_2, u_3$  respectively. The  $x$  and  $y$  axes are perpendicular axes in the middle plane of the plate where the  $z$ -axis is normal to the plane.  $u$  and  $v$  are in-plane displacement components and  $w$  indicates transverse deflection of the plate.

The Kirchhoff theory of thin plates\* assumes

- (a) Normals to the unstrained middle plane remain straight and normal to the strained middle surface after deformation.

---

\* for details of theories of plates, see Love<sup>231</sup> who also extended Kirchhoff's hypothesis to shell

- (b) The distance of any point of the plate from the middle surface remains unchanged by the deformation.

The first assumption sets shear strain components of  $e_{xz}$  and  $e_{yz}$  equal to zero and the second assumption sets the normal strain component of  $e_{zz}$  equal to zero. Hence, only three non-zero strain components,  $e_{xx}$ ,  $e_{yy}$ , and  $e_{xy}$  are left in Eq. 3.12. The simplified equations become

$$\begin{aligned} e_{xx} &= \frac{\partial u}{\partial x} + \frac{1}{2} \left[ \left( \frac{\partial u}{\partial x} \right)^2 + \left( \frac{\partial v}{\partial x} \right)^2 + \left( \frac{\partial w}{\partial x} \right)^2 \right] \\ e_{yy} &= \frac{\partial v}{\partial y} + \frac{1}{2} \left[ \left( \frac{\partial u}{\partial y} \right)^2 + \left( \frac{\partial v}{\partial y} \right)^2 + \left( \frac{\partial w}{\partial y} \right)^2 \right] \\ e_{xy} &= \frac{1}{2} \left[ \frac{\partial u}{\partial y} + \frac{\partial v}{\partial x} + \left( \frac{\partial u}{\partial x} \frac{\partial u}{\partial y} + \frac{\partial v}{\partial x} \frac{\partial v}{\partial y} + \frac{\partial w}{\partial x} \frac{\partial w}{\partial y} \right) \right] \end{aligned} \quad (3.22)$$

It is seen that the original three dimensional problem has been reduced to a two dimensional one. Eq. 3.22 is valid for the general large deflection-large strain problem. However, for the type of problems to be considered in this study, the strains remain small compared to unity and the squares of the derivatives of the in-plane displacements are small compared to other terms and may be neglected. This justifies retaining only the rotational contributions,  $\frac{\partial w}{\partial x}$  and  $\frac{\partial w}{\partial y}$ , among the higher order terms, resulting in:

$$\begin{pmatrix} \epsilon_{px} \\ \epsilon_{py} \\ \epsilon_{pxy} \end{pmatrix} = \begin{pmatrix} \frac{\partial u}{\partial x} + \frac{1}{2} \left( \frac{\partial w}{\partial x} \right)^2 \\ \frac{\partial v}{\partial y} + \frac{1}{2} \left( \frac{\partial w}{\partial y} \right)^2 \\ \frac{\partial u}{\partial y} + \frac{\partial v}{\partial x} + \frac{\partial w}{\partial x} \frac{\partial w}{\partial y} \end{pmatrix} \quad (3.23)$$

Note that in Eq. 3.23 the components are engineering strains and not tensor components as in Eq. 3.12 or Eq. 3.22. The subscript p indicates the in-plane or middle surface strains. This strain-displacement relationship is rendered nonlinear in the displacement gradients by the presence of quadratic terms  $(\frac{\partial w}{\partial x})^2$ , etc..

For the flexural strains, the Kirchhoff hypothesis implies that the higher order correcting terms due to shear deformation on strain components, can be ignored. Hence, strains vary linearly from the middle surface. With further simplification by deleting higher order terms in the expression for curvature<sup>219</sup>, the strains can then be written

$$\begin{pmatrix} \epsilon_{bx} \\ \epsilon_{by} \\ \epsilon_{bxy} \end{pmatrix} = \begin{pmatrix} -z\psi_{xx} \\ -z\psi_{yy} \\ -z\psi_{xy} \end{pmatrix} = \begin{pmatrix} -z\frac{\partial^2 w}{\partial x^2} \\ -z\frac{\partial^2 w}{\partial y^2} \\ -2z\frac{\partial^2 w}{\partial x \partial y} \end{pmatrix} \quad (3.24)$$

where b indicates strains due to bending.  $\psi_{xx}$  etc. are the curvatures along the x and y axes, and z is the distance from the middle surface along the normal.

Combining Eqs. 3.23 and 3.24, the total strains at any point in the plate are:

$$\{\epsilon\} = \begin{pmatrix} \epsilon_x \\ \epsilon_y \\ \epsilon_{xy} \end{pmatrix} = \begin{pmatrix} \frac{\partial u}{\partial x} + \frac{1}{2} \left( \frac{\partial w}{\partial x} \right)^2 - z \frac{\partial^2 w}{\partial x^2} \\ \frac{\partial v}{\partial y} + \frac{1}{2} \left( \frac{\partial w}{\partial y} \right)^2 - z \frac{\partial^2 w}{\partial y^2} \\ \frac{\partial v}{\partial x} + \frac{\partial u}{\partial y} + \left( \frac{\partial w}{\partial x} \right) \left( \frac{\partial w}{\partial y} \right) - 2z \frac{\partial^2 w}{\partial x \partial y} \end{pmatrix} \quad (3.25)$$

Eq. 3.25 leads to the formulation for the deformation of thin plates proposed by Von Karman<sup>14</sup>. It is worthwhile noting that Kirchhoff's hypothesis employed herein deals only with kinematic relationship and does not include any assumptions about the properties of the material of the plate. Thus it is equally applicable to materials which obey Hooke's law as well as those which do not.

Each strain component of Eq. 3.25 may be decomposed into linear and nonlinear parts and can be expressed in a way similar to that of Rajasekaran and Murray<sup>232</sup> as

$$\begin{aligned}\epsilon_i &= \epsilon_i^L + \epsilon_i^{NL} \\ &= {}^L A_i \{G\} + \frac{1}{2} {}^L G_i [H]_i \{G\}\end{aligned}\quad (3.26)$$

where:  $\epsilon_i$  ( $i=1,2,3$ ) denotes  $\epsilon_x$ ,  $\epsilon_y$ , and  $\epsilon_{xy}$  respectively  
 $A_i$  is a vector and is defined by

$$\begin{aligned}{}^L A_1 &= {}^L \begin{bmatrix} 1 & 0 & 0 & 0 & 0 & 0 & -z & 0 & 0 \end{bmatrix} \\ {}^L A_2 &= {}^L \begin{bmatrix} 0 & 0 & 0 & 1 & 0 & 0 & 0 & -z & 0 \end{bmatrix} \\ {}^L A_3 &= {}^L \begin{bmatrix} 0 & 1 & 1 & 0 & 0 & 0 & 0 & 0 & -2z \end{bmatrix}\end{aligned}\quad (3.27)$$

$[H]_i$ 's are  $9 \times 9$  symmetrical matrices where all the coefficients of the matrices are zero except for  $H_1(5,5) = H_2(6,6) = H_3(5,6) = H_3(6,5) = 1$ .  
 $\{G\}$  is a vector representing displacement gradients

$$\{G\}^T = {}^L \begin{bmatrix} \frac{\partial u}{\partial x}, \frac{\partial u}{\partial y}, \frac{\partial v}{\partial x}, \frac{\partial v}{\partial y}, \frac{\partial w}{\partial x}, \frac{\partial w}{\partial y}, \frac{\partial^2 w}{\partial x^2}, \frac{\partial^2 w}{\partial y^2}, \frac{\partial^2 w}{\partial x \partial y} \end{bmatrix}\quad (3.28)$$

Substitute Eq. 3.20 into Eq. 3.28 and, after mathematical manipulations, it can be written as

$$\{G\} = [D] \{q\} \quad (3.29)$$

[D] is shown explicitly in Appendix A-3. Substituting Eq. 3.29 into Eq. 3.26, and denoting

$$L_{A,i}^L = L_{A,i} [D] \quad (3.30)$$

$$L_{A,i}^{NL} = L_{G,i} [H]_i [D] \quad (3.31)$$

Eq. 3.26, after combining all three cases of  $i = 1, 2, 3$ , becomes

$$\{\epsilon\} = ([B^L] + \frac{1}{2} [B^{NL}]) \{q\} \quad (3.32)$$

If we take the variation of Eq. 3.26 with respect to displacements

$$\delta \epsilon_i = L_{A,i} \delta \{G\} + \frac{1}{2} \delta L_{G,i} [H]_i \{G\} + \frac{1}{2} L_{G,i} [H]_i \delta \{G\} \quad (3.33)$$

Note that the second and the third terms on the right hand side are equal and can be combined:

$$\delta \epsilon_i = L_{A,i} \delta \{G\} + L_{G,i} [H]_i \delta \{G\} \quad (3.34)$$

Substituting Eq. 3.29 into Eq. 3.34

$$\delta \epsilon_i = L_{A,i} [D] \delta \{q\} + L_{G,i} [H]_i [D] \delta \{q\} \quad (3.35)$$

combining all three cases of  $i = 1, 2, 3$ , we obtain:

$$\delta \{\epsilon\} = ([B^L] + [B^{NL}]) \delta \{q\} \quad (3.36)$$



### III.4.2 Incremental Strain-Displacement Relations

When strain-displacement relations are expressed in incremental form, a procedure similar to that above can be employed. Applying Eq. 3.14 to thin plate and adding flexural strain terms, we may write incremental nonlinear strains in the Lagrangian frame explicitly as

$$\{\Delta e\} = \begin{Bmatrix} \Delta e_x \\ \Delta e_y \\ \Delta e_{xy} \end{Bmatrix} = \begin{Bmatrix} \frac{\partial(\Delta u)}{\partial x} + \frac{\partial w}{\partial x} \frac{\partial(\Delta w)}{\partial x} + \frac{1}{2} \left[ \frac{\partial(\Delta w)}{\partial x} \right]^2 - z \frac{\partial^2(\Delta w)}{\partial x^2} \\ \frac{\partial(\Delta v)}{\partial y} + \frac{\partial w}{\partial y} \frac{\partial(\Delta w)}{\partial y} + \frac{1}{2} \left[ \frac{\partial(\Delta w)}{\partial y} \right]^2 - z \frac{\partial^2(\Delta w)}{\partial y^2} \\ \frac{\partial(\Delta v)}{\partial x} + \frac{\partial(\Delta u)}{\partial y} + \frac{\partial w}{\partial x} \frac{\partial(\Delta w)}{\partial y} + \frac{\partial w}{\partial y} \frac{\partial(\Delta w)}{\partial x} + \left[ \frac{\partial(\Delta w)}{\partial x} \frac{\partial(\Delta w)}{\partial y} \right] - 2z \frac{\partial^2(\Delta w)}{\partial x \partial y} \end{Bmatrix} \quad (3.37)$$

Note that Eq. 3.29 is now written in incremental form as:

$$\{\Delta G\} = [D]\{\Delta q\} \quad (3.38)$$

where the components of  $\{\Delta G\}^T$  are incremental displacement gradients,  $\frac{\partial(\Delta u)}{\partial x}$ , etc.. Each component of the incremental strains in Eq. 3.37 is decomposed into linear and nonlinear parts and is expressed as

$$\begin{aligned} \Delta e_i &= \Delta \epsilon_i + \Delta \theta_i \\ &= (\mathcal{L}A]_i \{\Delta G\} + \mathcal{L}G]_i [H]_i \{\Delta G\}) + \left( \frac{1}{2} \mathcal{L}AG]_i [H]_i \{\Delta G\} \right) \\ &= (\mathcal{L}A]_i [D] + \mathcal{L}G]_i [H]_i [D]) \{\Delta q\} + \left( \frac{1}{2} \mathcal{L}AG]_i [H]_i [D] \right) \{\Delta q\} \\ \text{or } \{\Delta e\} &= ([B^L] + [B^{NL}]) \{\Delta q\} + \frac{1}{2} [\Delta B^{NL}] \{\Delta q\} \end{aligned} \quad (3.39)$$

Here we define  $\Delta e_i$  ( $i = 1, 2, 3$ ) for  $\Delta e_x$ ,  $\Delta e_y$ , and  $\Delta e_{xy}$  respectively with similar definitions for  $\Delta \epsilon_i$  and  $\Delta \theta_i$ . We also define

$$\mathcal{L}AB^{NL}]_i = \mathcal{L}AG]_i [H]_i [D] \quad (3.40)$$

Taking the variation of Eq. 3.39 with respect to the incremental displacements, results in:

$$\begin{aligned}\delta\{\Delta\epsilon\} &= \delta\{\Delta\epsilon\} + \delta\{\Delta\theta\} \\ &= ([B^L] + [B^{NL}]) \delta\{\Delta q\} + [\Delta B^{NL}] \delta\{\Delta q\}\end{aligned}\quad (3.41)$$

Dropping higher order terms in Eqs. 3.39 and 3.41, we obtain the linearized incremental strains

$$\{\Delta\epsilon\} = ([B^L] + [B^{NL}]) \{\Delta q\} \quad (3.41a)$$

$$\delta\{\Delta\epsilon\} = ([B^L] + [B^{NL}]) \delta\{\Delta q\} \quad (3.41b)$$

### III.5 Incremental Theory of Plasticity

There are two major plasticity theories, namely, the total, or deformation theory<sup>235</sup> and the incremental, or flow theory<sup>236,237</sup>. The deformation theory assumes that a unique relation between total stresses and total strains exists. The total strain components are functions of the current state of stress and are independent of the loading path. This is in contradiction with the experimentally determined properties of materials, and hence its use is limited<sup>234</sup>. On the other hand, in the flow theory only incremental stresses and strains are related. The incremental plastic strain components at any instant of loading are assumed to be proportional to the corresponding instantaneous deviatoric stresses. Plastic deformations are traced by integrating the plastic strain increments over the previous loading history. Incremental and

deformation theories coincide in the case of proportional loading in which the stress vector remains fixed in direction. In some engineering problems where the loading path is not far from proportional loading, the deformation theory can be employed<sup>252</sup> provided that, when unloading occurs, the problem is separated into two parts: the loading part and the unloading part, which are governed by different laws.<sup>85,234</sup> However, the incremental theory is widely accepted and is adopted in this study due to its mathematical and physical consistency.

The plastic behaviour of a material in a multiaxial stress state can be described by specifying the following three parts which make up the content of the incremental theory of plasticity<sup>245</sup>.

1. a yield criterion which defines the elastic limit of the material in a multi-stress state
2. a hardening rule which specifies the changes in shape and orientation of the yield surface for subsequent yield from a plastic state.
3. a flow rule which provides the constitutive relations between incremental plastic strains and current state of stress

The basis of these three parts are discussed in the following section.

Details of the derivation are available in several well known plasticity books<sup>78-81,85,234,240,241</sup> and will not be repeated here.

### III.5.1 Yield Criterion

A yield condition can generally be described in the form

$$f(\sigma_{ij}, k) = 0 \quad (3.42)$$

where  $\sigma_{ij}$  are stress components and  $k$  are parameters such as plastic strains or hardening parameters. In this study it is assumed that the plastic behaviour of a material is independent of time and temperature. Eq. 3.42 can be expressed in an alternate form:

$$f(\sigma_{ij}) = c \quad (3.43)$$

where  $c$  represents some yielding parameter which is a constant for the case of initial yielding and is a function of the complete previous stress and strain history of the material and its hardening properties for the case of subsequent yielding from a plastic state. If the material is elastic-perfectly plastic (non-hardening),  $c$  remains a constant.

The function  $f$  of Eq. 3.42 is termed a yield function in the case of initial yielding and is referred to as a subsequent yield function or loading function in the case of subsequent yielding. This function represents a hypersurface to bound all the accessible states which can be achieved in an actual material element by some program of stressing<sup>81</sup>. By temporarily fixing  $k$  as a constant at an instantaneous time, the hypersurface can be projected onto the stress space and is called the yield surface. The yield surface, similar to the hypersurface, bounds the elastic region in the stress space for a particular stress-strain history ( $k$ ). Yield surfaces generated by changes in  $k$  during a stress program are referred to as the subsequent yield surfaces or loading surfaces.

Among many proposed yield criteria, the Tresca criterion<sup>238</sup> and the Von Mises criterion<sup>239</sup> are the two most commonly used for metallic materials. The Tresca criterion assumes that yielding will occur at a point when the maximum shear stress reaches the value of the maximum shear stress in a simple tension state (i.e. half the yield stress obtained from a uniaxial tensile test). When reduced to the two dimensional plane stress case, the yield surface postulated by Tresca is seen to be a six-sided polygon. The Tresca yield criterion is less widely used than the Von Mises criterion because of a few drawbacks. Firstly, experiments have shown that test points generally fall closer to the Von Mises yield condition than to Tresca's. Secondly, the Tresca criterion is expressed in terms of principal stresses and hence the maximum and minimum principal stresses have to be known in advance. The continuous calculation and checking of the relative sizes of the principal stresses is necessary and is tedious. Thirdly, consideration of the associated flow rules indicates that the discontinuities at corners of the Tresca yield surface are difficult to handle and can be avoided by the Von Mises criterion since the slope of the yield surface postulated by Von Mises is always continuous. It can be seen that by reducing to the two dimensional plane stress case, the Von Mises yield surface becomes an ellipse (See Fig. 4). In the light of these advantages, the Von Mises criterion and its associated flow rule are employed in this study.

The Von Mises yield criterion assumes that yielding begins when the distortion energy<sup>242</sup> equals the distortion energy at yield in simple

tension. Since the internal energy due to distortion can be expressed in terms of the octahedral shear stress or the second invariant of the deviatoric stress tensor ( $J_2$ ),<sup>243</sup> two alternate ways of stating the criterion are respectively: (1) Yielding begins when the octahedral shear stress exceeds a certain limit (i.e. the octahedral shear stress in simple tension). The octahedral plane is referred to the principal stress directions. And (2) Yielding begins when  $J_2$  reaches a critical value (i.e. the value of  $J_2$  in simple tension). Of the three forms of expression, the one using  $J_2$  is most commonly used. Introducing the critical value of  $J_2$  in a uniaxial tensile test, which is equal to  $\frac{1}{3} \sigma_0^2$ , the Von Mises yield criterion is written as

$$J_2 = \frac{1}{3} \sigma_0^2 \quad (3.44)$$

where  $\sigma_0$  is the initial yield stress in a uniaxial tensile test, and the second deviatoric stress invariant is defined by

$$J_2 = \frac{1}{2} \sigma'_{ij} \sigma'_{ij} \quad \text{or} \quad J_2 = \frac{1}{6} [(\sigma_x - \sigma_y)^2 + (\sigma_y - \sigma_z)^2 + (\sigma_z - \sigma_x)^2 + 6(\tau_{xy}^2 + \tau_{yz}^2 + \tau_{zx}^2)] \quad (3.45)$$

in which the deviatoric stresses are defined by

$$\sigma'_{ij} = \sigma_{ij} - \frac{1}{3} \sigma_{kk} \delta_{ij} \quad (3.46)$$

where  $\delta_{ij}$  denotes the Kronecker delta.

Introducing another term which is called the equivalent stress and is defined by

$$\sigma_e = \sqrt{3 J_2} \quad (3.47)$$

Eq. 3.44 can be expressed as

$$\sigma_e = \sigma_0 \quad (3.48)$$

Eq. 3.48 is a special form of Eq. 3.42 or 3.43.

For a plate which is a two dimensional case of plane stress, reduction of  $\sigma_e$  leads from Eq. 3.48 to an explicit form as:

$$(\sigma_x^2 - \sigma_x \sigma_y + \sigma_y^2 + 3 \tau_{xy}^2)^{1/2} = \sigma_0 \quad (3.49)$$

### III.5.2: Hardening Rule

When the stress state of the material lies on the yield surface (i.e. Eq. 3.42 or 3.43 is satisfied), the departure from the plastic state due to a further load increment may result in three different loading conditions for strain hardening material

Loading

$$df = \frac{\partial f}{\partial \sigma_{ij}} d\sigma_{ij} > 0$$

Neutral loading

$$df = \frac{\partial f}{\partial \sigma_{ij}} d\sigma_{ij} = 0 \quad (3.50)$$

Unloading

$$df = \frac{\partial f}{\partial \sigma_{ij}} d\sigma_{ij} < 0$$

The first case of  $df > 0$  means the stress state is moving out from the yield surface and plastic flow is occurring. The second case of  $df=0$  indicates the stress state is moving on the yield surface and represents perfectly plastic

behaviour. The third case of  $df < 0$  means the stress state is moving into the elastic region from the yield surface and is entirely an elastic behaviour.

In the case of a perfectly plastic material, the case of  $df > 0$  does not exist. Plastic flow occurs during the case of  $df = 0$ . Elastic unloading of  $df < 0$  is the same as for hardening material.

When loading occurs, a hardening rule is required to describe the manner in which the yield surface is modified as a result of plastic deformation. As a material is physically unable to maintain a stress state outside its yield surface, this modification is necessary to keep the stress state on the subsequent yield surface and to have material capable of maintaining a higher stress state due to work hardening. Many hardening rules have been proposed such as the isotropic hardening rule<sup>234</sup>, the Kinematic hardening rule<sup>244,245</sup>, the mechanical sublayer model<sup>246,247</sup> and the Mroz theory<sup>248</sup>. A discussion and comparison of these models is available elsewhere<sup>173,175</sup>. Of these various models, the isotropic hardening rule is most widely used and is employed in this study due to its simplicity and economy in computation. This model assumes plastic deformation to be an isotropic process. The subsequent yield surface is uniformly expanded from its initial yield surface and hence it retains the same shape as originally (Fig. 4). The disadvantage of using the isotropic model is the lack of consideration of the Bauschinger effect which is taken into account in other hardening rules such as the kinematic model. However, since cyclic loading is of no interest in the present study, this is not considered a serious drawback.



We now replace the  $\sigma_0$  of Eq. 3.48 by  $\bar{\sigma}$  to represent the subsequent yield stress on the stress-strain curve for uniaxial tensile and to account for previous plastic deformation. There are two hypotheses<sup>85</sup> often used to measure the amount of hardening.

(a) Work-hardening hypothesis

In this hypothesis, plastic work (shaded area in Fig. 5) is used for measurement, so  $\bar{\sigma}$  is a function of the plastic work done on the material

$$w^p = \int \sigma_{ij} d\epsilon_{ij}^p$$

or

$$w^p = \int \sigma_e d\epsilon_e^p \quad (3.51)$$

where the equivalent plastic strain increment is defined by

$$d\epsilon_e^p = \sqrt{\frac{2}{3}} (d\epsilon_{ij}^p d\epsilon_{ij}^p)^{1/2} \quad (3.52)$$

the loading function becomes

$$\sigma_e = F(w^p) \quad (3.53)$$

(b) Strain-hardening hypothesis

In this hypothesis, the equivalent plastic strain is used for measurement, so  $\bar{\sigma}$  is a function of the recorded equivalent plastic strain and is defined by:

$$\epsilon_e^p = \int d\epsilon_e^p \quad (3.54)$$

the loading function becomes

$$\sigma_e = H(\epsilon_e^p) \quad (3.55)$$

For the case of the Von Mises criterion assuming isotropic hardening, the two hypotheses are equivalent<sup>249</sup>. In general, however, they need not be equivalent because of anisotropy and the Bauschinger effect. Eqs. 3.53 and 3.55 are special forms of Eq. 3.43 and can be obtained from the experimental results of a uniaxial stress-strain test.

### III.5.3 Formulas for Uniaxial Stress-Strain Relation

In this study both perfectly plastic and hardening materials are considered. Two cases of hardening material are treated: linear hardening and nonlinear hardening. These two uniaxial stress-strain curves are shown in Fig. 5.

For the linear hardening material, the formula to express the stress-strain equation is unique. The strain which is composed of elastic and plastic parts can be written as

$$\epsilon = \frac{\sigma}{E} + \frac{1-m}{mE} (\sigma - \sigma_0) \quad (3.56)$$

where  $m = E_T/E$ ,  $E_T$  is the tangent modulus and  $E$  is Young's modulus.

For the nonlinear hardening material, numerous stress-strain formulas have been proposed<sup>85</sup>. Among them, the Ramberg-Osgood form<sup>250</sup> is most widely used in which the total strain is expressed as

$$\epsilon = \frac{\sigma}{E} + \frac{3\sigma}{7E} \left( \frac{\sigma}{\sigma_0} \right)^{n-1} \quad (3.57)$$

where  $n$  is an exponent and  $\sigma_{0.7}$  is the secant yield stress at  $0.7E$  (see Fig. 5). These two values can be obtained from experimental data by nonlinear curve fitting or by any other means.

An alternative form (e.g. see Ref. 118) which is appealing can be written as:

$$\epsilon = \frac{\sigma}{E} + 0.002 \left( \frac{\sigma - \sigma_0}{\sigma_2 - \sigma_0} \right)^n \quad (3.58)$$

where  $\sigma_2$  is the specified 0.2 per cent proof stress. There are three requirements for Eq. 3.58: (a) It should be tangent to the elastic line at  $\sigma = \sigma_0$  (b) The plastic strain should equal 0.002 at  $\sigma = \sigma_2$  and (c) The plastic strain should equal  $\epsilon_u^p$  at  $\sigma = \sigma_u$  ( $u$  denotes ultimate). The first two requirements are satisfied automatically.  $\sigma_0$  and  $n$  in Eq. 3.58 are adjusted so as to satisfy the third requirement.  $n$  is selected empirically thus

$$n = 10 \frac{\sigma_2}{\sigma_u} - 1.5 \quad (3.59)$$

$\sigma_0$  is then given by

$$\sigma_0 = \sigma_2 - \frac{\sigma_u - \sigma_2}{(500 \epsilon_u^p)^{1/n} - 1} \quad (3.60)$$

#### III.5.4 Flow Rule

Drucker's Postulate<sup>251</sup> of stability leads to the following two consequences:

1. The initial yield surface and all subsequent loading surfaces must be convex (convexity).

2. The plastic strain increment vector  $d\epsilon_{ij}^p$  must be normal to the yield or loading surface (normality)  
i.e.

$$d\epsilon_{ij}^p = d\lambda \frac{\partial f}{\partial \sigma_{ij}} \quad (3.61)$$

where  $d\lambda$  is the non-negative constant which varies throughout the loading history. The loading function,  $f$ , plays the same role as a plastic potential.

It is assumed that the relation between infinitesimals of plastic strain and stress is linear. This linearity can be established by showing  $d\lambda$  to be independent of all components of  $d\sigma_{ij}$  except the component in the direction of the normal  $\frac{\partial f}{\partial \sigma_{ij}}$ , then<sup>240</sup>

$$d\lambda = g \frac{\partial f}{\partial \sigma_{ij}} d\sigma_{ij} \quad (3.62)$$

where  $g$  is a positive scalar depending on the stress, strain, and the history of loading but is independent of  $d\sigma_{ij}$ . Substituting Eq. 3.62 into Eq. 3.61, then into Eq. 3.52, we obtain, with the aid of Eq. 3.62,

$$d\lambda = \sqrt{\frac{3}{2}} \frac{d\epsilon_e^p}{\left[ \left( \frac{\partial f}{\partial \sigma_{ij}} \right) \left( \frac{\partial f}{\partial \sigma_{ij}} \right) \right]^{1/2}} \quad (3.63)$$

Substituting Eq. 3.63 into Eq. 3.61, the general plastic stress-strain relation becomes<sup>85</sup>

$$d\epsilon_{ij}^p = \sqrt{\frac{3}{2}} \frac{\left( \frac{\partial f}{\partial \sigma_{ij}} \right) d\epsilon_e^p}{\left[ \left( \frac{\partial f}{\partial \sigma_{ij}} \right) \left( \frac{\partial f}{\partial \sigma_{ij}} \right) \right]^{1/2}}$$

$$\text{or } d\epsilon_{ij}^p = \sqrt{\frac{3}{2}} \frac{\left(\frac{\partial f}{\partial \sigma_{ij}}\right)}{H' \left[ \left(\frac{\partial f}{\partial \sigma_{ij}}\right) \left(\frac{\partial f}{\partial \sigma_{ij}}\right) \right]^{1/2}} d\sigma_e \quad (3.64)$$

where  $H' = d\sigma_e/d\epsilon_e^p$  is the slope of the uniaxial stress-plastic strain curve at the current value of  $\sigma_e$ . When substituting Von Mises yield function into Eq. 3.64, the associated flow rule of the Prandtl-Reuss relation is obtained.

$$\begin{aligned} d\epsilon_{ij}^p &= \frac{3}{2} \frac{d\sigma_e}{H' \sigma_e} \sigma_{ij}' \\ \text{or } &= \frac{3}{2} \frac{d\epsilon_e^p}{\sigma_e} \sigma_{ij}' \end{aligned} \quad (3.65)$$

Eq. 3.65 states that the plastic strain increment at any instant of loading is proportional to the instantaneous stress deviation. Eq. 3.65 can be written in matrix notation

$$\{d\epsilon^p\} = \left\{ \frac{\partial f}{\partial \sigma} \right\} d\epsilon_e^p \quad (3.66)$$

where,  $\frac{\partial f}{\partial \sigma_{ij}} = \frac{3}{2} \frac{\sigma_{ij}'}{\sigma_e}$  for the Von Mises yield criterion.

### III.5.5 Incremental Total Stress-Strain Relation

The theory of plasticity assumes that the incremental total strain can be decomposed into elastic and plastic components.

$$\{d\epsilon\} = \{d\epsilon^e\} + \{d\epsilon^p\} \quad (3.67)$$

Since only the elastic part of the strain is associated with the change of stress,

$$\{\mathrm{d}\sigma\} = [E_e] \{\mathrm{d}\epsilon^e\} = [E_e] (\{\mathrm{d}\epsilon\} - \{\mathrm{d}\epsilon^p\}) \quad (3.68)$$

where  $[E_e]$  is the conventional elasticity modulus matrix. Premultiply Eq. 3.68 by  $\frac{\partial f}{\partial \sigma}$  and get:

$$\frac{\partial f}{\partial \sigma} \{\mathrm{d}\sigma\} = \frac{\partial f}{\partial \sigma} [E_e] (\{\mathrm{d}\epsilon\} - \{\mathrm{d}\epsilon^p\}) \quad (3.69)$$

The left hand side of Eq. 3.69 represents the change of the loading function and is equal to the differential of the equivalent uniaxial stress,  $\mathrm{d}\sigma_e$ , for the Von Mises yield criterion. Substituting  $\mathrm{d}\sigma_e = H' \mathrm{d}\epsilon_e^p$  into the left hand side and Eq. 3.66 into the right hand side, Eq. 3.69 becomes:

$$H' \mathrm{d}\epsilon_e^p = \frac{\partial f}{\partial \sigma} [E_e] (\{\mathrm{d}\epsilon\} - \{\frac{\partial f}{\partial \sigma}\} \mathrm{d}\epsilon_e^p) \quad (3.70)$$

or, rearranging terms:

$$\mathrm{d}\epsilon_e^p = \frac{\frac{\partial f}{\partial \sigma} [E_e]}{H' + \frac{\partial f}{\partial \sigma} [E_e] \{\frac{\partial f}{\partial \sigma}\}} \{\mathrm{d}\epsilon\} \quad (3.71)$$

The equivalent plastic strain increment of Eq. 3.71 is evaluated at the stress and plastic strain level at the end of the previous load step.

Substituting Eq. 3.71 into Eq. 3.66 and then into Eq. 3.68, the final incremental stress-strain relation in the plastic region is obtained<sup>211</sup>

$$\begin{aligned} \{\mathrm{d}\sigma\} &= \left( [E_e] - \frac{[E_e] \{\frac{\partial f}{\partial \sigma}\} \frac{\partial f}{\partial \sigma} [E_e]}{H' + \frac{\partial f}{\partial \sigma} [E_e] \{\frac{\partial f}{\partial \sigma}\}} \right) \{\mathrm{d}\epsilon\} \\ &= [E_{ep}] \{\mathrm{d}\epsilon\} \end{aligned} \quad (3.72)$$

When the material is elastic, the second term inside the parentheses vanishes. Eq. 3.72 is then reduced to the generalized Hooke's law.

Eq. 3.72 has also been developed in an alternative form by Pifko et al<sup>253</sup> and in an explicit form by Yamada et al<sup>254</sup>. However, the explicit form does not provide any advantage for computation.

### III.6 Equilibrium Equations

#### III.6.1 Virtual Work Approach

We now write the principle of virtual work (Eq. 3.6) in matrix notation and with the implication that the finite element method is employed.

$$\int_V \delta\{\epsilon\}^T \{\sigma\} dv = \delta\{q\}^T \{p\} \quad (3.73)$$

Substituting Eq. 3.36 into the above equation, we obtain:

$$\int_V ([B^L] + [B^{NL}])^T \{\sigma\} dv = \{p\}$$

or

$$\{f\} = \{p\} - \int_V ([B^L] + [B^{NL}])^T \{\sigma\} dv \quad (3.74)$$

Eq. 3.74 is the basic equilibrium equation and is convenient to use for the equilibrium check when the stresses and displacements become known values.

When the stresses can be uniquely expressed in terms of strains, Eq. 3.74 becomes:

$$\int_V ([B^L] + [B^{NL}])^T [E] \{\epsilon\} dv = \{p\} \quad (3.75)$$

For simplicity,  $[E]$  is substituted for  $[E_e]$  in Eq. 3.75 with the understanding that the material is elastic. Substituting Eq. 3.32 into the above equation, results in:

$$\int_A t([B^L] + [B^{NL}])^T [E] ([B^L] + \frac{1}{2} [B^{NL}]) dA \{q\} = \{p\} \quad (3.76)$$

Regrouping,

$$\begin{aligned} & \left( \int_A t [B^L]^T [E] [B^L] dA + \int_A t ([B^{NL}]^T [E] [B^L] + \frac{1}{2} [B^L]^T [E] [B^{NL}] \right. \\ & \quad \left. + \frac{1}{2} [B^{NL}]^T [E] [B^{NL}]) dA \right) \{q\} = \{p\} \end{aligned}$$

$$\therefore ([K_0] + [K^*]) \{q\} = \{p\} \quad (3.77)$$

### III.6.2 Potential Energy Approach

An alternate formulation based on the principle of stationary potential energy is to first express the potential energy by

$$\begin{aligned} \phi &= \int_V \frac{1}{2} \{\epsilon\}^T \{\sigma\} dv - \{q\}^T \{p\} \\ &= \int_V \frac{1}{2} \{\epsilon\}^T [E] \{\epsilon\} dv - \{q\}^T \{p\} \end{aligned} \quad (3.78)$$

Taking the variation of potential energy with respect to displacements and setting equal to zero:

$$\delta\phi = \int_V \delta\{\epsilon\}^T [E] \{\epsilon\} dv - \delta\{q\}^T \{p\} = 0 \quad (3.79)$$

After substituting Eq. 3.32 and 3.36 into Eq. 3.79, Eq. 3.76 is reached.

The rest of the formulation is identical to that shown above by using the principle of virtual work and will not be repeated here.



### III.7 Element Tangent Stiffness Matrix

The nonlinear equilibrium equations derived in section III.6 are often solved using an iterative process. Among the available approaches, the Newton-Raphson method is the most widely used. We consider the principle of variation as applied to the element to formulate the element tangent stiffness matrix.

Let the force unbalance  $\{f\}_n$  be that corresponding to the  $n^{\text{th}}$  iteration for the displacement  $\{q\}_n$ . Expanding  $\{f\}_{n+1}$  in a first order Taylor's series about  $\{q\} = \{q\}_n$  for the improved displacements  $\{q\}_{n+1}$ , we seek for

$$\{f\}_{n+1} = \{f\}_n + \delta\{f\}_n = \{f\}_n + \frac{\partial}{\partial q_i} \{f\}_n \delta q_i = 0 \quad (3.80)$$

Substituting Eq. 3.74 into the above equation, results in:

$$\int_V (\delta([B^L] + [B^{NL}])^T \{\sigma\} + ([B^L] + [B^{NL}])^T [E] \delta \{\epsilon\}) dv = \{f\}_n \quad (3.81)$$

Noting  $[B^L]$  is independent of the displacement and using Eqs. 3.29, 3.31 and 3.36, Eq. 3.81 becomes

$$\int_V ([D]^T [\bar{K}_\sigma] [D] + ([B^L] + [B^{NL}])^T [E] ([B^L] + [B^{NL}])) dv \delta\{q\} = \{f\}_n \quad (3.82)$$

where  $[\bar{K}_\sigma] = \sum_{i=1}^3 [H]_i \sigma_i$ ,  $\sigma_i$  ( $i=1,2,3$ ) denotes  $\sigma_x$ ,  $\sigma_y$ ,  $\tau_{xy}$  respectively.

Now multiply out the second term of Eq. 3.82

$$\int_V ([D]^T [\bar{K}_\sigma] [D] + [B^L]^T [E] [B^L] + ([B^{NL}]^T [E] [B^L] + [B^L]^T [E] [B^{NL}] + [B^{NL}]^T [E] [B^{NL}])) dv \delta\{q\} = \{f\}_n \quad (3.83)$$

Using Eqs. 3.30 and 3.31 and with a large amount of manipulation, Eq. 3.83 can be finally written as:

$$\int_V ([D]^T [\bar{K}_\sigma] [D] + [D]^T [\bar{K}_L] [D] + [D]^T [\bar{K}_N] [D]) dv \delta\{q\} = \{f\}_n \quad (3.84)$$

Note that  $[D]$  is independent of  $z$ , the normal axis of the element, so let

$$\begin{aligned} [\hat{K}_\sigma] &= \int_t [\bar{K}_\sigma] dz \\ [\hat{K}_L] &= \int_t [\bar{K}_L] dz \\ [\hat{K}_N] &= \int_t [\bar{K}_N] dz \end{aligned} \quad (3.85)$$

Eq. 3.84 now becomes

$$\int_A ([D]^T ([\hat{K}_\sigma] + [\hat{K}_L] + [\hat{K}_N]) [D]) dA \cdot \delta\{q\} = \{f\}_n \quad (3.86)$$

or, in short,

$$[K_T] \delta\{q\} = \{f\}_n \quad (3.87)$$

where  $[K_T]$  is the tangent stiffness matrix which is used to define the corrections  $\delta\{q\}$  required to obtain the improved solution by the recursive formula:

$$\{q\}_{n+1} = \{q\}_n + \delta\{q\} \quad (3.88)$$

### III.8 Incremental Equilibrium Equations

There are several ways of putting the nonlinear equilibrium equations into a linear incremental form. Methods have been proposed by many researchers including Mallett and Marcal<sup>181</sup>, Gallagher<sup>210</sup>, and particularly Stricklin et al<sup>176,183,198-202</sup>. The most common methods using a first order Taylor's series expansion, an initial value problem formulation plus a simple Euler difference application, and self-correcting solution procedures also linked with an Euler difference formula, have already been discussed in Chapter II. In this section, however, the incremental equilibrium equation will be formulated by a direct application of the incremental variational principle.

#### III.8.1 Virtual Work Approach

We now write Eq. 3.17 in matrix notation with some manipulations:

$$\int_V [\delta\{\Delta\epsilon\}^T \{\Delta\sigma\} + \delta\{\Delta G\}^T [\bar{K}_0] \{\Delta G\}] dv - \delta\{\Delta q\}^T \{\Delta p\} + (\int_V \delta\{\Delta\epsilon\}^T \{\sigma\} - \delta\{\Delta q\}^T \{p\}) = 0 \quad (3.89)$$

All terms have been defined previously. Substituting Eqs. 3.38, 3.41a, 3.41b and 3.72 into the above equation, results in:

$$\delta\{\Delta q\}^T (\int_V [([B^L] + [B^{NL}])^T [E] ([B^L] + [B^{NL}]) \{\Delta q\} + [D]^T [\bar{K}_0] [D] \{\Delta q\}] dv - \{\Delta p\} - [\{p\} - \int_V ([B^L] + [B^{NL}])^T \{\sigma\} dv]) = 0 \quad (3.90)$$

Again, for simplicity, we use  $[E]$  to represent  $[E_e]$  for the elastic case and to represent  $[E_{ep}]$  for the plastic case. The quantities within the

last brackets of Eq. 3.90 represent the unbalanced residual forces at the end of the previous increment (see Eq. 3.74). Eq. 3.90 is then simplified to:

$$\int_V ([D]^T [R_o] [D] + ([B^L] + [B^{NL}])^T [E] ([B^L] + [B^{NL}])) dv \{\Delta q\} = \{\Delta p\} + \{f\} \quad (3.91)$$

The integral within the square brackets of Eq. 3.91 is the incremental stiffness matrix. Comparing this matrix with the tangent stiffness matrix shown in Eq. 3.82 of section III.7, we find that the two are the same. Further work is referred to in the previous section and is omitted here. We simply conclude the formulation by writing the final form of the incremental equilibrium equation as:

$$[K_T] \{\Delta q\} = \{\Delta p\} + \alpha \{f\} \quad (3.92)$$

Note that a factor denoted by  $\alpha^*$  is added to Eq. 3.92 so that the magnitude of the force unbalance can be flexibly adjusted.  $\alpha$  is generally kept as unity. However, when the solution is numerically stable, a value greater than unity (say 1.3 or 1.4) can be used to increase the rate of convergence. On the other hand, if numerical instability is encountered, a value less than unity should be used.

---

\*  $z(\Delta\lambda)$  was used for  $\alpha$  in the previous discussion in Chapter II

### III.8.2 Potential Energy Approach

To formulate the incremental equilibrium equations using the minimization of potential energy of the structure is rather trivial. It is simply a pure mathematical exercise in formulation procedures. To reach the  $(n+1)^{th}$  loading state from a given  $n^{th}$  loading state of equilibrium, the incremental potential energy can be written as:

$$\begin{aligned}\Delta\phi &= \int_V \frac{1}{2} \{\Delta e\}^T \{\Delta \sigma\} dv + \int_V \{\Delta e\}^T \{\sigma\} dv - \{\Delta q\}^T \{p + \Delta p\} - \{q\}^T \{\Delta p\} \\ &= \int_V \frac{1}{2} \{\Delta e\}^T [E] \{\Delta e\} dv + \int_V \{\Delta e\}^T \{\sigma\} dv - \{\Delta q\}^T \{p + \Delta p\} - \{q\}^T \{\Delta p\}\end{aligned}\quad (3.93)$$

Taking the variation with respect to the incremental displacements and setting equal to zero, results in:

$$\begin{aligned}\delta\Delta\phi &= \int_V \left( \frac{1}{2} \delta\{\Delta e\}^T [E] \{\Delta e\} + \frac{1}{2} \{\Delta e\}^T [E] \delta\{\Delta e\} \right) dv \\ &\quad + \int_V \delta\{\Delta e\}^T \{\sigma\} dv - \delta\{\Delta q\}^T \{p\} - \delta\{\Delta q\}^T \{\Delta p\} = 0\end{aligned}\quad (3.94)$$

Substituting Eqs. 3.39 and 3.41 into the above equation and neglecting the higher order terms so generated within the parentheses of Eq. 3.94, we obtain:

$$\begin{aligned}\int_V \delta\{\Delta e\}^T [E] \{\Delta e\} dv + \int_V \delta\{\Delta e\}^T \{\sigma\} dv + \int_V \delta\{\Delta \sigma\}^T \{\tilde{\sigma}\} \\ - \delta\{\Delta q\}^T \{p\} - \delta\{\Delta q\}^T \{\Delta p\} = 0\end{aligned}\quad (3.95)$$

and, with the aid of Eq. 3.39 through 3.41b,

$$\delta\{q\}^T \left( \int_V \left( [B^L] + [B^{NL}] \right)^T [E] \left( [B^L] + [B^{NL}] \right) \{\Delta q\} + [D]^T [\bar{K}_0] [D] \{\Delta q\} \right) dv - \{\Delta p\} - \{ \{p\} - \int_V \left( [B^L] + [B^{NL}] \right)^T \{\sigma\} dv \} = 0 \quad (3.96)$$

Eq. 3.96 is identical to Eq. 3.90 and this formulation is therefore not carried any further.

### III.9 Comments on the Tangent Stiffness Matrix

The integration of matrices through the thickness of the element (Eq. 3.85) has been evaluated exactly in advance when the material is elastic. When the material is in the plastic region, three basic techniques have been proposed to incorporate the effects of the variation of stiffness through the thickness. Levine et al<sup>175</sup> gave a detailed discussion of the subject which is briefed as follows:

The first technique is termed the layered approach. The plate thickness is divided into several layers. Plastic strains and stresses are evaluated for each layer at a specified number of points along the surface of the element (i.e. at nodes or Gaussian points). The stiffness matrix is then obtained by numerically integrating the properties through the thickness at each representative point and then over the element surface. This approach does not add any additional degree of freedom to the system but requires plasticity calculations to be performed at each integration point (layer) through the thickness.

The second approach is to assume a variation (often a linear variation) of plastic strain through the thickness. In this case, at

most, only four points need be monitored for plastic strains, the top and bottom surfaces and two possible elasto-plastic boundary locations through the thickness. The determination of the location of the elasto-plastic boundaries is relatively simple because of the Kirchhoff assumption of a linear variation of total strains. Disadvantages of the method are that it is only approximate and for unloading and reversed loading the total plastic strain distribution is no longer nearly linear. Nevertheless, for monotonic loading with, at most, simple isolated instances of unloading, it is efficient.

The third possibility is through the use of a moment resultant/stress resultant interaction curve. The advantage of this method is that no monitoring of points through the thickness is required. On the other hand, it is only approximate in nature and requires moment curvature tests for each structure considered. This explains why the method has not been widely accepted and its reduction in computing costs compared to other methods needs further investigation. This method would appear to have its most useful application with hybrid elements where the moment and stress resultants are the actual degrees of freedom of the problem and are calculated directly.

This study employs the layered method as it provides some advantages. In this method, because the stresses are monitored at points, they may vary arbitrarily through the thickness. Conventional stress yield criteria may be used and reversed loading, unloading and cyclic loading present no special problems. Only standard tensile stress-strain data are required for the plasticity calculation.

Several numerical integration schemes have been used to integrate the tangent stiffness through the thickness. These include trapezoidal integration, Simpson's rule and Gaussian quadrature. Simpson's rule is preferred because it converges faster than the trapezoidal rule and includes as integration points the top and bottom plate surfaces where plasticity must be initiated first due to the Kirchhoff hypothesis. On the other hand, even though Gaussian quadrature has been used by some researchers, it is not used in this study. Gaussian quadrature requires the stress at interior points within the thickness to exceed the yield stress before any contribution is obtained. Hence, it is not able to detect early yielding at the upper or lower surface. Most importantly, the Gaussian quadrature formulas assume the existence of continuous higher order derivatives for the plastic strain distribution. Physically, it is known that this is not necessarily the case. This inconsistency in the mathematical model could prove important for a complex distribution of plastic strains, particularly through the thickness of the element<sup>176,197</sup>.

Other comments on the tangent stiffness matrix are that all matrices used to form the tangent stiffness (Eq. 3.86) have been explicitly formed (see Appendices A-3 through A-10). The  $[D]$  matrix is a constant matrix and only needs evaluation once at the initial load increment. It is then stored for use in the rest of the load increments. Hence, the only matrices which have to be reevaluated are the  $9 \times 9$  matrices of  $[\hat{K}_\sigma]$  and  $[\hat{K}_N]$  where the merits of symmetry and sparseness



are provided. The advantage of avoiding the multiplication of zero coefficients in the matrices has been taken into account during the development of the computer program. If the three parts which compose the tangent (incremental) stiffness matrix were evaluated separately, they are respectively (from left to right as shown in Eq. 3.86) initial stress matrix, conventional elastic small displacement matrix, and initial displacement matrix. For elastic large displacement analysis, the total stress can be expressed in terms of strain and then in terms of displacement gradients. Combining the initial stress matrix and the initial displacement matrix and rearranging the coefficients, the so called  $N_1$  and  $N_2$  matrices as explicitly given by Mallet and Marcal<sup>181</sup> can be formed.

### III.10 Assemblage of Elements

The variational principle has been applied to a subdomain of the structure for deriving the individual element stiffnesses in the previous sections. To obtain the stiffness relationship for the total structure, the principle is applied to the whole domain by integrating over the entire structure. This is done by assembling the elements together to form an idealized structure using the topological conditions. Mathematically it is achieved by transforming the equilibrium equations for the elements to a common coordinate system and summing the corresponding element stiffness terms. The final equilibrium equations for the entire structure are then solved using any of the available solution procedures.

### III.11 Choice of Numerical Solution Procedure

The solution procedures used in this study are the Newton-Raphson method (including Modified Newton-Raphson method) and the incremental method with unbalanced force correction. The Newton-Raphson method is mainly used in the elastic range of the loading history. Due to its fast convergence and hence large step size, the Newton-Raphson method has proved to be more economical in computing costs and it provides a more accurate solution. The method can be extended to the initial post-yielding stage when material nonlinearity is still not very severe. However, the rate of convergence begins to be retarded quickly while the step size has to be continuously reduced and the method becomes expensive. It finally reaches a point where the incremental method must be used for the rest of the loading increments. The correcting term of force unbalance is added to the incremental equilibrium equation to prevent the solution from drifting from the true load-displacement path. The three methods are demonstrated graphically for the case of a single degree of freedom in Fig. 6.

### III.12 Modified Cholesky Decomposition Method

In the finite element displacement method, regardless of which type of formulation and solution procedure is being used for the nonlinear analysis at each iteration or at each load step, equations of the following form must be solved:

$$[K] \{q\} = \{p\} \quad (3.97)$$

in which  $[K]$  is the symmetrical, positive-definite stiffness matrix, and  $\{q\}$  and  $\{p\}$  are as defined previously. Eq. 3.97 herein is assumed to be the final form after the introduction of the kinematic constraints into the stiffness matrix.

The two most popular ways of solving Eq. 3.97 directly are the Gauss elimination method and the Cholesky decomposition method. Compared to Gauss elimination, the Cholesky algorithm is less accurate, mainly due to its process errors in forming the square roots. Despite this deficiency, the Cholesky method does have important data storage advantages.

This study employs a modified Cholesky decomposition<sup>256,257</sup> method which avoids taking square roots and hence retains the good features of both Gauss elimination and Cholesky decomposition. The algorithm is to decompose the stiffness matrix as follows:

$$[K] = [L][D]^{-1} [L]^T \quad (3.98)$$

where  $[L]$  is a lower triangular matrix,  $[D]$  is a diagonal matrix with element  $D_{ii}$  equal to diagonal elements of  $L_{ii}$ , and  $[L]^T$  is the transpose of  $[L]$ . The stiffness matrix,  $[K]$ , is assured of being positive-definite by checking that the diagonal elements of  $[D]$  are greater than zero. It is seen that only the  $[L]$  matrix has to be evaluated using the formula

$$L_{ij} = K_{ij} - \sum_{n=1}^{i-1} \frac{L_{nj} L_{ni}}{L_{nn}} \quad (\text{where } i \leq j) \quad (3.99)$$

Substituting Eq. 3.98 into Eq. 3.97, results

$$[L] \{Y\} = \{P\} \quad (3.100)$$

where  $[D]^{-1}[L]^T \{q\} = \{Y\}$  (3.101)

Eq. 3.100 is first solved for  $\{Y\}$  using forward substitution.  $\{q\}$  is then obtained by solving Eq. 3.101 using backward substitution.

The above algorithm proceeds with one equation at a time and thus requires only one row of the matrix to be in the core of the computer. This reduces the required core size to a minimum but it significantly increases the I/O time and may not necessarily be more economical.

A common alternative technique is to partition the stiffness matrix into a tridiagonal form\*. Eqs. 3.97 and 3.98 can now be written as

$$[K] \{q\} = \begin{bmatrix} A_1 & B_1^T & & \\ B_1 & A_2 & B_2^T & \\ & B_2 & A_3 & B_3^T \\ & & B_3 & A_4 \end{bmatrix} \begin{Bmatrix} q_1 \\ q_2 \\ q_3 \\ q_4 \end{Bmatrix} = \begin{Bmatrix} p_1 \\ p_2 \\ p_3 \\ p_4 \end{Bmatrix} \quad (3.102)$$

$$\begin{bmatrix} A_1 & B_1^T & & \\ B_1 & A_2 & B_2^T & \\ & B_2 & A_3 & B_3^T \\ & & B_3 & A_4 \end{bmatrix} = \begin{bmatrix} L_1 & & & \\ M_1 & L_2 & & \\ & M_2 & L_3 & \\ & & M_3 & L_4 \end{bmatrix} \begin{bmatrix} D_1^{-1} & & & \\ & D_2^{-1} & & \\ & & D_3^{-1} & \\ & & & D_4^{-1} \end{bmatrix} \begin{bmatrix} L_1^T & M_1^T & & \\ & L_2^T & M_2^T & \\ & & L_3^T & M_3^T \\ & & & L_4^T \end{bmatrix} \quad (3.103)$$

\* The case using the conventional Cholesky algorithm is described in Ref. 253.

For clarity, all the blocked submatrices will be represented by a capital letter without brackets. Now, at any time, it has one diagonal and one off-diagonal block retained in the core. The space can be used for other purposes, when equation solving is not executing, as a dynamic storage area.

The procedure to obtain submatrices  $L_i$  and  $M_i$  is as follows:

$$\begin{array}{ll}
 A_1 = L_1 D_1^{-1} L_1^T & \rightarrow L_1 D_1^{-1} L_1^T = A_1 \\
 B_1 = M_1 D_1^{-1} L_1^T & \rightarrow M_1 = B_1 (L_1^T)^{-1} D_1 \\
 A_2 = M_1 D_1^{-1} M_1^T + L_2 D_2^{-1} L_2^T & \rightarrow L_2 D_2^{-1} L_2^T = A_2 - M_1 D_1^{-1} M_1^T \\
 B_2 = M_2 D_2^{-1} L_2^T & \rightarrow M_2 = B_2 (L_2^T)^{-1} D_2 \\
 A_3 = M_2 D_2^{-1} M_2^T + L_3 D_3^{-1} L_3^T & \rightarrow L_3 D_3^{-1} L_3^T = A_3 - M_2 D_2^{-1} M_2^T \\
 B_3 = M_3 D_3^{-1} L_3^T & \rightarrow M_3 = B_3 (L_3^T)^{-1} D_3 \\
 & \text{etc.}
 \end{array} \quad (3.104)$$

These equations are used to determine  $L_1, M_1, L_2, M_2$  etc. to obtain each diagonal block by the modified Cholesky decomposition algorithm and each off-diagonal block by solving the corresponding equations.

The "forward" solution for Eq. 3.100 can be expressed as

$$\begin{bmatrix} L_1 & & & \\ M_1 & L_2 & & \\ & M_2 & L_3 & \\ & & M_3 & L_4 \end{bmatrix} \begin{Bmatrix} Y_1 \\ Y_2 \\ Y_3 \\ Y_4 \end{Bmatrix} = \begin{Bmatrix} P_1 \\ P_2 \\ P_3 \\ P_4 \end{Bmatrix} \quad (3.105)$$

which leads to

$$\begin{array}{ll}
 L_1 Y_1 & = P_1 \\
 L_2 Y_2 & = P_2 - M_1 Y_1 \\
 L_3 Y_3 & = P_3 - M_2 Y_2 \\
 & \text{etc.}
 \end{array} \quad (3.106)$$

These equations are solved for  $Y_1, Y_2, Y_3$ , etc..

The "backward" solution for Eq. 3.101 is now expressed as:

$$\begin{bmatrix} D_1^{-1} & & & \\ & D_2^{-1} & & \\ & & D_3^{-1} & \\ & & & D_4^{-1} \end{bmatrix} \begin{bmatrix} L_1^T & M_1^T & & \\ & L_2^T & M_2^T & \\ & & L_3^T & M_3^T \\ & & & L_4^T \end{bmatrix} \begin{pmatrix} q_1 \\ q_2 \\ q_3 \\ q_4 \end{pmatrix} = \begin{pmatrix} Y_1 \\ Y_2 \\ Y_3 \\ Y_4 \end{pmatrix} \quad (3.107)$$

$$\begin{bmatrix} D_1^{-1} L_1^T & D_1^{-1} M_1^T & & \\ & D_2^{-1} L_2^T & D_2^{-1} M_2^T & \\ & & D_3^{-1} L_3^T & D_3^{-1} M_3^T \\ & & & D_4^{-1} L_4^T \end{bmatrix} \begin{pmatrix} q_1 \\ q_2 \\ q_3 \\ q_4 \end{pmatrix} = \begin{pmatrix} Y_1 \\ Y_2 \\ Y_3 \\ Y_4 \end{pmatrix} \quad (3.108)$$

which leads to

$$\begin{aligned} (D_4^{-1} L_4^T) q_4 &= Y_4 \\ (D_3^{-1} L_3^T) q_3 &= Y_3 - D_3^{-1} M_3^T q_4 \\ (D_2^{-1} L_2^T) q_2 &= Y_2 - D_2^{-1} M_2^T q_3 \end{aligned} \quad (3.109)$$

etc.

Solving Eq. 3.109, the displacements  $q_i$  are obtained in reverse order.

## CHAPTER IV

### TEST EXAMPLES

A computer program (see Appendix B) using FORTRAN language (GI and H level) was developed. Prior to the application to thin-walled structural members, examples of beams and plates were tested and the results are presented in this Chapter. Examples were chosen so that different shapes, different loading patterns, various boundary conditions and different material properties can be tested. Direct comparisons with published results, using either the finite element method, an alternative theoretical approach, or experimental work, are made.

The stiffness matrix is evaluated numerically using Gaussian quadrature over the plane of the elements and Simpson's rule through the thickness. The number of integrating points is left to the user as input. It is judged that  $2 \times 2$  Gaussian points probably will not be able to provide adequate accuracy and a  $4 \times 4$  scheme is too expensive; hence a  $3 \times 3$  Gaussian quadrature is consistently used for all test examples. Either nine or eleven points (layers) are used through the thickness except for the first test of a restrained beam where seventeen are chosen instead. Seven layers may possibly give satisfactory results but has not been tried.

The transformation of the stiffness matrix and the displacement and load vectors between local and global coordinate systems are performed only for certain joints where non-coplanar elements meet and the local coordinate systems of these non-coplanar elements are different from the global. For those cases where an initial imperfection of the member is

introduced through joint coordinates, the four node transformation matrix as discussed in Section III.3 is employed.

Stresses and strains are evaluated at integrating points.

In this Chapter, only half of the beam is analyzed due to symmetry and only a quarter of each plate is analyzed due to double symmetry. The mesh idealizations are shown in their corresponding figures.

The test examples serve the following purposes:

1. To verify the mathematical formulation of the last chapter.
2. To check out the computer program.
3. To further explore the post-buckling behaviour and ultimate strength of plates and the factors which influence the behaviour and strength.
4. To study the accuracy and the convergency of the results with respect to the step size and fineness of the finite element idealization.

#### IV.1 Restrained Simply Supported Beam, Elastic-Perfectly Plastic Material

One of the earliest finite element applications considering combined geometrical and material nonlinearity was due to Armen, Pifko and Levine<sup>89</sup> who tested a restrained beam and a simply supported circular arch. The beam, which is simply supported under uniform lateral loads with its edges restrained from moving toward each other, was chosen for comparison because more detailed results were available. Results of two cases of investigation are shown in Fig. 7 and 8.



The previous investigation used beam elements, included material nonlinearity by using the initial strain method, and assumed a linear variation of plastic strain and of elastic-plastic boundary within the element. The present study uses a plate element, the tangent stiffness method and the layered approach. Hence the method and the elements used for the two cases of investigation are quite different.

The step size used in the previous investigation was reported as 30 lb (13.61 kg). In the present study, it varies from 120 lb (54.43 kg) to 240 lb (108.86 kg) in the elastic range and is, after initial yielding, gradually reduced to 30 lb (13.61 kg) at a load level of 95 lb/in (16.96 kg/cm). In order to speed up the investigation, the step size is again increased to 90 lb (40.82 kg) at a load level of 154 lb/in (27.5 kg/cm) and is maintained the same throughout the rest of the analysis. No iteration is performed during the course of the study.

Fig. 7 and 8 show very good agreement between the two studies up to a load level of about 150 lb /in (26.79 kg/cm). After that, the differences become more pronounced. The present results show that the beam is stiffer than that of the previous investigation and also shows that the softening of a member at the final stage of loading is slight. The difference is probably due to several causes. Firstly, it is attributed to the inclusion of a force unbalance at each increment and also the greater step size used in the present study. Secondly, even though the beam is softening due to plastification, its bending stiffness is increasing due to geometrical nonlinearity. The increase in bending stiffness by using the present element is probably greater than that of the previous

one. Thirdly, the previous investigation is a beam analysis, whereas the present study is a plate analysis. One only involved in single stress field while the other involves a multi-stress field. Hence, a slight difference may arise through computation, particularly in the plastic region where the theory of plasticity is used.

On the other hand, the solutions using different numbers of elements in the previous investigation (see Fig. 7) indicate a trend that the solution of the two investigations get closer when more elements are used. Hence it is believed that when the idealization of the present study is further refined, the difference between the two investigations should be even smaller. Furthermore, both results show identical progression of the plasticization pattern which initiated at the bottom and penetrated through the thickness toward the top of the beam, with only a small discrepancy at the edges (Element #12 in Fig. 8). This was because stresses were presumably evaluated at the nodal joints in the previous investigation but at the centroids of the elements, which is also one of the integration points, in the present study.

One interesting phenomenon observed during the analysis was that the longitudinal unbalanced forces gradually increased and oscillated along with the progression of the elastic-plastic boundary until it passed through approximately two-thirds of the depth of the beam and then started to diminish again (this phenomenon did not occur in later test examples of plates when the edges are free to move in the plane of the member). The larger longitudinal unbalanced forces are apparently due to very high membrane stresses generated due to the beam being restrained from moving in that direction. These unbalanced forces, even though higher than those in the transverse direction, remain small compared to

the total membrane force. However, it is felt necessary to reduce these unbalanced forces. Due to the slow improvement but rapid increase in computing cost, choosing a smaller step size is considered uneconomical. Therefore, it was felt best to reduce the magnitude of the unbalanced forces, which are used as correcting terms within the equilibrium equations for the next load step. The first attempt was an under-relaxation on unbalanced forces by letting  $\alpha < 1$  (see Eq. 3.92). This was not very successful because it was found that the proportionality constant,  $\alpha$ , is not necessarily the same for all unbalanced force components. Judging the character of the oscillation of these unbalanced forces, the method of generating the unbalanced forces used in the second-order self-correcting solution procedure as discussed in Chapter II is adopted to provide a better prediction for these correcting terms.

After a few trials, it is found that the value of parameters  $c$  and  $z$  of Eq. 2.31 can be best expressed as:

$$z = \frac{a}{\Delta p} \frac{1}{p^{0.125} \Delta p^{0.875}}$$

$$c = b\sqrt{z}$$

where  $a$  and  $b$  are scalar quantities,  $\Delta p$  is the current load increment, and  $p$  is the cumulative applied load. Similar forms were previously used in Refs. 199, 201, and 202 except that the exponents for each parameter were different and  $a$  and  $b$  were maintained as constants. In the present study, it was found that better results can be obtained by gradually adjusting the value of " $a$ " from 13 to 2.5 and " $b$ " from 1.8 to 0.2. The unbalanced forces are indeed gradually reduced to small values again and it is believed

that the improvement is partially due to the application of the second-order self-correcting procedure and partially due to its own nature of decreasing the residual forces at later stages of the analysis.

#### IV.2 Simply Supported Square Plates Beyond the Buckling Load

The post-buckling behaviour of simply supported square plates was studied previously by Levy<sup>21</sup>, Coan<sup>25</sup>, and Yamaki<sup>26</sup> using a double Fourier series approach and recently by many investigators<sup>51-57,61,144,149,229</sup> using the finite element method. Yamaki's classical solution is generally accepted as the most exact. Three problems were tested under this category and involve different width-thickness ratios, different materials, and different idealizations. In order to initiate a lateral deflection, imperfections are introduced as single half-sine waves in both directions with maximum magnitudes of ten percent of the thickness at the center of the plate:

$$w_0 = 0.1 t \sin \frac{\pi x}{L} \sin \frac{\pi y}{L}$$

The plates are uniformly compressed in one direction by imposing specified displacements along the loaded edges. The unloaded edges are free to move in the plane of the plates. The magnitudes of the required in-plane loads can be evaluated later by integrating the element stresses or by calculating the reactions after solving the equilibrium equations. The two are always in good agreement.

#### IV.2.A Width-Thickness Ratio = 192, Elastic-Perfectly Plastic Material

An identical plate 48" x 48" x 0.25" (122 cm x 122 cm x 0.635 cm) with  $E = 10^7$  psi ( $7.03 \times 10^5$  kg/cm<sup>2</sup>) and  $\nu = 0.316$ , which was previously tested in the elastic region by Khan et al.<sup>229</sup> was retested as the first test example of a plate in the current study. Results are shown in Fig. 9 where Yamaki's elastic solution is also plotted for comparison. The study of the elastic post-buckling behaviour of simply supported square plates has also been conducted by many other investigators whose results are not demonstrated in Fig. 9 for clarity.

In this particular test, Khan et al used a rectangular plate with five degrees of freedom and employed artificial stiffness coefficients corresponding to  $\theta_z$  as proposed by Zienkiewicz<sup>166</sup> for these coplanar elements. These artificial stiffness coefficients were not required in the present study since  $\theta_z$  itself is a degree of freedom.

Because the plate has a high width-thickness ratio which implies a small initial buckling load but large post-buckling strength, the analysis was mainly in the post-buckling range where the behaviour was highly nonlinear. Consequently, the step size should be small and the growth of stresses in the element was slow. In addition, the ultimate strength of this test plate was not comparable since both Yamaki's and Khan et al's work considered geometrical nonlinearity only. For these reasons, the yield stress of the material was set to a low value (10 ksi (703 kg/cm<sup>2</sup>)) so that the test could be terminated sooner.

Fig. 9 shows that the present result lies between the two previous investigations. After initial yielding, the increase in stiffness of the

plate due to large deflections is gradually more than compensated by the decrease in stiffness due to plastification. Probably due to the severe nonlinearities and the small step sizes that are used, the response of both loads and deflections were sluggish in the region of the ultimate load. The test was terminated when the loads ceased to grow.

#### IV.2.B Width-Thickness Ratio = 150

##### Case a: Elastic-Perfectly Plastic Material

Arai<sup>149</sup> used refined conforming triangular elements with three sub-elements to test a plate 600 mm x 600 mm x 4 mm with  $E = 2.1 \times 10^4$  kg/mm<sup>2</sup> and  $\sigma_y = 25$  kg/mm<sup>2</sup> ( $\nu$  was not reported). One coarse mesh of eight elements and one fine mesh of thirty-two elements were tested. An identical plate was retested using twenty-five rectangular elements and setting  $\nu = 0.31$

Comparing the results against Yamaki's<sup>26</sup> classical elastic solution in the pre-buckling and post-buckling region respectively, Fig. 10 shows that Arai's results changed from being on the stiff side to slightly on the flexible side. The present test almost coincides with Yamaki's but later becomes too stiff. The difference probably can be attributed to the following reasons:

1. The present study considers unloading even though it very rarely occurs in this test problem. In general, had unloading occurred, the stiffness would be evaluated based on the elastic properties of the material until yielding is reached again. Hence, the effect of unloading is essentially to stiffen the member.

2. It seems that Arai covered material nonlinearity by simply setting the stiffness to zero for the plastic portion of the member without further reference to the theory of plasticity. This may be the reason for his results being on the flexible side.
3. The present non-conforming rectangular element is too stiff in this particular problem.

Experimental results conducted by Arai are also reproduced in Fig. 10. No description of the work indicating how the loads were applied or how the boundary conditions were set was given.

Fig. 11 shows the history of the stress distribution near the loaded edge and near the centerline of the plate. It may be observed that the stress quickly drops toward the center of the plate after initial buckling and the ultimate strength is reached when the maximum stress at the edge yields and starts to decrease. This conforms with the concept of effective width initiated by Von Karman<sup>100</sup>. Note that the differences between the two tests are pronounced in Fig. 11a. The stress distribution pattern of the current study agrees with the classical solution (e.g. see Coan<sup>25</sup>) whereas Arai's result is actually closer to the case where the unloaded edges were kept straight. However, this is in conflict with his own choice of using Yamaki's solution for comparison (shown in Fig. 10) which implies that the unloaded edges were free to move in the plane of plate.

Figs. 12 and 13 compare the results on lateral deflection and extension of the plastic area. Generally speaking, the results of the two tests are similar.

Computing costs are also compared in Table 1. It is not certain that the computing time can be directly compared as Arai did not clearly define his computing time of 140 seconds, nor did he mention any attempt at iterations in each loading step. The time of 32 seconds in the present test is an average CPU time per iteration using H level Fortran language. Two or three iterations were used for each loading step depending on the step size. In most parts of the analysis, two iterations were more than adequate.

Case b: Elastic-Linear Strain Hardening Material

The same plate as Case (a) was retested using a different mesh and different material properties. The purpose is to compare results with different fineness of idealization and to check the computer subprogram for material with strain hardening. Fig. 10 shows that the degree of improvement on the result from a  $3 \times 3$  coarse mesh to a  $5 \times 5$  finer mesh is not proportional to the amount of extra computing cost required and this is quite a common conclusion in finite element analysis. However, the plate does have a higher strength due to strain hardening.

IV.3 Restrained Simply Supported Square Plate Under Uniform Pressure,  
Elastic-Perfectly Plastic Material

The classical elastic solution of this problem was previously found by Levy<sup>21</sup> who used double Fourier series to solve von Karman's<sup>14</sup> large deflection equation. Marcal<sup>142</sup> attacked the same problem using triangular elements at the earlier stage of development of combined nonlinear finite element analysis. Ohtsubo<sup>143</sup> later adopted the Ritz procedure with the



aid of the finite element method with the plastic analysis based on the initial strain concept. These works are compared with the present study for a plate 24 in x 24 in x 0.25 in (61 cm x 61 cm x 0.635 cm).

Fig. 14 indicates that the present study results indicate a less stiff plate than those of previous investigations. The Newton-Raphson procedure was employed up to the load level of  $pa^4/Et^4 = 334$  and it took twelve steps to reach this level. The number of iterations were varied from two at the beginning to twelve at the twelfth step where convergency became extremely slow due to severe plastification. The rest of the study was then carried out by strictly following the step by step procedure with a small incremental size. It is observed that both Ohtsubo's and Marcal's investigations terminated at an earlier stage comparing to the present study.

Crisfield<sup>144</sup> has recently used a rectangular element with five degrees of freedom to solve the nonlinear plate problem. He considered only geometrical nonlinearity in this particular problem and compared his result against Levy's classical solution. The elastic part of the solution of the present study is now added to this comparison and is shown in Figs. 15 and 16. It can be seen that, despite the coarse mesh being used in the present study, stresses are still in fairly good agreement.

Since it is the total stress calculated by the present computer program, the membrane and bending components are not explicitly separable after yielding. The post-yielding stresses are then presented in an alternate form as shown in Fig. 17 which shows the progression of plastification in the plate. It is clearly seen that yielding initiated along

the diagonal of the plate which is in agreement with yield line theory. However, due to the restraint along the edges of the plate which causes membrane stretching, the yielding zone, instead of being localized along the diagonal and through the thickness, gradually spread over the whole plate in a manner similar to the one dimensional restrained beam presented in Section IV.1. The test was terminated at a load level of  $pa^4/Et^4 = 423$  because the stored data (stresses, strains, displacements, etc) were unfortunately destroyed due to a human error. Note in this test that the in-plane unbalanced forces again increase at high load levels due to the building up of sizable membrane stresses. It is believed that a better prediction of the unbalanced forces which are used as correcting terms in the incremental equilibrium equations, using the second order self-correcting procedure of Section IV.1, should be helpful if the continuation of loading up to the plastification of the entire plate had been carried out.

#### IV.4 Simply Supported Rectangular Plates Beyond the Buckling Load

Two rectangular plates of different aspect ratios and different material properties were tested in this section. Again, the initial imperfection is introduced through the nodal coordinates using a sinusoidal curve. The plates are uniformly compressed in one direction by imposing specified displacements along the loaded edges.

##### IV.4.A Aspect Ratio (a/b) = 0.875, Width-Thickness Ratio (b/t) = 80, Elastic-Perfectly Plastic Material

Even though the behaviour of this plate, 222.25 mm x 254 mm x 3.175 mm, is similar to that of the square plate and the buckling form

involves only a single half wave, it was tested because a direct comparison with the results by Crisfield<sup>144,145</sup> is possible. Crisfield has used the Ilyushin yield criterion and a modified Ilyushin criterion to test this plate. He employed a rectangular element with five degrees of freedom at each node.

A single half sine wave is used in both directions for introducing an initial imperfection with a maximum amplitude of  $w_0 = 0.001 b = 0.254$  mm at the center of the plate. It took a total of seven steps to reach the ultimate strength prior to entering the region of load shedding. Within each increment, two iterations were used in the elastic range and three to four iterations in the range of post-yielding. Figs. 18 and 19 show excellent agreement between the two investigations which is probably due to the fact that a similar type of element was used in the two investigations. Moxham's nonfinite-element analysis, referred to by Crisfield, is also reproduced from Crisfield's report<sup>144,145</sup> in Figs. 18 and 19.

Crisfield has also provided information on his computing time. The computing times for the present study are added to Crisfield's in Table 2 as additional information. It should be noted that the computing times should not be compared directly because they depend on the computer model being used. Further, Crisfield used the Modified Newton-Raphson solution procedure, whereas the present study employs the unmodified Newton-Raphson method. Hence, the number of iterations listed in Table 2 should not be compared directly either.

IV.4.B Aspect Ratio (a/b) = 3.7, Width-Thickness Ratio (b/t) = 49,  
Elastic-Linear Strain Hardening Material

Dwight and Ractliffe<sup>118</sup> have conducted a series of experimental tests on steel plates and aluminum alloy plates to investigate the ultimate strength of plates under uniaxial compression. They have also performed theoretical calculations to predict the plate strengths. Their theoretical development (not a finite element method) was based on the analysis of a quadrant of a square plate using a few assumptions. One of the assumptions is that the strain in the y-direction (i.e. the direction parallel to that of the applied loads) varies only with x. The Tresca yield criterion was employed. The plasticity was checked at a number of points around the edge and corrections were made on the basis of appropriately reduced stresses in the plastic zones.

Among the specimens tested by Dwight and Ractliffe, one was arbitrarily chosen for re-analysis using the presently developed finite element program. The chosen specimen was a simply supported aluminum rectangular plate 45.5" x 12.225" x 0.25" (115.5 cm x 31.0 cm x 0.635 cm). The stress-strain relation of the aluminum alloy was linearized to elastic-linear hardening according to Dwight and Ractliffe. The initial imperfections were set in accordance with the formula

$$w_0 = 0.03 t \sin\left(\frac{\pi x}{b}\right) \sin\left(\frac{\pi y}{a/4}\right)$$

In this test the unloaded edges were allowed to move in the plane of the plate but must remain straight. This can usually be achieved by adding to the unloaded edges the rigid bar elements with two degrees of freedom (in-plane translation and rotation) at each node. In the present study, the in-plane rotation ( $\theta_z$ ) is a d.o.f. and can be restrained

accordingly. The restraint of translation was imposed by adding a large value to the corresponding coefficients of the stiffness matrix. Hence, no additional elements were actually added.

Fig. 20 shows the load-plate shortening response and the two investigations are in excellent agreement. Dwight and Ractliffe's theoretical result and their experimental results on the same plate but of different width are reproduced in Fig. 21 to further demonstrate the agreement between the two investigations. Fig. 22 shows the load-lateral deflection curves for the plate, where Nodes 9 and 25 are the locations of maximum magnitude of initial imperfection but in opposite directions and Node 33 represents the center of the plate. Since only a quarter of the plate is analysed, the boundary conditions at the center of the plate (i.e. Nodes 33 through 36) has been set by restraining the longitudinal slope at these nodes. This actually ruled out the possible anti-symmetric buckling modes. Fig. 23 clarifies this point by showing that the plate does buckle into three symmetrical half waves even though four half waves were initially introduced through initial imperfections.

The maximum load obtained in the present test is equal to an average compressive stress of  $8.26 \text{ T/in}^2$  ( $1300 \text{ kg/cm}^2$ ). Beyond that stress, the tangent stiffness matrix was detected as non-positive-definite which implied that the plate became unstable at a secondary point of bifurcation. This is also seen in Fig. 22 which demonstrates that the plate was stiffening in the initial post-buckling range but the stiffness of the plate later gradually decreased. This post-initial-buckling, stable, and rising equilibrium path is referred to as the primary path and is finally discontinued at the secondary bifurcation which implies either a

possible change in buckling pattern or a further instability phenomenon after the initial buckling. The post-branching behaviour is very complicated and has not been fully understood so far. Studies have been conducted by several researchers<sup>30,33,258,259</sup> in general terms using the structural model with two degrees of freedom to investigate the existence and the stability of the secondary equilibrium path which represents a higher buckling mode, and the coupling equilibrium path which branches from the primary path into a secondary path. Such coupling occurs in specific ways depending on the properties of the system, boundary conditions and method of control on applied loads. It is also imperfection sensitive. These properties are reflected in the topology and in the stability of the coupling paths. Stable coupling paths ensure a gradual statical transition between buckling modes while on unstable paths this transition is dynamic (e.g. snap through).

This complicated mode coupling and bifurcations from the primary paths require somewhat more refined post-critical load analysis than those which can be simulated using a single degree of freedom. It requires essentially an eigenvalue analysis and an investigation of the possible existence of a coupling path to connect the buckling modes. If such a transition curve exists and if the plate is compressed by controlled loading, the transition curve is unstable and the secondary buckling is of the snap through type. This is achieved in finite element analysis by adding loads incrementally above the bifurcation load and applying a Newton iteration at each load level. The iteration eventually will converge to the secondary path when the load is increased above snap-through load. On the other hand, if the plate is compressed by controlled

shortening, the transition curve is stable and indicates a gradual but rapid drop in loading before the stable and rising secondary path is reached. In this case the imperfection perturbation technique should be introduced in order to get the plate into the transition state.

In any case, the analysis after the secondary bifurcation is considered to be a purely academic exercise. The post-secondary-buckling strength can only be obtained through a dynamic disturbance or through a period of load shedding which is not acceptable for a practical structural member. In fact, the experiments (e.g. Fig. 20) would not show a higher buckling mode unless artificial restraints were introduced. Furthermore, there is always a possibility that the secondary bifurcation may indicate the total instability of the system and imply that no coupling path is available to link the primary path to the secondary path. Hence, the peak load of  $8.26 \text{ T/in}^2$  ( $1300 \text{ kg/cm}^2$ ) is justifiably considered to be the ultimate strength of the plate. At this ultimate load, yielding has been detected at a few integrating points on the surface of the plate. This indicates that the plate is approaching its ultimate strength due to yielding in any case.

#### IV.5 Discussion

Miscellaneous items, which were encountered during the course of testing specific examples and are general to all problems, are discussed under this section.

#### The merit of successive running of a problem

It is not recommended that a problem be completed in one computer run. Using the present computer program, successive running of one problem is possible and the resulting displacements, stresses, and strains are stored. This is preferred because it permits the user to have better control of the problem. The user can examine the results at an earlier stage of the analysis and can either terminate and restart the solution or make the necessary corrections if mistakes have been detected. In this way, he can take a close look at the results as well as study the progress of the analysis. Results which are unsatisfactory can be disregarded and re-run at the extra expense of that particular step only. The number of steps, step size, and maximum allowable number of iterations are all left as input data for each run and hence it is very convenient and flexible for the user.

#### Choice of step size

Step size is not necessarily kept the same throughout the analysis of a problem. Numerous simple algorithms can be incorporated into the computer program which change the step size automatically. For example, a criterion of tolerance can be set and the step size increased or decreased in accordance with a comparison of errors in the results against the allowable tolerance. A simple scheme is used in the present computer program such that the step size is automatically doubled when the error becomes less than ten per cent of the allowable tolerance and the step size is reduced to half when the error becomes greater than five times of the



allowable tolerance. If the error becomes ten times greater than the allowable tolerance, the computation is terminated for investigation before further continuation to the next load step. Besides, the criterion of tolerance is problem dependent and a different user may prefer a different accuracy. Hence, the value of the tolerance is treated as input data rather than a fixed value within the computer program.

Maximum economy of computing time is obtained, particularly in the elastic range, by keeping the step size as large as possible and having the required accuracy achieved with iterations. In other words, the Newton-Raphson method is more economical than the step by step method. Of course, the step size is also subject to certain limitations which depend on the type of problem being analyzed. In general, the step size should be kept small at the initial step and in the vicinity of a buckling load. However, it can be large in the pre- and post-buckling range where the structure is stable. The step size should gradually be reduced to a small value after the member starts to yield, to comply with the concept of the flow theory of plasticity and to cope with the slower convergence.

#### Choice of single or double precision

Double precision is used in the present computer program (half word for integers). Single precision was attempted, which gave good accuracy for displacements but not for stresses, and was therefore abandoned. This further confirmed the conclusion previously reported by Melosh<sup>257</sup>. The Modified Cholesky Decomposition method was adopted for solving the equilibrium equations, which should have improved the accuracy of the results. However, it was still not adequate to warrant the use of single precision in the present study.

Interpretation of accuracy of results (convergence)

The Euclidean norm, defined by

$$n = (\{\Delta\}^T \{\Delta\})^{1/2}$$

in which  $\{\Delta\}$  stands either for the iterative displacement changes, the total displacements, the unbalanced residual forces, or the total applied loads, is used as a basis for determining convergence in the present computer program. The errors are defined as the ratio of the Euclidean norm of the iterative displacement changes to the Euclidean norm of the total displacements, and as the ratio of the Euclidean norm of the unbalanced residual forces to the Euclidean norm of the total applied loads. The allowable tolerance for the error is usually set at one percent. When the plate is well into the plastic range and the solution procedure is performed using the incremental method without iterations, the error is evaluated only in terms of unbalanced residual forces and an error of five percent is generally considered tolerable.

In general, it is found that, in the pre-buckling range, errors calculated from unbalanced residual forces may be small while those from displacements are considerably larger. Hence, displacements instead of residual forces should be used for interpretation of accuracy. On the other hand, in the post-yielding range the opposite is true mainly because of the smaller step size being employed. In the range between post-buckling and pre-yielding, errors calculated in both displacements and residual forces respond very well and hence either one is reliable and can be used. In conclusion, the consistent use of only one parameter, displacement or residual force, to interpret the accuracy of results may be misleading in some range of the analysis. Of course, the best accuracy

can be obtained by having the error calculated from both parameters and have both tolerance allowances satisfied simultaneously. Apparently this will be compensated by higher computing costs and may not be worthwhile. Probably a good practice is to use the most reliable parameter for calculation of the error in the corresponding region and switch the term motivationally as is necessary during the course of analysis. This can be done very easily when the problem is analyzed successively.

It should be noted that the above discussion of errors and convergence is subject to the important question of the reliability of using the unbalanced residual forces to estimate the accuracy of the results<sup>57</sup>. Many investigators suggest that this residual check is unreliable. It is well known that to solve a set of simultaneous algebraic equations numerically, it is possible for an entirely erroneous solution to have a very small residual and it is possible for the more exact of two approximate solutions to have the larger residual particularly when the equations are not well conditioned<sup>260</sup>. Similarly, in finite element analysis, a satisfactory residual check may be obtained with stresses that are considerably in error or vice versa<sup>214</sup>. For example, if a support reaction  $R_i$  is computed by summing  $k_{ij}q_j$ , it may be nearly exact but displacements  $q_j$  may have appreciable error. If  $R_i$  is computed from element stresses, it is conceivable that stresses may be satisfactory while  $R_i$  is erroneous, since stresses at the element corners are less reliable than elsewhere.

Furthermore, the in-plane forces, transverse forces and moments may all be of different order. A beam or a plate which is laterally loaded and is restrained from movement in its own plane is a good example

to demonstrate this point. Consider the beam case which was tested in Section IV.1, where the in-plane forces were quickly built up and remained high in the plastic range. We may pick any node and evaluate the in-plane force at that node. Since there is no applied external force in the longitudinal direction, the two values of in-plane force computed from the stresses in adjacent elements on either side of the node should be equal and of opposite sign if the equilibrium condition is to be exactly satisfied. If not, the difference of the two values is the unbalanced residual force in that direction. This residual force is very small compared to the in-plane force but may be big when compared to the transverse incremental loading or the residual forces in other directions. The situation now arises that the Euclidean norm of the residual forces is contributed to mostly by residual forces in the longitudinal direction while the Euclidean norm of the total applied load is entirely due to the transverse loading. The two are neither in the same direction nor are the forces in the two directions of the same order. Hence, in this case, to use the ratio of the two Euclidean norms to measure the accuracy of the results may be erroneous. Consequently, some investigators simply use displacements to determine the convergence. This may be adequate for a non-linear elastic analysis but it is doubtful that checking on displacements alone will fully reflect the accuracy of stresses when material nonlinearity is involved. It is felt that the unbalanced residual forces are still worth checking as long as it is handled with caution. This is the reason for checking both displacements and residual forces in the present study.

It is worthwhile repeating that problems of convergence have been reported by several investigators when the Newton-Raphson procedure is used well into the plastic range. The present study also experienced slower convergence in the post-yielding stage along with the progression of plastification and the Newton-Raphson procedure was finally replaced by an incremental procedure not only because of slower convergence but also for reasons of economy. Stricklin et al<sup>202</sup> pointed out that since all the convergence proofs for the Newton-Raphson procedure assume a continuous first derivative, the stiffness matrix which takes account of plasticity,  $[K^P]$ , can have discrete discontinuities when unloading occurs, hence it can destroy any assurance of convergence when there is a possibility of elastic unloading. Furthermore, under such conditions, there is no unique solution for the deflections. On the other hand, Davis et al<sup>263</sup> stressed the importance of studying the sign of the rate of plastic work and making the necessary modifications to maintain a positive rate of work in all plastic areas. A negative rate of plastic work implies a physically impossible situation and should be removed by assuming that the plastic elements are elastic (elastic unloading). It is felt that information is limited and further investigation of methods for improving convergence in the plastic range is required.

#### Prediction of computing cost and behaviour of member

In addition to the method of analysis and efficiency in programming, it is clear that the cost of computing time is also highly dependent upon the type of problem and the member geometry. For example, compare a

laterally loaded beam or plate where edges are free to move in the plane of the member to the case where edges are restrained. The former will reach its ultimate strength shortly after its initial yielding and only a small portion of the member will have yielded while the rest of the member remains elastic. However, the latter case will not reach its ultimate strength until the whole member has yielded. Apparently the latter is more costly than the former.

Consider the classical problem of the uniformly compressed, simply supported square or rectangular plate as the second example. A plate with a high width-thickness ratio (thinner plate) will cost much more than the same plate with a lower width-thickness ratio (thicker plate). This is because the thinner plate has a smaller buckling load but a greater post-buckling strength. Hence most of the analysis is in the post-buckling range where nonlinearity is severe. Ultimate strength is not immediately reached after initial yielding but only after a significant range of gradual reduction in member stiffness. Even the load shedding part of the analysis performs in the same manner of slow and gradual decreasing. This implies that a smaller step size and more iterations are required and hence results in higher computing costs. On the other hand, the thicker plate has a greater buckling load and a shorter post-buckling range. Ultimate strength is reached very quickly after initial yielding and abrupt load shedding immediately follows.

Based on these considerations, an approximate prediction of computing costs and the behaviour of the plate may be attainable in advance.

## CHAPTER V

### APPLICATIONS TO THIN-WALLED SECTIONS

It is to be noted that a 3 x 3 Gaussian point integrating scheme over the element surface and 9 layers through the element thickness are used for all the problems treated in this Chapter.

#### V.1 A Cruciform Section Under Uniform Compression, Elastic-Nonlinear Strain Hardening Material

Similar to conventional hot rolled members, it is not uncommon for a thin-walled section to have an unstiffened flange which is supported by the web plate along one longitudinal edge with the other longitudinal edge free of support. To represent such an unstiffened flange, Stowell<sup>106</sup> chose a cruciform section loaded axially (Fig. 24). The dimensions were chosen in such a way that the individual flanges will buckle well before the Euler load for the entire column is reached. The column thus undergoes a torsional mode of buckling as the middle cross-section rotates about the longitudinal axis with respect to the end cross-sections which are restrained from moving in their own planes.

Stowell<sup>106</sup> has investigated several sections with different dimensions and the results were presented in a form of axial shortening vs maximum rotation except for one section whose results were presented in terms of stress distribution and strain distribution. The latter section was chosen for the present study using the finite element method. The reason for this choice was because in using the finite element displacement method,

a comparison of the two tests in terms of deformations might result in very good agreement while the comparison in terms of stresses may be substantially less so. By comparing stresses, the maximum difference between the present investigation and that of Stowell could then be obtained. It may be noted that Stowell used the deformation theory of plasticity, whereas the present study employs the flow theory. Hence the two are quite different.

Due to symmetry about the two axes, each flange of the cruciform section deforms identically. Mathematically, the problem is thus reduced to two dimensions as a single flange could be isolated and analysed. Further advantage of symmetry on a flange can be taken and hence only half of a single flange was actually investigated. The half flange is idealized by a mesh with 8 (rows) x 3 (columns) (Fig. 24). Actually a mesh of 8 x 2 will give a better aspect ratio (i.e. the ratio is closer to one) for each element. However, it was felt that a minimum of three elements across the width of the flange was necessary in order to faithfully describe the stress and strain distribution patterns. The mesh 8 x 3 was therefore chosen with the understanding that the accuracy may possibly be reduced due to higher aspect ratio in the elements.

The material for the section was aluminum alloy 24S-T4 whose stress-strain relation, which was used in the present study, is shown in Fig. 25. This stress-strain curve is expressed by a nonlinear formula using Eq. 3.58. Initial imperfections were introduced by applying a uniform lateral pressure of 0.03 psi ( $0.002 \text{ kg/cm}^2$ ). The column was compressed by controlled axial displacement.



The load-deformation relations for the cruciform section are shown in Figs. 26 and 27. No results are presented in these forms by Stowell for direct comparison. Fig. 26 demonstrates the relation between the axial stress and axial elongation which indicates the sluggish response in the ultimate load region and no pronounced load shedding was obtained. It is interesting to note that a similar behaviour also occurs in the case of axially compressed circular cylinders as shown in Ref. 175 where a different finite element scheme was used and the nonlinear hardening was incorporated using the Ramberg-Osgood equation (Eq. 3.57). In Fig. 27, the abscissa represents the maximum rotation which occurs at the middle cross-section of the column. The axial strain at torsional buckling, according to Stowell's theoretical formula, equal to  $2 \times 10^{-3}$  and is in excellent agreement with the present investigation. The present result is slightly lower due to introducing the initial imperfection.

Fig. 28 compares the axial strain and axial stress distributions from the two investigations. Stowell did not specify on which cross-section the strain and stress distributions were plotted. However, he mentioned that these distributions hold over the greater part of the flange where bending is negligible. The distributions of the present study are the results from a cross-section passing through the centroid of Elements 13, 14 and 15 (Fig. 24) which are some distance from the end and from the center of the flange. Hence, it represents the greater part of the flange. It is seen (Fig. 28.b) that, even though the maximum average stresses from the two investigations are close (32.4 ksi in the

present study and 32.1 ksi by Stowell), the difference between the two distributions becomes greater when the stress level increases. Compared to Stowell's, the stress in the present study grows faster near the supported edge while, at the same time, it also drops faster near the free edge. The result is that the increased amount of stress is cancelled by the decreased amount of stress thus explaining why the average stresses, which integrate to give the magnitude of the applied axial load, remains close. Fig. 28.a shows a substantial difference between the two strain distributions. This is easily explained by noting that when the material has yielded, the stress-strain curve is quickly flattened out (Fig. 25), hence, a small difference in stress may give a significant difference in strain.

## V.2 A Short Square Tube Column, Elastic-Perfectly Plastic Material

A square or rectangular tube column has generally been treated by considering each of its plate components as a simply supported rectangular plate under compression. Previous tests indicated (Fig. 34) that, when expressed in a non-dimensional form, the strength of a square tube is close to that of a rectangular plate with unloaded edges supported in V grooves. Graves-Smith<sup>119</sup> has studied both short and long rectangular tube columns with rigorous mathematical analysis. The main thrust of his work involved the application of a variational principle and plasticity, and solving the Von Karman equations for the plate. Recent research<sup>159</sup> on rectangular or square tube columns has applied the effective width concept to take into account the nonlinear effects due to locally buckled

plate components. In this section, a square tube column is analysed using an alternative approach, namely the finite element method.

Since the analysis of the uniformly compressed, simply supported rectangular plate has already been demonstrated in the previous chapter, the whole section of the tube will be analysed to take full account of the possible interaction between plate components. The material properties and the dimensions of the tube are chosen in accordance with Graves-Smith's so that a direct comparison of the two investigations is possible. Due to symmetries, only one-eighth of the tube is analysed and its idealization is shown in Fig. 29. At the initial step, a lateral load of four pounds was applied on those nodes that lay on the center line (in the longitudinal direction) of each plate component. The lateral loads were applied in the opposite direction at each alternate node so that a wave-form for the initial imperfection is generated. The maximum magnitude so generated was found to be equal to  $0.001a$ , where "a" is the width of the tube. The tube was compressed by controlled end displacements. per

Fig. 30 shows the response in terms of average axial stress vs. axial shortening and Fig. 31 in terms of axial stress vs. out of plane deflection. Both curves indicate excellent agreement with the results of Graves-Smith except that the ultimate strength of the present investigation is slightly lower. Fig. 32 shows the growth of the buckling form of each plate component and is rather straightforward. Fig. 33 shows the yielded zones at ultimate load and demonstrates clearly that the tube fails once its edge has fully yielded. It should be noted that, along the longitudinal center line of each plate component, those areas being

denoted as partially yielded have only yielded very slightly at the surface of the plate due to bending. This point can be easily seen by studying both Fig. 32 and Fig. 33 which indicate that the yielded areas adjacent to the longitudinal center line always correspond to the locations of maximum out-of-plane deflections. This surface yielding due to bending has not yet been reached for the region close to the middle of the column where the curvature at maximum deflection is smaller than at other locations (Fig. 32).

A summary of previous work on simply supported plates and square tubes under compression, which is available from Refs. 107, 111, 119, is reproduced in Fig. 34 on a log-log scale. The present study, using finite elements, which include four problems of square or rectangular plates in Chapter IV and the square tube in this Section, were added to this figure for comparison. If we consider the Mayers-Budiansky's<sup>107</sup> curve where the unloaded edges were kept straight for an extreme upper limit, and the experimental curve for V-groove plates which had the unloaded edges neither restrained from movement in its own plane nor fully restrained in the transverse direction as a lower limit, it is found that the present study (denoted by points A, B and C) which have the unloaded edges free to move in their own planes but restrained in the transverse directions indeed fall between the two extremes. The present investigation of a rectangular plate with the unloaded edge kept straight (denoted by point D) has a strength slightly higher than Mayers-Budiansky's but in very good agreement. It should be noted that the theory of Mayers-Budiansky was unable to describe the region of load shedding. Thus the

average compressive stress at a strain of 0.01 was taken as an indication of failure. Compared to Graves-Smith's result, the strength of a square tube column in the current study (denoted by point E) is in closer agreement to previous experiments.

### V.3 Hat Sections Under Compression, Elastic-Linear Strain Hardening Material

In this section, the assumption of a linear strain hardening type of material is assumed for two three dimensional thin-walled members. Two hat sections under compression were chosen for the test. In the first case, the column was loaded concentrically and a high value of linear hardening with a tangent modulus equal to 15% of its Young's modulus was used. In the second case, the column was loaded eccentrically and a low value of linear hardening with a tangent modulus equal to 1.5% of its Young's modulus is assumed. All the data including member dimensions and finite element idealizations are shown in Fig. 35.

In Figs. 36 and 39, the response of the two columns are plotted in terms of axial stress vs. axial shortening. In the first case (Fig. 36), it is seen that, even though the stiffness of the column is greatly decreased after yielding, the assumed high strain hardening character is adequate to provide sufficient stiffness to carry higher loads although at a greater rate of deformation. Since constant linear hardening is assumed to last indefinitely in this study, the computation is terminated at a load of 16.0 kips (7,257 kg) which gives an average axial stress of 25.9 ksi (1,821 kg/cm<sup>2</sup>) and is close enough to the yield stress of the material (26.0 ksi). This load-deformation curve can be lowered if a tri-linear stress-strain relation were assumed by adding a third section

of straight line representing zero strain hardening (a horizontal line) to halt the growth of strain hardening. In the second case (Fig. 39) where the assumed lower value of tangent modulus represents the amount of strain hardening usually possessed by the common aluminum alloys, the curve eventually flattens out at an ultimate load of 14.4 kips (6,531.7 kg) even though it does not show load shedding as it did in several previous investigations with perfect plastic material.

In Figs. 37 and 40, the profiles of lateral deflection along the longitudinal center line of the flange which is also the center line of the column are presented for both cases. The loads which cause local buckling in the flange are respectively 9.2 kips (4,173 kg) and 9.9 kips (4,490 kg). The familiar buckling pattern in wave-like forms are clearly developed. A close look at the last deflection profile corresponding to the highest load level in these two figures indicates that overall column buckling has also been initiated. The column in the second case buckles in the opposite direction with respect to the column buckling of the first case and is due to the eccentricity of the applied load.

Figs. 38 and 41 show the yielded areas on the members at the highest load levels. Plastification is seen to be widely spread and is extremely severe for the first case (Fig. 38). The column being able to sustain such heavy yielding is due to the aforementioned reason for high values of strain hardening. Note that the half inch wide lips play an important role in stiffening the member. This is seen by noting that the web and the lip are heavily yielded when compared to the flange, particularly to its center portion.

#### V.4 Short Span Hat-Section Beams Under Local Loads on the Webs, Elastic-Linear Strain Hardening Material

Local loads on webs is a common problem in the design of light gauge metal products. A theoretical analysis of this problem is extremely complex since it involves a combination of non-uniform stress distribution, elastic and plastic instability, local yielding in the immediate region of load application, and, furthermore, the bending produced by eccentric application of the load caused by the curved transition from the web to the bearing flange. In view of this analytical complexity, the codes<sup>1,4</sup> rely almost exclusively on experimental evidence. The purpose of the present study is to demonstrate the capability of using the finite element method to perform a theoretical analysis on such a complicated phenomenon. The failure due to web crippling is investigated and the results are examined in the light of the current codes on light gauge products<sup>3</sup> and compared against the previous experimental tests.

Previous experimental tests on short span, thin-walled aluminum beams were reported in Ref. 261 and 262. Two specimens, one with vertical webs and one with sloped webs, were chosen for the present theoretical analysis. The dimensions of the two beams are shown in Figs. 42 and 52. The material was aluminum alloy ALCAN 57S-H34, whereas the yield stresses cited for the two previous tests were different. The one in Ref. 262 is herein employed. The strain-hardening, which was not reported previously is also considered by assuming a linear variation.

According to Ref. 262, the beams were freely placed on 3/4 in (1.91 cm) wide steel bearing plates at each end, which left the beams with a clear span of 9.25 in (23.5 cm). The beams were loaded through

a 1.5 in (3.81 cm) wide, x 0.25 in. (0.635 cm) thick steel bar at the center. Laterally (horizontally), in order to simulate the effects of adjacent material extending in both directions as would be the case for a metal roof deck, a steel angle was placed against each outstanding lip. The steel angles were fixed to prevent the lips from moving laterally outward. However, no means was used to prevent them from moving inward.

Results of the present study for the two sections are now discussed separately.

#### V.4.A Hat-Section with Vertical Webs

Considering the symmetry in both directions, only one quarter of the beam was analyzed. The finite element idealization is shown in Fig. 42. In order to take into account the radiused bends between the webs and the flanges, a longitudinal row of elements was introduced at the web-flange junction. It was understood that this row of elements, with their smaller size and higher aspect ratio compared with adjacent rows of elements, might reduce the accuracy of the results. To improve this situation, the mesh could have been refined. This was not done after considering the substantial increase in computing costs that would result. The beam was restrained vertically at Nodes 55 and 63 and laterally along the bottom flange-lip junctions (i.e. Nodes 57-64). The load was applied at Nodes 17, 18 and 19.



The deflections in the direction normal to their plate elements at the center of the beam are plotted against the load in Fig. 43. This means that the curves for those nodes in the flanges (Nodes 1, 17 and 49) are vertical deflections while those for nodes in the web (Nodes 33 and 41) are lateral (horizontal) deflections. The curve for the deflection at the center (Node 1) does not indicate any clear local buckling phenomenon at the top flange. However, it does indicate that the top flange was initially stiffening due to the effect of the large deflection and that the stiffness, after a load level of approximately 550 lb (249.5 kg), gradually decreased due to the influence of plastification in nearby regions. The decrease in stiffness was exhibited even more strongly on the deflection curve for Node 17 where the stiffness started to decrease due to the yielding of the material at a load level of approximately 500 lb (226.8 kg) and the rate of decrease was faster than that of Node 1. This obviously demonstrates the phenomenon of local crushing in the region of Node 17 which is directly under the applied load. It seems that the center and lower portion of the web, which is represented by the deflection curves for Nodes 33, 41 and 49, has not been affected by local plastification in the flange-web junction and remains stiffening. The vertical deflection of Nodes 1 and 17 of the experimental test reported in Ref. 262 is reproduced in Fig. 43 for comparison. It may be seen that there is a substantial discrepancy between the experimental and theoretical investigations. This point will be discussed at the end of this section.

Similarly, the deflections for those nodes at the end of the beam are also plotted against the load in Fig. 44. This figure exhibits the interesting phenomenon of reversing the buckling form in both flange

and web. The change of buckling form was initiated at the top flange at a load level of 250 lb (113.4 kg) and was later followed by the web at 500 lb (226.8 kg). After the reversal of the buckling form, the deflections at both flange and web increased very quickly. This implied that the stiffness was diminishing rapidly at a higher load.

Figs. 45 and 46 show the subsequent distortion of the cross-section at midspan and at the end of the beam. These distortions are of the same form as those observed in the experimental test<sup>262</sup>. Fig. 46 clearly demonstrates the aforementioned rapid growth of deflection at the end of the beam at higher loads. Figs. 47 and 48 show the longitudinal profiles of the vertical deflection along the center of the top flange and of lateral deflection along the center of the web, where the deflection at the center of the web is obtained by averaging the deflection along nodal lines 33-40 and 41-48. Both figures exhibit the change of buckling form in the region near the end of the beam.

A comparison of the longitudinal strain on the interior face of the web between the theoretical and experimental investigations is presented in Fig. 49 at load levels of 200 lb (90.7 kg) and 400 lb (181.4 kg). For the experimental test, strain gauges were placed at 0.25 in. (0.635 cm) from the midspan. In the present study, strain was evaluated through the center of the first transverse row of elements, 0.1875 in from midspan. The difference in location for the measurement of strain is negligible and hence the strains can be compared directly. It is seen that the general form of strain distribution for the two investigations are similar and the strains in the upper and lower portion of the web are in fair agreement. However, the strains at the center of the web, where the web deflection is a maximum, are significantly different.

The initial yielding is detected in Element 15 at a load as low as 340 lb (154.2 kg). The analysis is terminated at a load of 790 lb (358.3 kg) which is believed to be well after local crushing of the web. Between the initial yielding and final termination, the yielding area in the region directly under the applied load is shown at four different load levels in Fig. 50 to demonstrate the progression of plastification.

It had already been observed in Ref. 261 during the previous experimental tests that the local deformation and yielding proceeded with increasing load, but the maximum load representing the longitudinal bending strength was only reached well after conspicuous local crushing had taken place. This behaviour raised the problem of defining failure. Consequently, each test was judged individually upon the degree of damage which represented failure being a severe permanent indentation in the specimen. It was pointed out that the possible variation in load which could be obtained by varying the opinion of severe damage might have been as high as fifteen percent. The same problem of defining failure is encountered in the present theoretical analysis. Judging from the load-deflection curve, the distortion of the section and the yielding area, it is believed reasonable to say that the crushing load in the present study is somewhere between 600 lb (272 kg) and 700 lb (317.5 kg).

The present Canadian code for the design of light gauge aluminum products (Clause 9.4 of CSA-S190-1968) controls local loads on webs by two criteria: the load which causes the elastic buckling of the web and the load which causes the yielding of the web due to direct bearing.

The maximum permissible load for a member should be the lesser of these two. Applying the code to the current hat-section beam, it is found that the maximum load is controlled by web buckling. After multiplying by a safety factor of 2 as used in the code and assuming that the web and flange were connected perfectly without a curved transition area, this failure load due to buckling is calculated to be 832 lb (377.4 kg). If an inside radius of bend equal to 1/8 in. is taken into account, the failure load is then reduced to 507 lb (230 kg).

For the previous experimental tests where the specimen had 1/8 in. radiused bends, the ultimate load reported in Ref. 262 was 691 lb (313.4 kg), and the failure load due to local crushing reported in Ref. 261 was 740 lb (335.7 kg). Note the yield stress of the specimen in Ref. 261 was reported to be 37 ksi (2600 kg/cm<sup>2</sup>) which was higher than the yield stress of 29 ksi (2024 kg/cm<sup>2</sup>) used in the present study. Reducing the load in accordance with the ratio of the two yield stresses, the approximate crushing load would then become 580 lb (263.1 kg).

In Ref. 261, Marsh also suggested a semi-empirical formula to predict the failure load due to local crushing. He used a simple idealization of a possible collapse mechanism for a point load to obtain a lower bound solution. Following this formula and after considering radiused bend, the failure load of the current beam appears to be 425 lb (192.8 kg).

It is seen that the present prediction of failure load is higher than that of the previous test results. One of the most important reasons is obviously because the present study analysed an ideal, perfect member, whereas the real specimens were by no means physically perfect. The initial imperfection of the member affects its strength very significantly, and

will be further discussed later. Also, the prediction of failure load based on the current code and based on Marsh's formula are less than the present one and hence are on the safe side. Whether these values are too conservative or not, requires further investigation. As a final note, the experience gained through the present study supports a conclusion drawn previously in Ref. 261 and 262 that a larger bend radius at the web flange junction does not reduce the member strength significantly. Therefore, the current code which suggests a reduction of allowable load by  $10 R/t$  per cent, where  $R$  is the inside radius of the bend and  $t$  the wall thickness, is considered to be excessively conservative.

Finally, the distribution of the longitudinal stress along the center line of the first transverse row of elements adjacent to the mid-span is plotted in Fig. 51. The stress is plotted at two different load levels. First, at a load of 340 lb (154.2 kg) when the initial yielding has just been detected and hence the beam basically is still elastic at this stage. Second, at a high load of 720 lb (326.6 kg) when local crushing has been fully developed. At this load level, in addition to the average stress through the wall thickness, the two extreme fiber stresses are also plotted to demonstrate their substantial differences. These differences are due to the local deformation as well as to the effect from the transverse bending stress which causes local yielding. Note that the highest stress has already reached yield, which implies that yielding at the top flange due to longitudinal bending of the beam has already started.

#### V.4.B Hat-Section with Sloping Webs

The idealization is shown in Fig. 52. Again, only a quarter of the beam is analysed. 90% of the load is applied to the ridge (Nodes 15 and 16) and 10% directly to the top flange (Nodes 8 and 9). The beam is vertically supported at Nodes 41 and 48, but for the lateral restraint, two different cases are initially investigated. In the first case, restraint is applied at the bottom flange-lip junction (i.e. Nodes 43-49) and in the second case at the bottom flange-web junction (i.e. Nodes 36-42). No radiused bends are considered in this beam.

Similar to the previous problem, the deflections in the normal direction are plotted against load in Fig. 53 for the midspan section and end section. It is seen that, for the two different lateral restraint conditions, the behaviours of the beam are almost identical. Consequently, the case with restraints along Nodes 36-42 is terminated at a load of 420 lbs (190.5 kgs) and only the case with restraint along Nodes 43-49 is carried further. Note that the deflection curves for Nodes 28 and 35 demonstrate clearly that the web at the end region of the beam buckles. The deflection curves for Nodes 1, 7, 22 and 29 become asymptotic when they are approaching the ultimate load of 890 lb (408.2 kg). This may be interpreted as a failure of the flange and web due to local bending. Actually the deflection curve for Node 15 also becomes asymptotic. However, in this case it indicates a failure due to longitudinal bending of the beam rather than a sign of local crushing as occurred in the previous problem. All these indications of collapse should become clearer when reference is made to Figs. 58 and 59. The vertical deflection at Node 1 from the experimental test in Ref. 262 is also reproduced in the

figure. This experimental curve was only reported for the lower load region and hence a direct comparison becomes rather difficult. However, judging by the trend of the curve, the difference between the two investigations is probably substantial.

Figs. 54 and 55 show the distortion of the section at midspan and at the end of the beam. Figs. 56 and 57 exhibit the longitudinal deflection profile along the center of the top flange and along the center of the web.

Initial yielding was detected in Element 1 at a load of 530 lb (240.4 kg). The yielding area of the beam is shown in Fig. 58 at a load level of 730 lb (331.1 kg) and 890 lb (403.7 kg). It is seen that the plastification in this case is quite different from that of the previous beam with the vertical webs. In this problem, the beam yielded mainly at the center portion of the top flange and web where a maximum bending stress is reached due to the large local deformations for each plate component (see Fig. 54). Note that full yielding at the ridge as shown at a load of 890 lb (403.7 kg) is actually due to the longitudinal bending of the beam as mentioned previously. This point is further clarified in Fig. 59 where both top and bottom fiber stress are shown in compression and have reached yield. This suggests that local crushing was not fully developed in this particular problem. Again, in Fig. 59, the distribution of longitudinal stress along the center line of the first transverse row of elements is plotted at 530 lb (240.4 kg), which represents the highest load level when the beam was still elastic, and at 890 lb, the ultimate load. The forms of distribution are similar to those of the previous problem. The substantial difference between the two extreme fibre stresses at the center of the top flange and web is due to the large local deformation.

Defining failure is rather easy for this section since the beam obviously failed by web buckling, which is in agreement with the previous experimental observations reported in Ref. 261. Referring to the deflection curve for Nodes 28 and 35 as shown in Fig. 53, if the inflection point of the curve is chosen to represent the buckling load, the failure load of the present study is approximately 500 lbs (226.8 kgs). According to Clause 9.4 of CSA-S190-1968, the buckling load predicted by the code is equal to 375 lb (170 kg) which is quite conservative. The failure loads reported from two previous tests are respectively 475 lb (215.5 kg) and 523 lb (237.3 kg).

For either the beam with vertical webs or that with sloping webs, the comparison in terms of deflection and strain between the present investigation and the test results reported in Ref. 262 is not very satisfactory. A few of the more important factors as described in Ref. 262 are summarized in the following to explain the reasons for such a discrepancy.

- (1) The initial imperfections in the specimens were numerous. The imperfections were not only due to the initial crookedness of the aluminum sheet, but also due to sagging because of the high thinness ratio of the plate elements as well as due to inexact manufacture in the dimensions and the radii of the bends. The effect due to imperfections was so great that, for the same two tests at the same location, the strain gauge readings for one test might be several times greater than the other test even with a reversed sign for certain cases.



- (2) The beam did not rest on the bearing plate evenly and did not really deform symmetrically.
- (3) Deflection at the ridge was not measured directly but rather through the interpretation of measurements at other locations.
- (4) Lateral restraint using fixed steel angles only prevented the outstanding lip from moving outward but not inward. Further, it was not clear whether the upper or lower tip of the lip was really against the steel angle. This type of boundary condition cannot be exactly simulated in a computer program.

On the other hand, the present study analysed an ideal and perfect structural member and hence the initial imperfections which reduce the strength of the member significantly was not taken into account. Therefore, the current theoretical investigation always shows a stiffer member than the test specimen.

#### V.5 Channel-Section Beam Subjected to Combined Bending and Torsion, Elastic-Perfectly Plastic Material


Although studies of thin-walled open-section beams subjected to combined bending and torsion for the linear elastic<sup>165</sup> and nonlinear elastic<sup>71</sup> cases have previously been attempted, studies considering material nonlinearity are lacking. In this section, a complete investigation considering both geometrical and material nonlinearities is presented.

An unlippped channel section (Fig. 60) was chosen for the test. The load (P) was applied uniformly to the top of the beam and in the plane of its web. It thus created a uniform torque of  $T = Pe$  on the beam,

where  $e$  (.65 in) is the distance from the shear center to the center line of the web. The material was assumed to be an aluminum alloy 6061-T6 whose ultimate stress is very close to its yield stress and hence strain hardening is neglected and its stress-strain relation is simplified to elastic-perfectly plastic. The beam was simply supported but restrained from twisting at both ends (i.e. at Nodes 3, 4, 5 and 6). Due to symmetry, only half span was analysed.

The results are shown in Fig. 61 in a relation between the applied load/torque and the angle of twist at the midspan cross-section. It was found from computer print out that the angle of twist at different locations (nodes) in the midspan section were almost identical except that slight differences arose at the flange tips. This indicated that in the midspan region the beam deflected and rotated without any pronounced local deformation of each plate component in this particular problem. Fig. 61 shows that the curve quickly flattened when it approached its ultimate load of 78 lb/in (13.93 kg/cm). Similar curves were also obtained in Fig. 62 where the result is expressed in terms of load and vertical deflection at midspan. Deflections at both flange tips and both flange-web junctions are plotted. Deflections at other nodes which include Node 44, whose curve lies between that of Nodes 43 and 45, and Nodes 46 and 47, whose curves lie between that of Nodes 45 and 48, were omitted for clarity.

Fig. 63 shows the variation of angle of twist along the longitudinal section at different locations. For the top half cross-section of the beam, the twisting angles increase monotonically and are only slightly different in magnitude at different sections. They are given in Fig. 63a,



where the longitudinal section is taken at one inch above the centerline of the web. Fig. 63b describes the variation for a section one inch below the centerline of the web and Fig. 63c at the junction of the web and the bottom flange. The variation of twisting angle at the bottom flange tip is similar to Fig. 63c (but different in magnitude), and hence is omitted. A study of Fig. 63b and 63c reveals that the bottom half cross-section of the beam in the region close to the end supports experienced a rotation in a reverse direction which later decreased and tended to recover toward the same rotational direction as the rest of the beam when the applied load was further increased.

This is obviously due to the fact that the web plate, which is under the direct compression of the applied load on the top, is also subjected to higher shear stresses adjacent to the end support. Thus locally, the web plate eventually buckled elastically toward the exterior side of the web plane. When the applied load was further increased toward its ultimate load, the effect due to twisting predominates over the effects due to compression and shear. Hence the dent created by local elastic buckling gradually disappeared and the rotational direction reversed to that of the applied torque.

The distortion of the beam is drawn at various transverse sections shown in Fig. 64. It is an alternative presentation describing the behaviour previously discussed in Fig. 61, 62 and 63.

The deflections along the span of the beam are plotted in Fig. 65, 66, and 67. Fig. 65 shows the vertical deflection at the top and bottom flange tips. The deflection at the bottom flange tip is considerably less than that of the top flange tip in the region close to

the end supports. This is caused by a significant amount of the downward deflection at the bottom flange tip due to bending and twisting being cancelled by the effect of local buckling of the web which caused the bottom flange tip to move upward. Fig. 66 shows the lateral (horizontal) deflection of the web plate. Longitudinal sections are taken at each third depth point. Again, in the region adjacent to the end supports, the deflection in the reverse direction for the upper longitudinal section (represented by solid lines) and the greater deflection than its deflection in the midspan region for the lower longitudinal section (represented by dotted lines) are due to local buckling of the web. Fig. 67 indicates the vertical deflection at both the top and bottom junctions of web and flange. The top junction deflects more than the bottom because the deflections due to bending and twisting at the top junction are both downward and are summed. However, the deflection due to twisting at the bottom junction is upward and is subtracted from its deflection due to bending.

The longitudinal stresses which are averaged through the plate thickness are plotted in Fig. 68 and 69 at an applied load of 68 lb/in (12.14 kg/cm) which is the load level at which the beam remains fully elastic but is just prior to initial yielding and at the ultimate load of 78 lb/in (13.93 kg/cm). Fig. 68 shows the distribution of longitudinal stress along the centerline of each transverse row of elements except the last section (Fig. 68f), which is taken through the midspan section (18 in from the support) by extrapolating the stresses to the midspan section. It is seen that the stress distribution at those sections near

the support is more nonlinear than the distribution at the section near midspan due to local buckling. Once the yield stress is reached, the maximum stress spreads to the adjacent areas as shown in Fig. 68e and 68f. Fig. 69 shows the distribution of longitudinal stresses along the centerline of each longitudinal row of elements. It is again indicated that the longitudinal stresses cease to grow when the yield stress is reached.

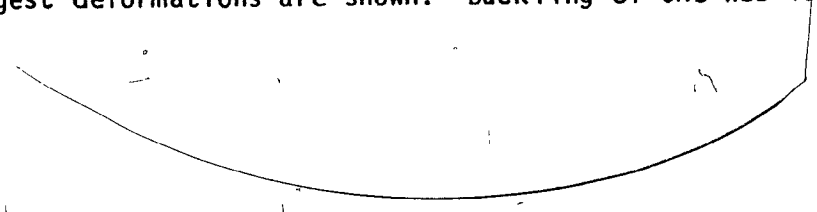
Fig. 70 shows the plastic area in the beam at the ultimate load.

A final test was to perform an elastic analysis based on small deformation theory on the channel section and investigate the difference between linear and nonlinear analysis. If the longitudinal stress is considered to be caused by bending only and conventional simple bending theory is applied, the load which causes the flanges to reach yield stress is found to be equal to 194.5 lb/in (34.73 kg/cm). This is 2.5 times greater than the ultimate load using nonlinear analysis. If the longitudinal stresses due to both bending and torsion (warping stress) are considered, the calculation following the procedure suggested in Ref. 165 indicates that the load level which causes initial yielding at the flange-web junction is equal to 105 lb/in (18.75 kg/cm). This is 1.35 times greater than the ultimate load by nonlinear analysis. However, a comparison between the load which causes initial yielding and the load which causes member failure is rather inconsistent. The ratio of ultimate load to initial yielding load using the nonlinear theory is equal to 1.13. If the same ratio is used for the case of linear analysis to predict the approximate load level which causes total collapse of the member, the ultimate load so evaluated is equal to 119 lb/in (21.25 kg/cm) which is 1.53 times greater than that using nonlinear analysis.

#### V.6 A Z-Section Beam Under Uniform Vertical Load, Elastic-Perfectly Plastic Material

An unlippped z-section beam is formed by simply moving the top flange of the previous channel section to the other side of the web. All other data including dimensions, material properties, boundary conditions, loading and idealization (see Fig. 71) remain the same. In this case, since the vertical load is applied in the plane of the web which is inclined with respect to the principal axes, the beam is subjected to unsymmetrical bending. Hence, the beam deflects laterally (horizontally) as well as vertically. Due to its lateral deflection and the local deformation of the plate elements, the applied loads are no longer in the same plane as the reactions at the ends and consequently the beam also twists about its longitudinal axis. The results are shown in a format similar to that of the previous investigation for the channel section so that a detailed explanation of each figure can be omitted to avoid repetition.

Figs. 72 and 73 show the twisting and the transverse deflection of the midspan of the beam. Note that in Fig. 73, the curves for Nodes 46 and 47 are lateral (horizontal) deflections while all other curves represent vertical deflections. The two figures clearly indicate that initial buckling occurred at a load of approximately 24 lb/in (4.3 kg/cm). Fig. 74 shows the distribution of twisting angle along different longitudinal sections. Fig. 75 indicates the distortion of the beam. Two cross sections, one at 6 in from the end and one at midspan, which exhibit the largest deformations are shown. Buckling of the web is clearly seen



in this figure and is buckled in the different direction for the two cross sections. Fig. 76 to 78 show the transverse deflections at different location along the span of the beam. The pronounced buckling of both flanges are shown in Fig. 76. In the present case, contrary to the previous channel section, the difference of vertical deflection between the top flange-web junction and the bottom flange-web junction is negligible. This is, of course, because twisting plays a less important role in the z-section. Consequently, only one set of curves is plotted in Fig. 78 which represents the vertical deflection profile of the beam at different load levels.

The computer program detected that the tangent stiffness matrix became non-positive-definite at a load level of 48 lb/in (8.6 kg/cm). After reducing the step size and restarting from the preceding step, the highest load which could be reached with the matrix still remaining positive-definite was 47.7 lb/in (8.5 kg/cm). This indicates that a secondary bifurcation point had been encountered (see further discussion in Section IV.4.B). A close look at the above-mentioned figures supports this point. For example, the curves for Nodes 43 and 45 in Fig. 72 and Nodes 43 and 49 in Fig. 73 show a tendency to reverse their direction of deformation in the region of 48 lb/in (8.6 kg/cm). This is even more pronounced in Fig. 74a and 74b where a reversal in buckling form has clearly been initiated in the center of the beam. The evidence is further demonstrated by the deflection curve for the top flange tip in Fig. 76. It is seen that, in the center region of the beam, the deflection was originally decreasing after initial buckling but later increased again at higher loads.

Using a smaller step size and restarting from the previous step as was done for the case of initial buckling seemed insufficient to bypass this secondary bifurcation point indicated by the illconditioning in the stiffness matrix. Actually, the problem could be continued by further increasing the load and temporarily disregarding the non-positive-definiteness of the tangent stiffness matrix. It would eventually converge to its secondary path within a few load steps through a "snap through" type of buckling, providing a secondary path indeed exists and the applied load step size is small enough. Application of an iterative technique within each step is preferred in this case. However, the "snap through" type of buckling occurs with a dynamic disturbance and is unacceptable for a structural member in service. Computation was consequently terminated and it was concluded that the beam failed due to elastic instability.

The distribution of average longitudinal stresses corresponding to the failure load of 47.7 lb/in (8.5 kg/cm) is shown in Fig. 79 and 80. In Fig. 79, the stress is plotted at a section through the center of the last transverse row of elements adjacent to the midspan section. The variation is almost entirely linear and is mainly due to there being no material-nonlinearity involved. It is seen that the stresses in the flanges vary from compression to tension or vice versa, and are different in magnitude. This indicates that the effect of lateral bending is significant. Fig. 79 and 80 show that the stress in the beam is still mainly controlled by vertical bending as expected.

According to the CSA Standard (Clause 9.2 of CSA S190-1968), the gross cross-section of the beam may be used for the calculation of deflection in the working range. Based on such an assumption and following



the approximate solution method suggested in Ref. 264, the vertical deflection of the beam is calculated and plotted as a dotted line in Fig. 78. The error at the center of the beam, compared to the non-linear analysis, is about 15%.

In this Z-section beam, the maximum stress occurred at the flange-web junctions. If the gross cross-section is considered fully effective in carrying loads (i.e. the effect due to local buckling is ignored), a linear elastic analysis based on Ref. 264 shows that yielding will occur at a load of 97.2 lb/in (17.4 kg/cm). If local buckling is considered by employing the effective section in accordance with Clause 12.4 of CSA S190-1968, the allowable load which causes the maximum allowable stress of 19.0 ksi ( $1335.8 \text{ kg/cm}^2$ ) as specified by the code, is found to be 32.8 lb/in (5.86 kg/cm). When this load is multiplied by a ratio of the yield stress of 35 ksi ( $2,460 \text{ kg/cm}^2$ ) to the allowable stress, the yield load as predicted by the Standard becomes 60.4 lb/in (10.8 kg/cm). It should be noted that these linear elastic analyses based on Ref. 264 do not include the effect due to twisting. Furthermore, these loads are the failure loads corresponding to the yielding of the beam whereas, the 47.7 lb/in (8.5 kg/cm) load of the present study is the failure load defined by the secondary bifurcation point (elastic instability) of the member.

## CHAPTER VI

### SUMMARY AND CONCLUSIONS

#### VI.1 Summary

The definition and methods of fabrication of thin-walled members and the problems associated with two types of nonlinearity is first introduced. A comprehensive survey of published literature on the geometric and/or material nonlinear behaviour and the ultimate strength of thin-walled structures has been attempted with particular emphasis on the post-buckling aspects of the problem. After identifying some of the inadequacies of available methods of analysis, a finite element displacement model is proposed as the most promising vehicle for a comprehensive study of nonlinear problems.

The general technique of using the finite element method to solve nonlinear problems is summarized and presented in a simple conceptual manner. The different available coordinate systems for such a formulation are described and different methods for handling nonlinear terms are introduced and examined. All the current commonly used solution procedures have been classified and briefly described. The references relevant to nonlinear finite element analysis are also cited.

The present formulation is then developed in detail based on the principle of virtual work and the related variational principle of potential energy. The element selected is a flat rectangular element with six degrees of freedom per node which can be identified as physical quantities (i.e. linear displacements and rotations) and transformed as vector components. The present formulation differs from others published recently,

in that the degrees of freedom chosen permit the analysis of non-planar structures involving slope discontinuities. The strain-displacement relations and the incremental theory of plasticity which incorporate geometric and material nonlinearity respectively, are described briefly. Both the equilibrium equations and the incremental equilibrium equations have been developed. The equations which are formulated based on the principle of virtual work and the principle of stationary potential energy are proved to be identical. Finally, the Modified Cholesky Decomposition Scheme in tridiagonal form and in matrix notation are presented in detail.

A computer program is then developed to incorporate the above mathematical formulation. The computer program has the following main features:

1. No limitation on the size of the problem: All the Dimension Statements in the computer program are written with variable arguments. Only one-dimension statement card in the main program needs to be changed to incorporate the problem size. Hence the storage used will be neither insufficient nor wasteful.
2. Matrix transformation only performed at non-coplanar joints: This permits saving of storage required and computing time which may be significant, particularly for larger sized problems.
3. Choice of number of integrating points: The number of Gaussian points and layers are read into the computer as input data. Hence, the user may choose the preferred accuracy for each problem.

4. Restart facility: The displacements, stresses and strains after each step are stored on disks so that they can be read as input data for a subsequent run, if the analysis is to be continued further or if the program has, for some reason (e.g. insufficient time, computer breakdown, etc.), terminated before the required load level is reached.
5. Variable load increments, maximum number of iterations, and allowable error tolerance: All these quantities are treated as input data, thereby permitting complete flexibility to allow the user to control the problem. The structure may be loaded either by specifying forces or displacements.
6. Automatic change of step size and number of iterations: The error of the result is compared against the allowable tolerance at each iteration and at each step. When the comparison is favourable, the computing is immediately shifted to the next load step with a lesser number of iterations being performed. The step size is also adjusted to be greater, the same, or smaller in accordance with the result of the comparison. If the error suddenly grows and becomes rather high, the analysis will be terminated automatically for investigation.
7. Detection of ill-conditioned stiffness matrix: The character of positive-definiteness in the tangent stiffness matrix of the structure is always checked and assured throughout the analysis.

The computer program was used to analyse a variety of plate problems and when compared with other published solutions, good agreement was found in all cases. In some cases, the analysis was continued beyond the load for which other solutions were available. The agreement with

experimental results, when available, was also found to be very good.

A comparison of CPU time was attempted whenever possible, which indicated that the present computer program is quite efficient.

Finally, a few of the most commonly used thin-walled sections were analysed from zero load up to failure. Members were loaded as columns as well as beams. Different types of material with respect to their strain hardening characteristics were involved. Comparisons with experiments carried out by others were good in some cases. However, in other cases, some discrepancies did exist. The reasons for such discrepancies were explained. In a few problems, a comparison of the results with the current Canadian Standard for Light Gauge Aluminum and with conventional linear elastic analysis have also been made.

## VI.2 General Conclusions

The structures analysed in Chapters IV and V amply demonstrate the feasibility as well as the reliability of the present formulation in representing the nonlinear behaviour and the ultimate strength of thin-walled planar and non-planar structures. The choice of the finite element method as the method of analysis permits the program to handle arbitrary loading, cross-section geometry, boundary conditions and material properties.

Comparing the results with other solutions indicates that the present results are sometimes stiffer and sometimes more flexible. This is actually the character of the ACM element<sup>225,226</sup> which is employed as the bending part of the present element. In most cases, the present element gives results somewhat on the stiffer side.

As for the solution procedure, experience from the present study indicates that the Newton-Raphson method is more favourable in the elastic range. Even though this method requires the regeneration of the stiffness matrix, actually the extra computing time is paid back by rapid convergence and with better accuracy. It is recommended that the Newton-Raphson method should be used as far as possible. For the type of problem where the structure fails immediately after initial yielding, the Newton-Raphson method can be used throughout the entire loading history without difficulty. However, for problems where the structure only fails after heavy yielding, the Newton-Raphson method generally will encounter convergence problems due to severe plastification prior to the collapse of the structure. In this case, the strict step-by-step procedure should be applied instead and often one is forced to use a smaller step size and a higher error tolerance. It is felt that the problem has not really been solved but rather avoided by a sacrifice in the computing cost and in the accuracy of the results. Some technique is needed to attack this problem which should be a challenging topic for further research.

Another problem is the lack of general agreement on which terms (displacements, stresses, or others) should be used to evaluate the accuracy of the results and how they should be evaluated. It is hoped that a conclusion which is acceptable to all researchers can be found in the near future.

### VI.3 Behaviour and Ultimate Strength of Thin-Walled Sections

Owing to the large variety of shapes and sizes in which thin-walled sections are produced, it is rather difficult to draw general conclusions. The emphasis in this dissertation has been on developing a computer program such that particular situations could be studied in detail. However, the following observations, although strictly applicable to the types of structures analysed in the last chapter, may be of more general interest.

The ultimate strength of the structure, in addition to being affected by the boundary conditions, seems also to be somewhat affected by the loading conditions. When the member is loaded as a column, the stress distribution is simpler. The main stress is the longitudinal stress in the direction of loading while the transverse stress and shear stress remain comparatively low. Each component plate does not seem to be influenced appreciably by the presence of adjoining plates. The member generally fails quickly after initial yielding. On the other hand, if the member is loaded as a beam, the stress distribution is more complicated. The influence from adjacent plates is significant and the transverse stress and shear stress may also become high. The member, then, generally seems able to carry a somewhat higher load after initial yielding.

The inclusion of strain hardening may significantly increase the ultimate strength of the structure.

The initial local buckling load often has no marked significance as far as the growth of deflections and stresses are concerned.

The strength of webs loaded locally may be significantly underestimated by the existing CSA/Standard formula.

The calculation of deflections at working loads on the basis of beam theory using the gross cross-section as permitted by the CSA Standard may be quite inaccurate. Since it is almost certain that local buckling will always occur in thin-walled sections, a calculation based on an effective section would be more reasonable.

The ultimate strength of thin-walled sections is generally reached only well after initial elastic buckling. At the stage of ultimate load, the structure is often greatly deformed. Consequently, the serviceability of the structure becomes doubtful prior to reaching the ultimate load. Hence, a close examination of serviceability may be more meaningful than the blind use of the full extent of post-buckling strength up to the yielding or ultimate strength of the structure.

Secondary buckling which may be encountered in thin-walled members is not considered in the present CSA code. Current literature has dealt with this problem in qualitative terms only and further investigation and understanding of this problem for thin-walled sections is needed.

The conventional linear elastic analysis over-estimates the strength of thin-walled section greatly and may not even be a useful approximation.

Finally, it should be noted that many of the aspects noted above such as the distortion of the cross-section, the effect of lateral restraints, the determination of deflections in the post-buckling range and the progress of the yielding area, can not be analysed satisfactorily by other methods. Furthermore, although thin-walled sections have been



the main topic of interest in this dissertation, the program developed herein should be applicable to a much wider range of problems involving geometric and/or material nonlinearities.

#### VI.4 Recommendations for Future Work

The following recommendations are suggested to extend the scope of the computer program developed herein for the purpose of more general usage.

1. Consider the material to be anisotropic: The treatment of anisotropy in the theory of plasticity can be found in Ref. 234. The relevant work done by Pifko et al.<sup>173,253</sup> is worth consulting.
2. Take account of strain hardening due to cold-forming: Advantage of using higher yield stresses in the cold-bended regions is currently permitted in the design of cold-formed steel members. This provision might lead the present program to be more realistic when applied to cold-formed structures.
3. Provide a feature to include initial stress: One of the most common types of initial stress is the residual stress generated due to welding. With this feature, the present program can be applied to thin-walled plate girders which are widely used in bridge and industrial building construction. Work by Crisfield<sup>144,145</sup> can be consulted.
4. Develop a subprogram to generate the stiffness matrix using triangular elements: The geometry of thin-walled sections in the present study is limited to the folded-plate type. With

the facility of triangular elements being available, the present program could be used to analyse a larger variety of thin-walled structures such as spherical shells, cylinders, etc..

5. Carry out a systematic study of thin-walled members: Parameters such as the geometry of lips, the optimum width of compression flanges, and the geometry of spacing of stiffeners should be investigated. This could be achieved, for example, by starting with a simple rectangular plate and adding lips of varying sizes (or shapes) and loading them in axial compression or simple bending.

#### VI.5 Discussion of Computing Cost in Non-Linear Analysis

Even though research on the use of finite elements to solve either geometric or material nonlinear problems has been conducted extensively during the last fifteen years, work on combined nonlinear problems has been rare. The most important reason is obviously due to the high computing cost. It is not uncommon for many researchers to prefer to perform experimental tests in their investigations simply because it is less expensive. However, it should be remembered that almost all these experiments are conducted within university laboratories and the main cost is the test specimens which are relatively inexpensive. It is doubtful that a comparison between the material cost in the one case and the computing cost in the other is fair. If the same experimental work were performed by an industrial consulting firm, the salaries paid for technicians and others working on the project may perhaps be as much, or even more, than the computing costs. In that sense, computing costs are not as high as is generally believed.

Furthermore, a theoretical analysis provides a number of advantages over an experimental investigation. In addition to its availability for the detailed study in deflection, stress, strain, yielding, etc., as previously pointed out in Chapter I, another important factor is time. The results, which can be obtained from a computer in a matter of minutes can only be achieved by performing experimental tests in days or even weeks.

Due to the necessity of iterative procedures in solving nonlinear problems, computing costs are always higher than for linear elastic analysis no matter whether the finite element or any other method is used. This must be accepted as a fact as long as a nonlinear analysis has to be performed. It is felt that it should not be a question of whether a theoretical analysis is to be conducted or not. Theoretical analyses should always be encouraged. It is really a matter of how to develop new techniques to further reduce the computing cost in both software and hardware. Other ideas such as using a less accurate formulation but having the advantage of a considerable saving in computer time should also be promoted. Crisfield<sup>144</sup>, who proposed an "area approach" formulation using an approximate Ilyushin yield criterion (a similar method using finite differences was proposed by Massonnet<sup>123</sup>) provides a good example. In conclusion, more research should be conducted on the improvement of efficiency in the formulation and solution procedures to reduce unnecessary computing to a minimum.

FIGURES

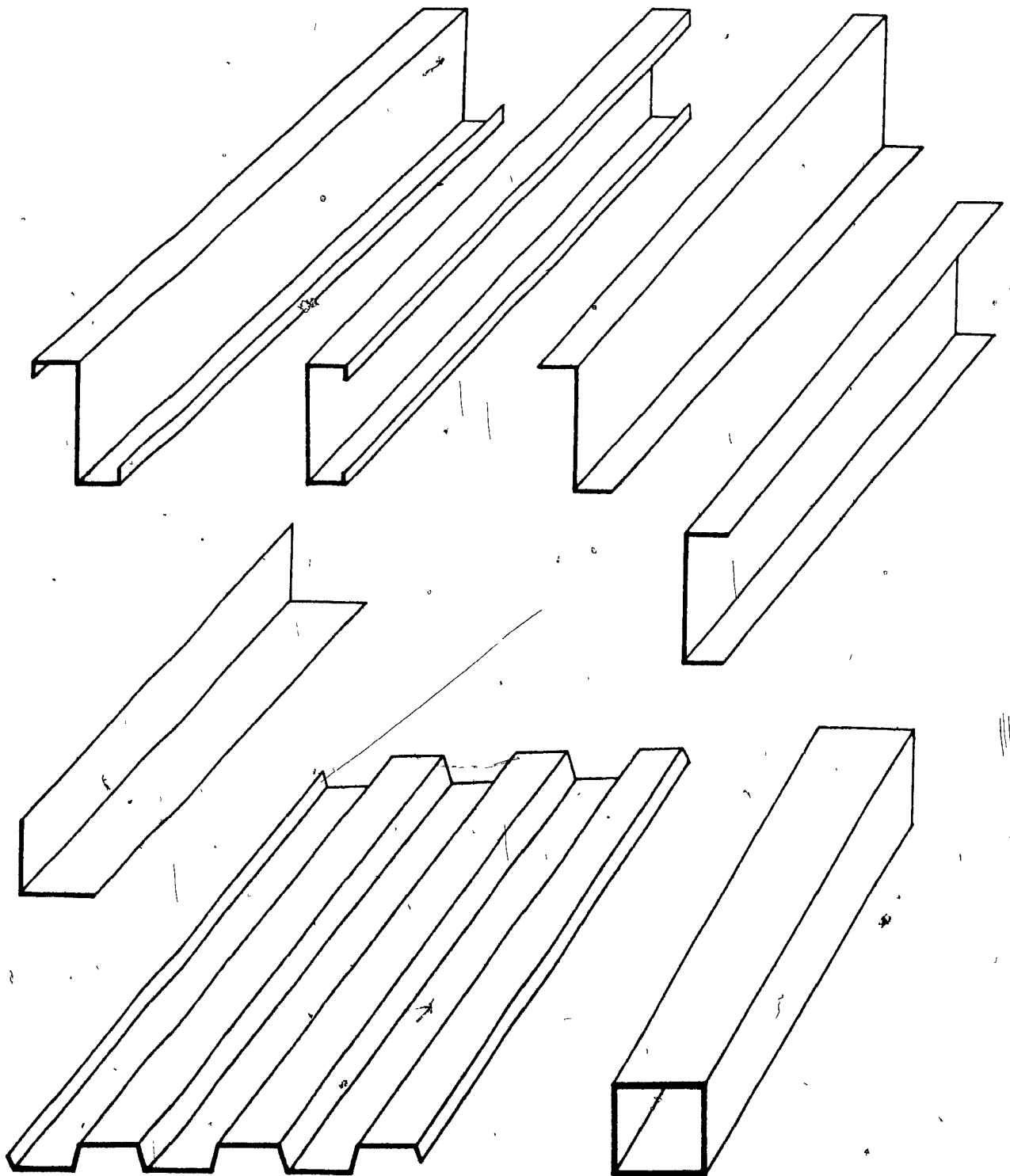
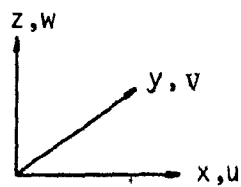
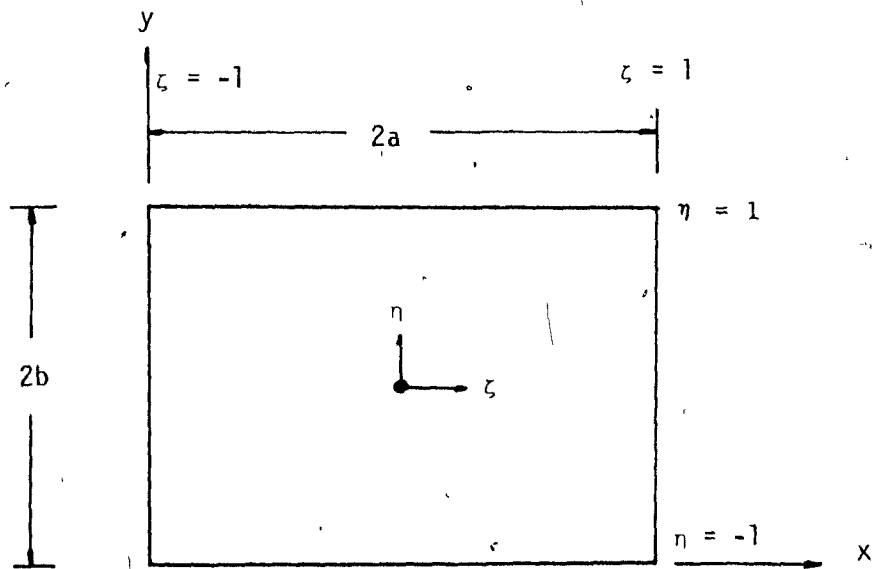
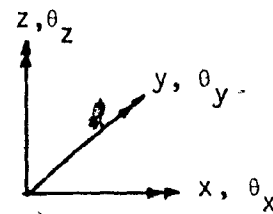


Figure 1      Some Common Shapes of Thin-Walled Members



translation



rotation

$u_i$

$v_i$

$w_i$

$$\theta_{zi} = \left( \frac{\partial v}{\partial x} \right)_i$$

$$\theta_{xi} = \left( \frac{\partial w}{\partial y} \right)_i$$

$$\theta_{yi} = - \left( \frac{\partial w}{\partial x} \right)_i$$

Figure 2 Geometry of the Element and Degrees of Freedom

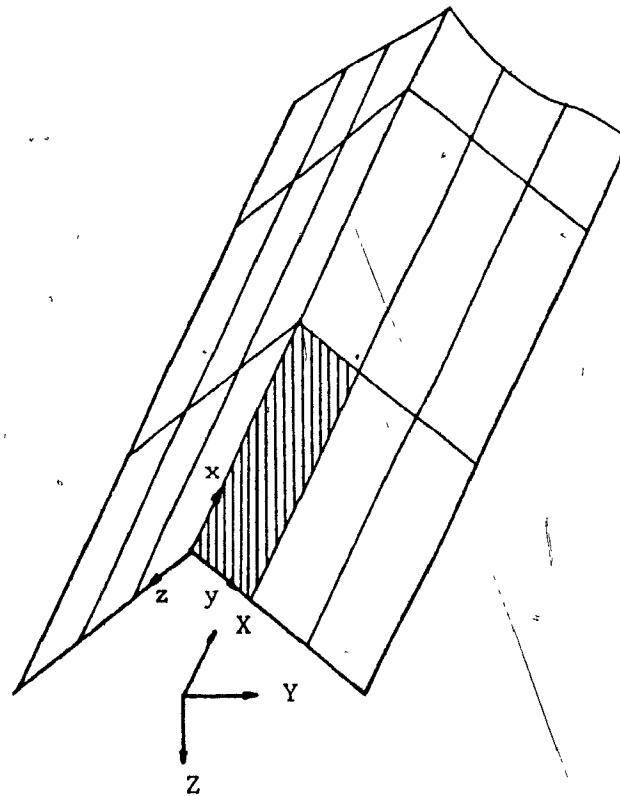


Figure 3 Global and Local Coordinates

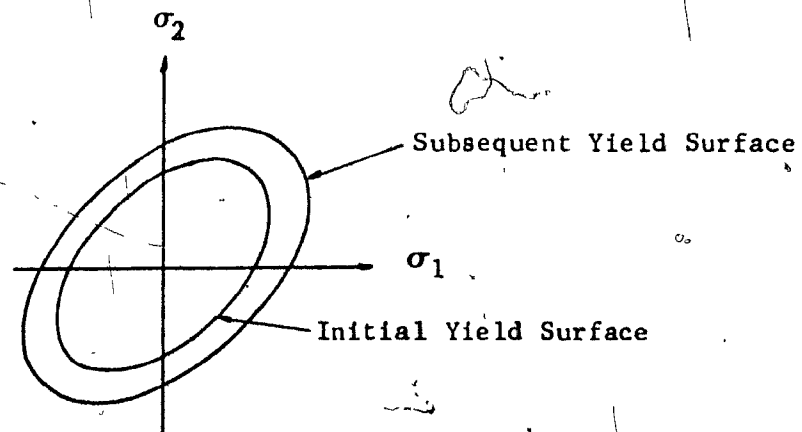


Figure 4 Von Mises Yield Surface and Isotropic Hardening

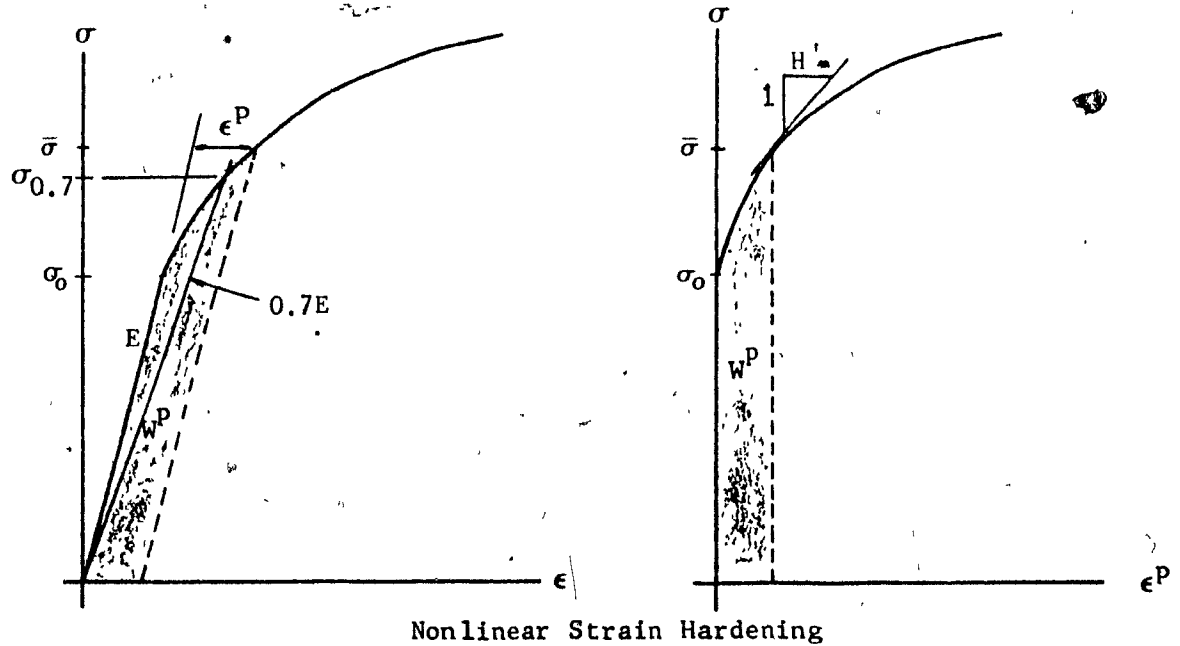
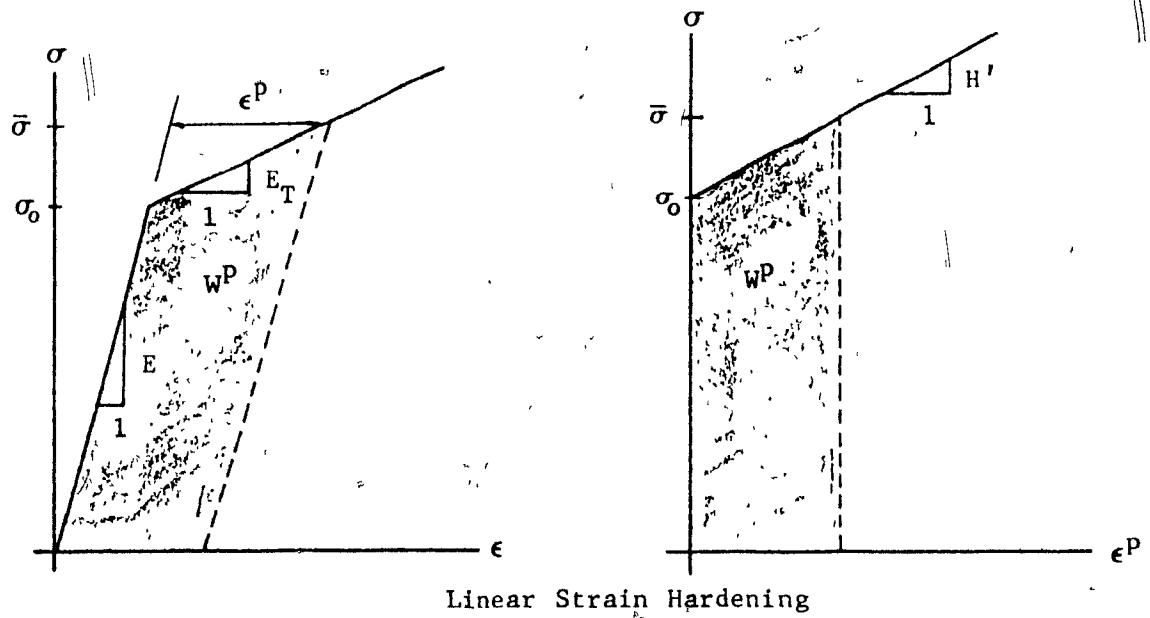


Figure 5 Uniaxial Stress-Strain and Stress-Plastic Strain Curves



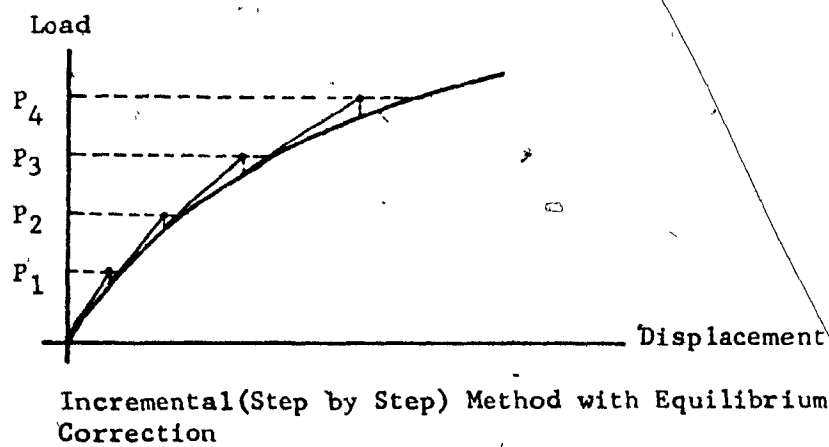
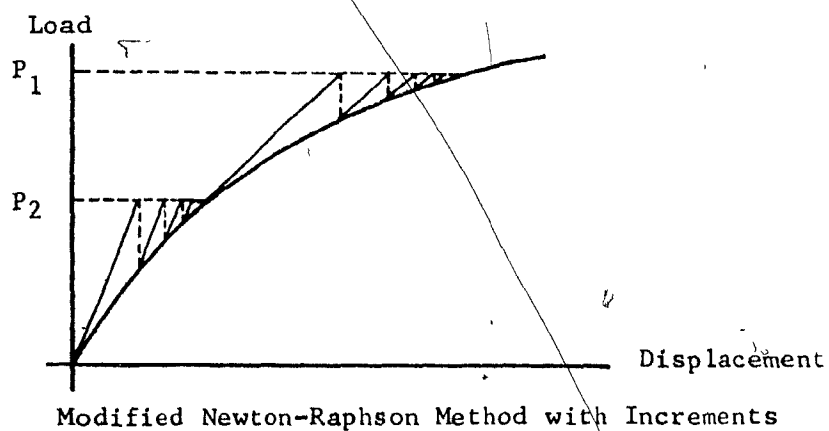
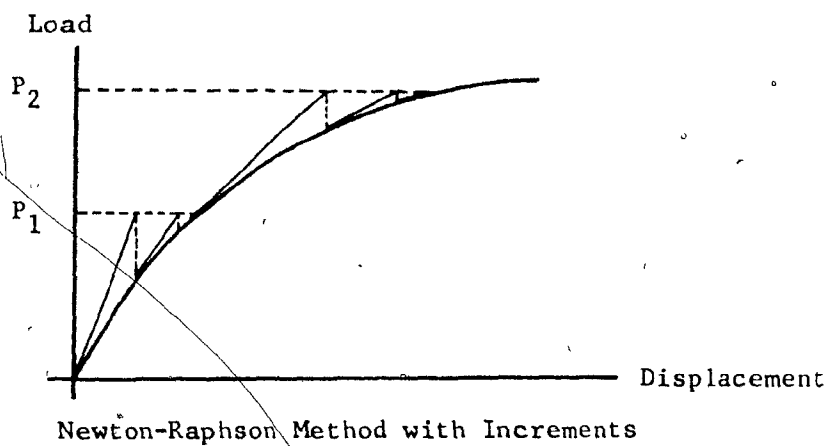


Figure 6 Numerical Solution Methods

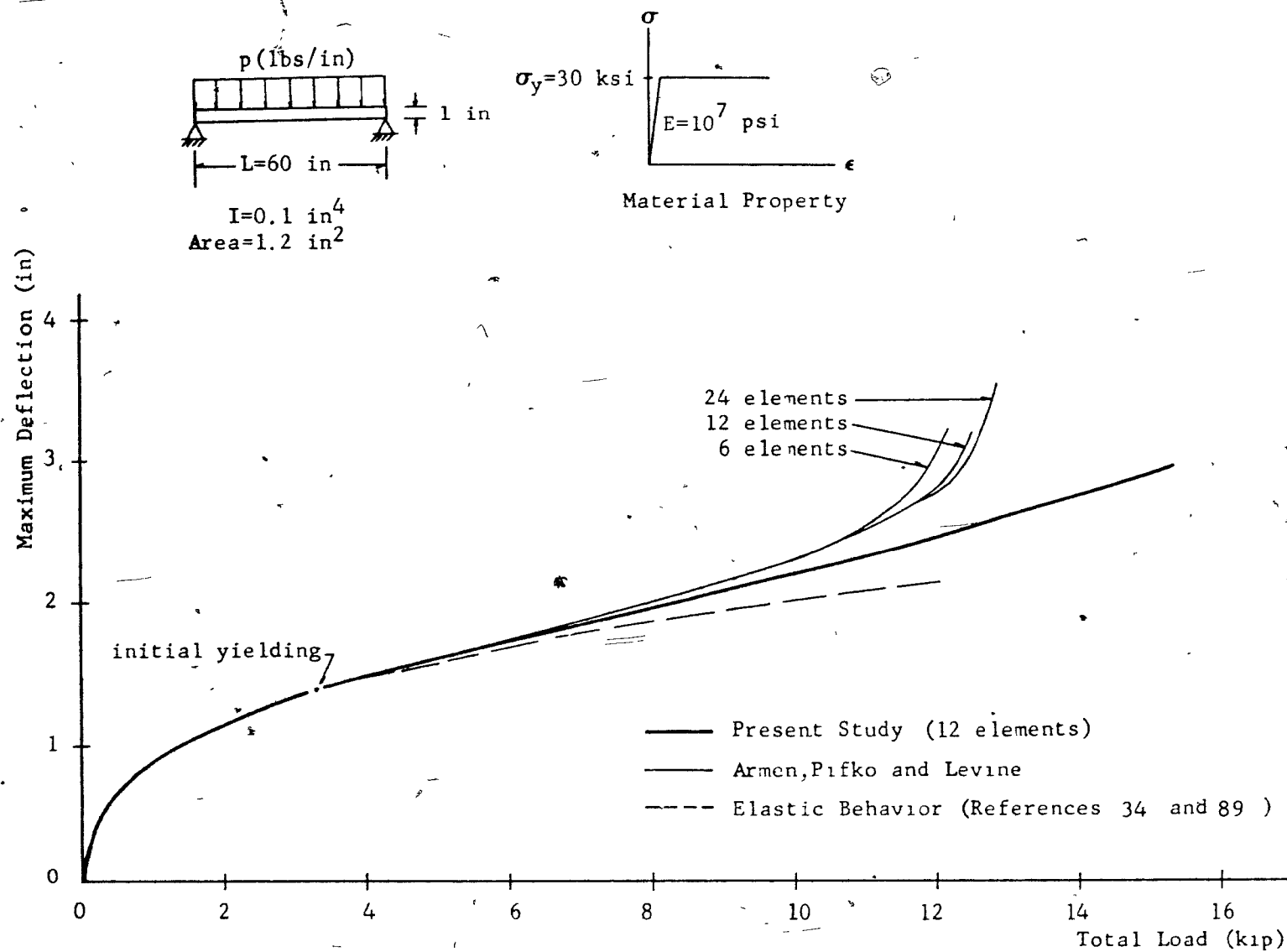


Figure 7 Elastic-Plastic Response of a Restrained Beam

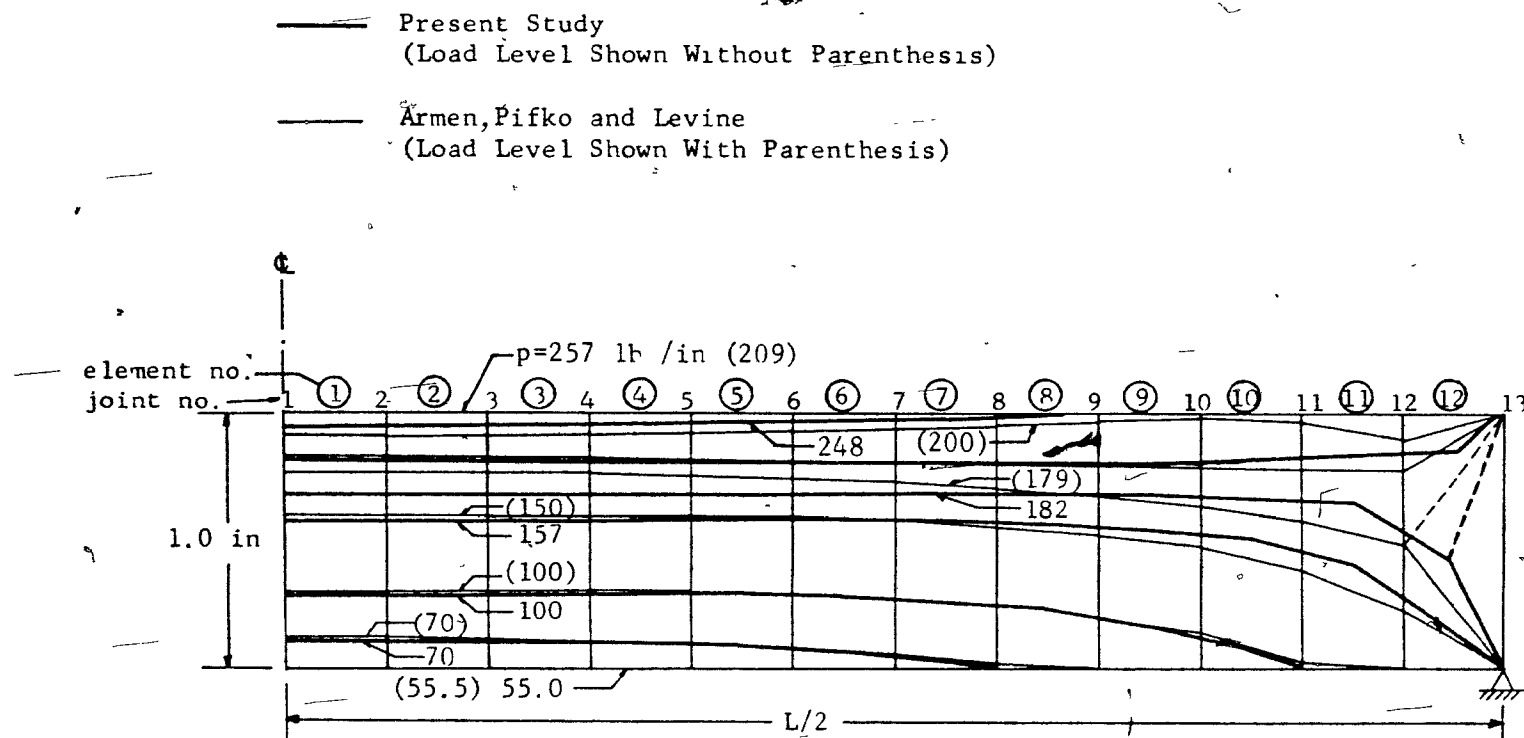


Figure 8 - Progression of Elastic-Plastic Boundary in a Restrained Beam for Increasing Load

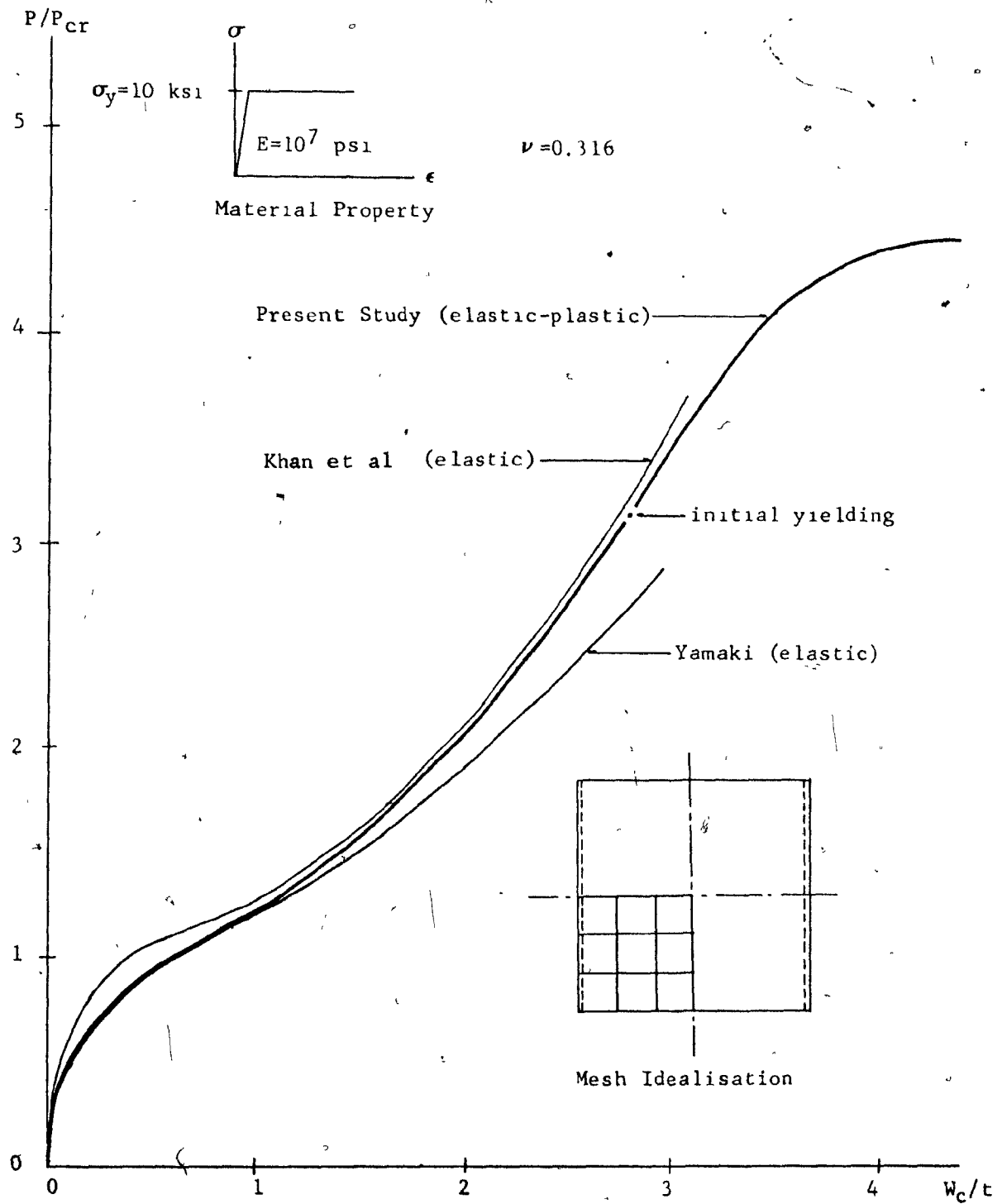


Figure 9 Simply Supported Square Plate With In-Plane Load, (  $b/t=192$  )

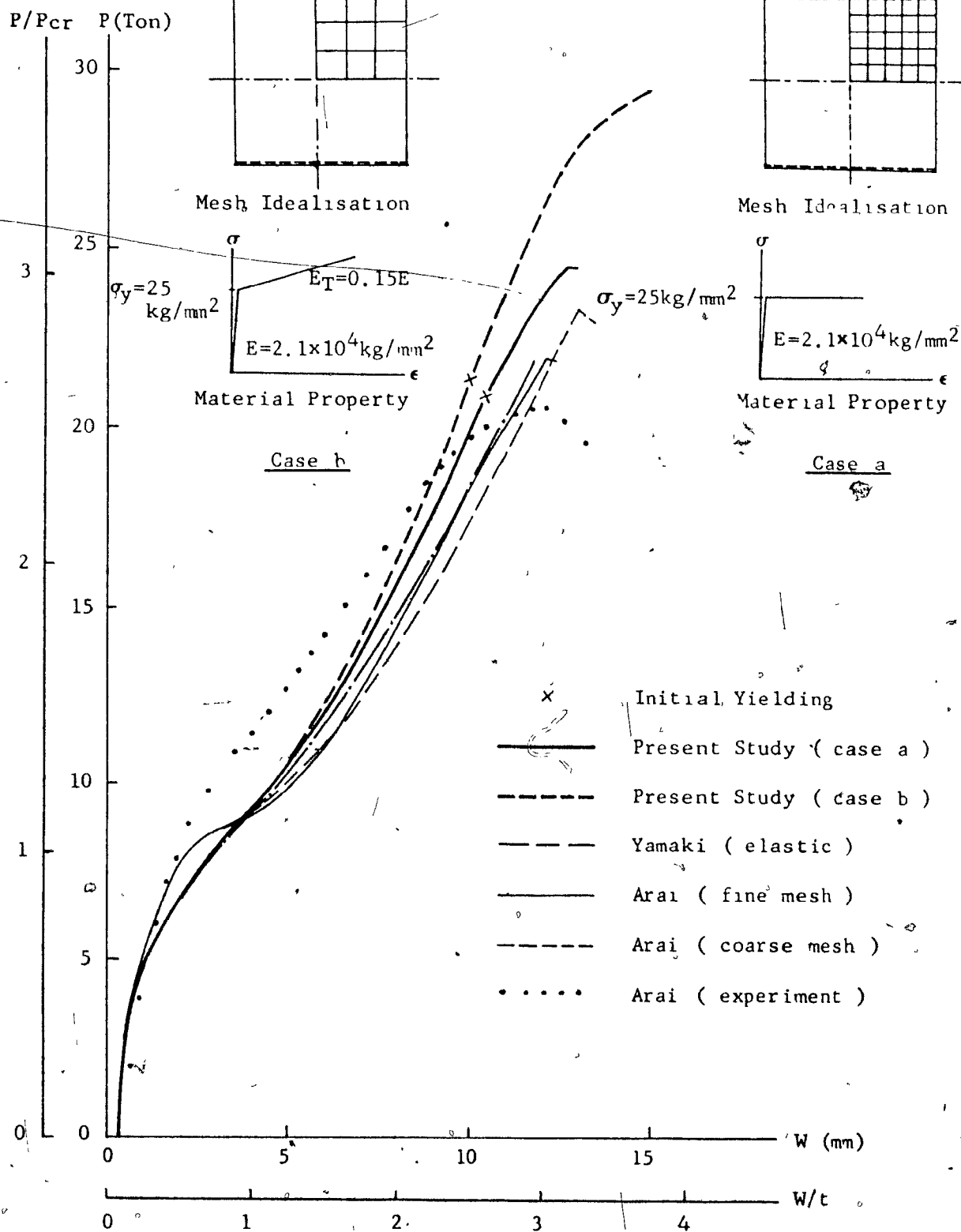


Figure 10 Load-Deflection Curves of Simply Supported Square Plate ( $b/t=150$ )

— Present Study  
(Load Level Shown Without Parenthesis)

- - - Arai  
(Load Level Shown With Parenthesis)

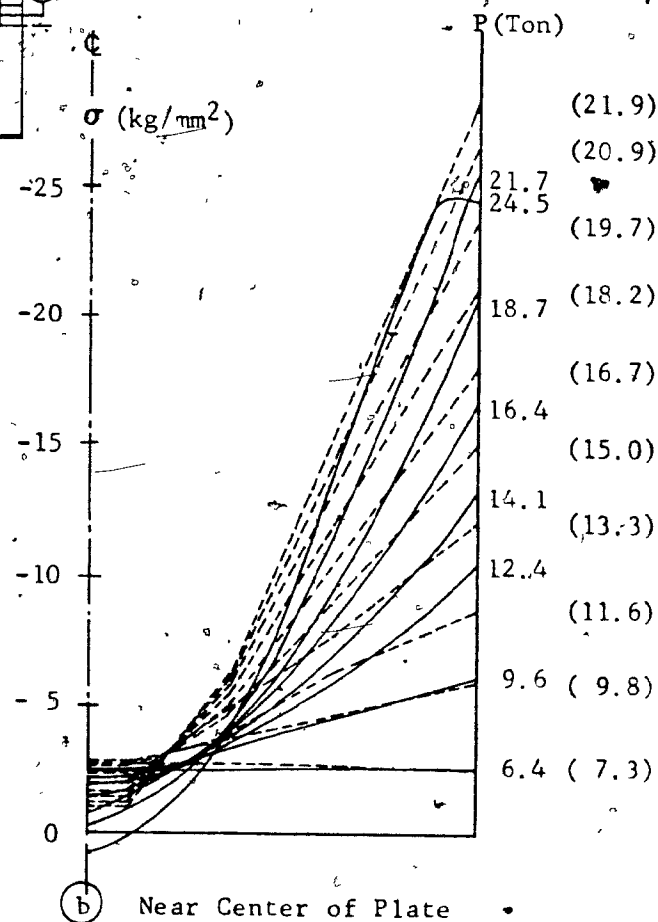
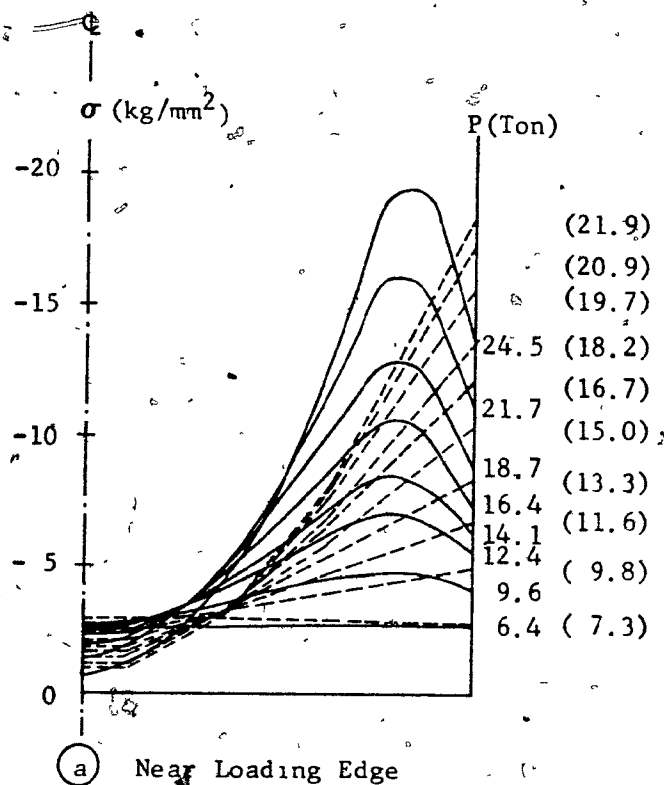
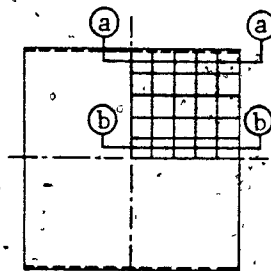


Figure 11 Stress Distribution of Simply Supported Square Plate

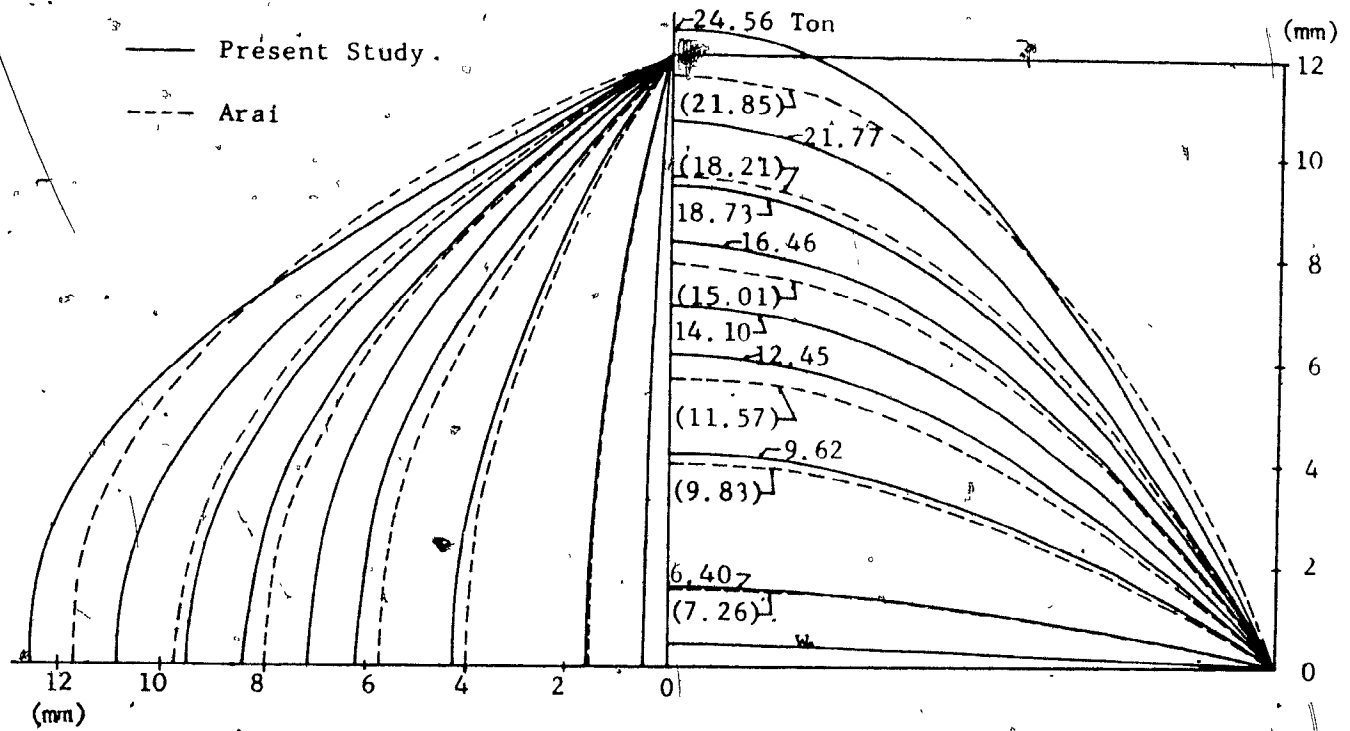


Figure 12 Lateral Deflection of Simply Supported Square Plate

	Arai	Present Study
Computer Model	IBM 370-155	IBM 360-75
Number of Elements	32 Triangular	25 Rectangular
Number of Joints	25	36
Core Memory Required	256 K	186 K
Computing Time Per One Loading Step Per One Iteration	140 Seconds	32 Seconds

Table 1 Comparison of Computing Time

Arai

Present Study

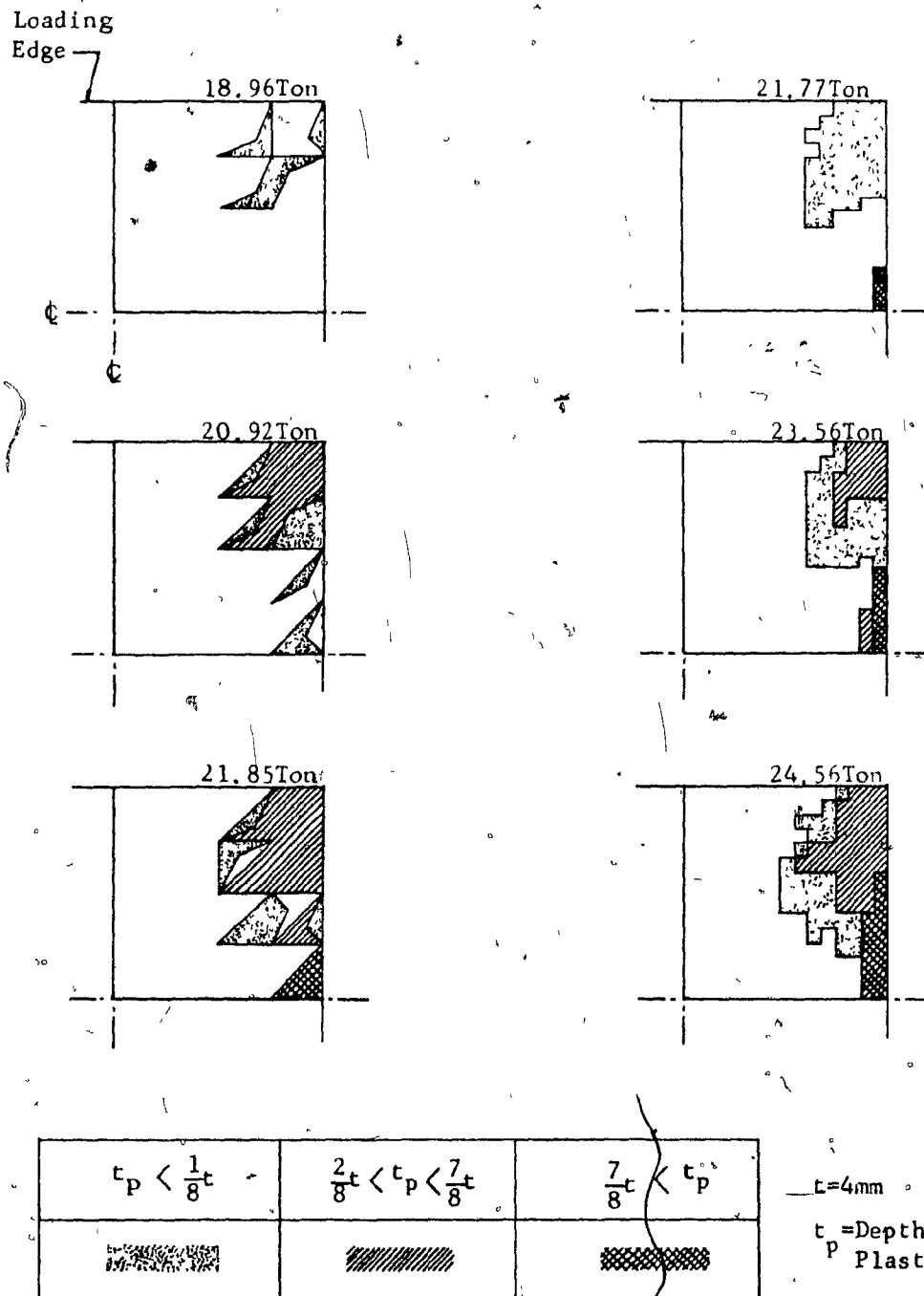


Figure 13 Extension of Plastic Area in Square Plate



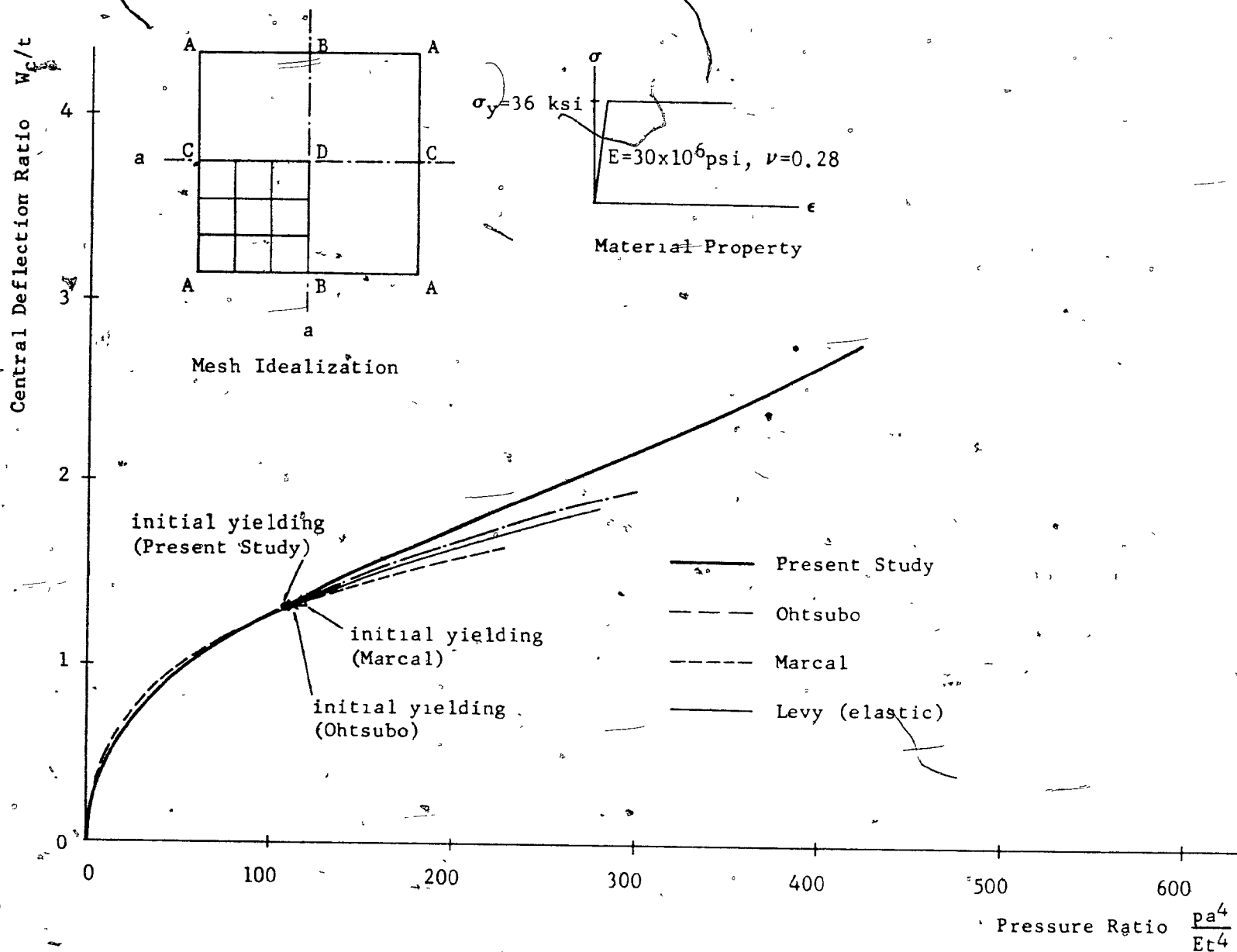


Figure 14 Response of Restrained Square Plate Under Uniform Pressure

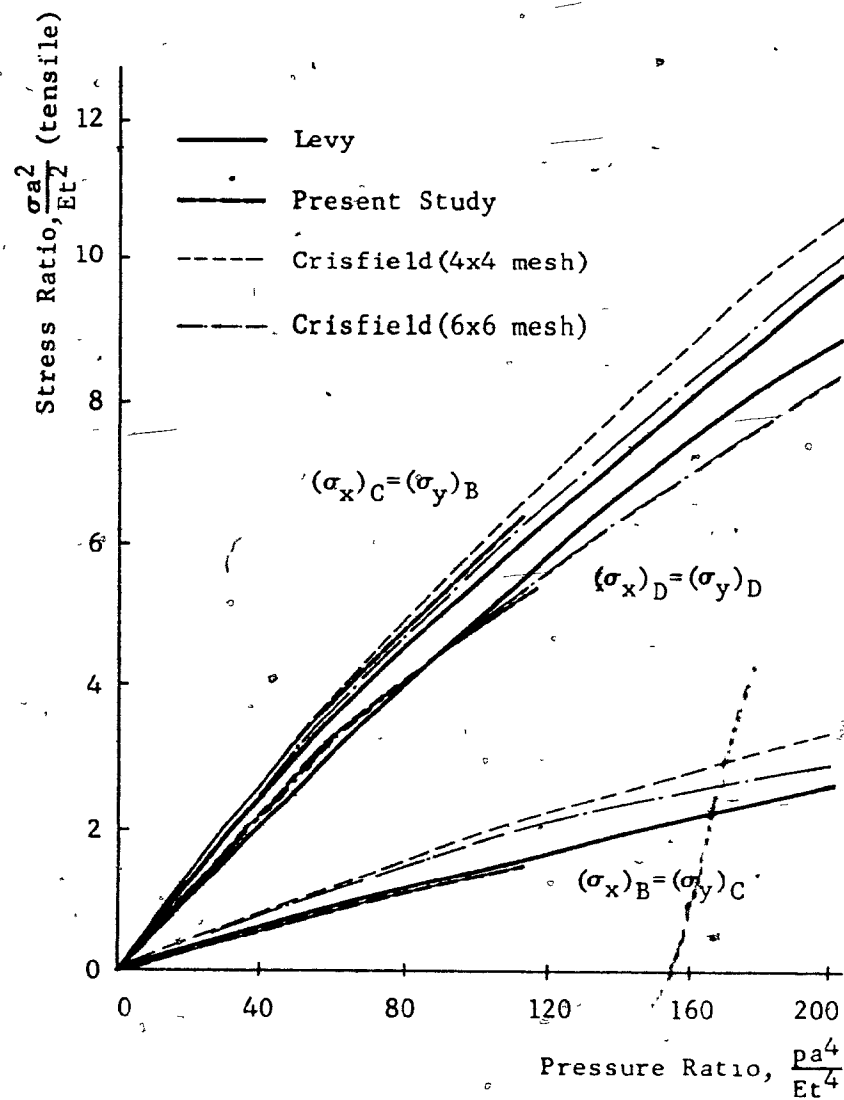


Figure 15. Restrained Plate Under Uniform Pressure.  
Elastic Membrane Stresses

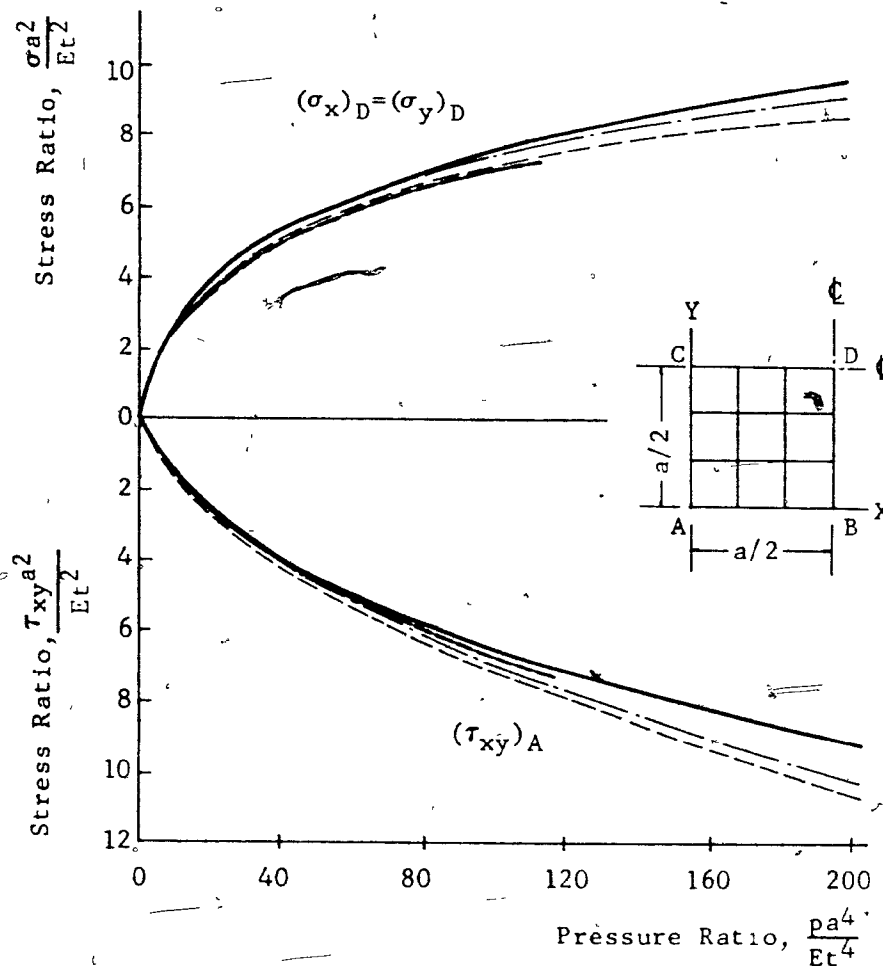
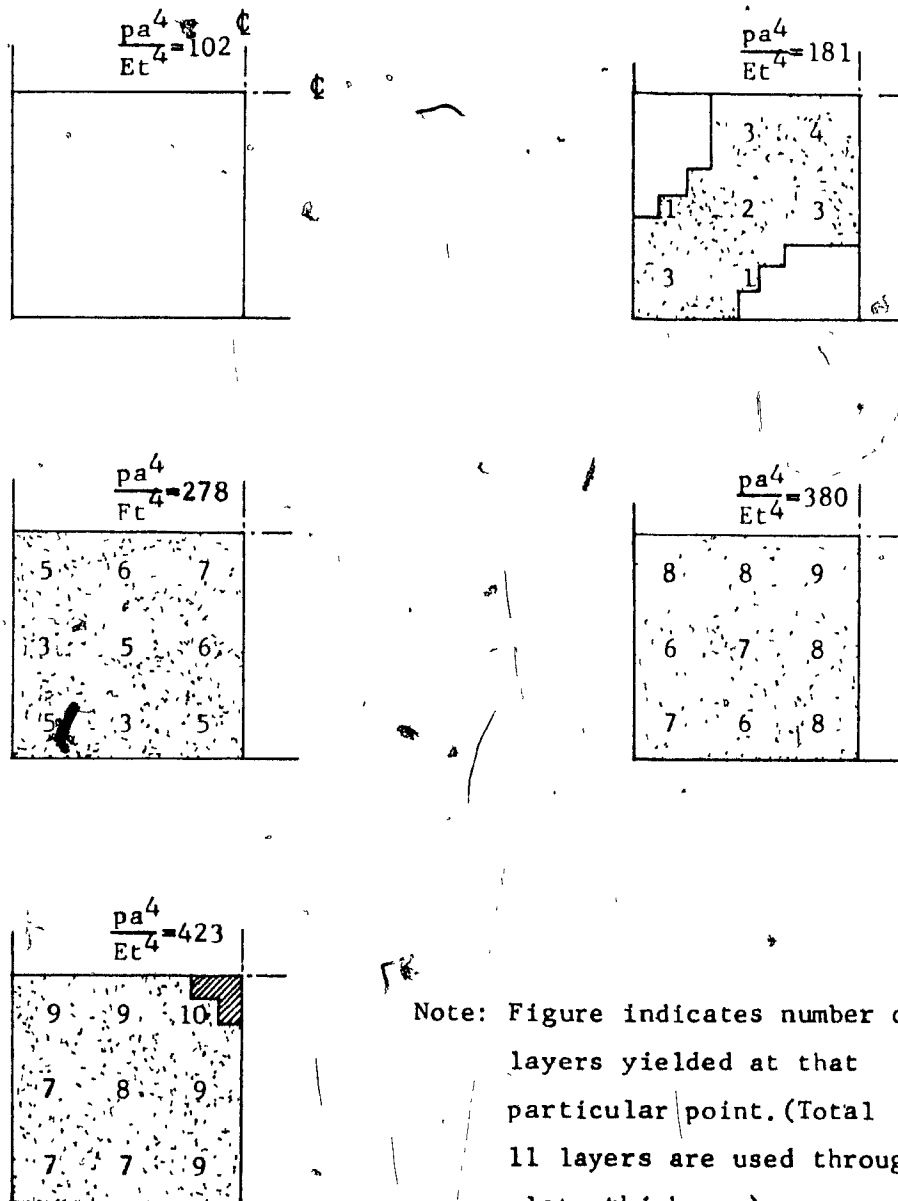


Figure 16. Restrained Plate Under Uniform Pressure.  
Elastic Extreme Fibre Bending Stresses



Note: Figure indicates number of layers yielded at that particular point. (Total of 11 layers are used through plate thickness)

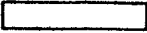


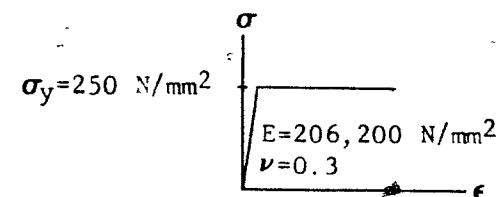
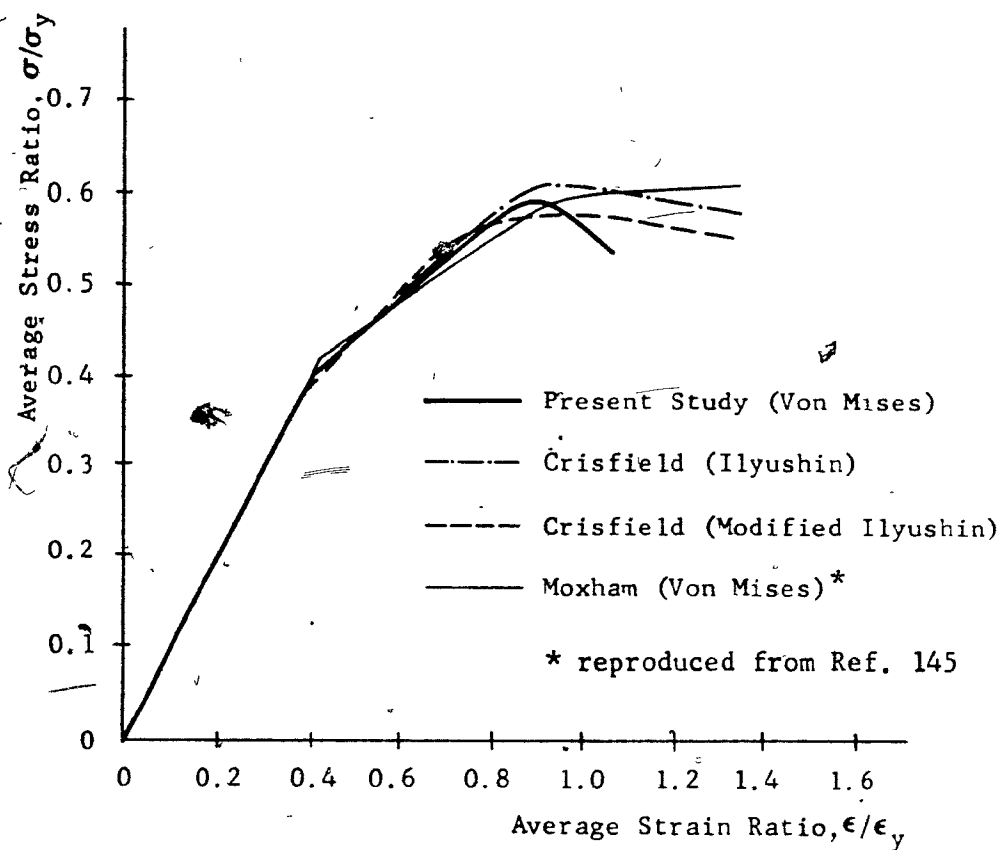
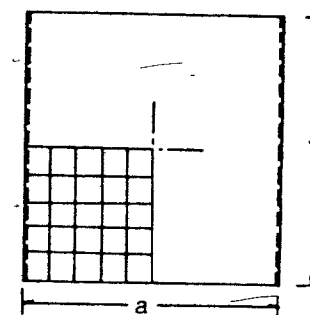
Fully Elastic	Partially Yielded	Fully Yielded
		

Figure 17 Progression of Plastic Zone in Restrained Plate



Material Property



Mesh Idealization

$b/t=80$ ,  $a/b=0.875$

$t=3.175 \text{ mm}$

Figure 18 Average Stress - Average Strain for Simply Supported Rectangular Plate ( $a/b=0.875$ )

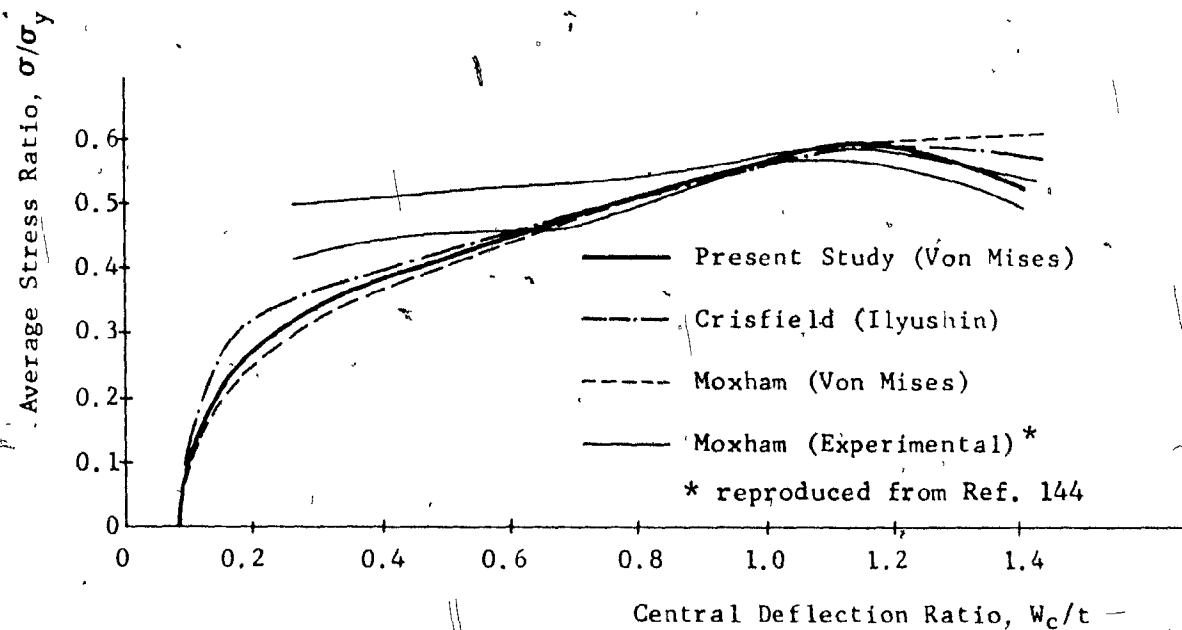
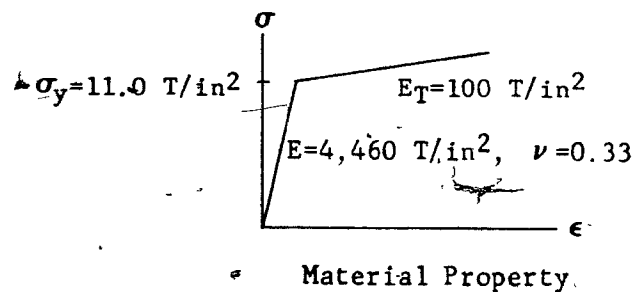


Figure 19 Average Stress - Central Deflection for Simply Supported Plate

Program	Computer Model	Core Memory	Type of Increment	Mesh	No. of N-R Iterations	Time - Mins.	
						CPU	Total
LADEP or LADEP2	TRRL ICL 4/70	107 K (Single Precision)	elastic	4x4	1 - 2	1.1	2.3
LADEP			plastic	4x4	1 - 2	1.2	3.0
LADEP2			plastic	4x4(x3)	5 - 6	2.9	5.5
LADEP2			plastic	4x4(x5)	5 - 6	4.1	8.0
Present Study	IBM 360/75	186 K (Double Precision)	elastic	5x5	2	1.06	1.36
			plastic	5x5(x9)	4	2.22	2.76

Table 2 Computer Times per Increment



$a/b = 3.72$   
 $b/t = 48.9$   
 $t = 0.25 \text{ in}$

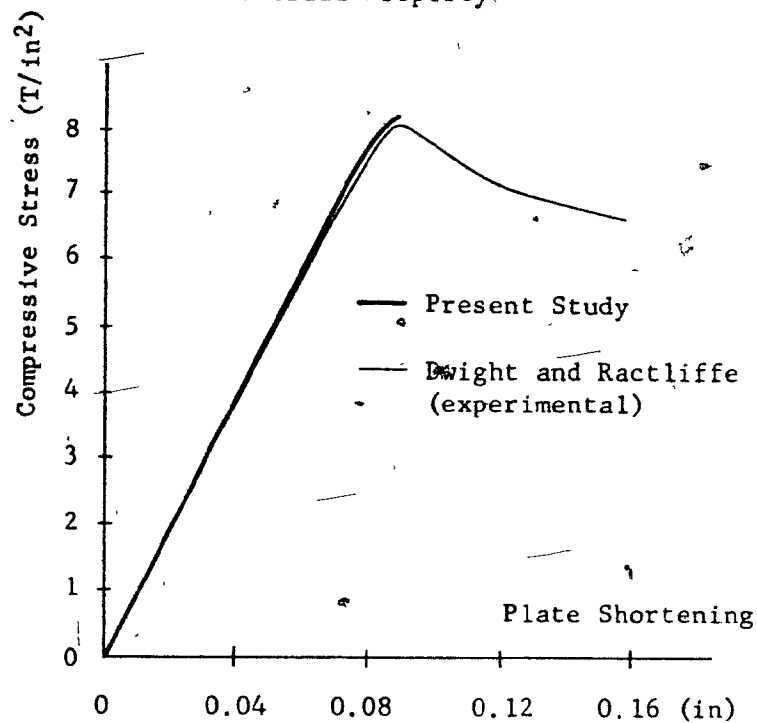
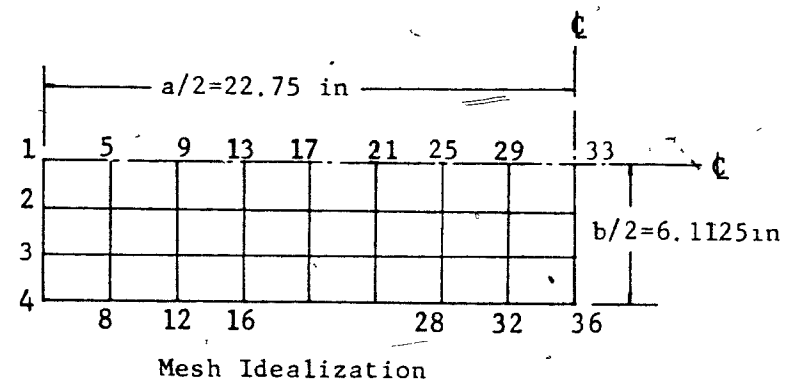


Figure 20 Load - Shortening Curve for Simply Supported Rectangular Plate

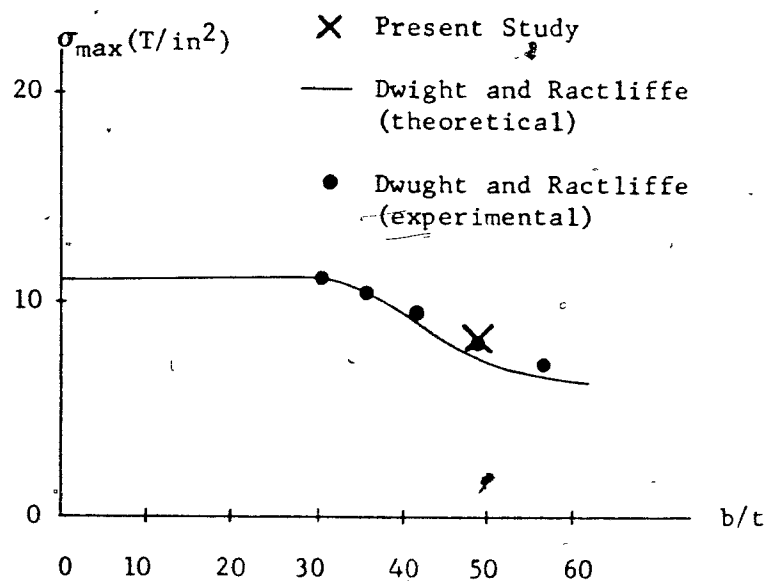


Figure 21 Relation Between Ultimate Strength and Width-Thickness Ratio for Simply Supported Rectangular Plate

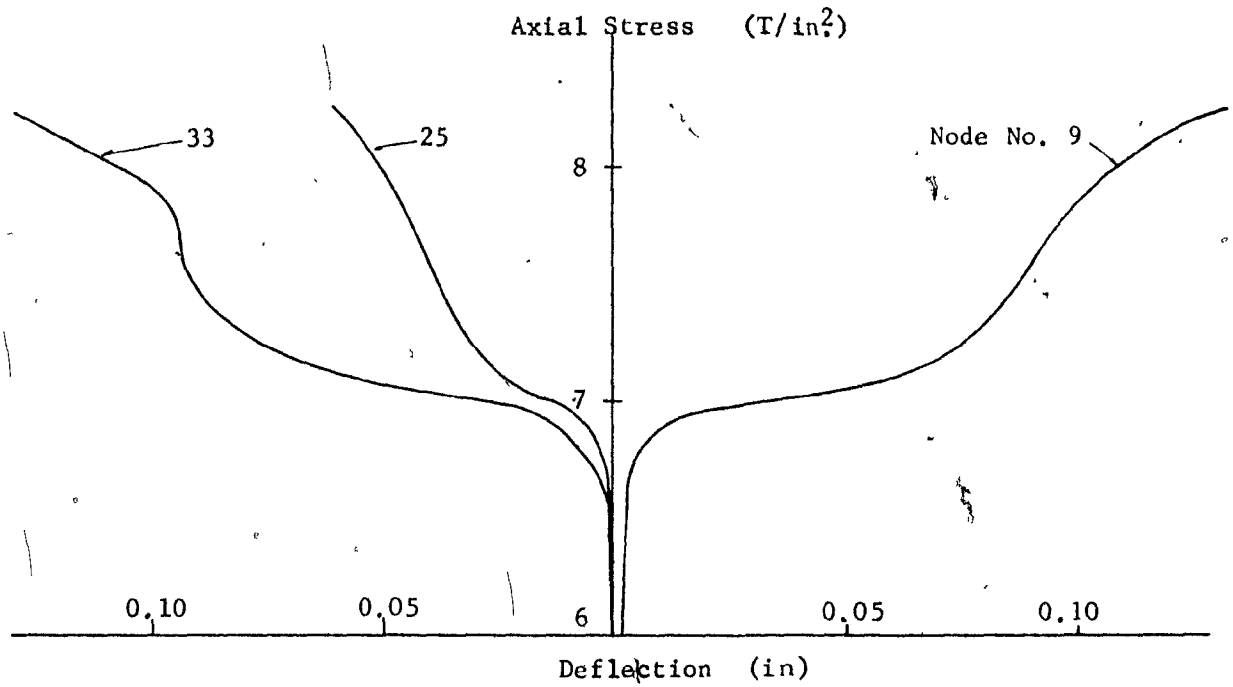


Figure 22 Load-Deflection Curves for Simply Supported Rectangular Plate

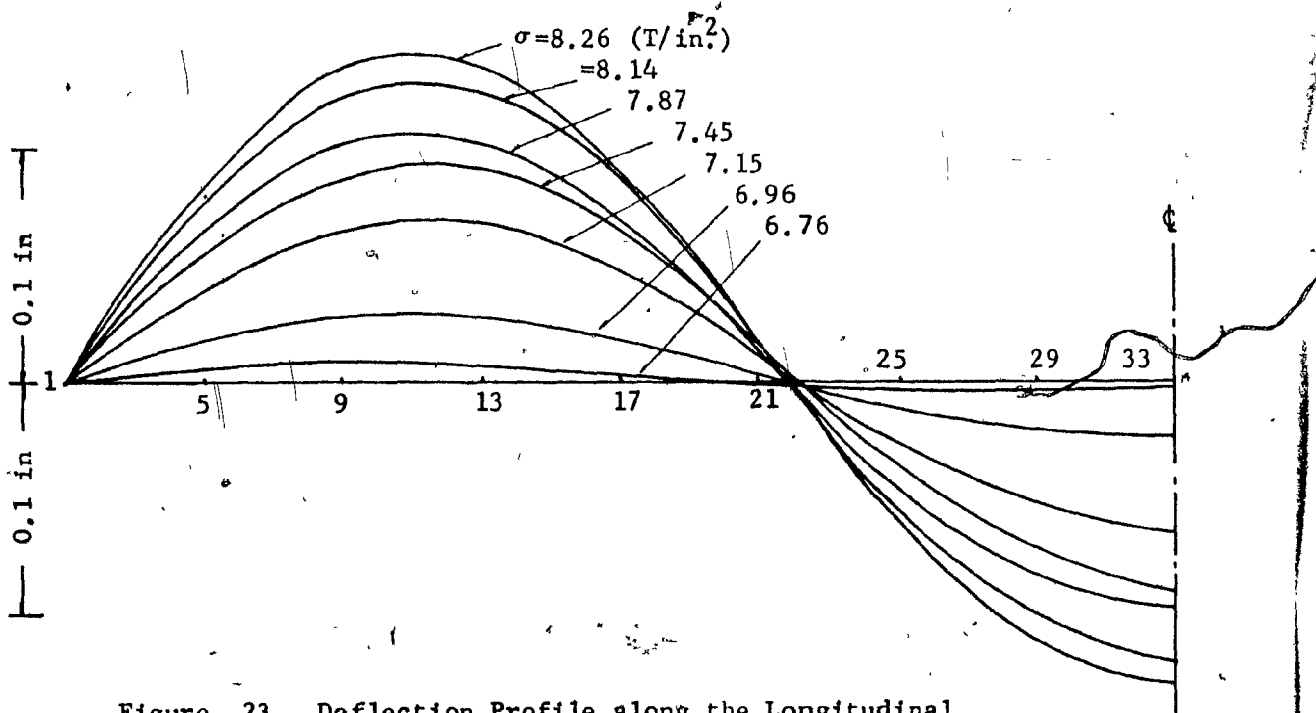


Figure 23 Deflection Profile along the Longitudinal Center Line of Rectangular Plate

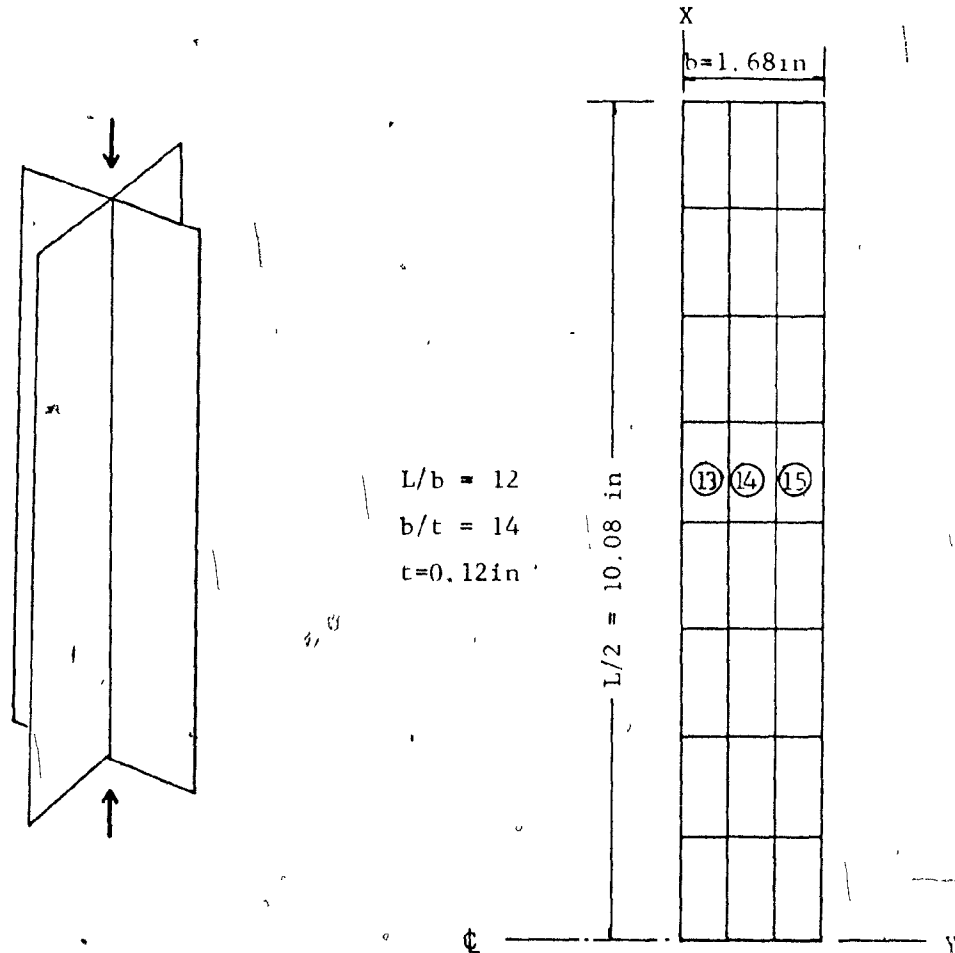


Figure 24 A Cruciform Section and Idealization

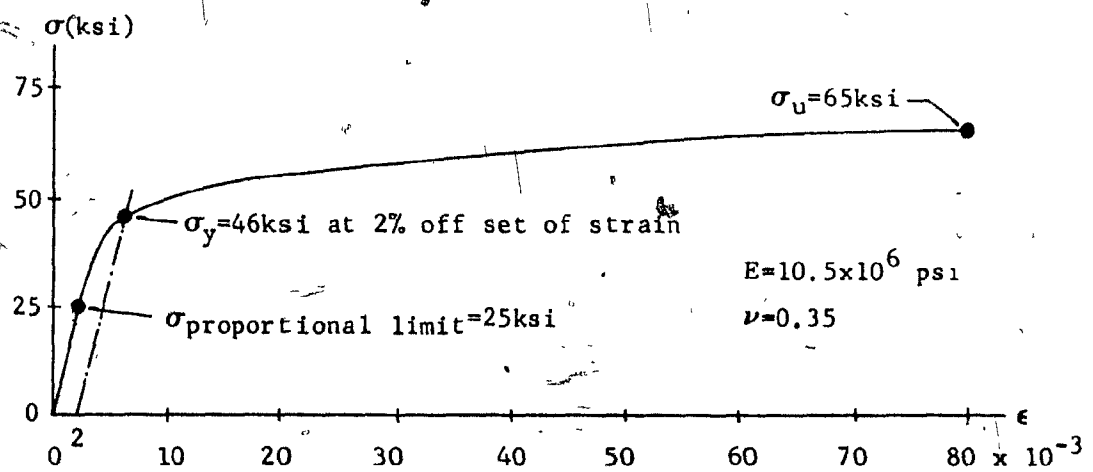


Figure 25 Material Property of Cruciform



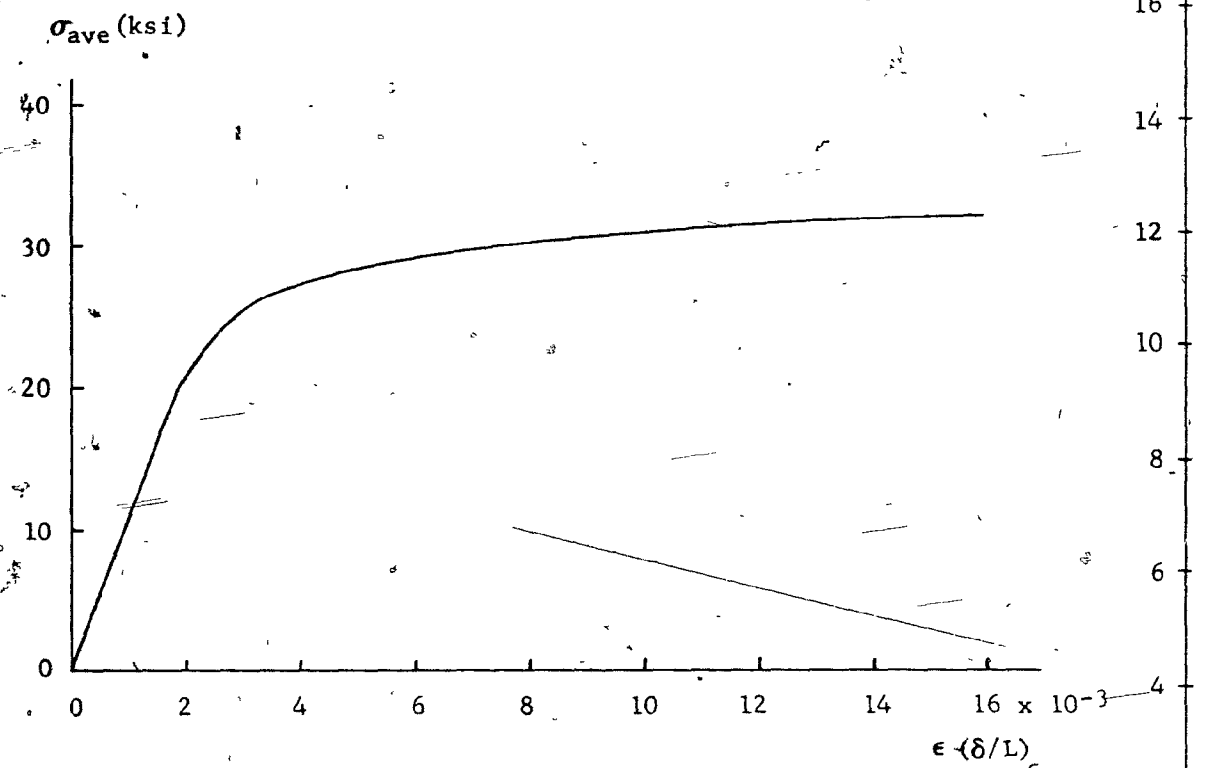


Figure 26 Average Stress - Average Strain for Cruciform Section

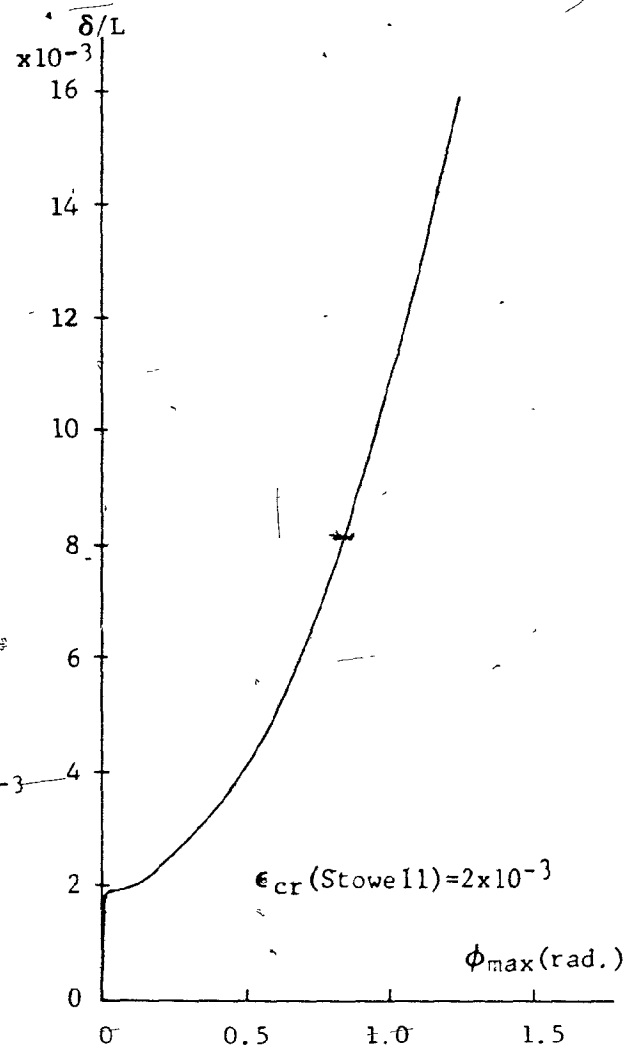
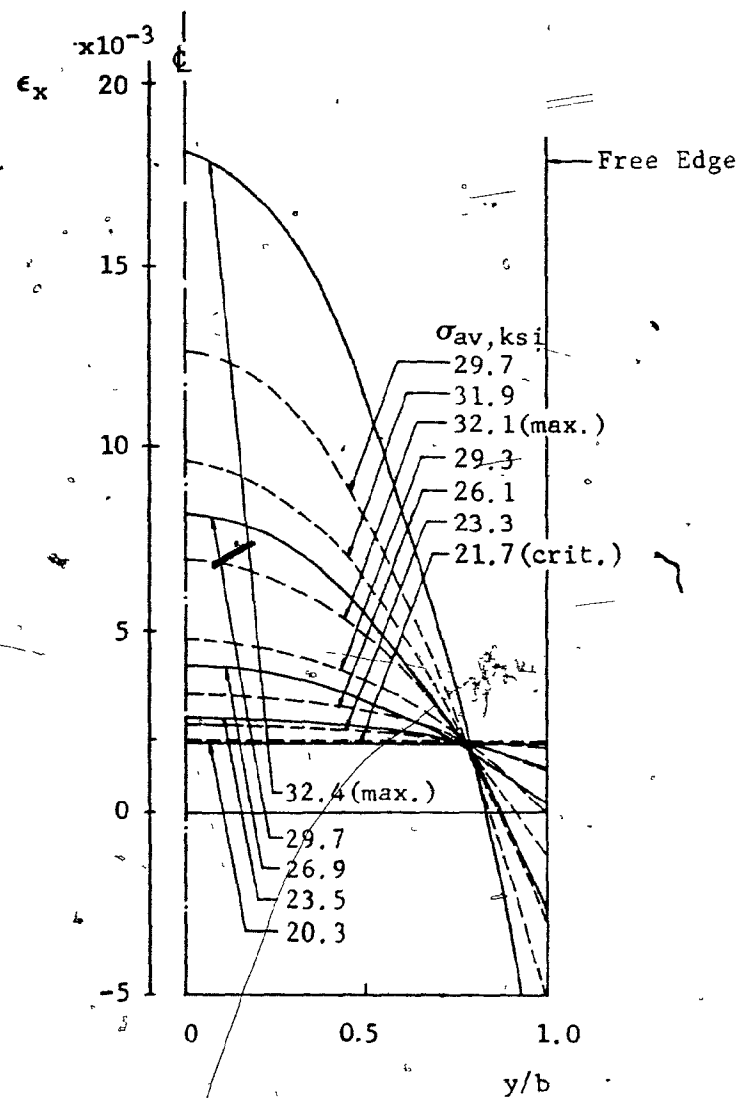
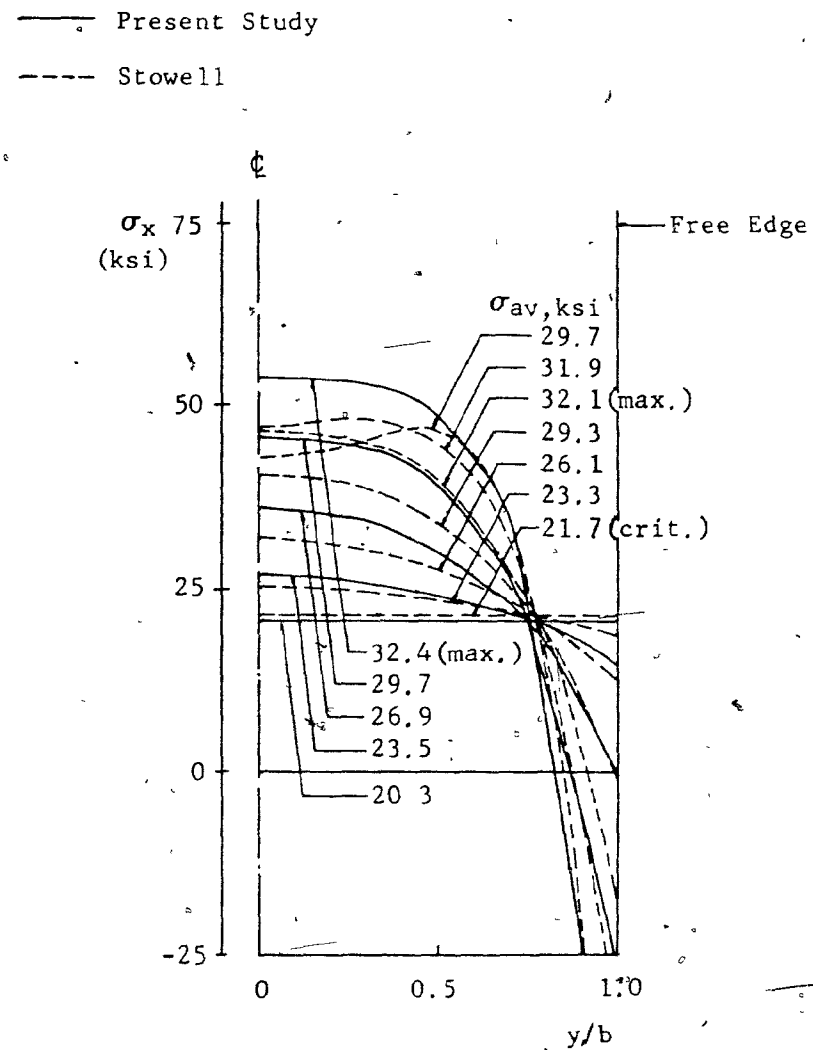


Figure 27 Shortening - Rotation of Cruciform Section



(a) Strain Distribution



(b) Stress Distribution

Figure 28 Strain and Stress Distribution Across a Flange of a Cruciform

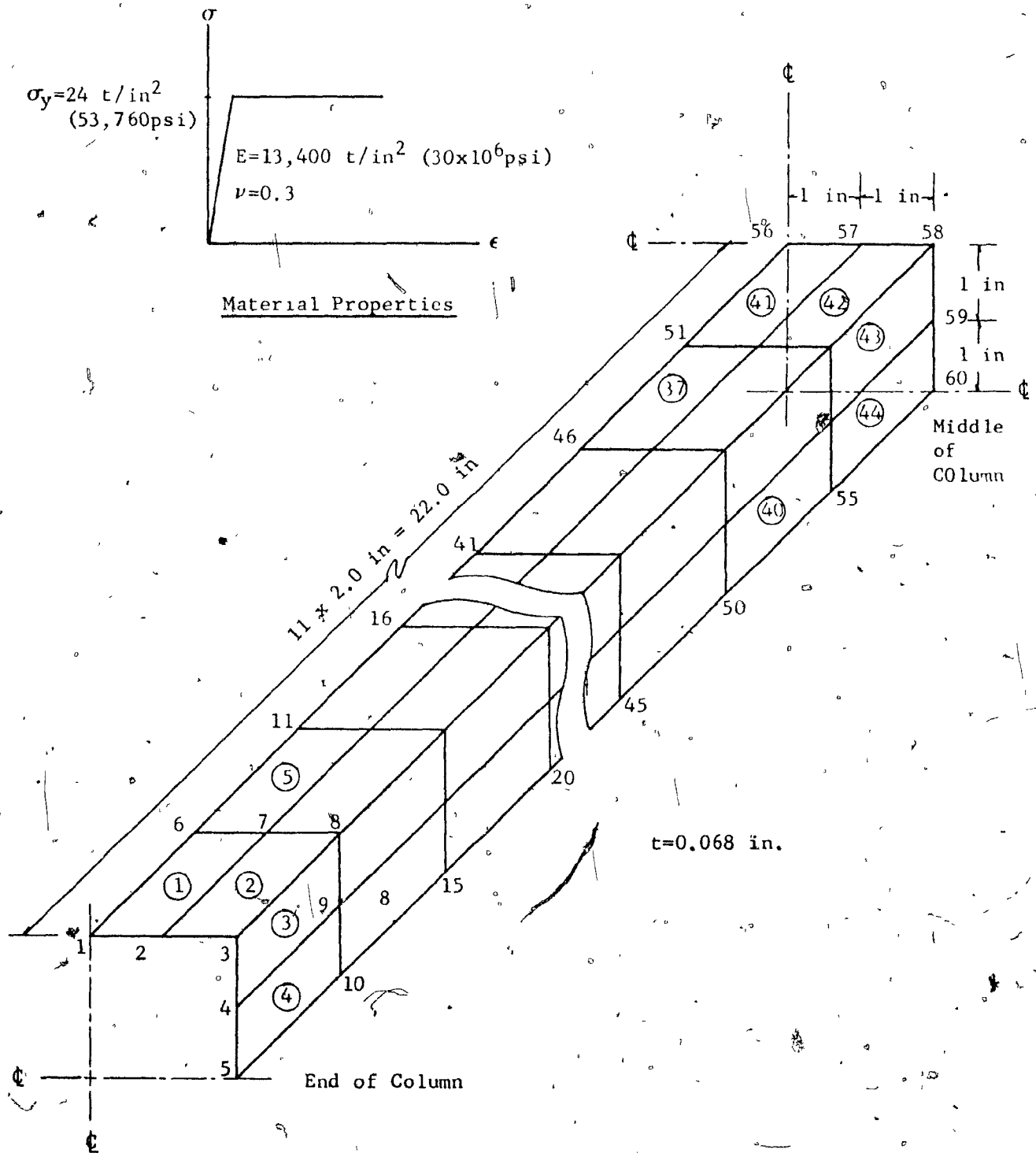


Figure 29

Idealization for Square Column

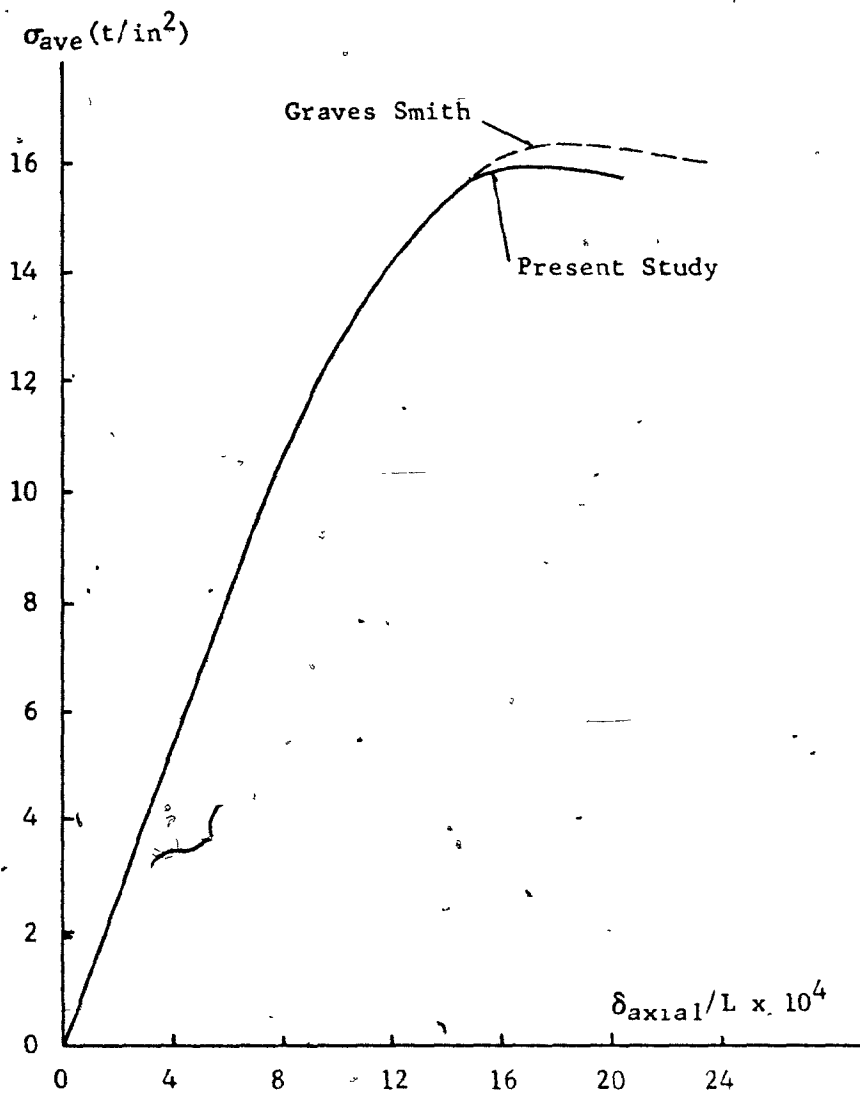


Figure 30 Stress - Strain Curve of Square Column

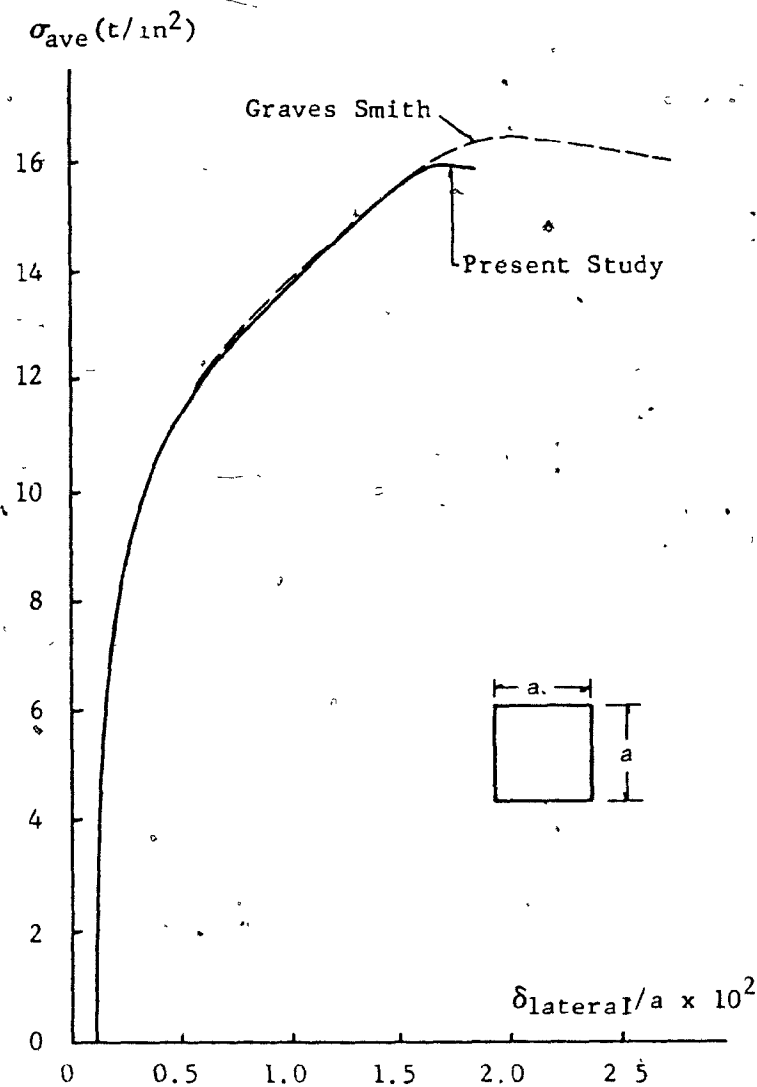


Figure 31 Out-Of-Plane Deflection of Square Column

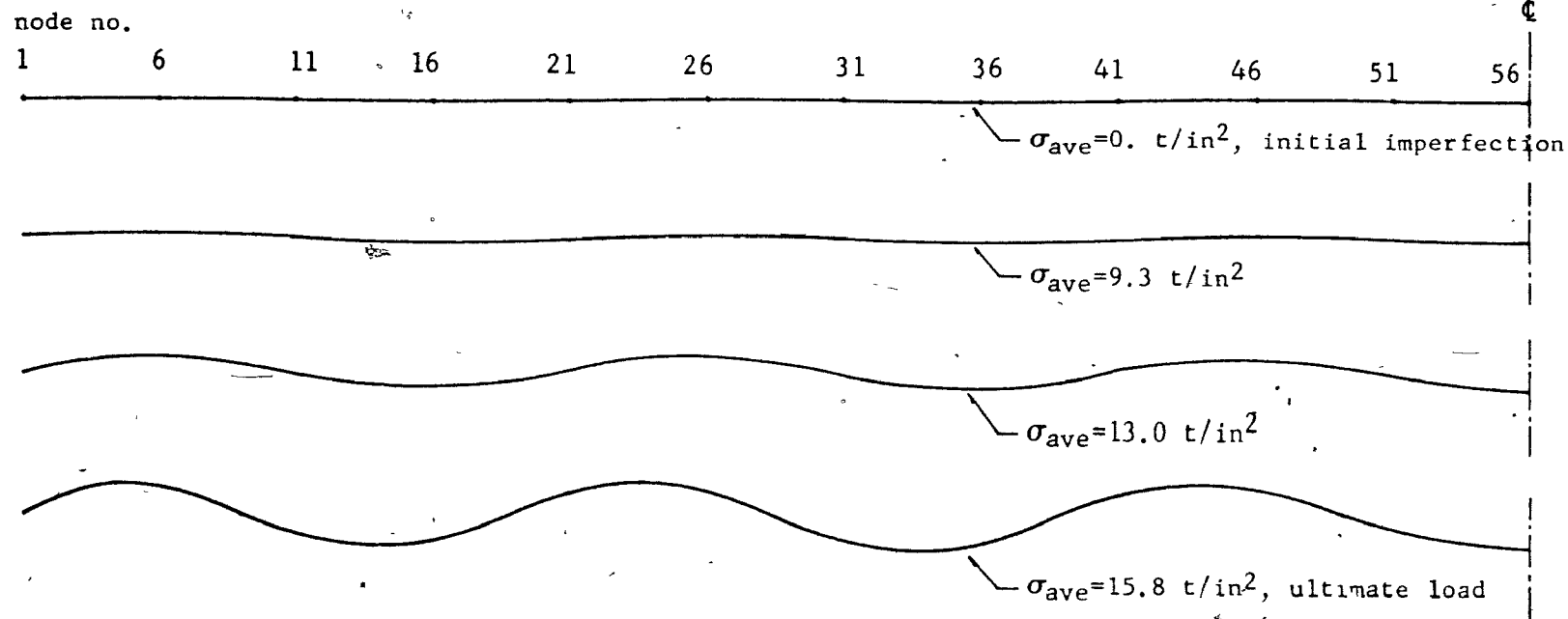


Figure 32 Deflection Profile Along the Longitudinal Center Line of a Plate Element of Square Column

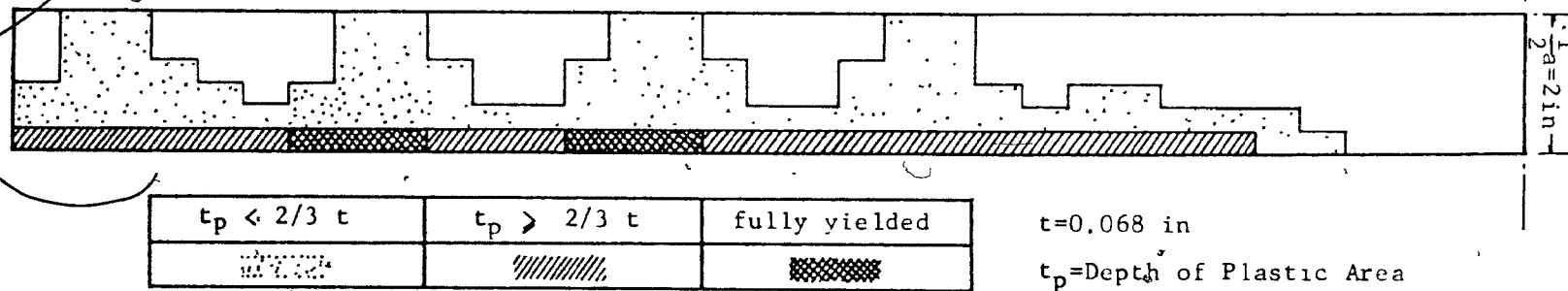


Figure 33 Yielded Zone of Square Column at Ultimate Load ( $\sigma_{ave} = 15.8 t/in^2$ )

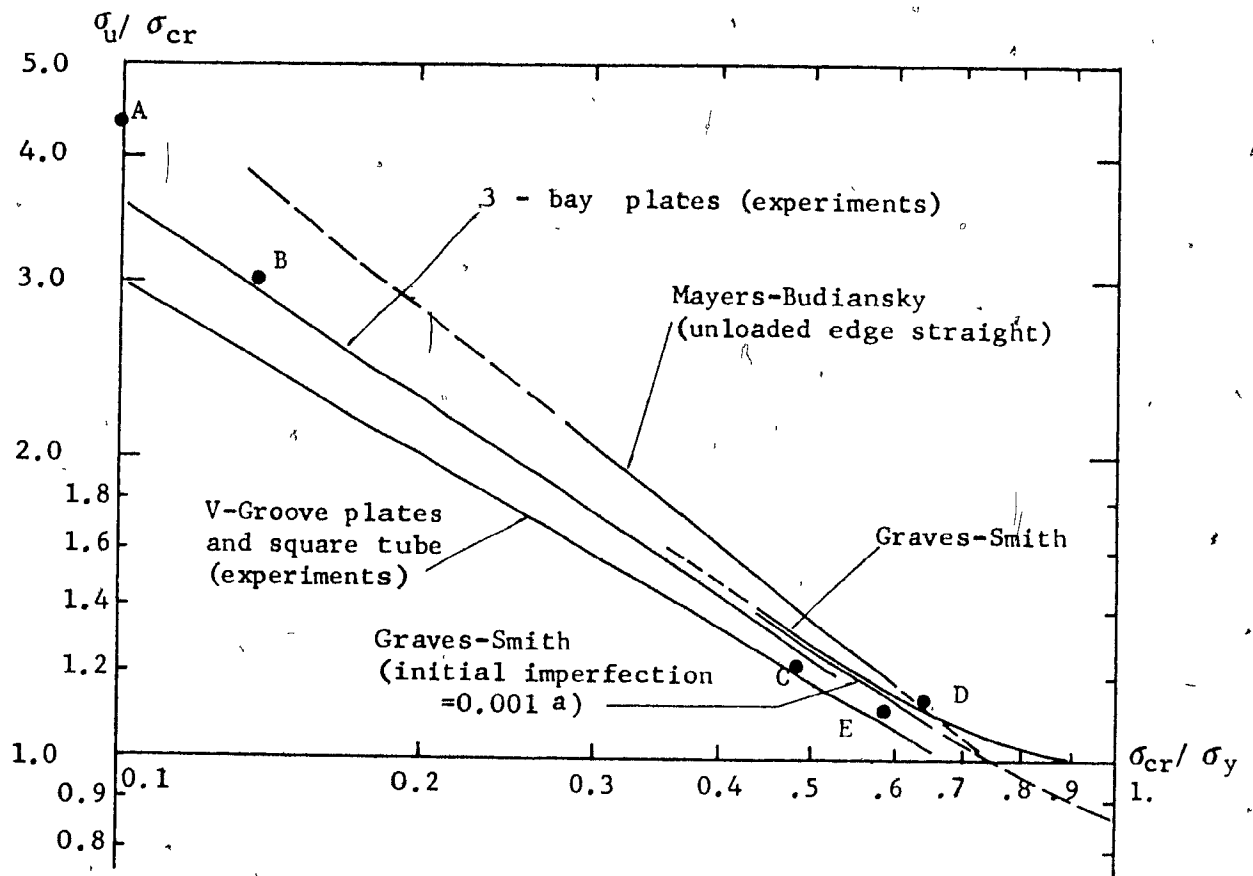


Figure 34 Curves of  $\sigma_u / \sigma_{cr}$  Versus  $\sigma_{cr} / \sigma_y$  for Square Tube Columns and Plates

- A. Chapter IV, Section IV.2.A
- B. Chapter IV, Section IV.2.B.a
- C. Chapter IV, Section IV.4.A
- D. Chapter IV, Section IV.4.B
- E. Chapter V, Section V.2

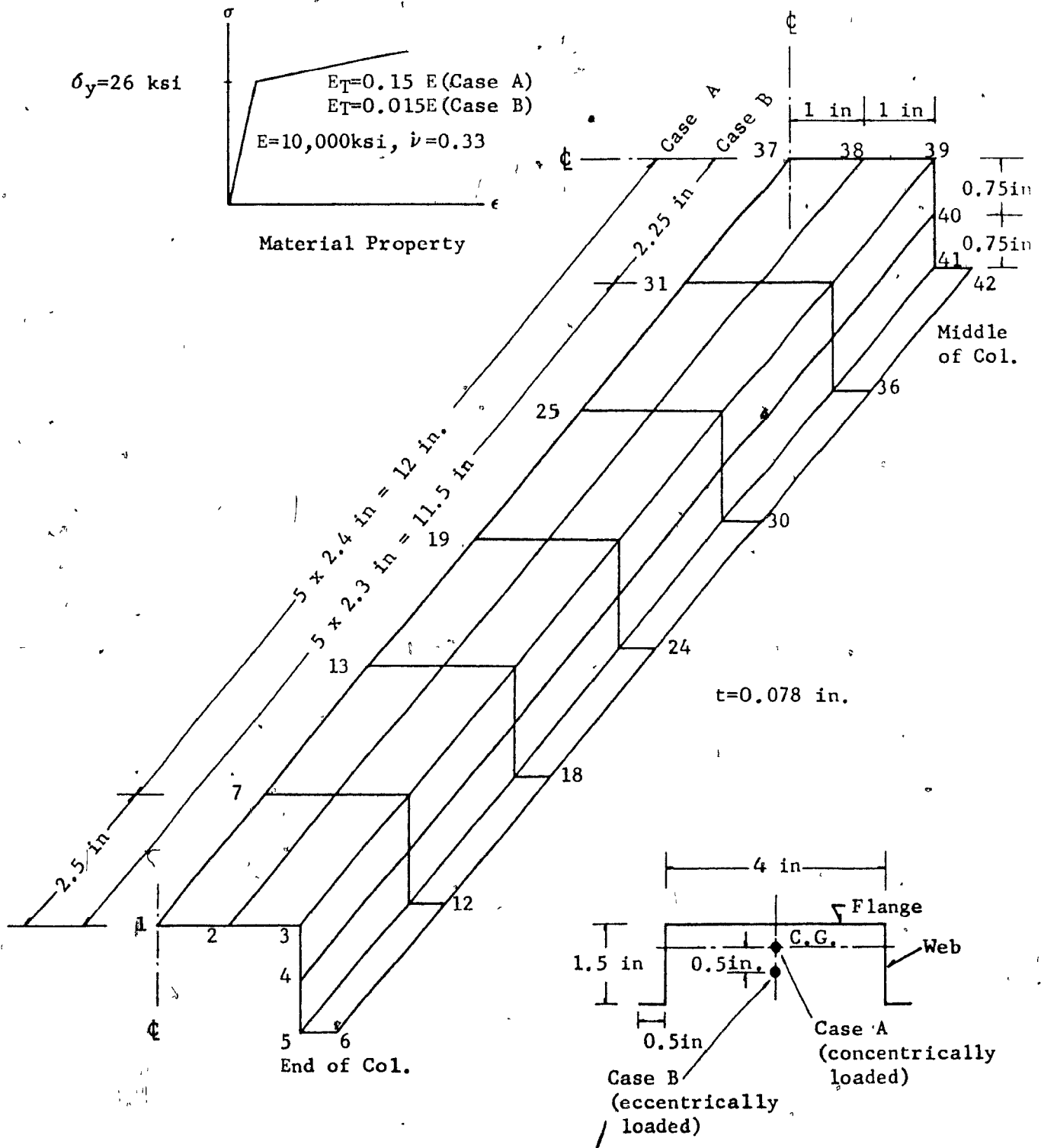


Figure 35

Idealization for Hat-Section Columns

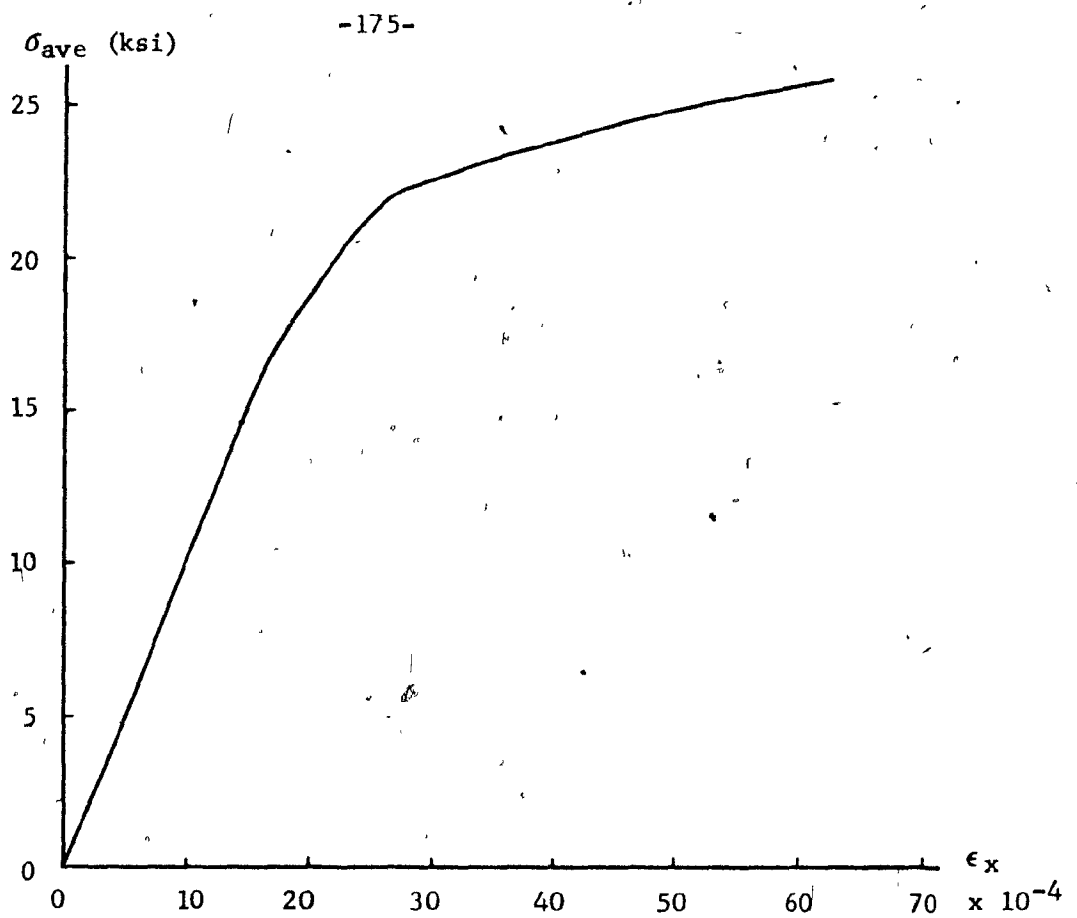


Figure 36 Stress - Shortening of Hat-Section Under Concentric Load

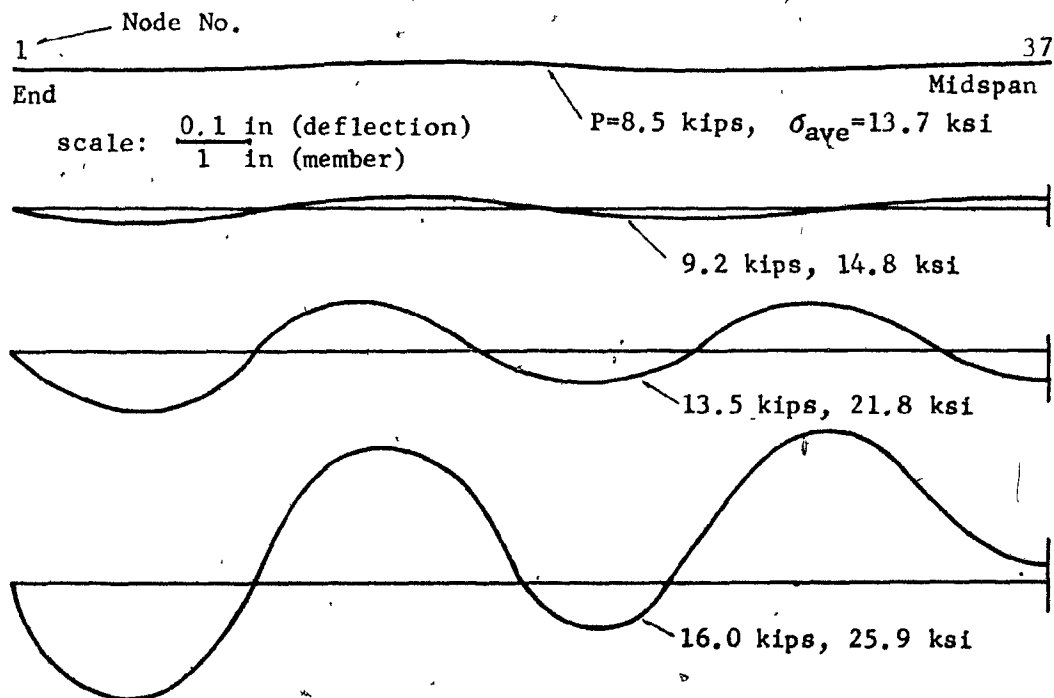


Figure 37 Deflection Profile for Concentrically Loaded Hat-Section



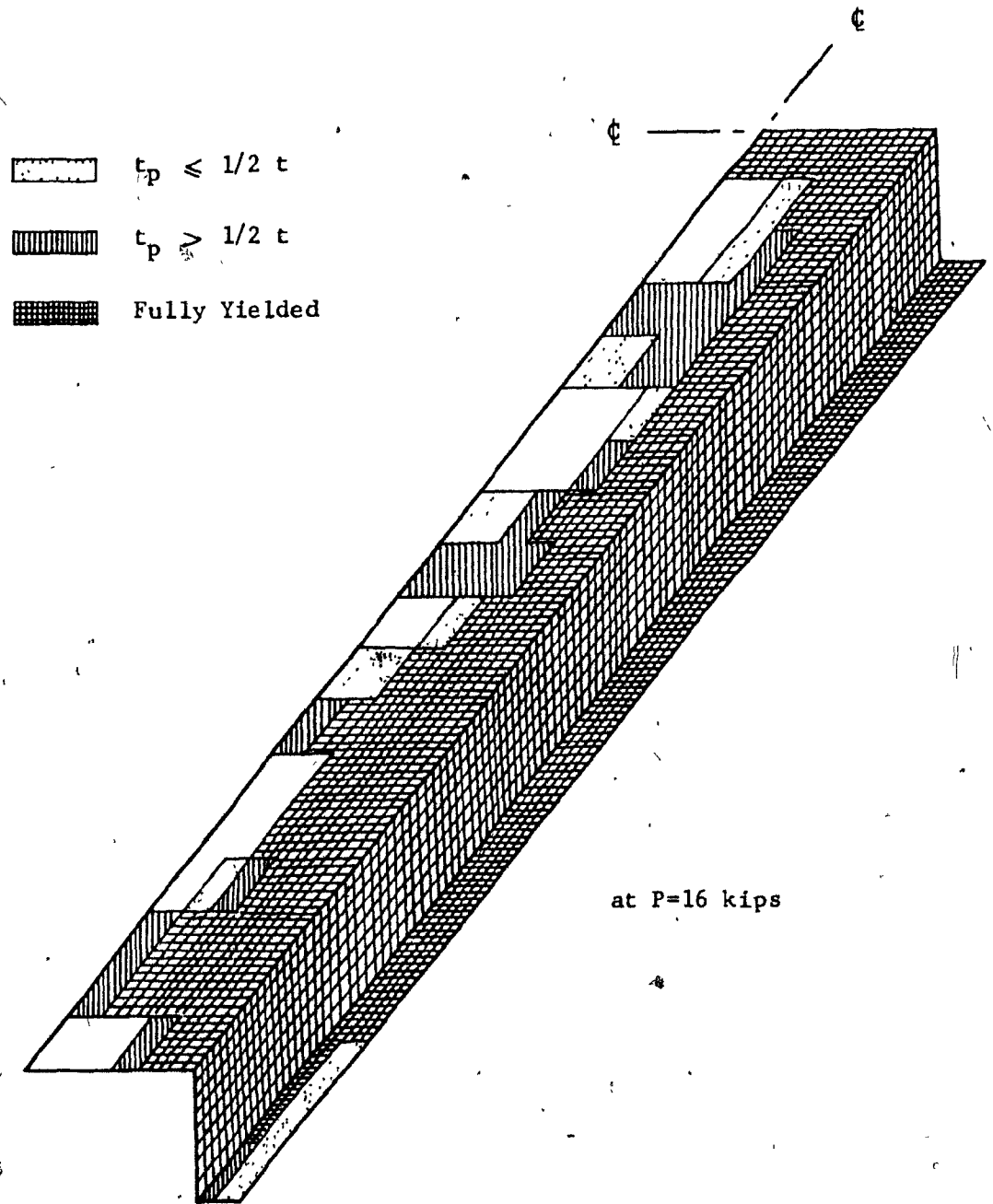


Figure 38 Yielded Zones for Concentrically Loaded Hat-Section

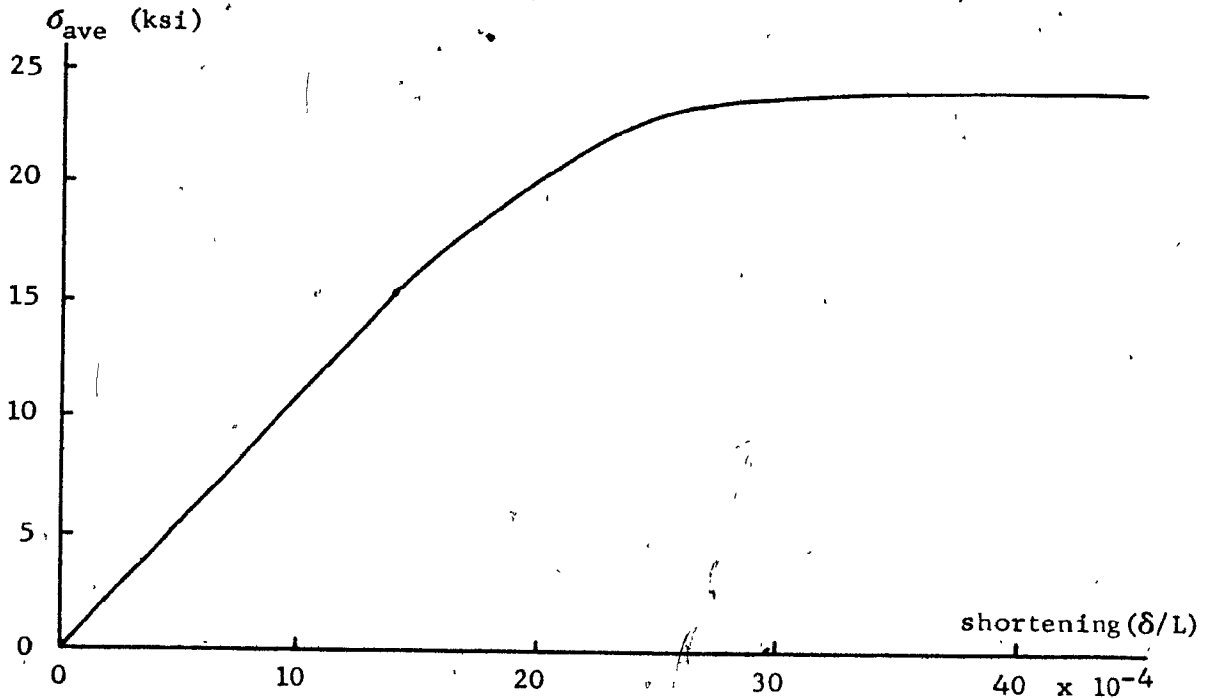


Figure 39 Stress - Shortening of Hat-Section Under Eccentric Load

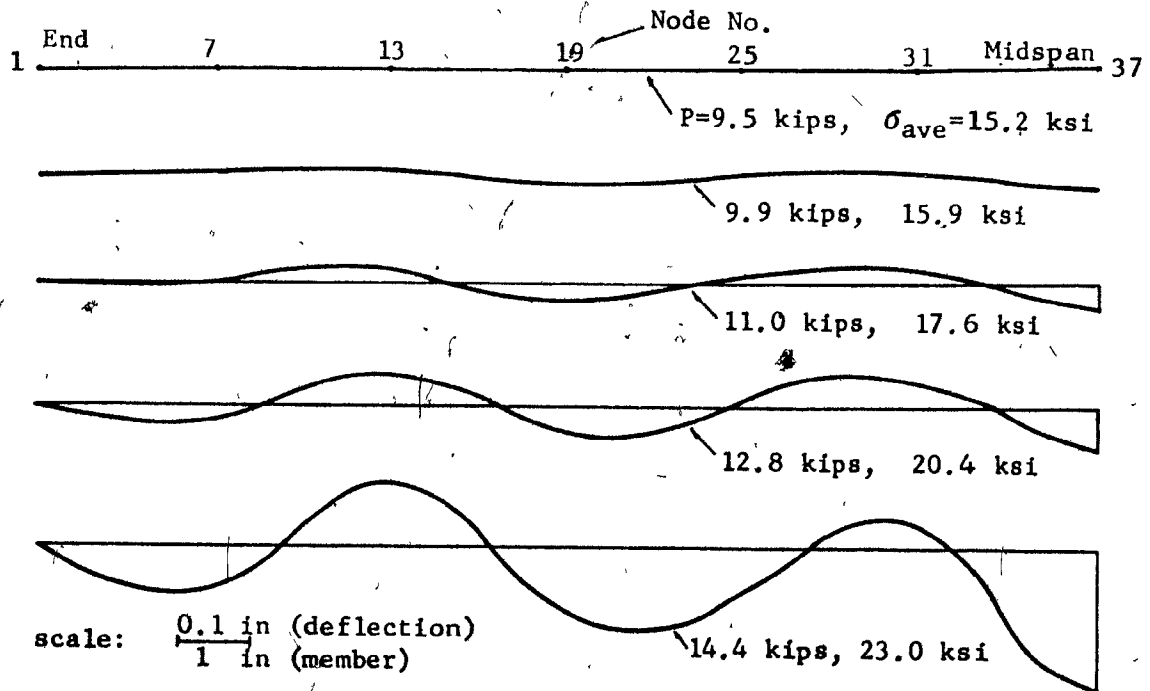


Figure 40 Deflection Profile for Eccentrically Loaded Hat-Section

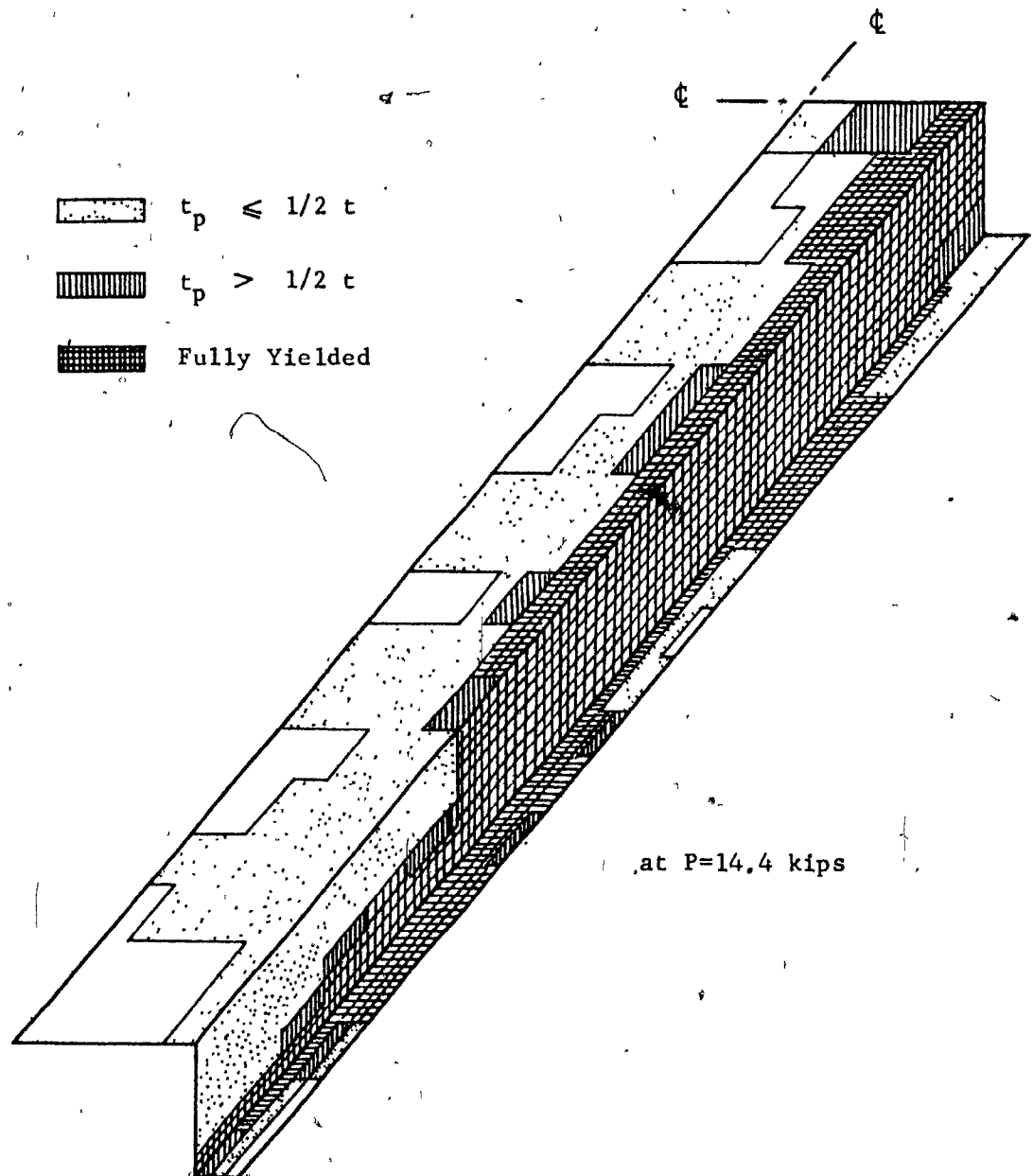


Figure 41 Yielded Zones for Eccentrically Loaded Hat-Section

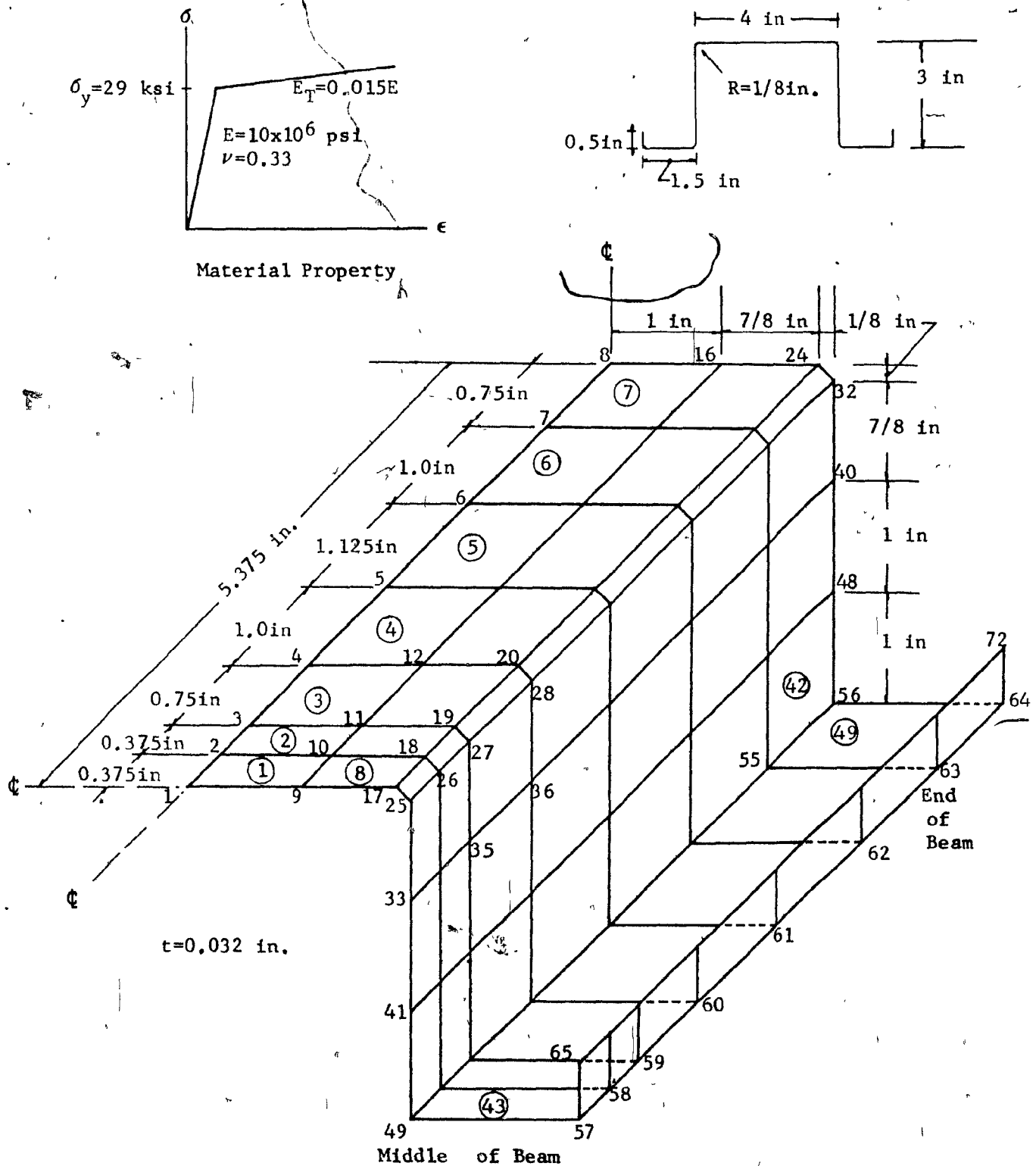


Figure 42 . Idealization for a Hat-Section Beam with Vertical Webs

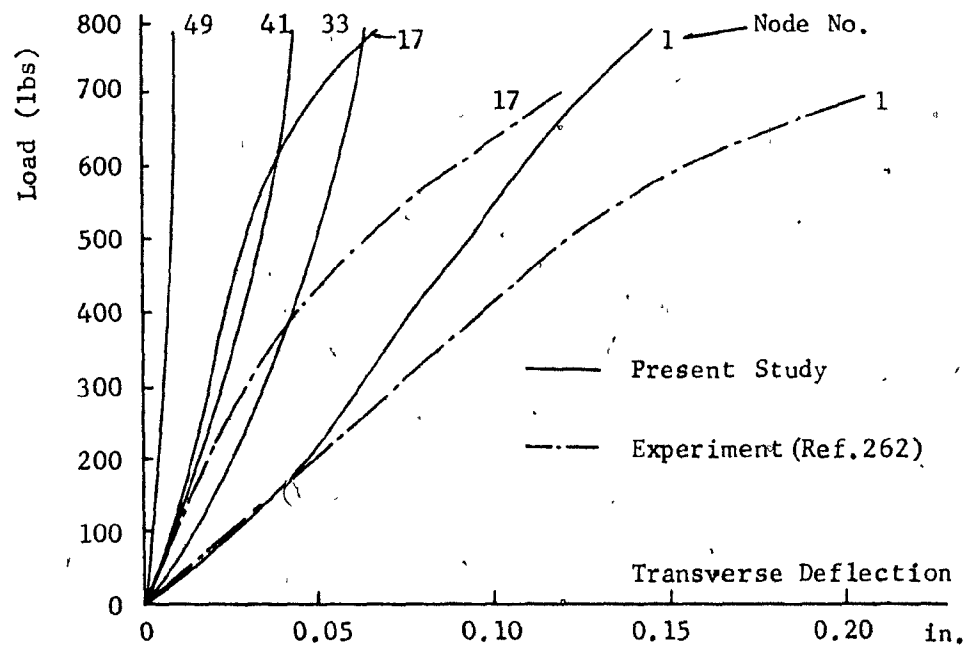


Figure 43 Transverse Deflection at Midspan of Hat-Section Beam with Vertical Webs

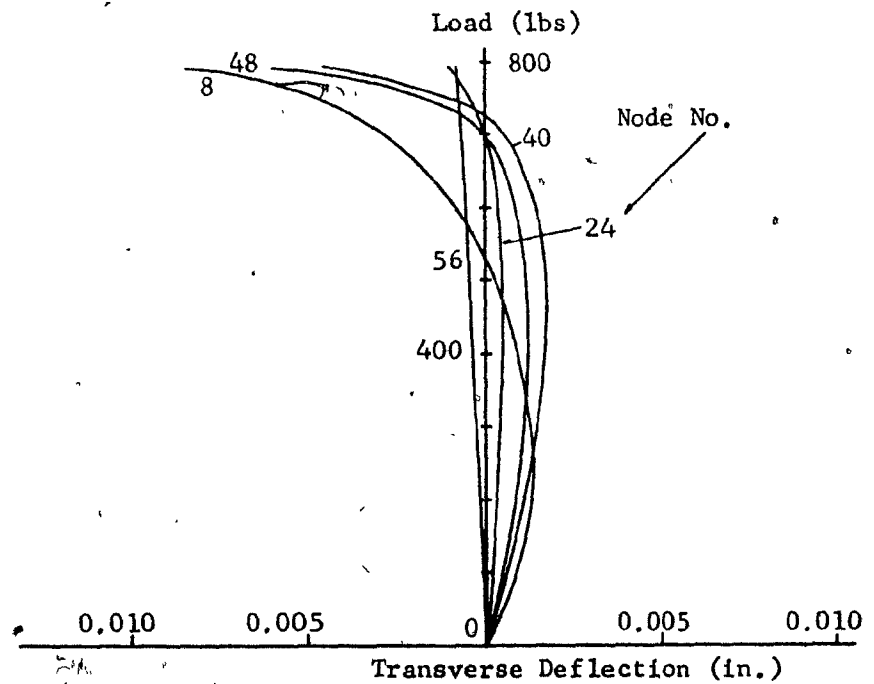


Figure 44 Transverse Deflection at End of Hat-Section Beam with Vertical Webs

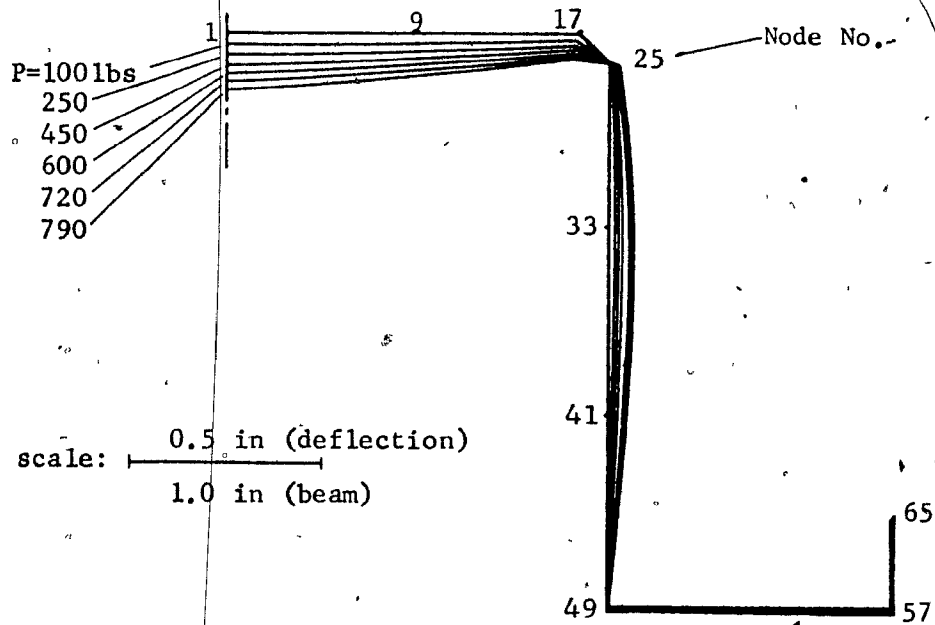


Figure 45 Deflection Profile at Midspan Cross-Section

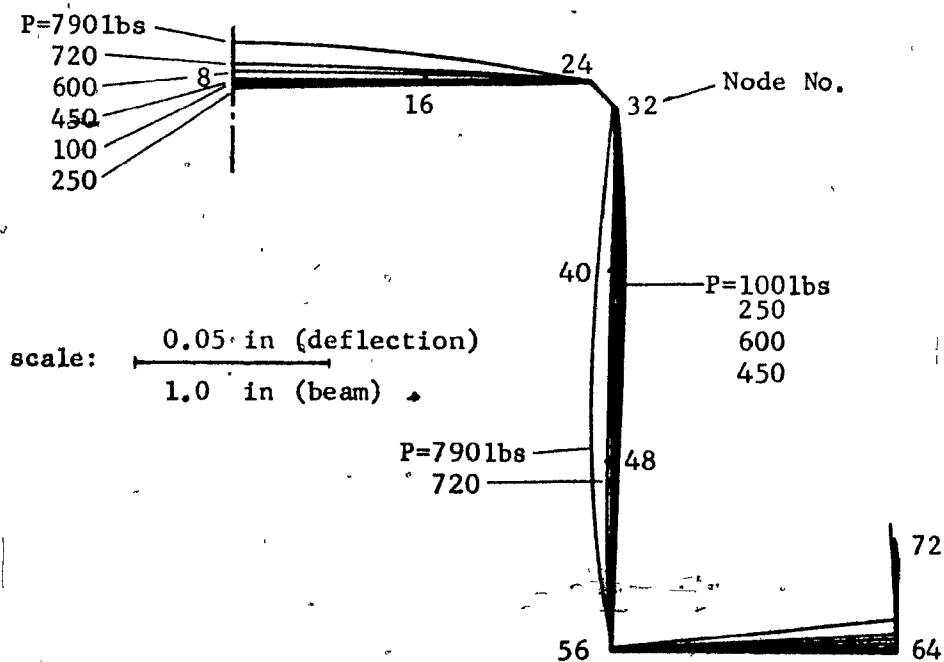


Figure 46 Deflection Profile at End Cross-Section

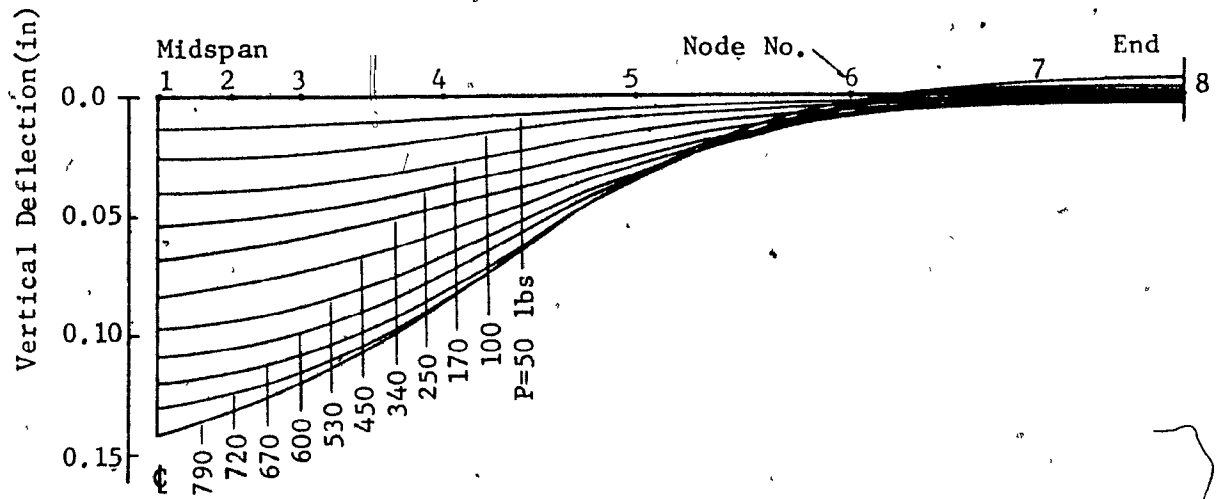


Figure 47 Deflection Profile Along the Longitudinal Center Line of Top Flange of Hat-Section Beam with Vertical Webs

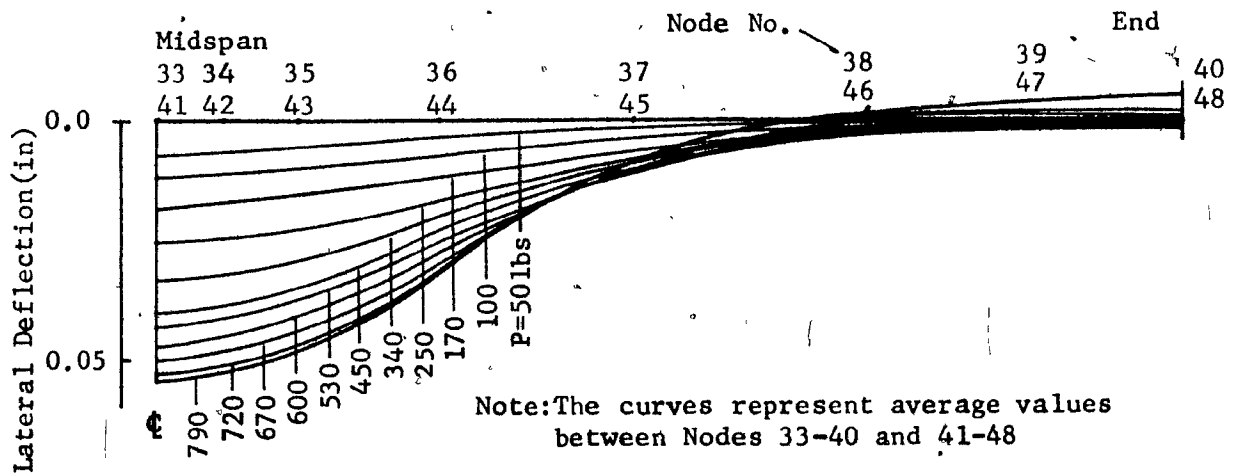


Figure 48 Deflection Profile Along the Longitudinal Center Line of Web of Hat-Section Beam with Vertical Webs

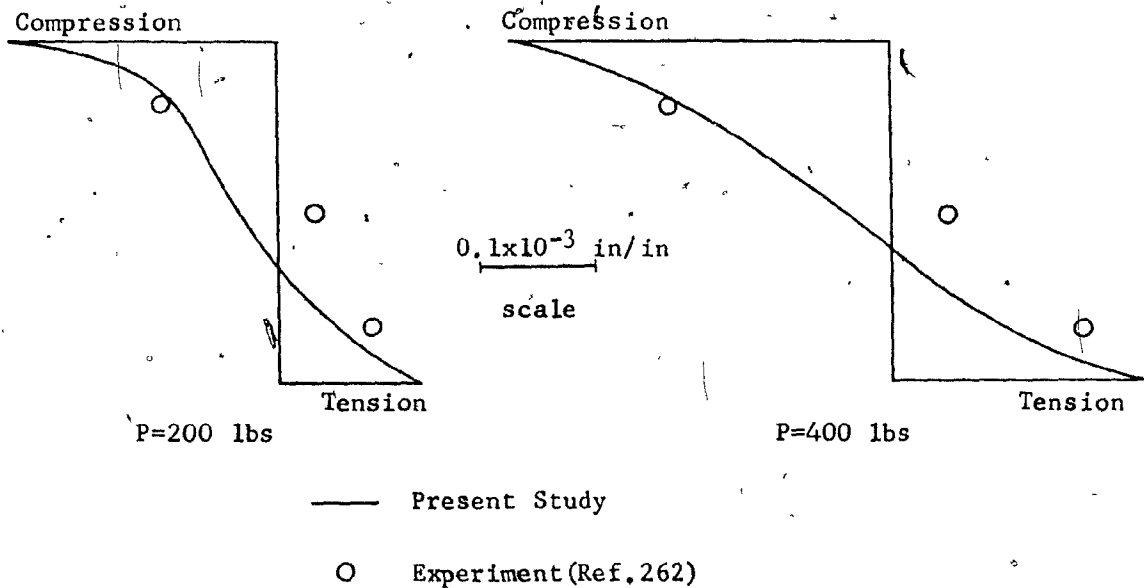


Figure 49 Longitudinal Strain Distribution on Inner Face of Web Near Midspan

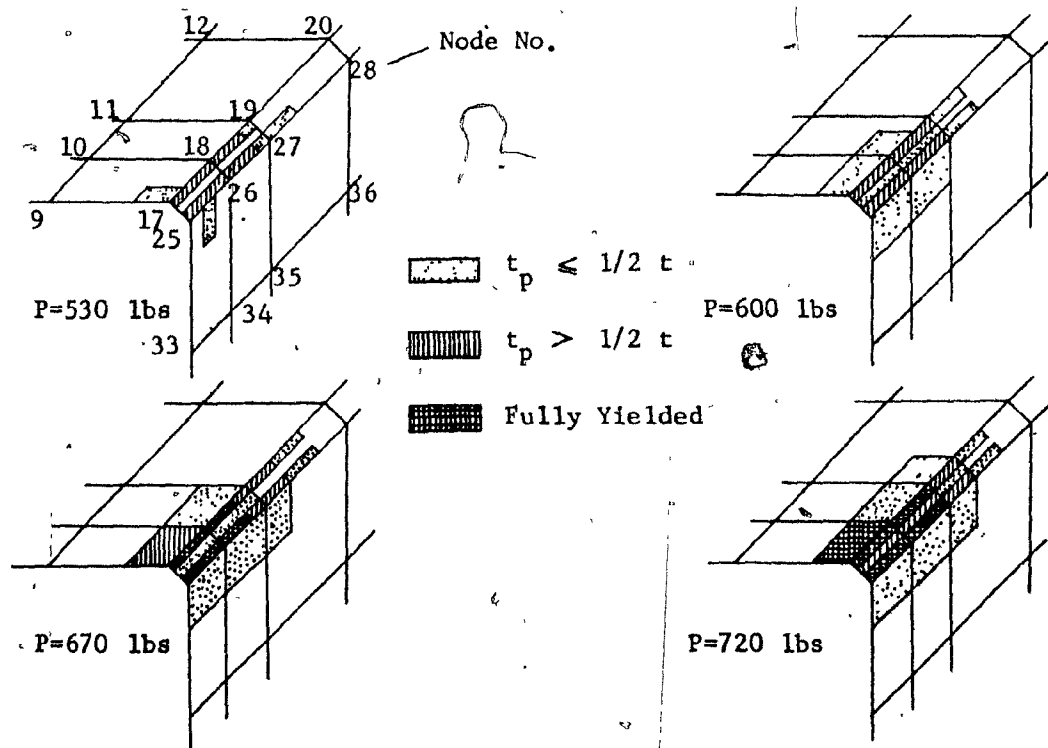


Figure 50 Plastic Zone of Hat-Section Beam with Vertical Webs



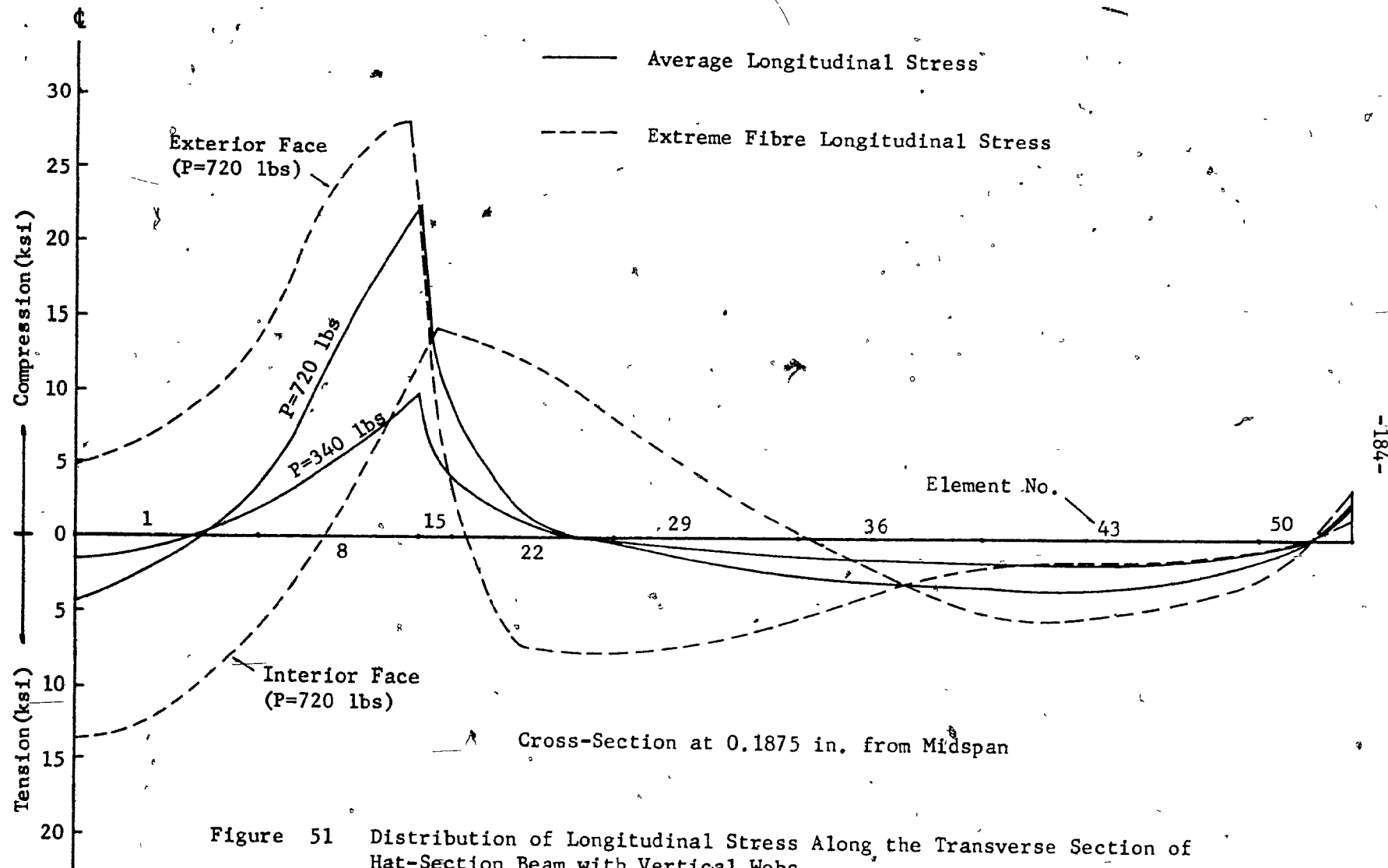


Figure 51 Distribution of Longitudinal Stress Along the Transverse Section of Hat-Section Beam with Vertical Webs



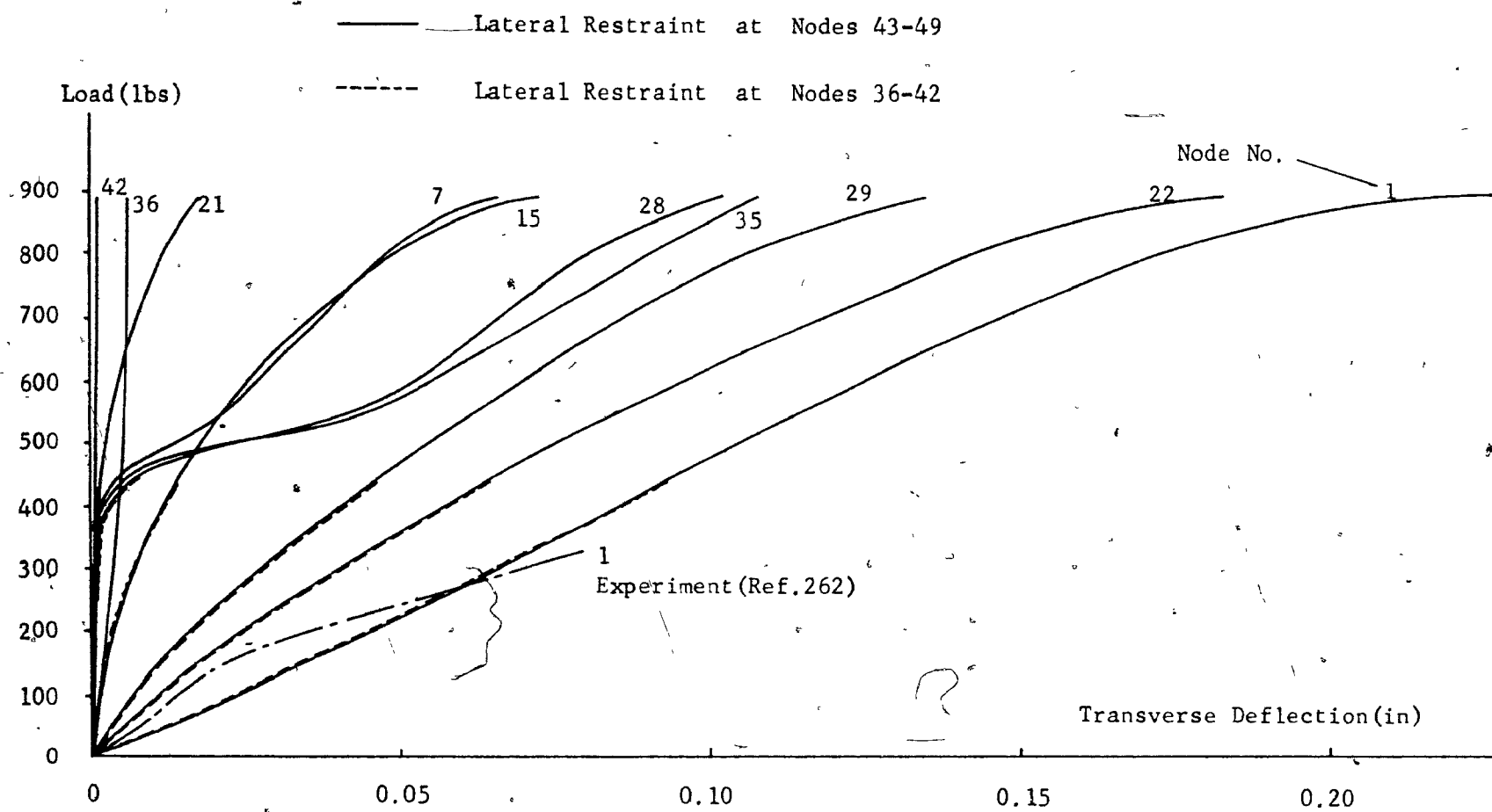


Figure 53 Transverse Deflection at Midspan and at End of Hat-Section Beam with Sloped Webs

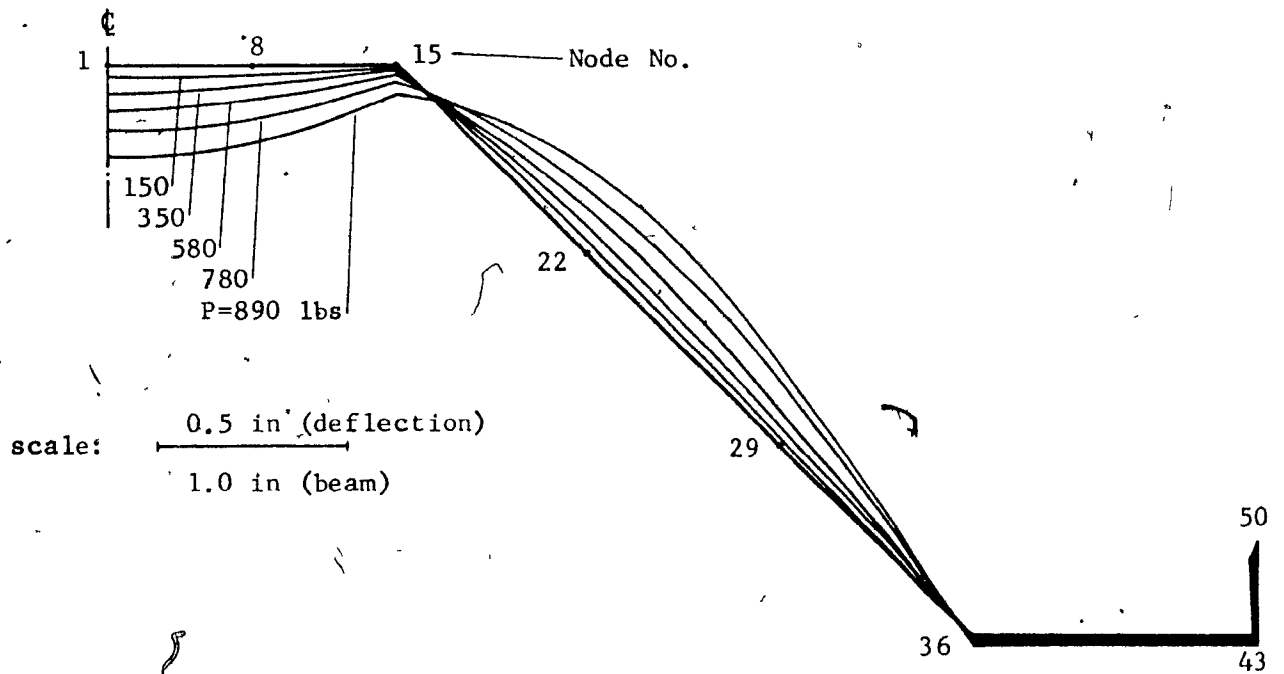


Figure 54 Deflection Profile at Midspan Cross-Section

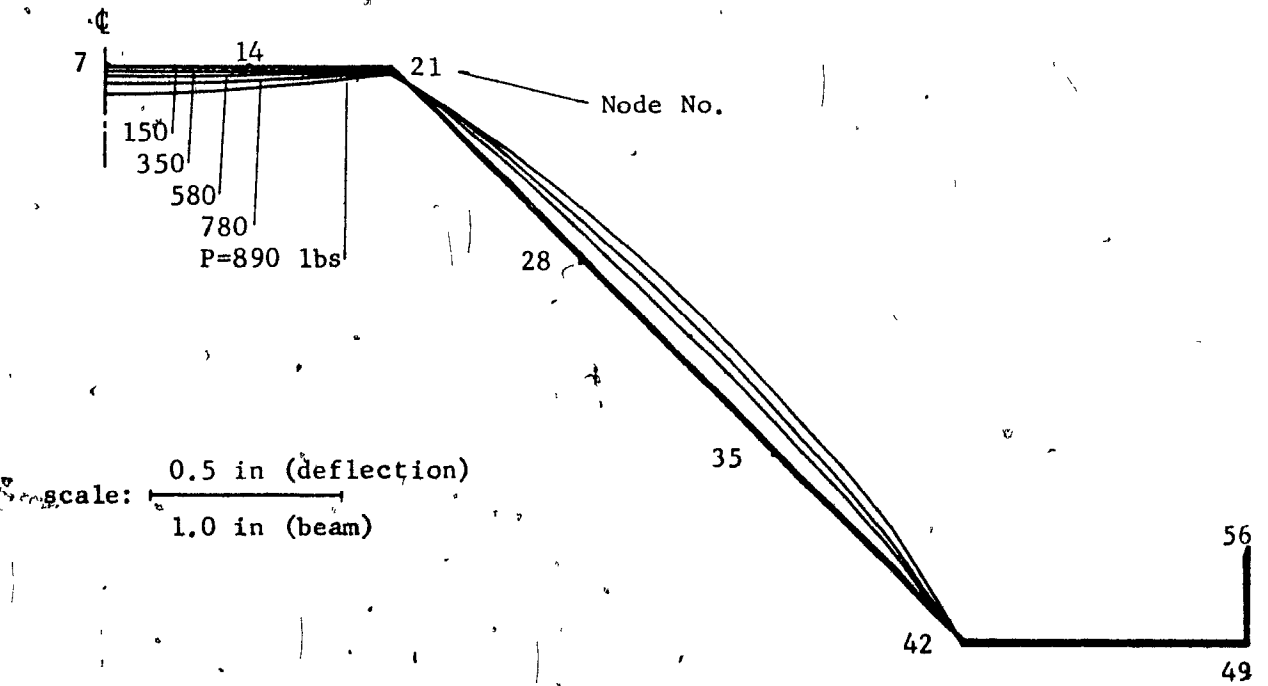


Figure 55 Deflection Profile at End Cross-Section

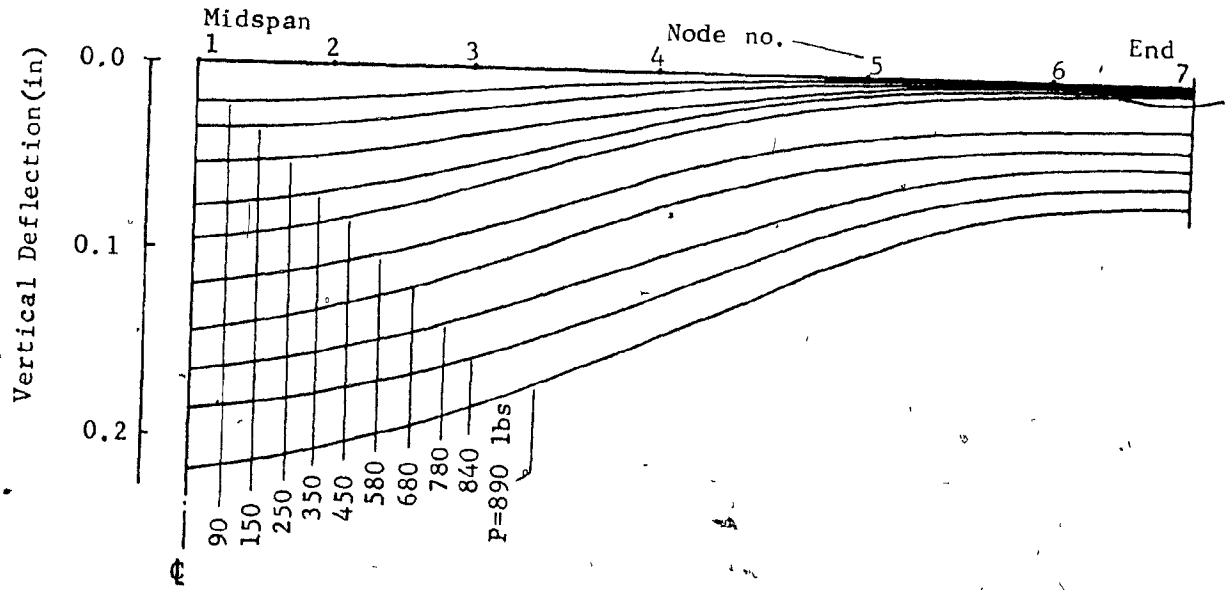


Figure 56 Deflection Profile Along the Longitudinal Center Line of Top Flange of Hat-Section Beam with Sloped Webs

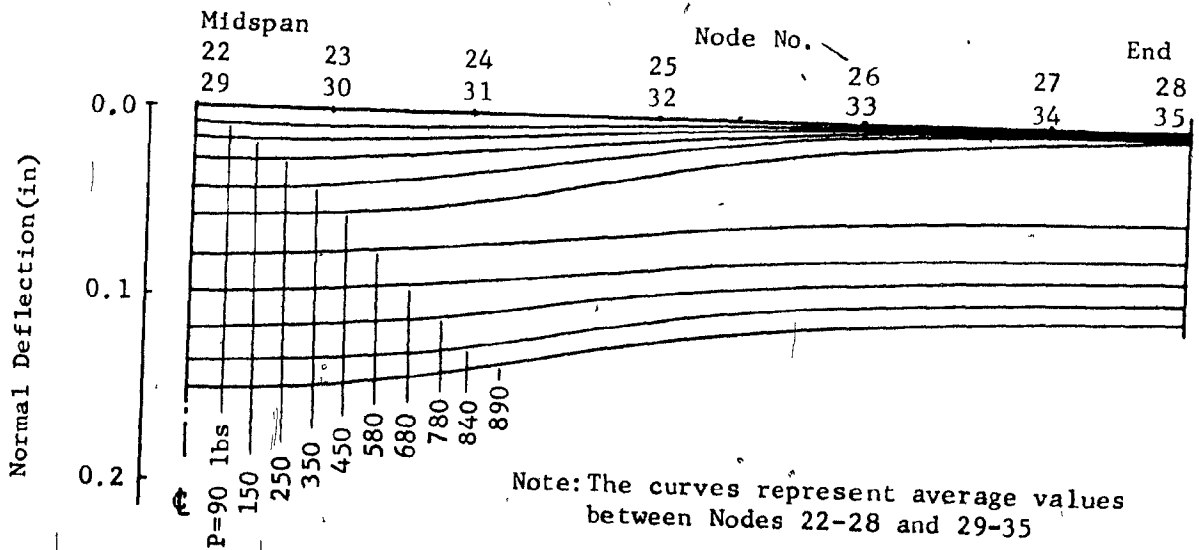


Figure 57 Deflection Profile Along the Longitudinal Center Line of Web of Hat-Section Beam with Sloped Webs

Initial Yield at  
P=530 lbs

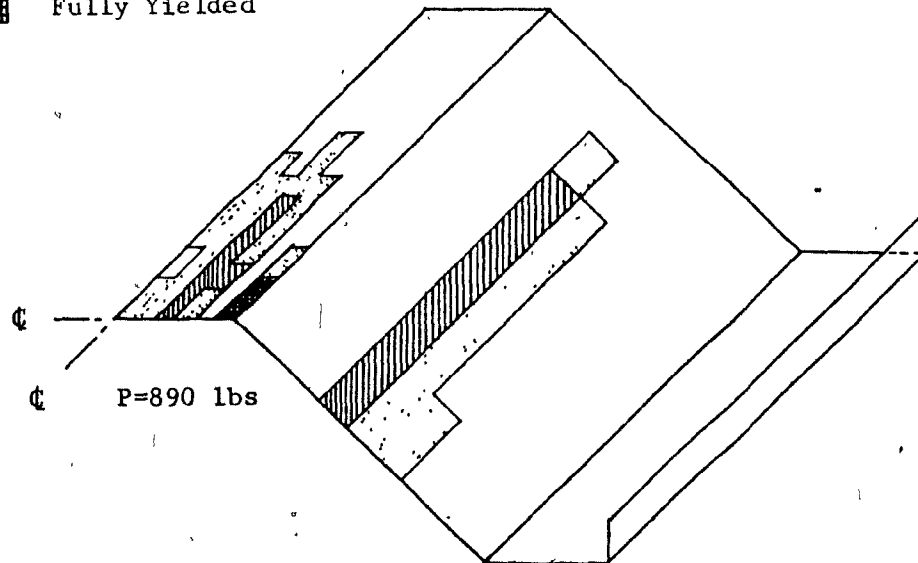
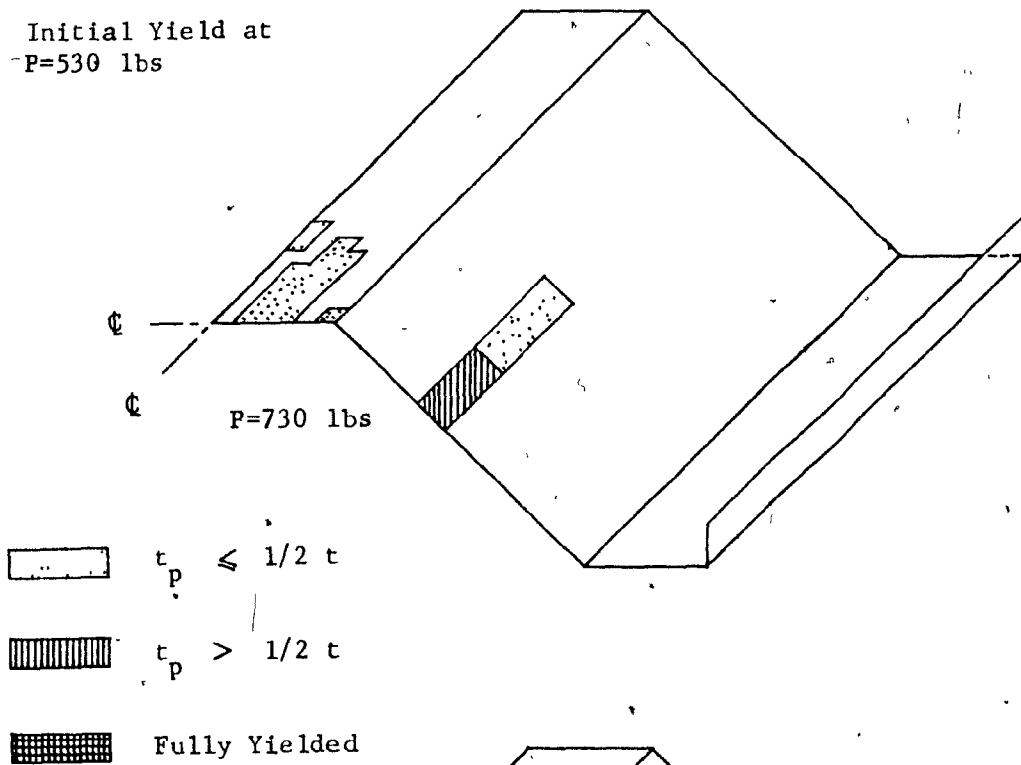


Figure 58 Plastic Zone of Hat-Section with Sloped Webs

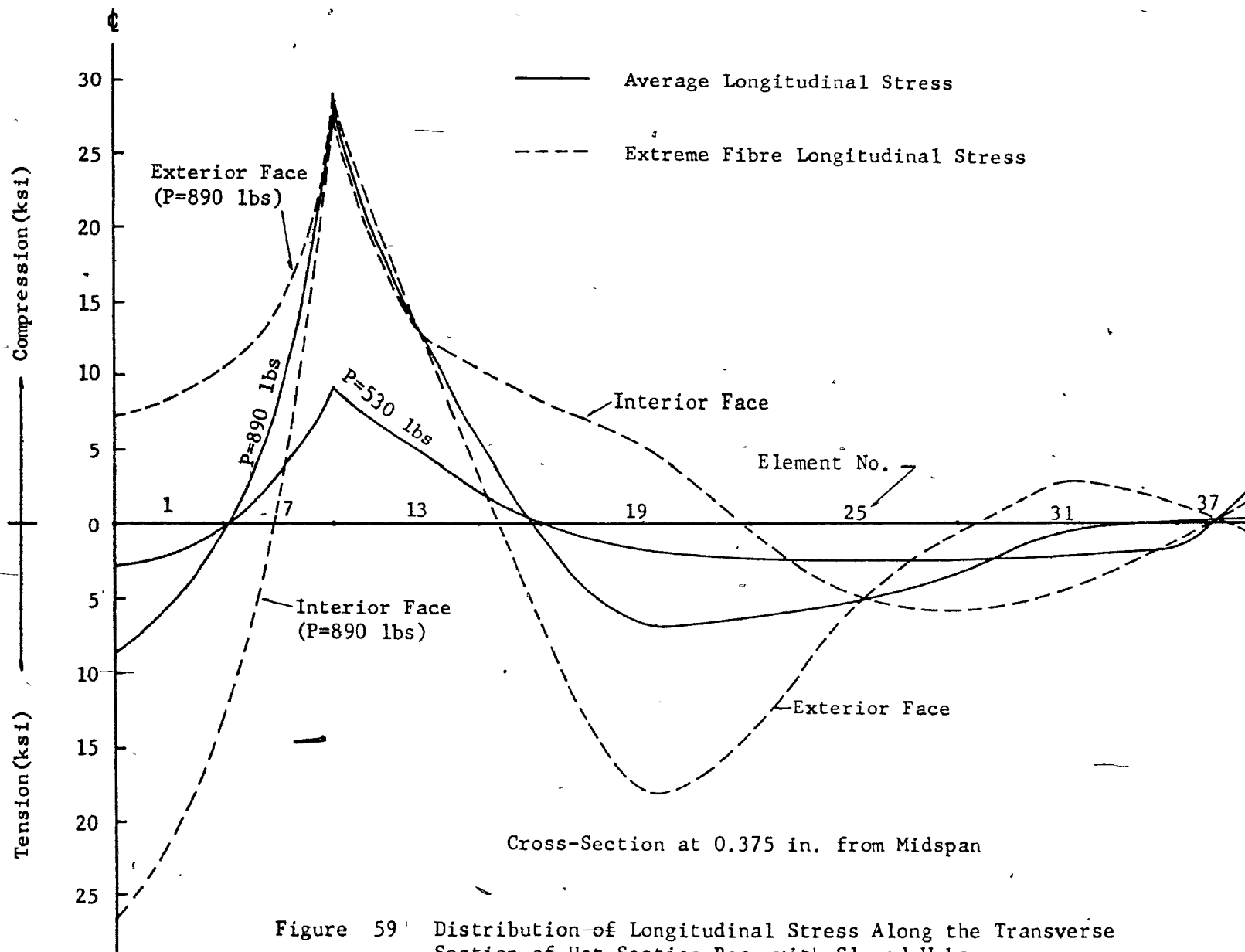


Figure 59 Distribution of Longitudinal Stress Along the Transverse Section of Hat-Section Beam with Sloped Webs

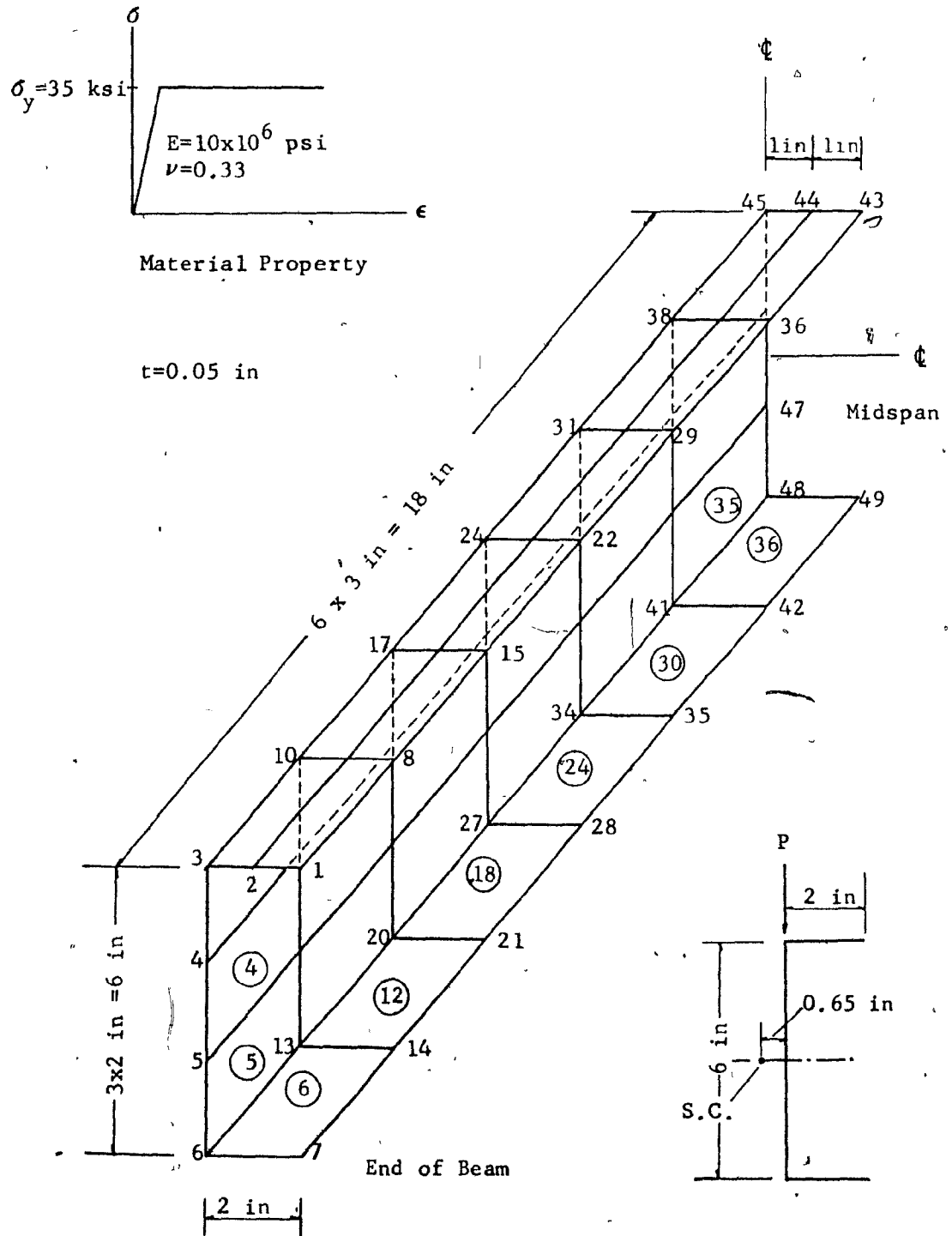


Figure 60

Idealization for a Channel-Section Beam



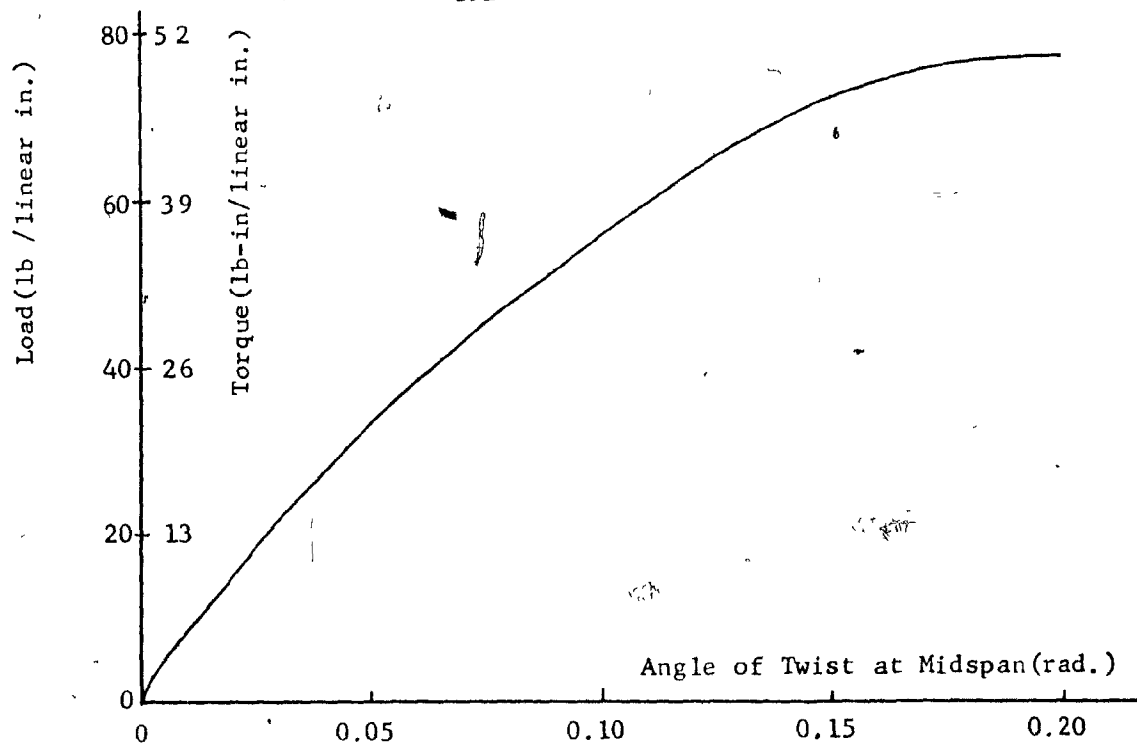


Figure 61 Load/Torque - Angle of Twist Relation of Channel-Section

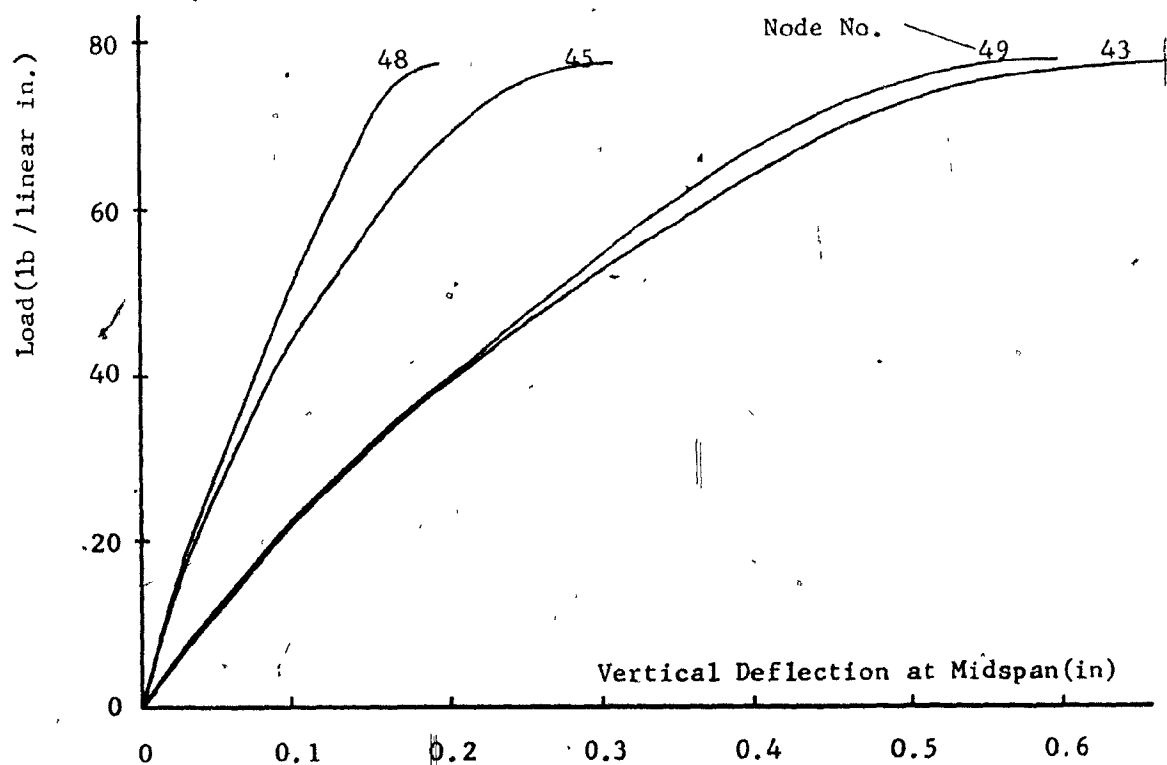


Figure 62 Load-Deflection Relation of Channel-Section

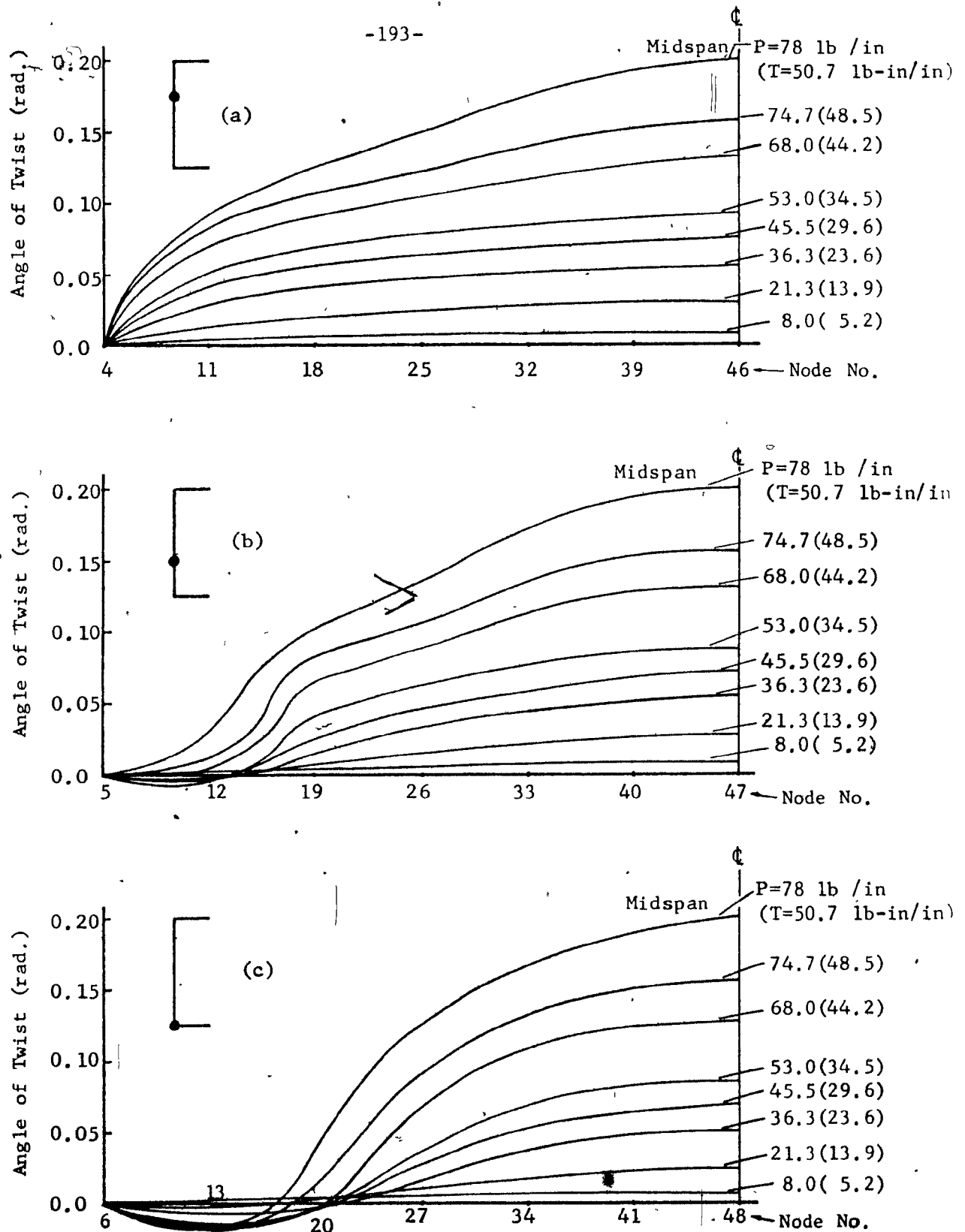


Figure 63 Distribution of Angle of Twist Along the Span of Channel-Section

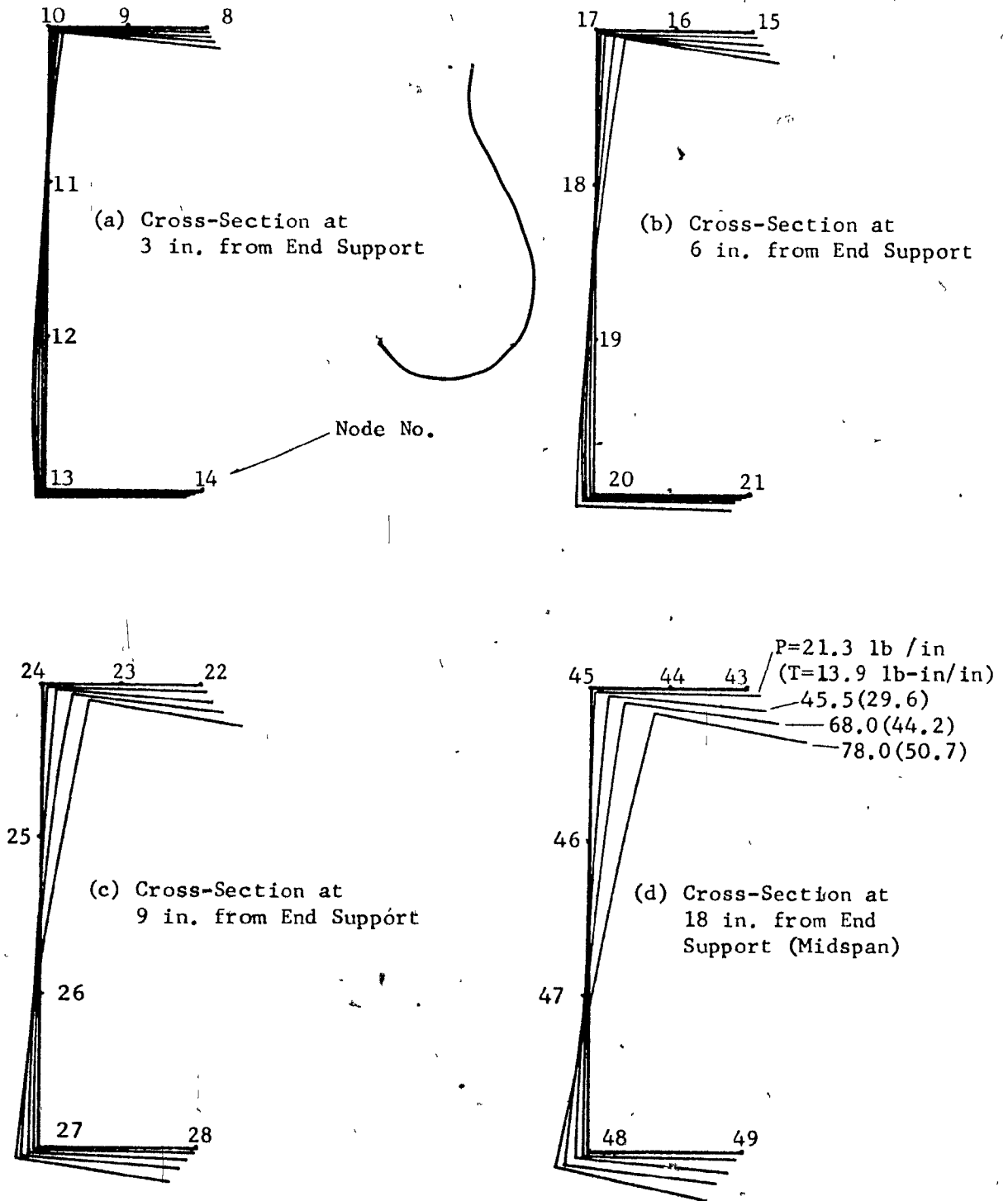


Figure 64 Distortion of the Channel-Section

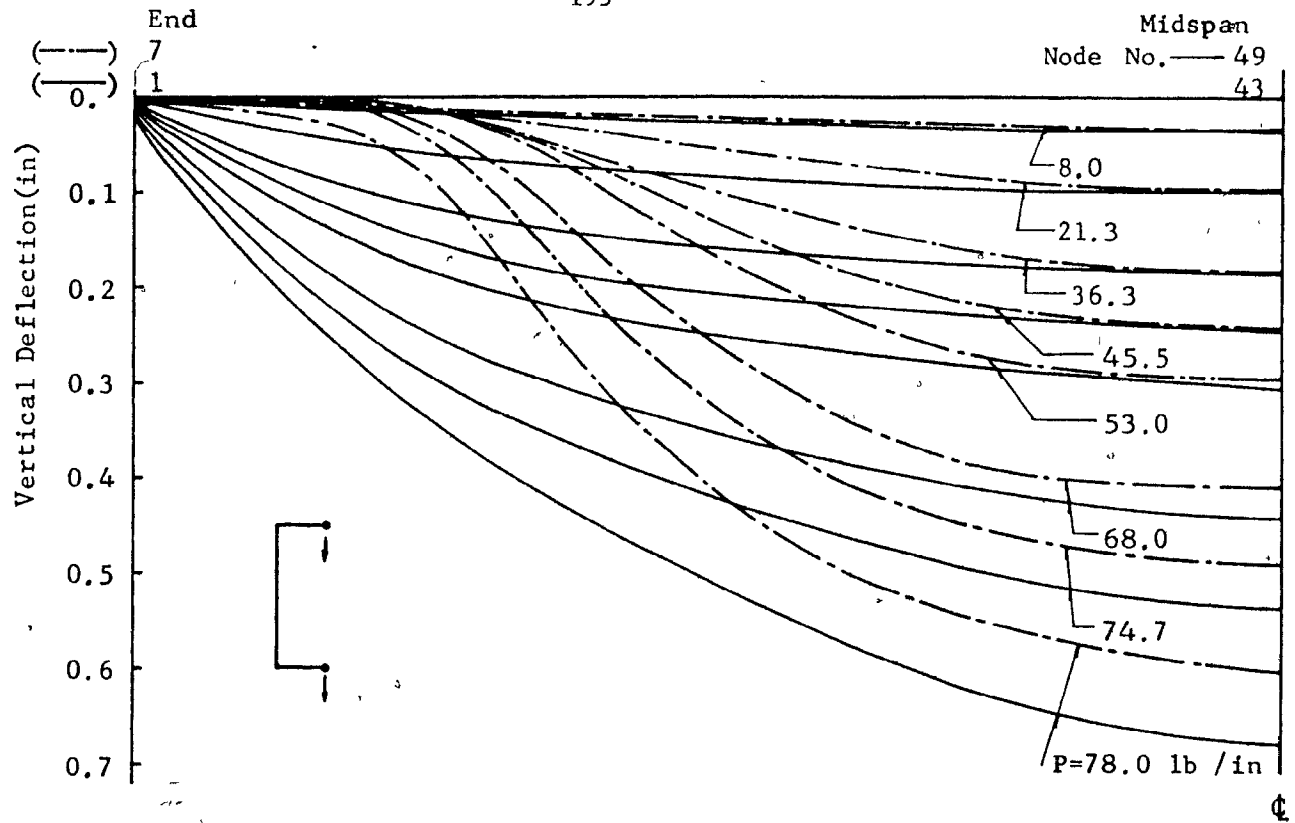


Figure 65 Vertical Deflection Profile Along the Flange Tips of Channel-Section

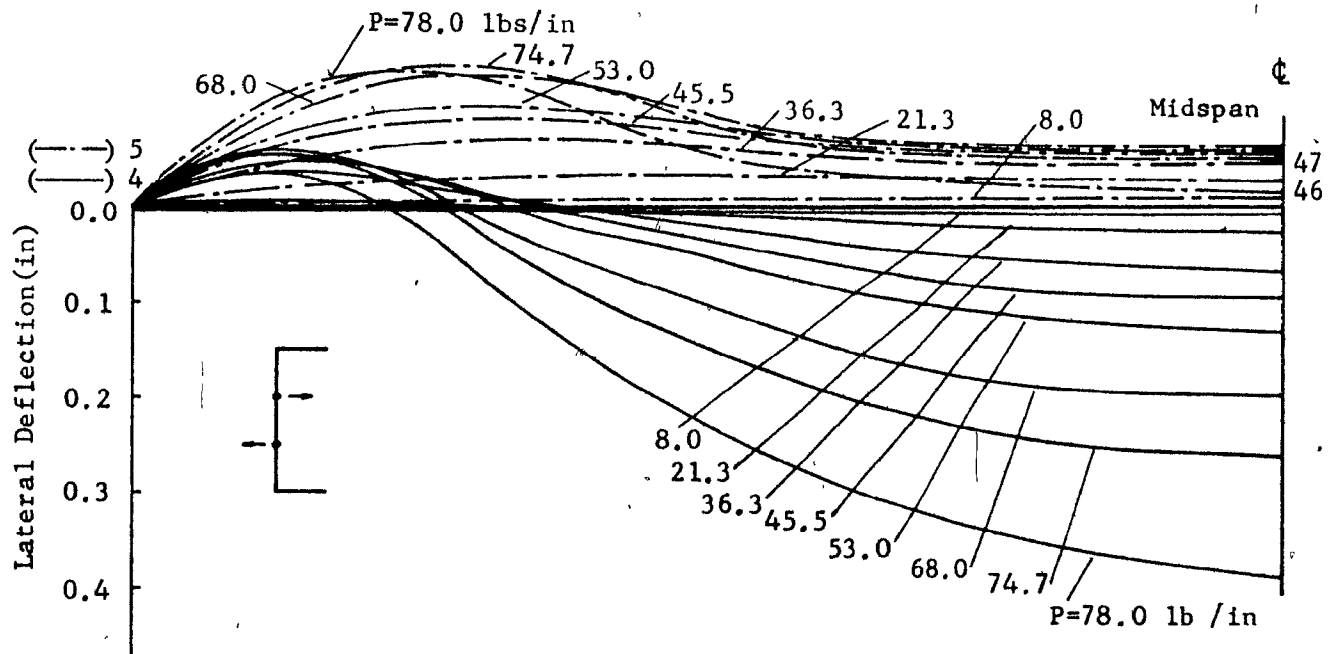


Figure 66 Lateral Deflection Profile of Web of Channel-Section

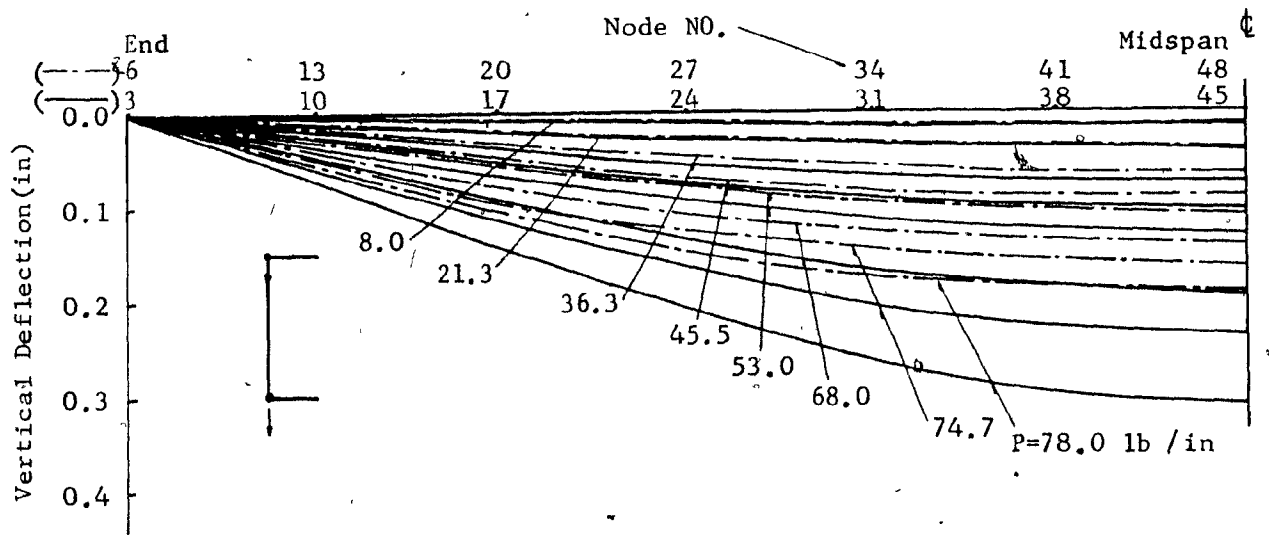


Figure 67 Vertical Deflection Profile of Channel-Section

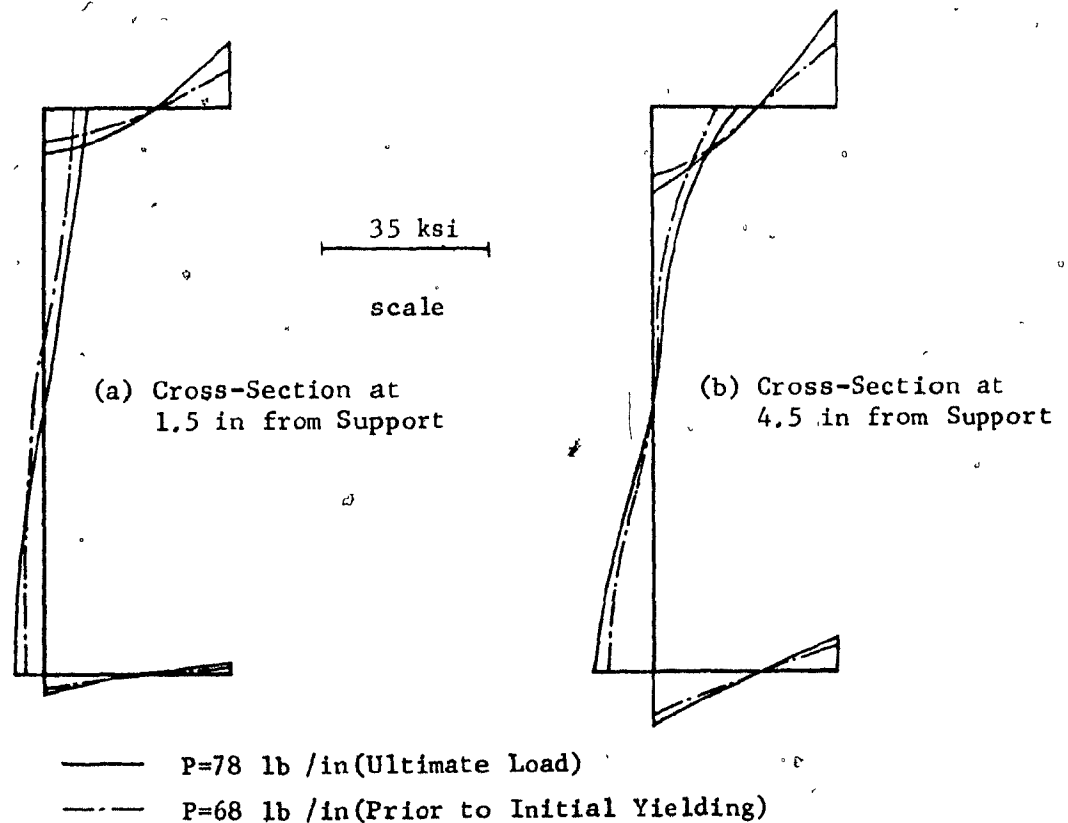


Figure 68 Longitudinal Stress Distribution Along the Transverse Sections of Channel-Section Beam

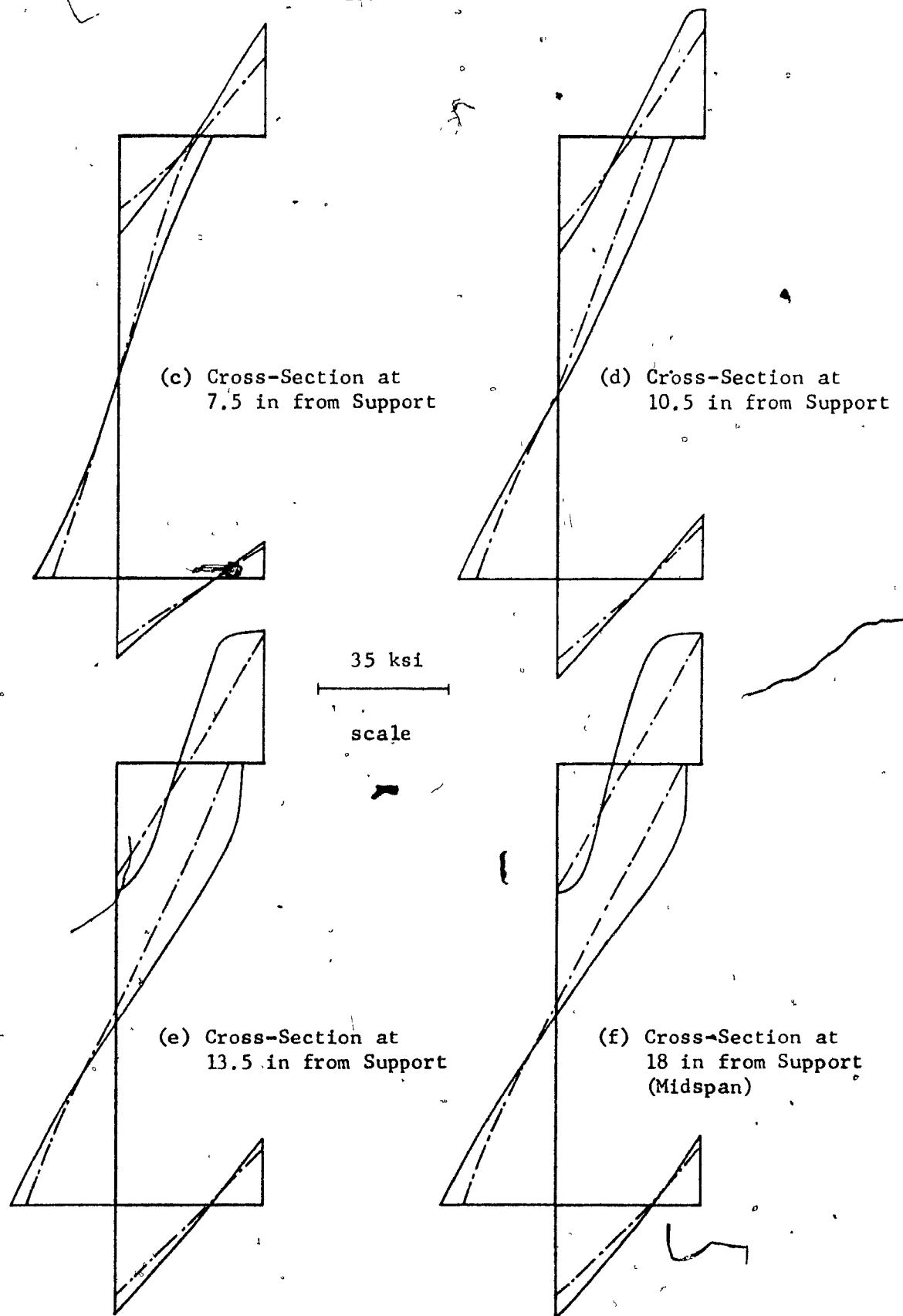


Figure 68 Continued

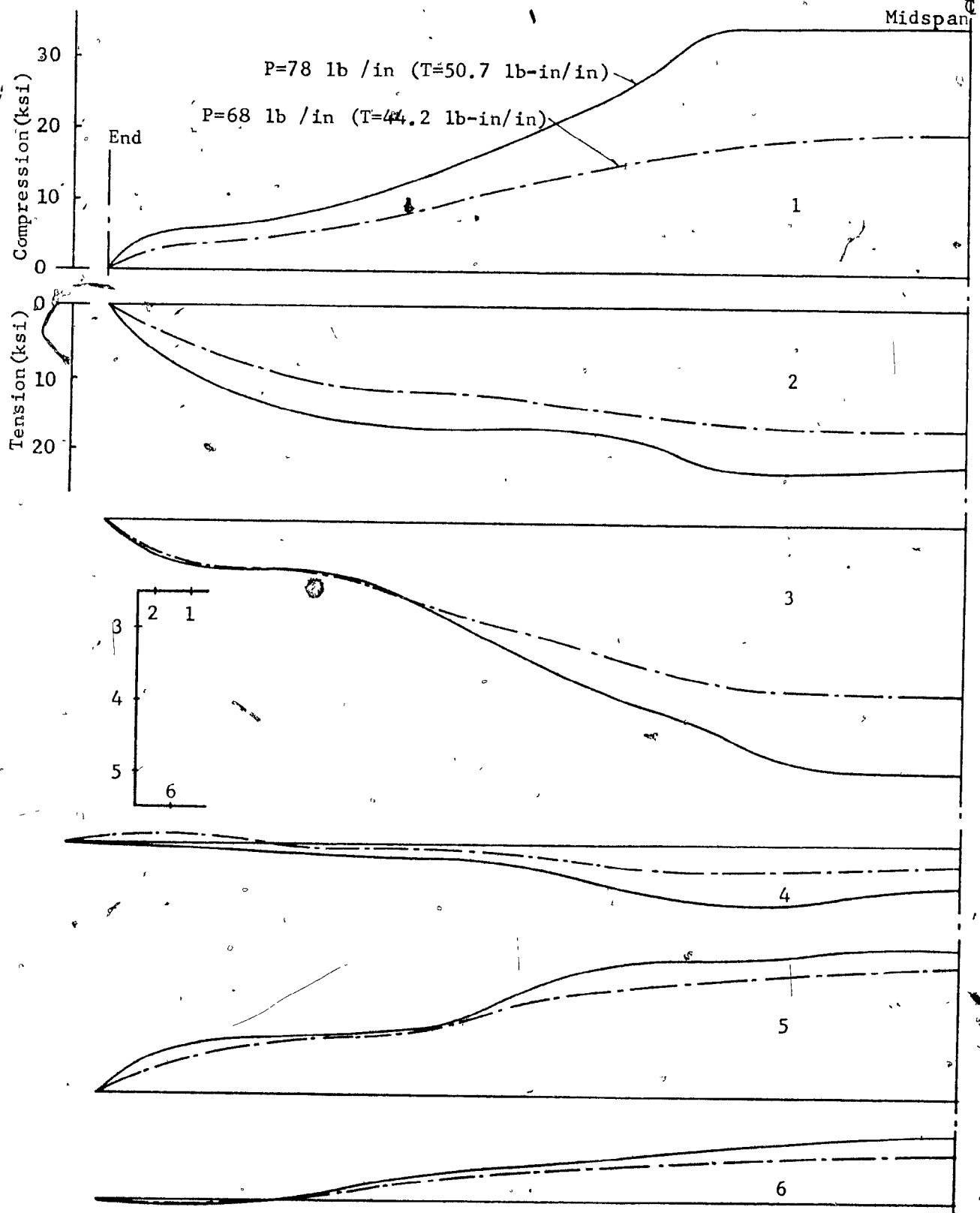

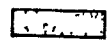
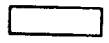


Figure 69 Distribution of Average Longitudinal Stress Along the Longitudinal Sections of Channel-Section Beam

 Fully Yielded

 Partially Yielded

 Fully Elastic

$$P_{ult} = 78 \text{ lb/in}$$

$$T_{ult} = 50.7 \text{ lb-in/in}$$

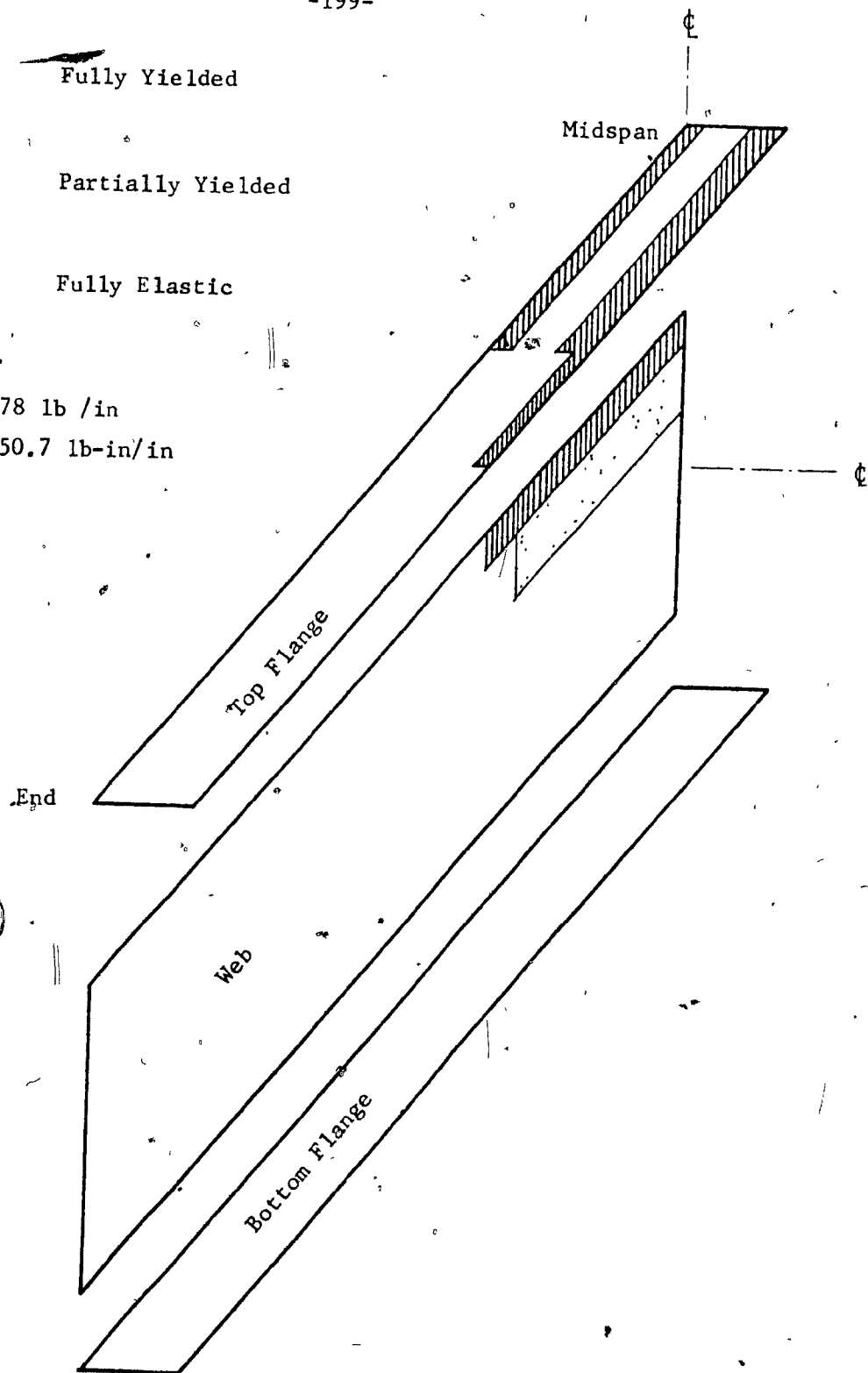


Figure 70 Plastic Zone of Channel-Section at Ultimate Load



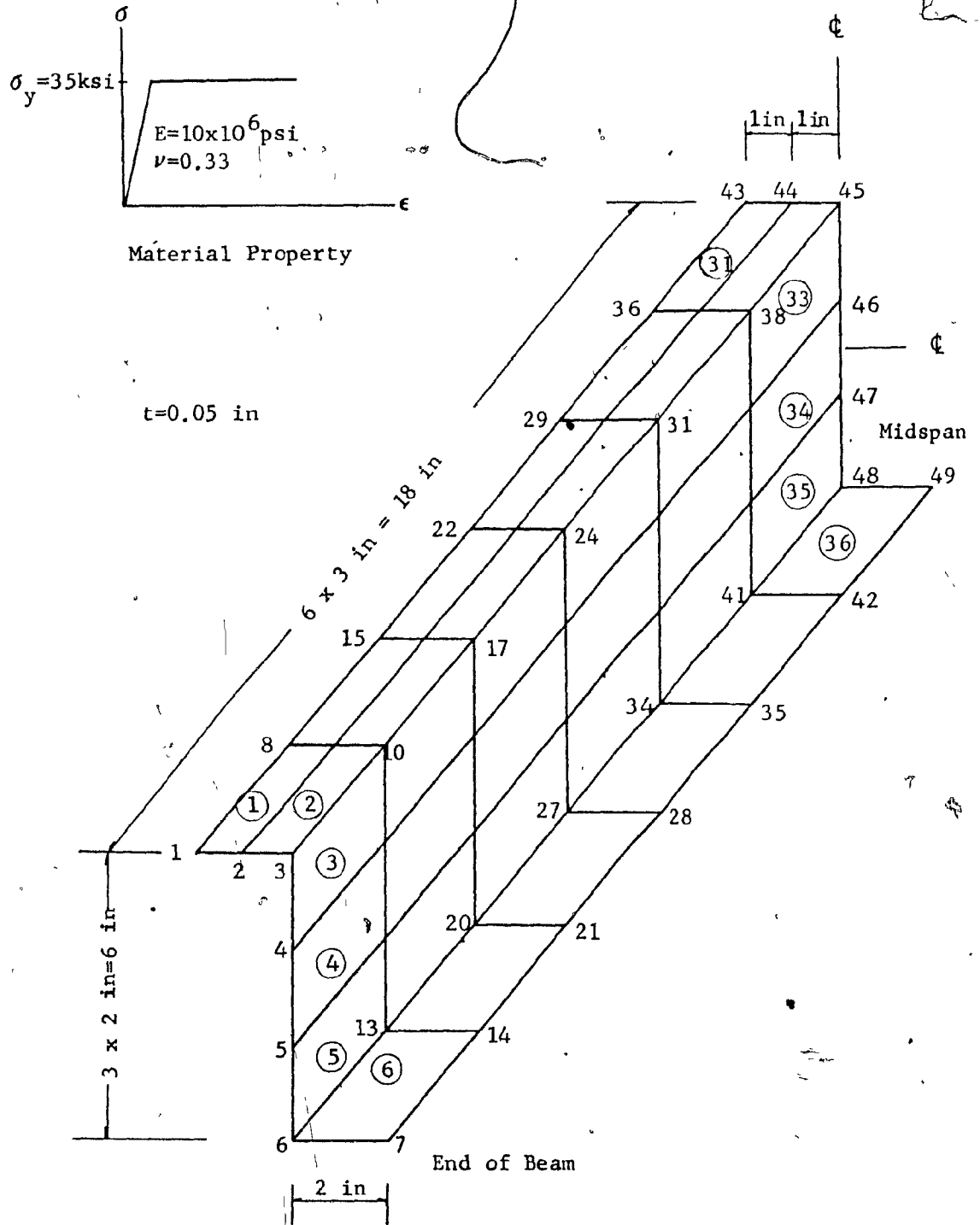


Figure 71

Idealization for a Z-Section Beam

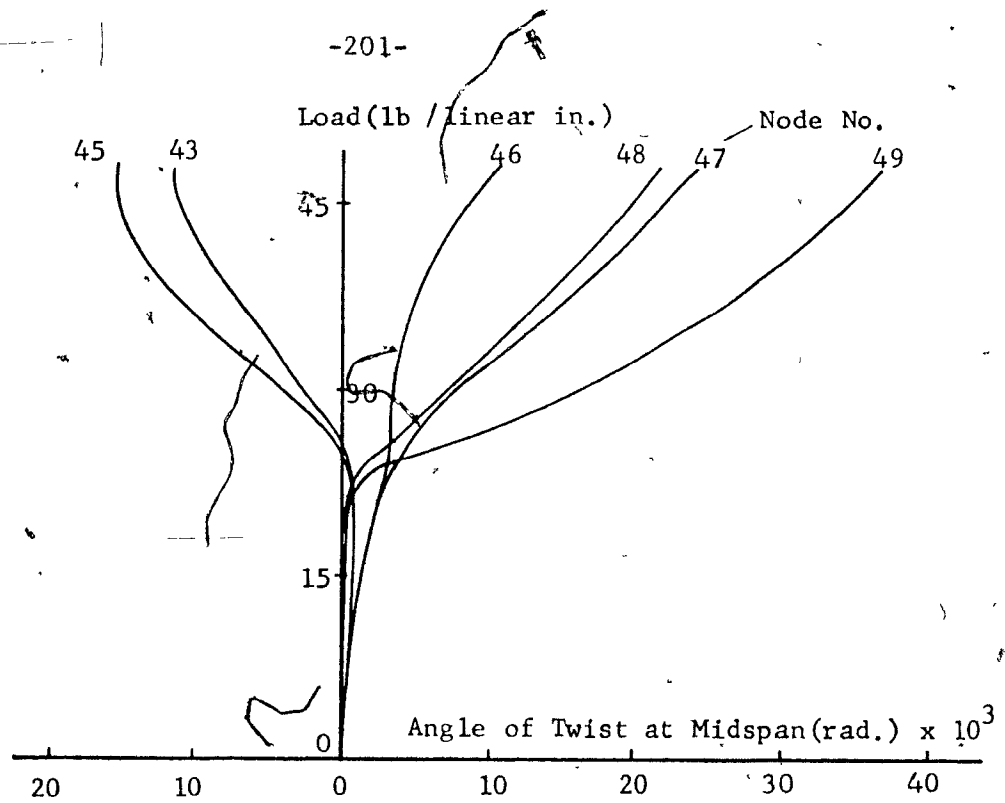


Figure 72 Load-Angle of Twist Relation of Z-Section

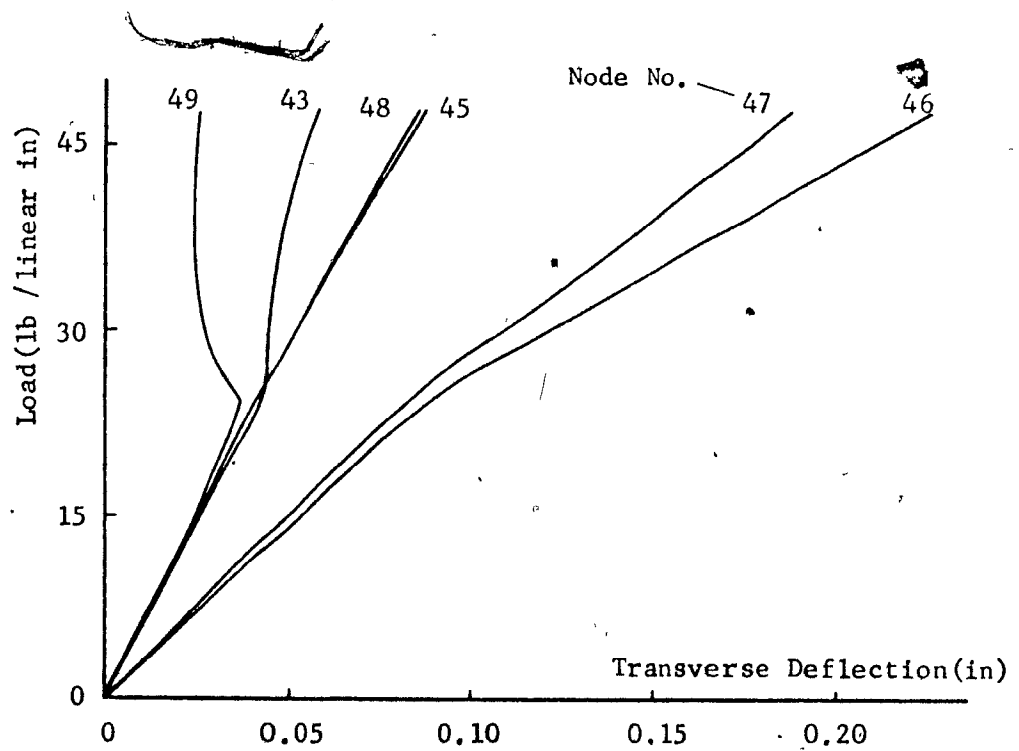


Figure 73 Load-Deflection Relation of Z-Section

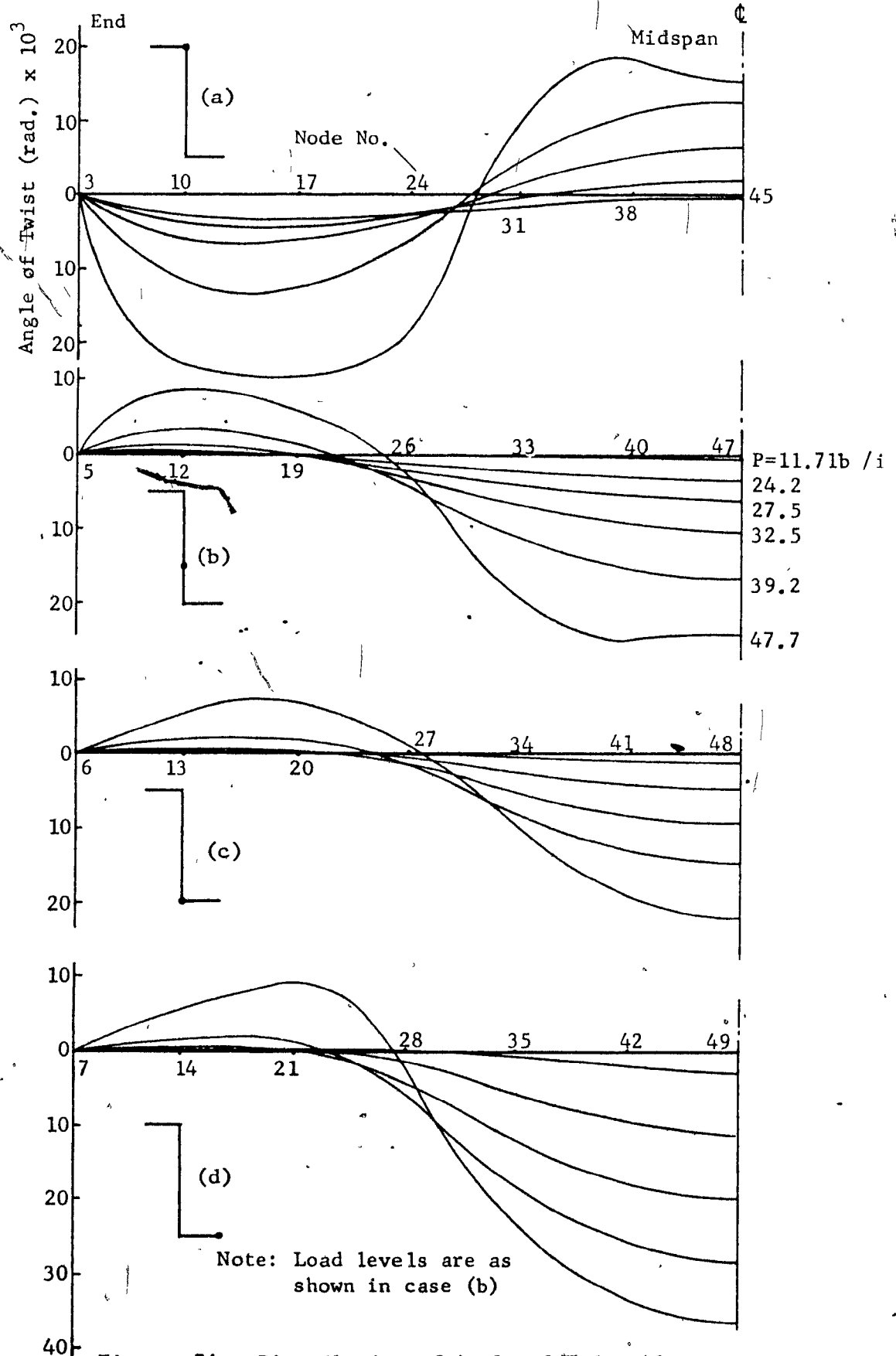


Figure 74 Distribution of Angle of Twist Along the Span of Z-Section

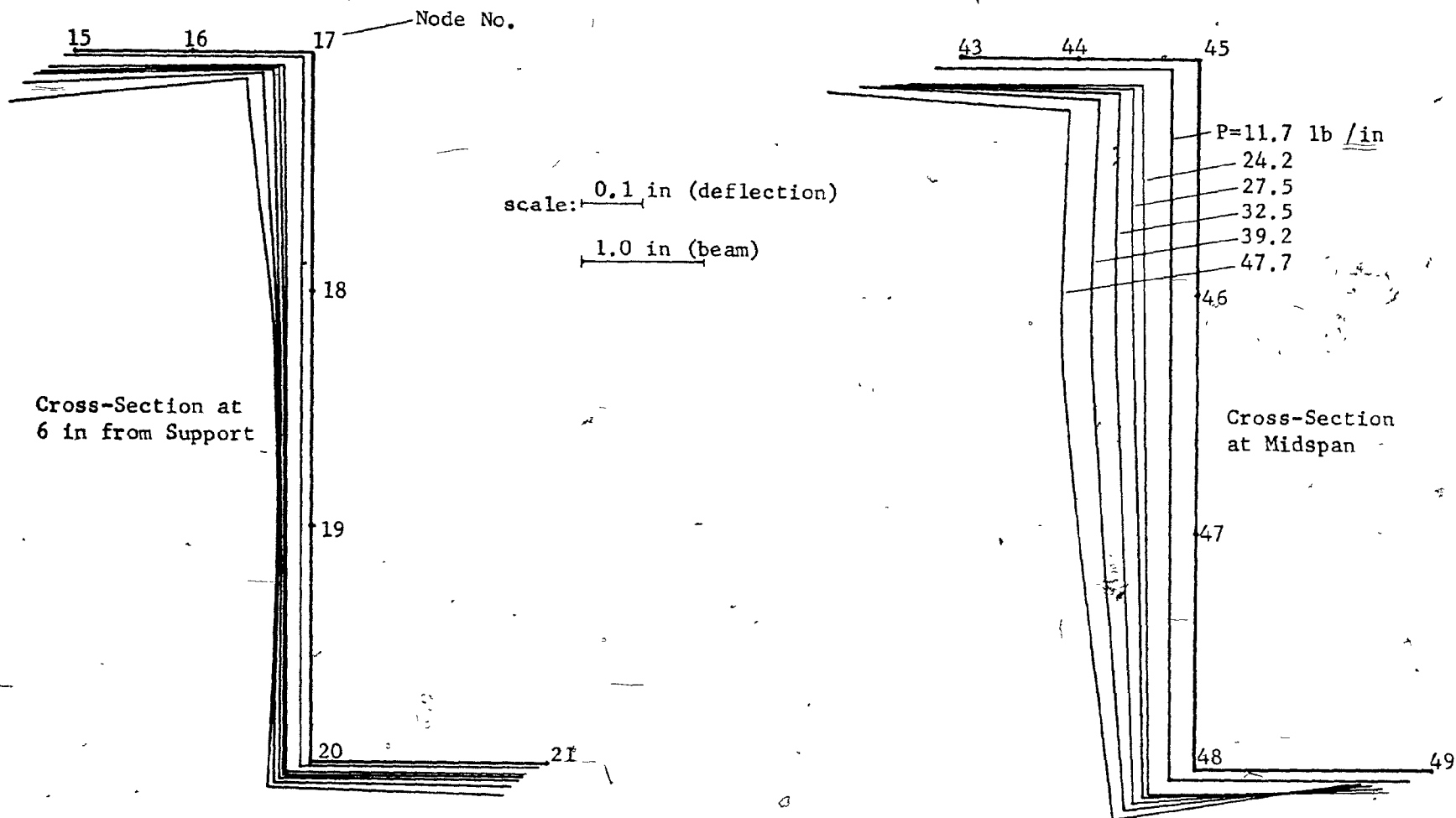


Figure 75 Distortion of the Z-Section

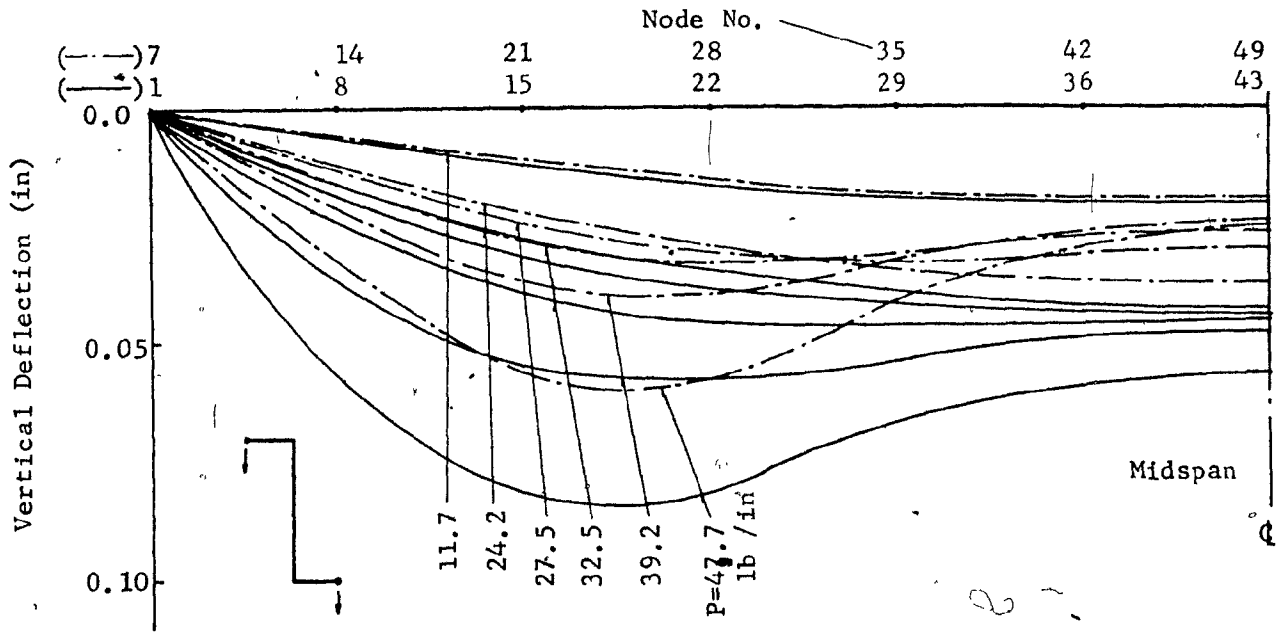


Figure 76 Vertical Deflection Profile Along the Flange Tips of Z-Section

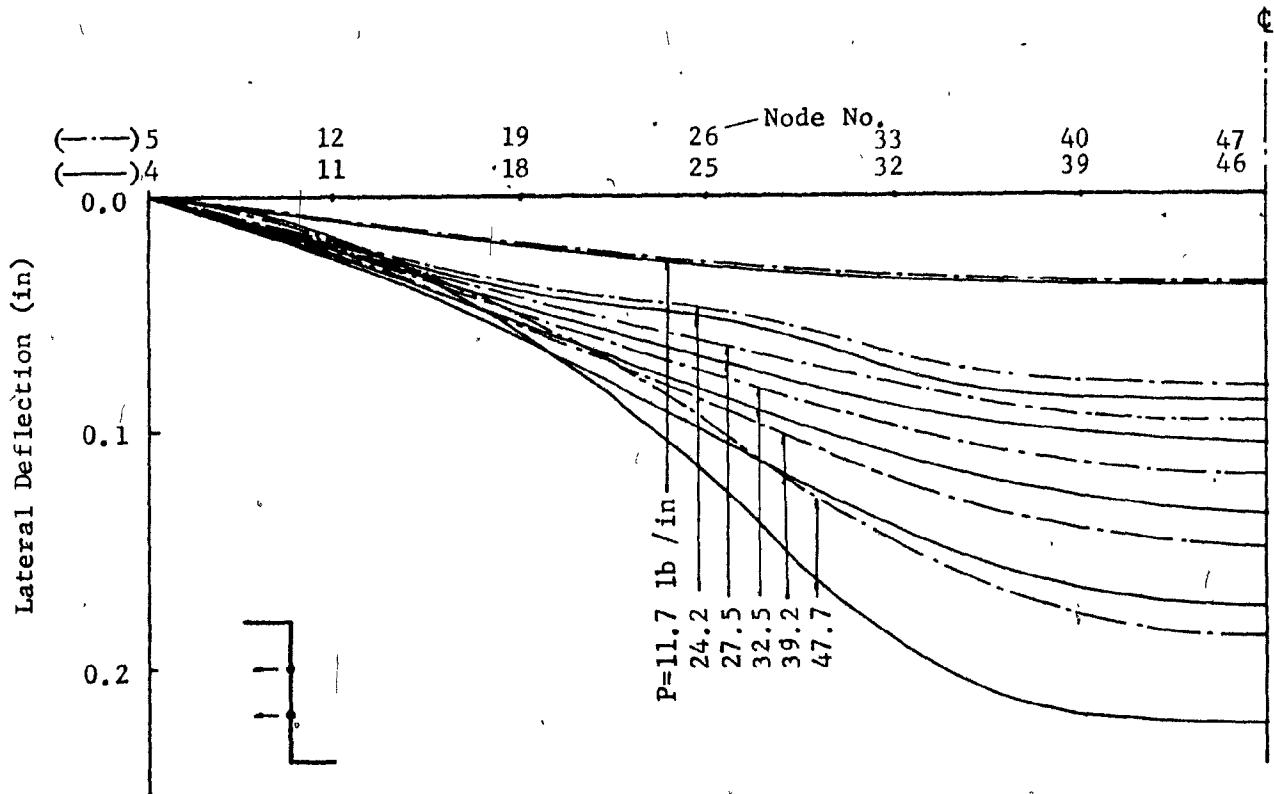


Figure 77 Lateral Deflection Profile of Web of Z-Section

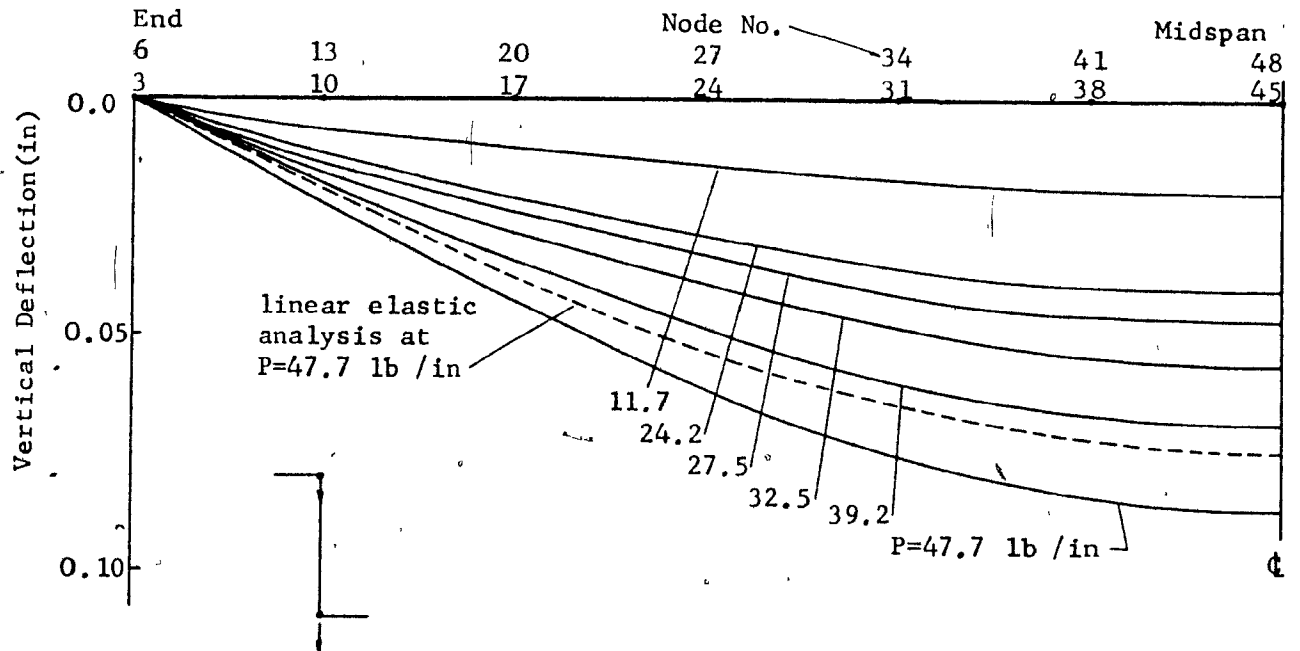


Figure 78 Vertical Deflection Profile of Z-Section

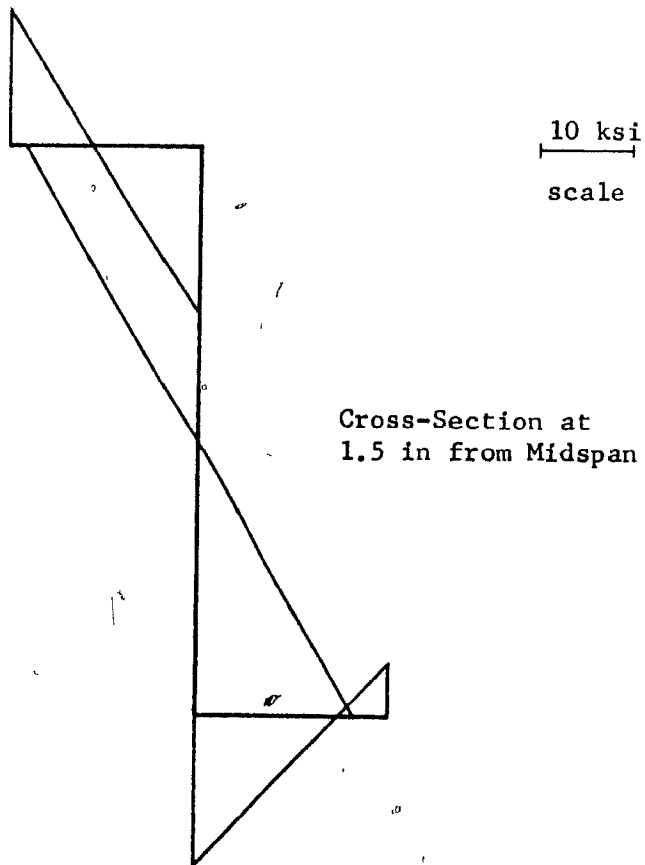


Figure 79 Longitudinal Stress Distribution Along the Transverse Section of Z-Section

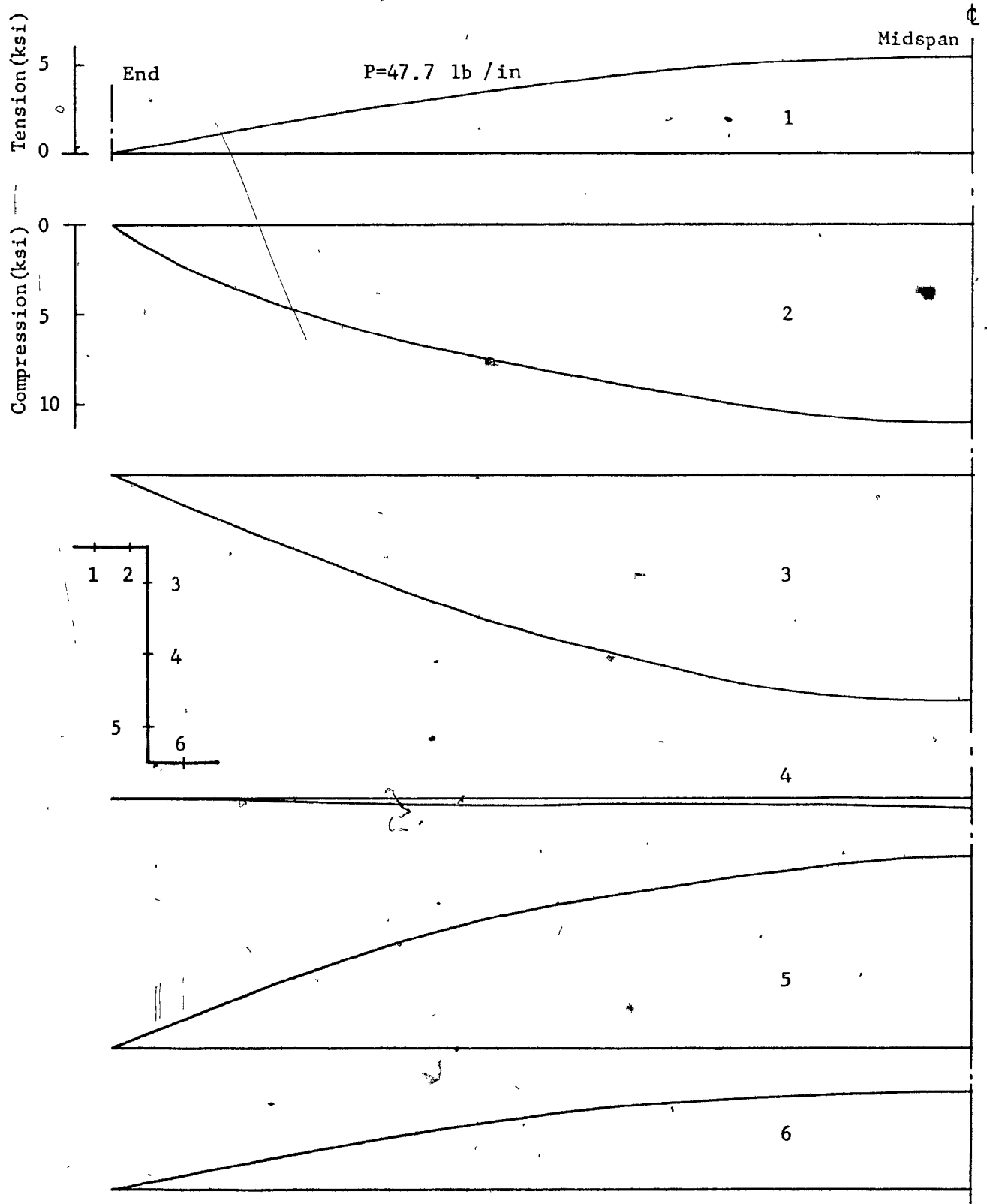


Figure 80 Distribution of Longitudinal Stress Along the Longitudinal Sections of Z-Section Beam

REFERENCES

1. Canadian Standards Association, "Cold Formed Steel Structural Members" CSA Standard S139-1974
2. "Commentary on Cold Formed Steel Structural Members" Canadian Standards Association, CSA Standard S136-1974.
3. Canadian Standards Association, "Design of Light Gauge Aluminum Products" CSA Standard S190-1968
4. American Iron and Steel Institute, "Specification for the Design of Cold-Formed Steel Structural Members", 1968.
5. Winter, G., "Commentary on the 1968 Edition of The Specification for the Design of Cold-Formed Steel Structural Members", American Iron and Steel Institute, 1970
6. British Standards Institution, "Specification for the Use of Cold-Formed Steel Sections in Building", Addendum No. 1 to British Standard 449(PD4064), 1974
7. Yu, W.W., "Cold-Formed Steel Structures", McGraw-Hill Book Co., N.Y., 1973
8. Walker, A.C., ed. "Design and Analysis of Cold Formed Sections", John Wiley & Sons, N.Y., 1975
9. Kirchhoff, G., "Vorlesungen Uber Mathematik", Physik und Mechanik, 2nd ed., Leipzig, 1877 (3rd ed. in 1883)
10. Vlasov, V.Z., "Thin-walled Elastic Beams", Translated from Russian by Y. Schechtman, Israel Program for Scientific Translations, Jerusalem, 1961. Also see Zbirohowski-Koscia, K. "Thin-Walled Beams", Grosby Lockwood & Sons Ltd., London, 1967.
11. Bleich, F., "Buckling Strength of Metal Structures", ed. by Bleich, H. McGraw-Hill, N.Y., 1952
12. Timoshenko, S.P., "Strength of Materials", Part II: Advanced Theory and Problems, 3rd ed., D. Van Nostrand Co. N.Y., 1956
13. Timoshenko, S.P., and Gere, J.M., "Theory of Elastic Stability", McGraw-Hill, N.Y., 1961.
14. Von Karman, Th., "Festigkeitsprobleme in Maschinenbau", Encyklopadie der Mathematischen Wissenschaften, Vol. 4, 1910, p. 349
15. Timoshenko, S., "Theory of Elastic Stability", McGraw-Hill Book Co. Inc., N.Y., N.Y., 1936



16. Marguerre, K. and Trefftz, E., "Über die Tragfähigkeit eines längsbelasteten Plattenstreifens nach Überschreiten der Beullast", Z.f.a.M.M., Bd. 17, Heft 2, Apr. 1937, pp 85-100
17. Way, S., "Uniformly Loaded, Clamped, Rectangular Plates with Large Deflection", Proceedings, 5th International Congress for Applied Mechanics, Cambridge, Mass, 1938.
18. Wang, C.T., "Non-Linear Large Deflection Boundary Value Problem of Rectangular Plates", NACA TN 1425, 1948
19. Wang, C.T., "Bending of Rectangular Plate with Large Deflection", NACA TN 1462, 1948
20. Chien, W.Z. and Yeh, K.Y., "On the Large Deflection of Rectangular Plate", Proc. 9th Int. Cong. for Appl. Mech., Brussels, Vol. 6, 1957, pp 403-412.
21. Levy, S., "Bending of Rectangular Plates with Large Deflections", NACA Report No. 737, Also NACA Tech. Notes No. 846, 1942
22. Levy, S., "Square Plate with Clamped Edges under Normal Pressure Producing Large Deflections", NACA Report No. 740, Also NACA Tech. Notes No. 847, 1942.
23. Levy, S., Goldenberg, D. and Zibritsky, G., "Simply Supported Long Rectangular Plate under Combined Axial Load and Normal Pressure", NACA TN. 949, Oct. 1944.
24. Hu, Pai. C., Lundquist, E.E. and Batdorf, S.B., "Effect of Small Deviations from Flatness on Effective Width and Buckling of Plates in Compression", NACA TN.1124, 1946.
25. Coan, J.M., "Large-Deflection Theory for Plates with Small Initial Curvature Loaded in Edge Compression", Journal of Applied Mechanics, Vol. 18, Trans. ASME Vol. 73, 1951, pp 143-151
26. Yamaki, N., "Post-Buckling Behaviour of Rectangular Plates with Small Initial Curvature Loaded in Edge Compression", Journal of Applied Mechanics, Trans. ASME Vol. 81, 1959, pp 407-414
27. Koiter, W.T., "On the Stability of Elastic Equilibrium", Ph.D. Thesis, Delft, Netherlands, 1945, English Translation, NASA TTF-10, 1967.
28. Berger, H.M., "A New Approach to the Analysis of Large Deflections of Plates", J. of Appl. Mech., ASME Trans., Vol. 22, No. 4, Dec. 1955, pp 465-472
29. Stein, M., "Load and Deflections of Buckled Rectangular Plates", NASA TR R-40, 1959.

30. Stein, M., "The Phenomenon of Change in Buckle Pattern in Elastic Structures", NASA TR R-39, 1959
31. Supple, W.J. and Chilver, A.H., "Elastic Post-Buckling of Compressed Rectangular Flat Plates", Thin-Walled Structures, edited by A.H. Chilver, John-Wiley and Sons, N.Y., 1967
32. Supple, W.J., "On the Change in Buckle Pattern in Elastic Structures", Int. J. of Mechanical Sciences, Vol. 10, pp 737-745, 1968.
33. Supple, W.J., "Change of Wave-Form of Plates in the Post-Buckling Range", Int. J. of Solid and Structures, Vol. 6, 1970, pp 1243-1258
34. Timoshenko, S. and S. Woinowsky-Krieger, "Theory of Plates and Shells", McGraw-Hill Book Co., N.Y., 1959.
35. Walker, A.C., "The Post-Buckling Behaviour of Simply Supported Square Plates", Aero. Quarterly, Vol. 20, Aug. 1969, pp 203-222.
36. Dawson, R.G. and Walker, A.C., "Post-Buckling of Geometrically Imperfect Plates", ASCE, J. of Struct. Div., ST 1, Jan. 1972, pp 75-94
37. Williams, D.G. and Walker, A.C., "Explicit Solutions for the Design of Initially Deformed Plates Subject to Compression", Proc. Inst. Civil Engrs., Part 2, 1975, 59, Dec. pp 763-787.
38. Chandra, R. and Raju, B.B., "Post-Buckling Analysis of Rectangular Orthotropic Plates", Int. J. of Mech. Sci., Vol. 15, Jan. 1973, pp 81-98
39. Rushton, K.R., "Post-Buckling of Rectangular Plates with Various Boundary Conditions", Aeronautical Quarterly, May 1970, pp 163-181.
40. Rushton, K.R., "Large Deflection of Rectangular Plates with Initial Curvature", Int. J. Mech. Sci., Vol. 12, 1970, pp 1037-1051 (also discussion Vol. 13, 489-491, 1971)
41. Rushton, K.R., "Large Deflection of Plates with Unsupported Edges", J. of Strain Analysis, Vol. 7, No. 1, 1972, pp 44-53.
42. Rushton, K.R., "Buckling of Laterally Loaded Plates Having Initial Curvature", Int. J. Mech. Sci., Vol. 14, pp 667-680, 1972.
43. Rhodes, J. and Harvey, J.M., "Plates in Uniaxial Compression with Various Support Conditions at the Unloaded Boundaries", Int. J. of Mech. Sci., Vol. 13, 1971, pp 787-802.
44. Rhodes, J. and Harvey, J.M., "Effects of Eccentricity of Load or Compression on the Buckling and Post-Buckling Behaviour of Flat Plates", Int. J. Mech. Sci. Vol. 13, 867-879, 1971.

45. Rhodes, J. and Harvey, J.M., "The Post-Buckling Behaviour of Thin Flat Plates in Compression with the Unloaded Edges Elastically Restrained Against Rotation", J. of Mech. Eng. Sci., Vol. 13, No. 2, 1971, pp 82-91
46. Basu, A.K. and Chapman, J.C., "Large Deflection Behaviour of Transversely Loaded Rectangular Orthotropic Plates", Proc. ICE, Vol. 35, Sept. 1966, pp 79-110
47. Aalami, B. and Chapman, J.C., "Large Deflection Behaviour of Rectangular Orthotropic Plate under Transverse and In-Plane Loads", Proc. ICE, Vol. 42, March 1969, pp 347-382
48. Hutchison, J.W. and Koiter, W.T., "Post-Buckling Theory", Applied Mechanics Review, Vol. 232, pp 1353-1366, 1970
49. Bieniek, M.P., "Post-Critical Behaviour", Introductory Report, 9th Congress of IABSE, May 1972, pp 25-53
50. Murray, D.W. and Wilson, E.L., "Finite Element Large Deflection Analysis of Plates", ASCE, J. EML, Vol. 95, 1969, pp 143-165
51. Murray, D.W. and Wilson, E.L., "Finite Element Post-Buckling Analysis of Thin Elastic Plates", AIAA J., Vol. 7, No. 10, 1969, pp 1915-1920
52. Lang, T.E. and Hartz, B.J., "Finite Element Matrix Formulation of Post-Buckling Stability and Imperfection Sensitivity", IUTAM Colloquium on High Speed Computing of Elastic Structures, Liege, Belgium, 1970
53. Roberts, T.M. and Ashwell, D.G., "The Use of Finite Element Mid-Increment Stiffness Matrices in the Post-Buckling Analysis of Imperfect Structures", Int. J. Solids Struct., 7, 1971, pp 805-823
54. Kawai, T. and Yoshimura, N., "Analysis of Large Deflection of Plates by the Finite Element Method", Int. J. for Num. Meth. in Eng., Vol. 1, 1969, pp 123-133.
55. Kawai, T., "Finite Element Analysis of the Geometrically Nonlinear Problems of Elastic Plates", Recent Advances in Matrix Methods of Structural Analysis and Design (1st U.S.-Japan Seminar held at Tokyo, 1969) eds. R.H. Gallagher, Y. Yamada, and J.T. Oden, The University of Alabama Press, 1971. pp 383-414.
56. Vos, R.G. and Vann, W.P., "A Finite Element Tensor Approach to Plate Buckling and Post-Buckling", Int. J. for Num. Meth. in Eng., Jan. 1973, pp 351-365, Vol. 5.
57. Bergan, P.G., "Nonlinear Analysis of Plates Considering Geometric and Material Effects", 2nd Report No. 72-1, Div. of Structural Mechanics, The Norwegian Institute of Technology, The University of Trondheim, Norway, May 1972.

58. Yang, H.T.Y., "Flexible Plate Finite Element on Elastic Foundation", ASCE, Struct. Div., Oct. 1970, pp 2083-2101
59. Yang, H.T.Y., "A Finite Element Procedure for Large Deflection Analysis of Plates with Initial Deflections", AIAA J., Vol. 9, Aug. 1971, pp 1468-1473
60. Yang, H.T.Y., "Nonlinear Buckling of Thin-Walled Components", Proc. 1st Specialty Conf. on Cold-Formed Steel Structures, Aug. 1971, ed. W.W. Tu, University of Missouri-Rolla, pp 31-36
61. Yang, H.T.Y., "Elastic Post-Buckling Predictions of Plates Using Discrete Elements", AIAA J., Vol. 9, Sept. 1971, pp 1665-1666
62. Yang, H.T.Y., "Finite Displacement Plate Flexure by Use of Matrix Incremental Approach", Int. J. for Num. Meth. in Eng., Vol. 4, No. 3, 1972, pp 415-432
63. Bagchi, D.K. and Rockey, K.C., "Post-Buckling Behaviour of a Web Plate under Partial Edge Loading", Third Int. Specialty Conf. on Cold-Formed Steel Structures, ed. W.W. Yu and J.H. Senne, University of Missouri-Rolla, Nov. 1975, pp 251-284.
64. Schmit, L.A., Bogner, F.K. and Fox, R.C., "Finite Deflection Analysis Using Plate and Shell Discrete Elements", AIAA J., Vol. 6, May 1968, pp 781-791
65. Brebbia, C. and Connor, J., "Geometrically Non-Linear Finite Element Analysis", ASCE, J. of Eng. Mech. Div., EM2, Vol. 95, April 1969, pp 463-486
66. Tezcan, S., Mahapatra, B.C. and Mathews, C., "Tangent Stiffness Matrix for Finite Elements", Publication of IABSE 30-1, 1970, pp 217-246
67. Gallagher, R.H., Lien, S., and Mau, S.T., "A Procedure for Finite Element Plate and Shell Pre- and Post-Buckling Analysis", Proc. of Third Air Force Conf. on Matrix Methods in Struct. Mech., Dayton Ohio, 1971, pp 857-879.
68. Mau, S. and Gallagher, R.H., "A Finite Element Procedure for Nonlinear Prebuckling and Initial Post-Buckling Analysis", NASA CR-1936, Jan. 1972.
69. Bergan, P.G. and Clough, R.W., "Large Deflection Analysis of Plates and Shallow Shells Using Finite Element Methods", Int. J. for Num. Meth. in Eng., Vol. 5, pp 543-556, 1973.
70. Gass, N. and Tabarrok, B., "A Large Deformation Analysis of Plates and Cylindrical Shells by a Mixed Finite Element Method", Int. J. for Num. Method. in Eng., Vol. 10, 1976, pp 731-746.

71. Black, M., "Non-Linear Behaviour of Thin-Walled Unsymmetrical Beam-Sections Subjected to Bending and Torsion", Thin-Walled Structures, A.H. Chilver, ed., John Wiley and Sons, N.Y., 1967, pp 87-102
72. Soltis, L.A. and Christiano, P., "Finite Deformation of Biaxially Loaded Columns", J. of Struct. Div., ASCE, Vol. 98, No. ST12, Dec. 1972, pp 2647-2662
73. Ghobarah, A.A., and Tso, W.K., "A Non-Linear Thin-Walled Beam Theory", Int. J. Mech. Sci., Vol. 13, 1971, pp 1025-1038
74. Tso, W.K. and Ghobarah, A.A., "Non-Linear Non-Uniform Torsion of Thin-Walled Beams", Int. J. Mech. Sci., Vol. 13, 1971, pp 1039-1047
75. Mikhail, M.L. and Guralnick, S.A., "The Non-Linear Response of Transversely-Loaded Folded Plate Structures", Int. J. Non-Linear Mechanics, Vol. 6, 1971, pp 81-99
76. Khan, A.Q., and Harris, P.J., "Post-Buckling Behaviour of Thin-Walled Members", Proc. Int. Conf. of Computational Methods in Nonlinear Mechanics, Univ. of Texas, Austin, Sept. 1974.
77. Rajasekaran, S. and Murray, D.W., "Finite Element Large Deflection Analysis of Thin-Walled Beams of Open Section", Proc. of the 1974 Int. Conf. on Finite Element Methods in Engineering, eds. V.A. Pulmano and A.P. Kabaila, University of New South Wales, Australia, Aug. 1974, pp. 435-453.
78. Prager, W. and Hodge, P.G., Jr., "Theory of Perfectly Plastic Solids", John Wiley and Sons, Inc., New York, 1951.
79. Hodge, P.G., Jr., "Numerical Applications of Minimum Principles in Plasticity", Engineering Plasticity, eds. J. Heyman and F.A. Leckie, Cambridge University Press, 1968, pp 237-256.
80. Johnson, W. and Mellor, P.B., "Engineering Plasticity", Van Nostrand Reinhold Co., London, 1973:
81. Martin, J.B., "Plasticity: Fundamental and General Results", the MIT Press, Cambridge, Mass., 1975.
82. Massonnet, C.H., "Theorie Generals des Plaques Elasto-Plastiques", IABSE Publications, Vol. XXVI, 1966, pp 289-300.
83. Cornelis, A., "Etude a Laide D'une Calculatrice Electronique du Comportement Elastique des Plaques", IABSE Publications, Vol. XXVI 1966, pp 301-311.
84. Ang, A.H.S., and Lopez, L.A., "Discrete Model Analysis of Elastic-Plastic Plates", J. of Eng. Mech. Div., Proc. ASCE, Vol. 94, EM1, Feb. 1968, pp 271-293.

85. Mendelson, A., "Plasticity: Theory and Application", the Macmillian Co., New York, 1968
86. Lin, T.H. and Ho, E.Y., "Elasto-Plastic Bending of Rectangular Plates", J. of Eng. Mech., Proc. of ASCE, Vol. 94, EM1, Feb. 1968, pp 199-209
87. Lin, T.H., "Theory of Inelastic Structures", John Wiley and Sons, Inc., New York, 1968.
88. Marcal, P.V. and Mallett, R.H., "Elastic-Plastic Analysis of Flat Plates by the Finite Element Method", Proc. ASME Winter Annual Meeting, Paper No. 68-WA/PVP-10, Dec. 1968
89. Armen, H. Jr., Pifko, A., and Levine, H.S., "Finite Element Method for the Plastic Bending Analysis of Structures", Proc. 2nd Conf. on Matrix Methods in Struct. Mechanics, AFFDL-TR-68-150, 1968, pp 1301-1339
90. Armen, H. Jr., Pifko, A., and Levine, H.S., "Finite Element Analysis of Structures in the Plastic Range", NASA CR 1649, 1971
91. Whang, B., "Elasto-Plastic Orthotropic Plates and Shells", Proc. Symposium on Application of Finite Element Methods in Civil Engineering, Vanderbilt University, ASCE, Nov. 1969, pp 481-515
92. Bergan, P.G. and Clough, R.W., "Elasto-Plastic Analysis of Plates Using the Finite Element Method", 3rd Conf. on Matrix Method in Struct. Mech., Wright Patterson Air Force Base, Ohio, 1971 pp 929-957
93. Wegmuller, A.W., "Full Range Analysis of Eccentrically Stiffened Plates", Proc. ASCE, J. St. Div., ST.1, Jan. 1974, Vol. 100, pp 143-159
94. Wegmuller, A.W., "Elastic-Plastic Finite Element Analysis of Plates", Proc. Instn. Civ. Engrs., Part 2, 1974, Vol. 54, Sept., pp 535-543
95. Barnard, A.J. and Sharman, P.W., "The Elasto-Plastic Analysis of Plates Using Hybrid Finite Elements", Int. J. for Num. Meth. in Eng., Vol. 10, 1976, pp 1343-1356.
96. Rajaskaran, S., and Murray, D.W., "Finite Element Solution of Inelastic Beam Equations", J. of Struct. Div., Proc. ASCE, Vol. 99, No. ST6, June 1973, pp 1025-1041
97. Lundgren, K., "Vlasov Torsion of Non-Linear Elastic Beams of Thin-Walled Open Cross-Section", Int. J. Mech. Sci., Vol. 16, pp 289-295, 1974.
98. Lundgren, K., "Vlasov Torsion of Elastic-Ideally-Plastic Beams of Thin-Walled Open Cross-Section", Int. J. Mech. Sci., Vol. 18, 1976, pp 105-109.

99. Schuman, L. and Back, G., "Strength of Rectangular Flat Plates under Edge Compression", NACA Report No. 356, 1930, (Also NACA TN No. 356, 1930).
100. Von Karman, T., Sechler, E.E. and Donnell, L.H., "The Strength of Thin Plates in Compression", ASME. Trans., Vol. 5, 1932, APM-54-5, pp 53-57
101. Sechler, E.E., "The Ultimate Strength of Thin Flat Sheets in Compression", Publication No. 27, Guggenheim Aeronautics Laboratory, California Inst. of Tech., Pasadena, 1933.
102. Cox, H.L., "Buckling of Thin Plates in Compression", British Aeronautical Research Council, Report and Memorandum No. 1554, 1933.
103. Cox, H.L., "The Buckling of a Flat Rectangular Plate Under Axial Compression and its Behaviour after Buckling", Aeron. Res. Council, R and M 2041, 1945.
104. Marguerre, K., "The Apparent Width of the Plate in Compression", NACA TM 833, 1937.
105. Kromm, A. and Marguerre, K., "Behaviour of a Plate Strip Under Shear and Compressive Stresses Beyond the Buckling Limit", NACA TM 870, 1938.
106. Stowell, E.Z., "Compressive Strength of Flanges", NACA TN 2020, 1950 (also NACA Report 1029, 1951).
107. Mayers, J. and Budiansky, B., "Analysis of Behaviour of Simply Supported Flat Plates Compressed Beyond the Buckling Load Into the Plastic Range", NACA TN 3368, 1955.
108. Heimerl, G.J., "Determination of Plate Compressive Strengths", NACA TN 1480, 1947.
109. Schuette, E.H., "Observations of the Maximum Average Stress of Flat Plates Buckled in Edge Compression", NACA TN 1625, 1949.
110. Needham, R.A., "The Ultimate Strength of Aluminum-Alloy Formed Structural Shapes in Compression", J. Aero. Sci., Vol. 21, No. 4, April 1954, pp 217-229.
111. Gerard, G., "Handbook of Structural Stability", Part IV and V. NACA TN 3784 and 3785, Aug. 1957
112. Gerard, G., "Introduction to Structural Stability Theory", McGraw-Hill, N.Y., 1962.
113. Winter, G., "Strength of Thin Steel Compression Flanges", Engineering Experiment Station, Reprint No. 32, Cornell Univ. 1947.
114. Winter, G., Lansing, W. and McCalley, R.B. Jr., "Four Papers on the Performance of Thin-Walled Steel Structures", Engineering Experiment Station ; Reprint No. 33, Cornell University, 1950.

115. Chilver, A.H., "The Stability and Strength of Thin-Walled Steel Struts", *The Engineer*, Aug. 7, 1953, pp 180-183
116. Jombock, J.R. and Clark, J.W., "Postbuckling Behaviour of Flat Plates", *ASCE, J. of Struct. Div.*, ST5, June 1961, pp 17-33.
117. Campus, F. et Massonnet, CH. (editeurs), "Colloque International sur le Comportement Post-Critique des Plaques Utilisees en Construction Metallique", (Symposium on the post-buckling behaviour of plates), Liege, Institut de Genie Civil, 1963
118. Dwight, J.B. and Ractliffe, A.T., "The Strength of Thin Plates in Compression", *Thin Walled Steel Structures - Their Design and Use in Building*, Symposium at University of College of Swansea, Sept. 1967, eds. K.C. Rockey and H.V. Hill, Gordon and Breach Sci. Pub., pp 3-34, 1969.
119. Graves-Smith, T.R., "The Ultimate Strength of Locally Buckled Columns of Arbitrary Length", *Thin Walled Steel Structures - Their Design and Use in Building*, Symposium at University of College of Swansea, Sept. 1967, eds. K.C. Rockey and H.V. Hill, Gordon and Breach Sci. Pub., pp 35-60, 1969.
120. Graves-Smith, T.R., "The Post-Buckling Strength of Thin-Walled Columns", *Final Report, 8th Congress of IABSE*, 1968, pp 311-320.
121. Graves-Smith, T.R., "The Effect of Initial Imperfections on the Strength of Thin-Walled Box Column", *Int. J. Mech. Sci.*, Vol. 13, pp 911-925, 1971.
122. Graves-Smith, T.R., "The Post-Buckled Behaviour of a Thin-Walled Box Beam in Pure Bending", *Int. J. of Mech. Science*, Vol. 14, Nov. 1972, pp 711-722.
123. Massonnet, Ch., "General Theory of Elasto-Plastic Membrane-Plates", *Engineering Plasticity*, eds. J. Heyman and F.A. Leckie, Cambridge University Press, 1968, pp 443-471.
124. Reiss, M. and Chilver, A.H., "Computation of the Post-Buckling Strength of Thin-Walled Sections", *Final Report, 8th Congress of IABSE*, 1968, pp 299-309.
125. Bulson, P.S., "The Stability of Flat Plates", *American Elsevier Publishing Co., Inc.*, N.Y., 1969.
126. Abdel-Sayed, G., "Effective Width of Thin Plates in Compression", *J. of Struct. Div.*, *ASCE*, ST10, Oct. 1969, pp 2183-2203.
127. Rhodes, J., Harvey, J.M. and Fox, W.C., "The Load-Carrying Capacity of Initially Imperfect Eccentrically Loaded Plates", *Int. J. Mech. Sci.*, Vol. 17, 1975, pp 161-175.



128. Sherbourne, A.N., C.Y. Liaw, and C. Marsh, "Stiffened Plates in Uniaxial Compression", Publications, IABSE, Vol. 31-1, 1971, pp 145-177
129. Korol, R.M. and A.N. Sherbourne, "Strength Predictions of Plates in Uniaxial Compression", ASCE, St. Div., Vol. 98, Sept. 1972, pp 1965-1986.
130. Sherbourne, A.G. and R.M. Korol, "Post-Buckling of Axially Compressed Plates", ASCE, St. Div., Vol. 98, Oct. 1972, pp 2223-2234
131. Wang, S.T., "Nonlinear Analysis of Thin-Walled Continuous Beams", Second Specialty Conference on Cold-Formed Steel Structures, ed. W.W. Yu, University of Missouri-Rolla, 1973, pp 107-138
132. Rockey, K.C., El-gaaly, M.A. and Bagchi, D.K., "Failure of Thin-Walled Members Under Patch Loading", J. of Struct. Div., ASCE, No. ST12, Vol. 98, Dec. 1972, pp 2739-2752
133. El-gaaly, M.A. and Rockey, K.C., "Ultimate Strength of Thin-Walled Members Under Patch Loading and Bending", Second Specialty Conference on Cold-Formed Steel Structures, ed. W.W. Yu, University of Missouri, 1973, pp 139-167
134. Rockey, K.C., Porter, D.M. and Evans, H.R., "Ultimate Load Capacity of the Webs of Thin-Walled Members", Second Specialty Conference on Cold-Formed Steel Structures, ed. W.W. Yu, University of Missouri-Rolla, 1973, pp 169-200
135. Venkataramaiah, K.R., "Thin-Walled Columns", Ph.D. Thesis, University of Waterloo, 1973.
136. Lind, N.C., Ravindra, M.K. and Power, J., "A Review of the Effective Width Formula", Proc. 1st Speciality Conf. on Cold-Formed Steel Structures, 1971, ed. W.W. Yu, University of Missouri-Rolla, pp 37-42.
137. Lind, N.C., "Recent Developments in Cold-Formed Steel Design Requirements", Design in Cold Formed Steel, ed. R.M. Schuster, 1974, pp 213-223, Solid Mech. Div., University of Waterloo Press.
138. Lind, N.C., Ravindra, M.K. and Schorn, G., "Empirical Effective Width Formula," J. of Struc. Div., Proc. of ASCE, ST9, Sept. 1976, pp 1741-1757.
139. Lin, T.H., Lin, S.R. and Mazelsky, B., "Elastoplastic Bending of Rectangular Plates with Large Deflection", J. of Applied Mech., Dec. 1972, pp 978-982.
140. Davies, P., Kemp, K.O. and Walker, A.C., "An Analysis of Failure Mechanism of an Axially Loaded Simply Supported Steel Plate", Proc. Inst. of Civil Engrs., Part 2, 1975, 59, Dec. pp 645-658.

141. Murray, D.W. and Wilson, E.L., "An Approximate Nonlinear Analysis of Thin Plates", Proc. 2nd Conf. On Matrix Methods in Struct. Mech., AFFDL-TR-68-150, 1968, pp 1207-1230
142. Marcal, P.V., "Large Deflection Analysis of Elastic-Plastic Plates and Shells", Proc. First Int. Conf. on Pressure Vessel Tech., ASME/Royal Netherlands Engineering Society, Delft, Sept. 1969, pp. 75-87.
143. Ohtsubo, H., "A Method of Elastic-Plastic Analysis of Largely Deformed Plate Problems", Advances in Computational Methods in Structural Mechanics and Design, eds. J.T. Oden, R.W. Clough and Y. Yamamoto, The University of Alabama Press, 1972, pp 439-456
144. Crisfield, M.A., "Large-Deflection Elasto-Plastic Buckling Analysis of Plate Using Finite Elements", TRRL Report LR 593, Crowthorne, Berkshire, 1973.
145. Crisfield, M.A., "Collapse Analysis of Box-Girder Components Using Finite Elements", Presented at Symposium on Non-Linear Tech. and Behaviour in Structural Analysis, Transport and Road Research Laboratory, Crowthorne, Berkshire, Dec. 1974.
146. Crisfield, M.A., "Combined Material and Geometric Non-Linearity for Thin Steel Plates", World Congress on Finite Element Methods in Structural Mechanics, ed. J. Robinson, Bournemouth, 1975.
147. Crisfield, M.A., "Full-Range Analysis of Steel Plates and Stiffened Plating Under Uniaxial Compression", Proc. ICE, Part 2, Vol. 59, Dec. 1975, pp 595-624
148. Crisfield, M.A., "Large-Deflection Elasto-Plastic Buckling Analysis of Eccentrically Stiffened Plates Using Finite Elements", TRRL Laboratory Report 725, Crowthorne, Berkshire 1976.
149. Arai, H., "Analysis on the Large Deformation of Plate Structures", Proc. of the 1974 Int. Conf. on Finite Element Methods in Engineering, eds. V.A. Pulmano and A.P. Kabaila, University of New South Wales, Australia, Aug. 1974, pp 299-313.
150. Murray, D.W. and Rajasekaran, S., "Technique for Formulating Beam Equations", J. of Engineering Mechanics, ASCE, EM5, Oct. 1975, pp 561-573
151. Moan, T. and Soreide, T.H., "Analysis of Stiffened Plates Considering Non-Linear Material and Geometric Behaviour Using Finite Elements", World Congress on Finite Element Methods in Structural Mechanics, ed. J. Robinson, Bournemouth, 1975.

152. Soreide, T.H., Bergan, P.G., Moan, T., "Ultimate Collapse Behaviour of Stiffened Plates Using Alternative Finite Element Formulations", Presented at Int. Conf. on Steel Plated Structures, Imperial College, London, July 1976.
153. Bijlaard, P.P. and Fisher, G.P., "Column Strength of H-Sections and Square Tubes in Postbuckling Range of Component Plates", NACA TN 2994, 1953
154. Cherry, S., "The Stability of Beams with Buckled Compression Flanges", The Structural Engineer, Sept. 1960, pp 277-285
155. Jomback, J.R. and Clark, J.W., "Bending Strength of Aluminum Formed Sheet Members", J. of Struct. Div., ASCE, No. ST2, Feb. 1968, pp 511-528
156. Bulson, P.S., "Local Stability and Strength of Structural Sections", Thin-Walled Structures, ed. A.H. Chilver, John Wiley and Sons, Inc., N.Y., 1967
157. Ghobarah, A.A. and Tso, W.K., "Overall and Local Buckling of Channel Columns", ASCE, J. of Eng. Mech. Div., EM2, Vol. 95, April 1969, pp 447-462. Also Discussion on EM5, Vol. 96, Oct. 1970, pp 783-785.
158. Sharp, M.L., "Strength of Beams or Columns with Buckled Elements", J. of Struct. Div., ASCE, Vol. 96, No. ST5, May 1970, pp 1011-1015
159. Wang, S.T. and Tien, Y.L., "Post-Local-Buckling Behaviour of Thin-Walled Columns", Second Specialty Conference on Cold-Formed Steel Structures, ed. W.W. Yu, University of Missouri-Rolla, 1973, pp 53-81
160. De Wolf, J.T., Pekoz, T. and Winter, G., "Interaction of Postcritical Plate Buckling with Overall Column Buckling of Thin-Walled Members", ASCE, J. St. Div., Vol. 100, No. 10, Oct. 1974, pp 2017-2036
161. De Wolf, J.T., "Local Buckling in Channel Columns", Proc. 3rd Int. Specialty Conf. on Cold-Formed Steel Structures. eds. W.W. Yu and J. M. Senne, Univ. of Missouri-Rolla, 1975, pp 27-49
162. Kalganaraman, V., Pekoz, T. and Winter, G., "Unstiffened Compression Elements", ASCE Annual Convention and Exposition, Philadelphia Sept. 27 - Oct. 1, 1976.
163. Rhodes, J. and Harvey, J.M., "Alternative Approach to Light-Gage Beam Design", ASCE, ST8, Aug. 1971, pp 2119-2135
164. Rhodes, J. and Harvey, J.M., "The Local Buckling and Post Local Buckling Behaviour of Thin-Walled Beams", Aeronautical Quarterly, Vol. 22, Nov. 1971, pp 363-388.

165. Black, M.M., "The Analysis and Design of Thin-Walled Open-Section Beams", Thin Walled Steel Structures - Their Design and Use in Building, Symposium at University of College of Swansea, Sept. 1967, eds. K.C. Rockey and H.V. Hill, Gordon and Breach Sci. Pub., pp 173-196, 1969
166. Zienkiewicz, O.C., "The Finite Element Method in Engineering Science", McGraw-Hill, London, 1971
167. Gallagher, R.H., "Finite Element Analysis-Fundamentals", Prentice-Hall, Inc., Englewood Cliffs, N.J., 1975.
168. Washizu, K., "Variational Methods in Elasticity and Plasticity", Pergamon Press, N.Y., 2nd Edition, 1975.
169. Oden, J.T. and Reddy, J.N., "Variational Methods in Theoretical Mechanics", Springer-Verlag, N.Y., 1976
170. Turner, M.J., Dill, E.H., Martin, H.C. and Melosh, R.J., "Large Deflections of Structures Subjected to Heating and External Loads", J. of the Aerospace Science, Vol. 27, 1960, pp 97-106, 127.
171. Turner, M.J., Martin, H.C. and Weikel, R.C., "Further Development and Applications of the Stiffness Method", AGARDograph 72, Pergamon Press, 1964, pp 203-266
172. Martin, H.C., "On the Derivation of Stiffness Matrices for the Analysis of Large Deflection and Stability Problems", Proc. of Conf. on Matrix Method in Structural Mechanics, Wright-Patterson Air Force Base, Ohio, 1965, AFFDL-TR-66-80, pp 697-716
173. Armen, H. Jr., Levine, H., Pifko, A. and Levy, A., "Nonlinear Analysis of Structures", NASA CR-2351, March 1974
174. Levine, H.S., Armen, H. Jr., Winter, R. and Pifko, A. "Non-Linear Behaviour of Shells of Revolution Under Cyclic Loading", Int. J. of Computer and Structures, Vol. 3, 1973, pp 589-617.
175. Levine, H.S., Winter, R., Armen, H. Jr. and Pifko, A., "Application of the Finite Element Method to Inelastic Shell Analysis", Presented at Conf. on Approximations and Numerical Methods for Inelastic Shells at Georgian Inst. of Tech., May 1975.
176. Stricklin, J.A., Von Riesenmann, W.A., Tillerson, J.R. and Haisler, W.E., "Static Geometric and Material Nonlinear Analysis", Advances in Computational Methods in Structural Mechanics and Design, eds. J.T. Oden, R.W. Clough, and Y. Yamamoto, The University of Alabama Press, 1972, pp 301-324.

177. Argyris, J.H., Kelsey, S. and Kamel, H., "Matrix Method of Structural Analysis - A Precis of Recent Development", AGARDograph 72, Pergamon Press, 1964, pp 1-164
178. Argyris, J.H., "Continua and Discontinua", Proc. of Conf. on Matrix Methods in Structural Mechanics, Wright-Patterson Air Force Base, Ohio, 1965, AFFDL-TR-66-80, pp 11-189.
179. Gallagher, R.H. and Padlog, J., "Discrete Element Approach to Structural Instability Analysis", AIAA J., Vol. 1, No. 6, June 1963, pp 1437-1439
180. Oden, J.T., "Finite Element Applications in Nonlinear Structural Analysis", Proceedings of the Symposium Application of Finite Element Method in Civil Engineering, eds. W.H. Rowan, Jr. and R.M. Hackett, Vanderbilt University, 1969, pp 419-456
181. Mallett, R.H. and Marcal, P.V., "Finite Element Analysis of Nonlinear Structures", Proc. ASCE, J. of the Structural Division, ST9, Sept. 1968, pp 2081-2105
182. Mallett, R.H. and Schmit, L.A., "Nonlinear Structural Analysis by Energy Search", J. of the Struct. Div., ASCE, Vol. 93, ST3, June 1967, pp 221-234
183. Stricklin, J.A., Haisler, W.E., and Von Rieseemann, W.A., "Geometrically Nonlinear Structural Analysis by Direct Stiffness Method", J. of Struct. Div., ASCE, No. ST9, Sept. 1971, pp 2299-2314
184. Zienkiewicz, O.C. and Nayak, G.C., "A General Approach to Problems of Plasticity and Large Deformation Using Isoparametric Elements", Proc. of the 3rd Conf. on Matrix Methods in Structural Mechanics held at Wright-Patterson Air Force Base, Ohio, 1971 pp 881-928
185. Yamada, Y., "Incremental Formulation for Problems with Geometric and Material Nonlinearities", Advances in Computational Method in Structural Mechanics and Design, eds. J.T. Oden, R.W. Clough and Y. Yamamoto, The University of Alabama Press, 1972, pp 325-355
186. Pope, G.G., "The Application of the Matrix Displacement Method in Plan Elasto-Plastic Problems", Proc. of 1st Conf. on Matrix Methods in Structural Mechanics, Wright-Patterson Air Force Base, Ohio, 1965, pp 635-654.
187. Swedlow, J.L. and Young, W.H., "Stiffness Analysis of Elastic-Plastic Plates", Graduate Aeronautical Laboratory, Calif. Inst. of Tech., SM 65-10, 1965.
188. Marcal, P.V., and King, I.P., "Elastic-Plastic Analysis of Two-Dimensional Stress System by the Finite Element Method", Int. J. Mech. Sci., Vol. 9, 1967, pp 143-155

189. Yamada, Y., Kawai, T., Yoshimura, N. and Sakurai, T., "Analysis of the Elastic-Plastic Problem by the Matrix Displacement Method", Proc. of the 2nd Conf. on Matrix Methods in Structural Mechanics held at Wright-Patterson Air Force Base, Ohio, 1968, pp 1271-1299
190. Y. Yamada, "Recent Developments in Matrix Displacement Method for Elastic-Plastic Problems in Japan", Recent Advances in Matrix Methods of Structural Analysis and Design, eds. R.H. Gallagher, Y. Yamada, and J.T. Oden, The University of Alabama Press, 1971, pp 283-316
191. Mendelson, A., and Manson, S., "Practical Solution of Plastic Deformation Problems in the Elastic-Plastic Range", NASA TR-R-28 1959
192. Padlog, J., Huff, R.O. and Holloway, G.F., "The Unelastic Behaviour of Structures Subjected to Cyclic, Thermal and Mechanical Stressing Conditions", Bell Aerosystem Company Report WPADD TR 60-271, 1960
193. Gallagher, R.H., Padlog, J. and Bijlaard, P.P., "Stress Analysis of Heated Complex Shapes", J. of the American Rocket Society, Vol. 32, No. 5, May 1962, pp 700-707
194. Lansing, W., Jensen, W. and Falby, W., "Matrix Analysis Method for Inelastic Structures", Proc. of 1st Conf. on Matrix Methods in Structural Mechanics, Wright-Patterson Air Force Base, Ohio, 1965, pp 605-633.
195. Zienkiewicz, O.C., Valliappan, S. and King, I.P., "Elasto-Plastic Solutions of Engineering Problems. Initial-Stress, Finite Element Approach", Int. J. Num. Meth. in Eng., Vol. 1, 1969, pp 75-100
196. Marcal, P.V., "A Comparative Study of Numerical Method of Elastic-Plastic Analysis", AIAA J., Vol. 6, No. 1, 1967, pp 157-158.
197. Stricklin, J.A., Haisler, W.E. and Von Reisemann, W.A., "Computation and Solution Procedures for Non-Linear Analysis by Combined Finite Element-Finite Difference Methods", Int. J. of Computer and Structures, Vol. 2, 1972, pp 955-974.
198. Stricklin, J.A., Haisler, W.E. and Von Riesemann, W.A., "Formulation, Computation, and Solution Procedures for Material and/or Geometric Nonlinear Structural Analysis by the Finite Element Methods", SC-CR-72-3102, Sandia Laboratories, Albuquerque, New Mexico, 1972.
199. Massett, D.A. and Stricklin, J.A., "Self-Correcting Incremental Approach in Nonlinear Structural Mechanics", AIAA Journal, Vol. 9, No. 12, Dec. 1971, pp 2464-2466.
200. Haisler, W.A., Stricklin, J.A. and Stebbins, F.J., "Development and Evaluation of Solution Procedures for Geometrically Non-Linear Structural Analysis", AIAA Journal, Vol. 10, No. 3, March 1972, pp 264-272.

201. Tillerson, J.R., "A Treatise on Nonlinear Finite Element Analysis", Ph.D. Dissertation, Texas A & M University, Dec. 1973
202. Stricklin, J.A., Haisler, W.E. and Von Riesenmann, W.A., "Evaluation of Solution Procedures for Material and/or Geometrically Nonlinear Structural Analysis", AIAA Journal, Vol. 11, No. 3, March 1973, pp 292-299
203. Thompson, J.M.T. and Walker, A.C., "The Nonlinear Perturbation Analysis of Discrete Structural Systems", Int. J. of Solids and Structures, Vol. 4, No. 7, July 1968, pp 757-768.
204. Connor, J. and Morin, N., "Perturbation Techniques in the Analysis of Geometrically Nonlinear Shells", IUTAM Colloquim on High Speed Computing of Elastic Structures, Liege, Belgium, August 1970, 683-705.
205. Mallett, R.H. and Haftka, R.T., "Progress in Nonlinear Finite Element Analysis using Asymptotic Solution Techniques", Advance in Computational Methods in Structural Mechanics and Design, eds. J.T. Oden, R.W. Clough, and Y. Yamamoto, University of Alabama Press, 1972, pp 357-373
206. Hangai, Y. and Kawamata, S., "Perturbation Method in the Analysis of Geometrically Nonlinear and Stability Problems", Advances in Computational Methods in Structural Mechanics and Design, eds. J.T. Oden, R.W. Clough, and Y. Yamamoto, University of Alabama Press, 1972, pp 473-489
207. Yokoo, Y., Nakamura, T., and Uetani, K., "The Incremental Perturbation Method for Large Displacement Analysis of Elastic-Plastic Structures", Int. J. for Num. Meth. in Eng., Vol. 10, 1976, pp 503-525
208. Martin, H.C., "Finite Elements and the Analysis of Geometrically Nonlinear Problems", Recent Advances in Matrix Methods of Structural Analysis and Design, eds. R.H. Gallagher, Y. Yamada and J.T. Oden, The University of Alabama Press, 1971, pp 343-381.
209. Hartz, B.J. and Nathan, N.D., "Finite Element Formulation of Geometrically Nonlinear Problems of Elasticity", Recent Advances in Matrix Methods of Structural Analysis and Design, eds. R.H. Gallagher, Y. Yamada, and J.T. Oden, The University of Alabama Press, 1971, pp 415-437
210. Gallagher, R.H., "Geometrically Nonlinear Finite Element Analysis", Proceedings of the Specialty Conference on Finite Element Method in Civil Engineering, eds. J.O. McCutcheon, M.S. Mirza, and A.A. Mufti, McGill University, 1972, pp 3-33.
211. Marcal, P.V., "Finite Element Analysis with Material Non-Linearities Theory and Practice", Proc. of the Specialty Conference on Finite Element Method in Civil Engineering, eds. J.O. McCutcheon, M.S. Mirza, and A.A. Mufti, McGill University, 1972, pp 35-69.

212. Desai, C.S. and Abel, J.F., "Introduction to the Finite Element Method", Van Nostrand Reinhold Co., N.Y., 1972
213. Martin, H.C. and Carey, G.F., "Introduction to Finite Element Analysis", McGraw-Hill, N.Y., 1973
214. Cook, R.O., "Concepts and Applications of Finite Element Analysis", John Wiley and Sons, Inc., N.Y., 1974
215. Oden, J.T., "Finite Elements on Nonlinear Continua", McGraw-Hill, N.Y., 1972
216. Holand, I. and Moan, T., "The Finite Element Method in Plate Buckling", Finite Element Methods in Stress Analysis, eds. I. Holland and K. Bell, Tapir Press, Trondheim, Norway, 1969, Chapter 16, pp 475-500
217. Fung, Y.C., "Foundations of Solid Mechanics", Prentice-Hall Inc., Englewood Cliffs, N.J., 1965
218. Sokolnikoff, I.S., "Mathematical Theory of Elasticity", 2nd ed., McGraw-Hill, N.Y., 1956
219. Novozhilov, V.V., "Foundations of the Non-Linear Theory of Elasticity", Graylock Press, N.Y., 1953
220. Bogner, F.K., Fox, R.L. and Schmit, L.A., Jr., "The Generation of Inter-Element-Compatible Stiffness and Mass Matrix by the Use of Interpolation Formulas", Proc. of Conf. on Matrix Method in Structural Mechanics, Wright-Patterson Air Force Base, Ohio, 1965, AFFDL-TR-66-80, pp 397-443
221. Gopalacharyulu, S., "A Higher Order Conforming Rectangular Plate Element", Int. J. for Num. Meth. in Eng., Vol. 6, 1973, pp 305-308, (Also Discussions: Vol. 6, 1973, pp 308-309, Vol. 8, 1974, pp 209-212 and pp 429-430, and Vol. 10, 1976, pp 471-474).
222. Watkin, D.S., "On the Construction of Conforming Rectangular Plate Elements", Int. J. for Num. Meth. in Eng., Vol. 10, 1976, pp 925-933
223. Smith, I.M. and Duncan, W., "The Effectiveness of Excessive Nodal Continuities in the Finite Element Analysis of Thin Rectangular and Skew Plates in Bending", Int. J. for Num. Meth. in Eng., Vol. 2, 1970, pp 253-257.
224. Sabir, A.B., "The Nodal Solution Routine for the Large Number of Linear Simultaneous Equations in the Finite Element Analysis of Plates and Shells", Finite Elements for Thin Shells and Curved Members, eds. D.G. Ashwell and R.H. Gallagher, John Wiley & Sons, 1976, Chapter 5, pp 63-89.



225. Melosh, R.J., "Basic for Derivation of Matrices for the Direct Stiffness Method", AIAA J., Vol. 1, 1963, pp 1631-1637
226. Clough, R.W. and Tocher, J.L., "Finite Element Stiffness Matrices for Analysis of Plate Bending", Proc. of Conf. on Matrix Method in Structural Mechanics, Wright-Patterson Air Force Base, Ohio, 1965, AFFDL-TR-66-80, pp 515-545
227. Walz, J.E., Fulton, R.E., and Cyrus, N.J., "Accuracy and Convergence of Finite Element Approximations", Proc. of 2nd Conf. on Matrix Method in Structural Mechanics, Wright-Patterson Air Force Base, Ohio, 1968, AFFDL-TR-68-150, pp 995-1027
228. Abel, J.F., and Desai, C.S., "Comparison of Finite Elements for Plate Bending", Proc. of ASCE, J. of Structural Div., Vol. 98, No. ST9, 1972, pp 2143-2148
229. Khan, A.Q., Mufti, A.A. and Harris, P.J., "Post-Buckling of Thin Plates and Shells", Variational Methods in Engineering, eds. C.A. Brebbia and H. Tottenham, Proc. of an Int. Conf. held at the University of Southampton, Sept. 1972, Vol. II, pp 7/54-7/65
230. Sisodiya, R.G., Cheung, Y.K. and Ghali, A., "New Finite Element with Application to Box Girder Bridges", Proc. of Instn. of Civil Engrs., Vol. Supplement, No. (x), 1972, paper No. 74795, pp 207-225
231. Love, A.E.H., "A Treatise on the Mathematical Theory of Elasticity", Dover Publications, N.Y., 1944.
232. Rajasekaran, S. and Murray, D.W., "Incremental Finite Element Matrices", Proc. of ASCE, J. of Struct. Div., Vol. 99, No. ST12, Dec. 1973, pp 2423-2438
233. Biot, M.A., "Mechanics of Incremental Deformations", John Wiley and Sons, Inc., N.Y., 1965
234. Hill, R., "The Mathematical Theory of Plasticity", The Oxford University Press, 1950
235. Hencky, H., "Zur Theorie Plastischer Deformationen und der hierdurch in Material hervorgerufenen Nebenspannungen", Vol. 4, Z. Angew. Math. Mech., 1924, pp 323-334
236. Prandtl, L., "Spannungsverteilung in Plastischen Korpern", Proc. 1st Int. Cong. App. Mech., Delft, 1924, pp 43-54.
237. Reuss, A., "Berucksichtigung der elastischen Formanderung in der Plastizitatstheorie", Z. Angew. Math. Mech., Vol. 10, 1930, pp 266-274

238. Tresca, H., "Memoire Sur Lecoulement des Corps Solides Soumis a des fortes Pressions", Comptes Rendus de l'Academie des Sciences, Vol. 59, 1864, pp 754
239. Von Mises, R., "Mechanik der Festen Korper in Plastisch Deformablen Zustand", Gottinger Nachr. Math. Phys. Kl., 1913, pp 582-592
240. Drucker, D.C., "Plasticity", Structural Mechanics, Proc. of the First Symposium on Naval Structural Mechanics, eds. J.N. Goodier and N.J. Hoff, Pergamon Press, 1960, pp 407-455.
241. Naghdi, P.M., "Stress-Strain Relation in Plasticity and Thermo-plasticity" Plasticity, Proc. of the Second Symposium on Naval Structural Mechanics, eds. E.H. Lee and P.S. Symonds, Pergamon Press, 1960, pp 121-169
242. Hencky, H., "Zur Theorie Plastischer Deformationen und der Hierdurch in Material Hervorgerufenen Nebenspannungen", Proc. 1st Int. Cong. Appl. Mech., Delft, 1924, pp 312-317
243. Nadai, A. "Plastic Behaviour of Metals in the Strain Hardening Range", J. Appl. Phys., Vol. 8, 1937, pp 205
244. Prager, W., "The Theory of Plasticity: A Survey of Recent Achievements", Proc. of the Instn. of Mech. Engrs., London, Vol. 169, No. 21, 1955, pp 41-57
245. Ziegler, H., "A Modification of Prager's Hardening Rule", Quarterly of Applied Mechanics, Vol. 17, No. 1, 1959, pp 55-65
246. Duwez, P., "On the Plasticity of Crystals", Physical Review, 1935, pp 494
247. White, G.N., Jr., "Application of the Theory of Perfectly Plastic Solids to Stress Analysis of Strain Hardening Solids", Graduate Div. of Applied Mathematics, Brown University, Tech. Report No. 51, 1950.
248. Mroz, Z., "On the Description of Anisotropic Workhardening", J. of the Mech. and Phys. of Solids, Vol. 15, 1967, pp 163-175
249. Bland, D.R., "The Two Measures of Work-Hardening", Proc. of 9th Int. Cong. of Appl. Mech., Univ. de Bruxelles, 1957, pp 45-50
250. Ramberg, W. and Osgood, W.R., "Description of Stress-Strain Curves by Three Parameters", NACA TN-902, 1943
251. Drucker, D.C. "A More Fundamental Approach to Plastic Stress-Strain Relations", Proc. of 1st U.S. Natl. Cong. of Appl. Mech., ASME, N.Y., 1952, pp 487-491

252. Budiansky, B., "A Reassessment of Deformation Theories of Plasticity", J. Appl. Mech., Trans. ASME, Vol. 81, June 1959, pp 259-264
253. Pifko, A., Levine, H.S. and Armen, H. Jr., "PLAN - A Finite Element Program for Nonlinear Analysis of Structures, Vol. I - Theoretical Manual", Research Department Grumman Aerospace Corporation, Bethpage, N.Y., Aug. 1974
254. Yamada, Y., Yoshimura, N. and Sakurai, T., "Plastic Stress-Strain Matrix and its Application for the Solution of Elastic-Plastic Problems by the Finite Element Method", Int. J. of Mech. Sci., Vol. 10, 1968, pp 343-354
255. Trefftz, E., "Über die Ableitung der Stabilitäts-Kriterien des Elastischen Gleichgewichtes aus der Elastizitäts Theorie Endlicher Deformationen", Proc. of the 3rd Int. Cong. for Appl. Mech., Stockholm 1930, pp 44-50
256. Melosh, R.J. and Bamford, R.M., "Efficient Solution of Load-Deflection Equations", Proc. ASCE, J. of Struct. Div., Vol. 95, No. ST4, April 1969, pp 661-676
257. Melosh, R.J., "Manipulation Errors in Finite Element Analysis", Recent Advances in Matrix Methods of Structural Analysis and Design, eds. R.H. Gallagher, Y. Yamada and J.T. Oden, The University of Alabama Press, 1971, pp 857-877
258. Croll, J.G.A., and Walker, A.C., "Elements of Structural Stability", MacMillan, London, 1972.
259. Britvec, S.J., "The Stability of Elastic Systems", Pergamon Press Inc., N.Y., 1973
260. Noble, B., "Applied Linear Algebra", Prentice-Hall, Inc., Englewood Cliffs, N.J., 1969.
261. Marsh, C., "Web Crushing in Formed Aluminum Profiles", University of Waterloo Report, May 1968.
262. Fabien, Y., "Buckling of Light-Gauge Aluminum Flexural Members", Master Thesis, Structural Mechanics Report No. 75-2, McGill University, 1975.
263. Davis, E.H., Ring, G.J., and Booker, J.R., "The Significance of the Rate of Plastic Work in Elasto-Plastic Analysis", Proc. of the 1974 Int. Conf. on Finite Element Methods in Engineering, eds. V.A. Pulmano and A.P. Kappala, University of New South Wales, Australia, Aug. 1974, pp 327-335
264. Zetlin, L. and Winter, G., "Unsymmetrical Bending of Beams With and Without Lateral Bracing", Proc. ASCE, Vol. 81, 1955, pp 744-1 to 744-20.

APPENDIX

A-1

$$\begin{aligned}
 N_1 &= \frac{1}{4} (1-\zeta) (1-\eta) \\
 N_2 &= \frac{1}{4} (1+\zeta) (1-\eta) \\
 N_3 &= \frac{1}{4} (1+\zeta) (1+\eta) \\
 N_4 &= \frac{1}{4} (1-\zeta) (1+\eta) \\
 N_5 &= \frac{1}{8} (2-3\zeta+\zeta^3) (1-\eta) \\
 N_6 &= \frac{1}{8} (2+3\zeta-\zeta^3) (1-\eta) \\
 N_7 &= \frac{1}{8} (2+3\zeta-\zeta^3) (1+\eta) \\
 N_8 &= \frac{1}{8} (2-3\zeta+\zeta^3) (1+\eta) \\
 N_9 &= \frac{a}{8} (1-\zeta-\zeta^2+\zeta^3) (1-\eta) \\
 N_{10} &= -\frac{a}{8} (1+\zeta-\zeta^2-\zeta^3) (1-\eta) \\
 N_{11} &= -\frac{a}{8} (1+\zeta-\zeta^2-\zeta^3) (1+\eta) \\
 N_{12} &= \frac{a}{8} (1-\zeta-\zeta^2+\zeta^3) (1+\eta) \\
 N_{13} &= \frac{1}{8} (1-\zeta) (1-\eta) (2-\zeta-\eta-\zeta^2-\eta^2) \\
 N_{14} &= \frac{1}{8} (1+\zeta) (1-\eta) (2+\zeta-\eta-\zeta^2-\eta^2) \\
 N_{15} &= \frac{1}{8} (1+\zeta) (1+\eta) (2+\zeta+\eta-\zeta^2-\eta^2) \\
 N_{16} &= \frac{1}{8} (1-\zeta) (1+\eta) (2-\zeta+\eta-\zeta^2-\eta^2) \\
 N_{17} &= \frac{b}{8} (1-\zeta) (1-\eta)^2 (1+\eta) \\
 N_{18} &= \frac{b}{8} (1+\zeta) (1-\eta)^2 (1+\eta) \\
 N_{19} &= -\frac{b}{8} (1+\zeta) (1+\eta)^2 (1-\eta) \\
 N_{20} &= -\frac{b}{8} (1-\zeta) (1+\eta)^2 (1-\eta) \\
 N_{21} &= -\frac{a}{8} (1-\zeta)^2 (1+\zeta) (1-\eta) \\
 N_{22} &= \frac{a}{8} (1+\zeta)^2 (1-\zeta) (1-\eta) \\
 N_{23} &= \frac{a}{8} (1+\zeta)^2 (1-\zeta) (1+\eta) \\
 N_{24} &= -\frac{a}{8} (1-\zeta)^2 (1+\zeta) (1+\eta)
 \end{aligned}$$

Shape Functions

A-2.

$$\begin{Bmatrix} u \\ v \\ w \end{Bmatrix} = \begin{bmatrix} N_1 & & & & & & & & & & & \\ & N_2 & & & & & & & & & & \\ & & N_3 & & & & & & & & & \\ & & & N_4 & & & & & & & & \\ & N_5 & & & & & & & & & & \\ & & N_9 & & & & & & & & & \\ & & & N_6 & & & & & & & & \\ & & & & N_{10} & & & & & & & \\ & & & & & N_7 & & & & & & \\ & & & & & & N_{11} & & & & & \\ & & & & & & & N_8 & & & & \\ & & & & & & & & N_{12} & & & \\ & N_{13} & N_{17} & N_{21} & & & & & & & & \\ & & & & N_{14} & N_{18} & N_{22} & & & & & \\ & & & & & & & N_{15} & N_{19} & N_{23} & & \\ & & & & & & & & & & N_{16} & N_{20} & N_{24} \end{bmatrix}$$

Explicit Form of Eq. 3.20

$$\begin{Bmatrix} u_1 \\ v_1 \\ w_1 \\ \theta_{x1} \\ \theta_{y1} \\ \theta_{z1} \\ u_2 \\ v_2 \\ w_2 \\ \theta_{x2} \\ \theta_{y2} \\ \theta_{z2} \\ u_3 \\ v_3 \\ w_3 \\ \theta_{x3} \\ \theta_{y3} \\ \theta_{z3} \\ u_4 \\ v_4 \\ w_4 \\ \theta_{x4} \\ \theta_{y4} \\ \theta_{z4} \end{Bmatrix}$$

$\frac{-1}{4a} \cdot (1-\eta)$	$-D(1,1)$	$\frac{1}{4a} \cdot (1+\eta)$	$-D(1,13)$
$\frac{-1}{4b} \cdot (1-\xi)$	$\frac{-1}{4b} \cdot (1+\xi)$	$-D(2,7)$	$-D(2,1)$
$\frac{-3}{8a} (1-\xi^2) \cdot (1-\eta)$	$\frac{-1}{8} (1+2\xi - 3\xi^2) \cdot (1-\eta)$	$\frac{-1}{8} (1-2\xi - 3\xi^2) \cdot (1-\eta)$	$\frac{-1}{8} (1+2\xi - 3\xi^2) \cdot (1+\eta)$
$\frac{-1}{8b} (2-3\xi+\xi^3)$	$\frac{-a}{8b} (1-\xi - \xi^2+\xi^3)$	$\frac{a}{8b} (1+\xi - \xi^2-\xi^3)$	$\frac{-1}{8} (1-2\xi - 3\xi^2) \cdot (1+\eta)$
	$-D(3,2)$	$-D(4,8)$	$-D(3,14)$
$\frac{-1}{8a} (1-\eta) - \frac{b}{8a} (1-\eta)^2 \cdot (3-\eta - \frac{3}{8a} (1-\eta)^2) \cdot (1+\eta)$	$-D(5,3) - D(5,4) - D(3,12)$	$\frac{1}{8a} (1+\eta) - \frac{b}{8a} \cdot (3+\eta) \cdot (1+\eta)^2 - D(3,18) - 3\xi^2 - \eta^2 \cdot (1-\eta)$	$-D(5,15) - D(5,16) - D(3,24)$
$\frac{-1}{8b} (1-\eta) - \frac{1}{8} (1-\xi) \cdot (3-\xi - \xi^2 + 1+2\eta - 3\eta^2 - 3\eta^2)$	$\frac{-1}{8b} (1+\xi) - \frac{1}{8} (1+\xi) \cdot (3+\xi - (1+2\eta - 3\eta^2 - 3\eta^2))$	$\frac{-1}{8} (1+\xi) \cdot (1-2\eta - 3\eta^2) - D(6,11)$	$\frac{-1}{8} (1-\xi) \cdot (1-2\eta - 3\eta^2) - D(6,5)$
$\frac{3}{4a^2} \xi \cdot \frac{1}{4a} (1-3\xi) \cdot (1-\eta)$	$-D(7,3)$	$\frac{-3}{4a^2} \xi \cdot \frac{1}{4a} \cdot (1+\eta) \cdot (1+3\xi) \cdot (1-\eta)$	$-D(7,15)$
$\frac{3}{4b^2} \cdot \frac{-1}{4b} (1-\eta) \cdot (1-\xi) \eta \cdot (1-3\eta)$	$\frac{3}{4b^2} \cdot \frac{-1}{4b} (1+\xi) \cdot (1+\xi) \eta \cdot (1-3\eta)$	$-D(8,9) \cdot \frac{1}{4b} (1+\xi) \cdot (1+3\eta)$	$-D(8,3) \cdot \frac{1}{4b} (1-\xi) \cdot (1+3\eta)$
$\frac{1}{8ab} (4 - \frac{1}{8a} (1+\frac{1}{8b} (1+3\xi^2-3\eta^2) 2\eta - 3\eta^2) 2\xi - 3\xi^2)$	$-D(9,3) - D(9,4) - \frac{1}{8b} \cdot (1-2\xi - 3\xi^2)$	$D(9,3) \cdot \frac{-1}{8a} (1-2\eta - 3\eta^2) - D(9,11)$	$-D(9,3) - D(9,16) - D(9,5)$

A-4

$$\hat{K}_\sigma = \int_t \bar{K}_\sigma dZ$$

$$\bar{k}_\sigma =$$



A-5

$$\hat{K}_L = \int_t \bar{K}_L dZ$$

$$\bar{K}_L = \begin{bmatrix} \begin{bmatrix} E_{11} & E_{13} & E_{13} & E_{12} & \cdot & \cdot \\ & E_{33} & E_{33} & E_{23} & \cdot & \cdot \\ & & E_{33} & E_{23} & \cdot & \cdot \\ & & & E_{22} & \cdot & \cdot \\ & & & & \cdot & \cdot \\ & & & & & \cdot \end{bmatrix} & \begin{bmatrix} E_{11} & E_{12} & 2E_{13} \\ E_{13} & E_{23} & 2E_{33} \\ E_{13} & E_{23} & 2E_{33} \\ E_{12} & E_{22} & 2E_{23} \\ \cdot & \cdot & \cdot \\ \cdot & \cdot & \cdot \end{bmatrix} \\ \text{sym.} & \begin{bmatrix} E_{11} & E_{12} & 2E_{13} \\ & E_{22} & 2E_{23} \\ & & 4E_{33} \end{bmatrix} \end{bmatrix} \begin{matrix} Z \times \\ \\ Z^2 \times \end{matrix}$$

NOTE:  $E_{ij}$ 's in this matrix are components of elasto-plastic matrix  $[E]$

$\bar{K}_L =$ 

$$\begin{bmatrix}
 \begin{bmatrix}
 E_{11} & \cdot & \cdot & E_{12} & \cdot & \cdot \\
 \cdot & E_{33} & E_{33} & \cdot & \cdot & \cdot \\
 \cdot & \cdot & E_{33} & \cdot & \cdot & \cdot \\
 \cdot & \cdot & \cdot & E_{22} & \cdot & \cdot \\
 \cdot & \cdot & \cdot & \cdot & \cdot & \cdot \\
 \cdot & \cdot & \cdot & \cdot & \cdot & \cdot
 \end{bmatrix} &
 \begin{bmatrix}
 E_{11} & E_{12} & \cdot \\
 \cdot & \cdot & 2E_{33} \\
 \cdot & \cdot & 2E_{33} \\
 E_{12} & E_{22} & \cdot \\
 \cdot & \cdot & \cdot \\
 \cdot & \cdot & \cdot
 \end{bmatrix} \\
 \text{sym.} & \\
 \text{NOTE: } E_{ij} \text{'s in this matrix are components} & \\
 \text{of conventional elasticity matrix} & \\
 [E_e] &
 \begin{bmatrix}
 E_{11} & E_{12} & \cdot \\
 \cdot & E_{22} & \cdot \\
 \cdot & \cdot & 4E_{33}
 \end{bmatrix}
 \end{bmatrix}$$

$Z \times$

$Z^2 \times$

(This matrix is only for elastic layers, simplified from Appendix A-5)

**A-7**

$$\hat{K}_L = \int_{\Gamma} \bar{K}_L \, dZ =$$

-234-

(This matrix is for the case that all layers through thickness are elastic, simplified from Appendix A-6)

$$\hat{K}_N = \int_t \bar{K}_N dZ$$

A-8

$\bar{K}_N =$

sym.

NOTE:  $E_{ij}$ 's in this matrix are components of elasto-plastic matrix [E]

$$\begin{bmatrix} E_{11} \frac{\partial W}{\partial x} + E_{13} \frac{\partial W}{\partial y} & E_{12} \frac{\partial W}{\partial y} + E_{13} \frac{\partial W}{\partial x} \\ E_{33} \frac{\partial W}{\partial y} + E_{13} \frac{\partial W}{\partial x} & E_{33} \frac{\partial W}{\partial x} + E_{23} \frac{\partial W}{\partial y} \\ E_{12} \frac{\partial W}{\partial x} + E_{23} \frac{\partial W}{\partial y} & E_{22} \frac{\partial W}{\partial y} + E_{23} \frac{\partial W}{\partial x} \\ E_{11} \left( \frac{\partial W}{\partial x} \right)^2 + E_{33} \left( \frac{\partial W}{\partial y} \right)^2 + 2E_{13} \left( \frac{\partial W}{\partial x} \right) \left( \frac{\partial W}{\partial y} \right) & E_{12} \left( \frac{\partial W}{\partial x} \right) \left( \frac{\partial W}{\partial y} \right) + E_{33} \left( \frac{\partial W}{\partial x} \right) \left( \frac{\partial W}{\partial y} \right) + E_{13} \left( \frac{\partial W}{\partial x} \right)^2 + E_{23} \left( \frac{\partial W}{\partial y} \right)^2 + E_{22} \left( \frac{\partial W}{\partial y} \right)^2 + E_{33} \left( \frac{\partial W}{\partial x} \right)^2 + 2E_{23} \left( \frac{\partial W}{\partial x} \right) \left( \frac{\partial W}{\partial y} \right) \end{bmatrix}$$

$$\begin{bmatrix} E_{11} \frac{\partial W}{\partial x} + E_{13} \frac{\partial W}{\partial y} & E_{12} \frac{\partial W}{\partial x} + E_{23} \frac{\partial W}{\partial y} & 2E_{33} \frac{\partial W}{\partial y} + E_{13} \frac{\partial W}{\partial x} \\ E_{12} \frac{\partial W}{\partial y} + E_{23} \frac{\partial W}{\partial x} & E_{22} \frac{\partial W}{\partial y} + E_{23} \frac{\partial W}{\partial x} & 2E_{33} \frac{\partial W}{\partial x} + E_{23} \frac{\partial W}{\partial y} \end{bmatrix}$$

Zx

$\bar{K}_N =$ 

sym.

NOTE:  $E_{ij}$ 's in this matrix  
are components of  
conventional elasticity  
matrix  $[E_e]$

$$\begin{bmatrix} E_{11} \frac{\partial w}{\partial x} & E_{12} \frac{\partial w}{\partial y} \\ E_{33} \frac{\partial w}{\partial y} & E_{33} \frac{\partial w}{\partial x} \\ E_{33} \frac{\partial w}{\partial y} & E_{33} \frac{\partial w}{\partial x} \\ E_{12} \frac{\partial w}{\partial x} & E_{22} \frac{\partial w}{\partial y} \\ E_{11} \left( \frac{\partial w}{\partial x} \right)^2 + E_{33} \left( \frac{\partial w}{\partial y} \right)^2 & E_{12} \left( \frac{\partial w}{\partial x} \right) \left( \frac{\partial w}{\partial y} \right) + E_{33} \left( \frac{\partial w}{\partial x} \right) \left( \frac{\partial w}{\partial y} \right) \\ E_{22} \left( \frac{\partial w}{\partial y} \right)^2 + E_{33} \left( \frac{\partial w}{\partial x} \right)^2 \end{bmatrix}$$

Z x

$$\begin{bmatrix} E_{11} \frac{\partial w}{\partial x} & E_{12} \frac{\partial w}{\partial x} & 2E_{33} \frac{\partial w}{\partial y} \\ E_{12} \frac{\partial w}{\partial y} & E_{22} \frac{\partial w}{\partial y} & 2E_{33} \frac{\partial w}{\partial x} \end{bmatrix}$$

(This matrix is only for elastic layers, simplified from Appendix A-8)

$$\hat{K}_N = \int_t \bar{K}_N dZ = t \times$$

$$\begin{bmatrix} \cdot & \cdot & \cdot & \cdot & E_{11} \frac{\partial w}{\partial x} & E_{12} \frac{\partial w}{\partial y} & \cdot & \cdot \\ \cdot & \cdot & \cdot & \cdot & E_{33} \frac{\partial w}{\partial y} & E_{33} \frac{\partial w}{\partial x} & \cdot & \cdot \\ \cdot & \cdot & \cdot & \cdot & E_{33} \frac{\partial w}{\partial y} & E_{33} \frac{\partial w}{\partial x} & \cdot & \cdot \\ \cdot & \cdot & \cdot & \cdot & E_{12} \frac{\partial w}{\partial x} & E_{22} \frac{\partial w}{\partial y} & \cdot & \cdot \\ \cdot & \cdot & \cdot & \cdot & E_{11} \left( \frac{\partial w}{\partial x} \right)^2 & E_{12} \left( \frac{\partial w}{\partial x} \right) \left( \frac{\partial w}{\partial y} \right) & \cdot & \cdot \\ & & & & + & + & \cdot & \cdot \\ \cdot & \cdot & \cdot & \cdot & E_{33} \left( \frac{\partial w}{\partial y} \right)^2 & E_{33} \left( \frac{\partial w}{\partial x} \right) \left( \frac{\partial w}{\partial y} \right) & \cdot & \cdot \\ & & & & & E_{22} \left( \frac{\partial w}{\partial y} \right)^2 & \cdot & \cdot \\ & & & & & + & \cdot & \cdot \\ & & & & & E_{33} \left( \frac{\partial w}{\partial x} \right)^2 & \cdot & \cdot \end{bmatrix}$$

sym.

(This matrix is for the case that all layers through thickness are elastic, simplified from Appendix A-9)

## Appendix B

## Computer Program

RELEASE 2.0

MAIN

DATE = 77154

11/22/35

RELEASE 2.0

MAIN

DATE = 77154

11/22/35

```

IMPLICIT REAL*8 (A-H,O-Z), INTEGER*2 (I-N)
INTEGER NJOINT,NPART,NOISP,NELEM,NONCOP,NBOUN,NLOAD,NGAUSS,NLAYER,
NIMPER,NFREE,NTOTAL,MMAX,MTWICE,NREAD,NWRITE
DIMENSION BOOK(6950),NBOOK(985)

C
C DISK #1 FOR ST
C DISK #2 FOR ST
C DISK #3 FOR ST
C DISK #4 FOR D
C DISK #11 FOR RESULT STORAGE
C DISK #12 FOR RESULT STORAGE
C DISK #13 INSURANCE DISK
C

READ(5,10) NJOINT,NPART,NELEM,NONCOP,NBOUN,NLOAD,NOISP,NGAUSS,
NLAYER,NIMPER,NFREE,NTOTAL,MMAX,MTWICE,NREAD,NWRITE
10 FORMAT(14I6,2F5.0)
NREF=6
NT=INIT+NSTEP
NTOTAL=NFREE+NJOINT
100 CALL COUNT(NJOINT,NPART,NOISP,NELEM,NONCOP,NBOUN,NLOAD,NGAUSS,
NLAYER,NIMPER,NFREE,NTOTAL,
11,12,13,14,15,16,17,18,19,110,111,112,113,114,115,116,
11,12,13,14,15,16,17,18,19,110,111,112,113,114,115,116)
CALL INPUT(NJOINT,NPART,NELEM,NBOUN,NLOAD,INIT,NOISP,NFREE,FLAS,V,
SYIELD,NHARD,EXPON,507,ET,ITOTAL,MMAX,MTWICE,NTOTAL,
BOOK(1),BOOK(14),BOOK(15),BOOK(16),BOOK(18),BOOK(19),
BOOK(21),BOOK(22),BOOK(23),BOOK(24),
BOOK(25),BOOK(26),BOOK(27),BOOK(28),BOOK(29),
BOOK(310),BOOK(311))
117=116+MMAX*MMAX
CALL TRANS(NJOINT,NELEM,NONCOP,NIMPER,BOOK(13),BOOK(15),BOOK(16),
BOOK(17),BOOK(26),BOOK(25))
CALL SET ( NELEM,NLAYER,NGAUSS,INIT,NTOTAL, ELAS,V,
SYIELD,NHARD,EXPON,507,ET,NPRIME,EXX,EXY,EYY,EZZ,
BOOK(11),BOOK(12),BOOK(110),BOOK(111),BOOK(113),
BOOK(114),BOOK(115), NBOOK(J12),NREAD)
IF(NREAD.EQ.11) NWRITE=12
IF(NREAD.EQ.12) NWRITE=11
DO 300 ISTEP=INIT,NT
DO 700 ITERA=1,NITER
IF(ISTEP.EQ.INIT.OR.ISTEP.EQ.NT.OR.NITER.LE.2) GO TO 150
IF(ITERA.EQ.1.AND.ERRORR.LE.TOLNCE) GO TO 620
150 REWIND 1
REWIND 2
REWIND 3
REWIND 4
REWIND NWRITE
11(ISTEP,NE,1,OP,ITERA,NE,1) REWIND NREAD
IF(ISTEP.LE.(INIT+1).AND.NITER.EQ.1) GO TO 200
IF(ISTEP.EQ.INIT.AND.ITERA.LE.2) GO TO 200
170 READ
NREAD=NWRITE
NWRITE=1
200 DO 600 LK=1,NELEM

```

```

K1=14+LK-1
K2=15+LK-1
K3=16+LK-1
L1=J5+LK-1
CALL READY(NJOINT,NELEM,NONCOP,NGAUSS,NLAYER,NFREE,LK,NIMPER,ISTEP,
INIT,NTOTAL,NREAD,NWRITE,BOOK(17),BOOK(111),BOOK(113),
BOOK(114),BOOK(115),NBOOK(J1),NBOOK(J4),NBOOK(L1),
NBOOK(J12),ITERA)
CALL DISGRD( NGAUSS,ISTEP,INIT,LK,BOOK(11),BOOK(K2),BOOK(K3),
BOOK(116),ITERA)
DO 500 I1=1,NGAUSS
DO 500 JJ=1,NGAUSS
IYIELD=0
IF(ISTEP.EQ.1.AND.ITERA.EQ.1) GO TO 450
CALL STRAIN(NGAUSS,NLAYER,JJ,I1,BOOK(K1),BOOK(112),BOOK(115),
BOOK(116),ISTEP,INIT,ITERA)
CALL STRESS(NGAUSS,NLAYER,JJ,I1,LK,ELAS,SYIELD,NHARD,EXPON,507,
EXX,EXY,EYY,EZZ,IYIELD,ISTEP,INIT,NPRIME,NWRITE,
BOOK(13),BOOK(112),BOOK(113),BOOK(114),BOOK(115),
NBOOK(J12),NT,ITERA)
300 CALL TRUEPT(NGAUSS,NLAYER,JJ,I1,BOOK(12),BOOK(K1),BOOK(K2),
BOOK(K3),BOOK(113),ISTEP,INIT,ITERA)
400 IF(ISTEP.EQ.NT) GO TO 500
450 CALL STIFF(NGAUSS,NLAYER,JJ,I1,ISTEP,IYIELD,EXX,EXY,EYY,EZZ,
BOOK(12),BOOK(13),BOOK(K1),BOOK(K2),BOOK(K3),BOOK(113),
ITERA)
500 CONTINUE
IF(NBOOK(L1).NE.0) CALL ROT(NJOINT,NELEM,ISTEP,NT,LK,BOOK(17),
NBOOK(J1),NBOOK(J4),NBOOK(L1),NONCOP,NIMPER,
INIT,ITERA)
IF(ISTEP.NE.NT) CALL STORE(NPART,NLAYER,NFREE,LK,MMAX,MTWICE,BOOK(11),
NBOOK(J2),NBOOK(J3),NBOOK(J4),NBOOK(J5),
NBOOK(J10),NTOTAL)
IF(ISTEP.EQ.INIT.AND.ITERA.EQ.1) GO TO 600
CALL SUM(NJOINT,NELEM,NFREE,NTOTAL,BOOK(110),NBOOK(J1),NBOOK(J4),
LK)
600 CONTINUE
IF(ISTEP.EQ.INIT.AND.ITERA.EQ.1) GO TO 620
CALL RES(NJOINT,NLOAD,NFREE,NOISP,ISTEP,INIT,NT,SIZE,BOOK(19),
BOOK(19),BOOK(110),BOOK(112),NBOOK(J1),NBOOK(J5),
BOOK(J9),NBOOK(J11),ITOTAL,NWRITE,NREAD,NITER,ITERA,
TOLNCE,DISERR,ERRORR,XLEVEL)
IF(ISTEP.LT.(NT-1).AND.ITERA.GT.2.AND.FRPRD.LT.TOLNCE) GO TO 620
620 CALL NEW(NELEM,NLOAD,NGAUSS,NLAYER,NFREE,NTOTAL,ISTEP,INIT,NT,
NITER,ITERA,NWRITE,SIZE,XLEVEL,BOOK(14),BOOK(111),BOOK(112),
BOOK(113),BOOK(114),BOOK(115),NBOOK(J9),NBOOK(J12),
NREAD,FRPRD,TOLNCE)
650 CALL FIX(NPART,NOISP,NFREE,NBOUN,NTOTAL,MMAX,MTWICE,SIZE,BOOK(17),
BOOK(112),BOOK(116),
BOOK(J2),NBOOK(J3),NBOOK(J6),NBOOK(J11),ITERA)
CALL SOLVE(NJOINT,NPART,NOISP,NFREE,MMAX,ITOTAL,NTOTAL,NBOUN,
BOOK(110),BOOK(111),BOOK(114),BOOK(117),
NBOOK(J1),NBOOK(J2),NBOOK(J6),DISERR,ITERA)
IF(ISTEP.EQ.INIT.AND.ITERA.EQ.1) GO TO 700

```

RELEASE 2.0

MAIN

DATE = 77154

11/22/35

RELEASE 2.0

COUNT

DATE = 77154

11/22/35

```

IF(ISTEP.EQ.(NT-1).AND.ITERA.GT.2.AND.ERROR.LT.TOLNCE) GO TO 800
700 CONTINUE
800 CONTINUE
STOP
END

```

```

EFFECT* NOTFRM.ID.EBCDIC.SOURCE.NOLIST.NODECK.LOAD.NOMAP.NOTEST
EFFECT* NAME = MAIN . LINECNT = 56
SOURCE STATEMENTS = 64 PROGRAM SIZE = 63120
NO DIAGNOSTICS GENERATED

```

```

SUBROUTINE COUNT(NJOINT,NPART,NDISP,NLEFM,NONCOP,NPOUN,NLOAD,
* NGAUSS,NLAYER,NIMPER,NFREE,NTOTAL,I1,I2,I3,I4,I5,
* I6,I7,I8,I9,I10,I11,I12,I13,I14,I15,I16,
* J1,J2,J3,J4,J5,J6,J7,J8,J9,J10,J11,J12)
IMPLICIT INTEGER*2 (I-N)
INTEGER NJOINT,NPART,NDISP,NLEFM,NONCOP,NPOUN,NLOAD,NGAUSS,NLAYER,
* NIMPER,NFREE,NTOTAL,MAX0

```

```

I1=1
I2=I1+NGAUSS
I3=I2+NGAUSS
I4=I3+MAX0(3*NJOINT,3*3*NLAYER)
I5=I4+NELEM
I6=I5+NELEM
I7=I6+NELEM
IF(NONCOP.EQ.0) NONCOP=1
I8=I7+3*NIMPER*NONCOP
IF(NLOAD.EQ.0) NLOAD=1
I9=I8+NFREE*NLOAD
IF(NDISP.EQ.0) NDISP=1
I10=I9+NREF*NDISP
I11=I10+NTOTAL
I12=I11+NTOTAL
I13=I12+3*NLAYER
I14=I13+3*NLAYER*NGAUSS*NGAUSS
I15=I14+NLAYER*NGAUSS*NGAUSS
I16=MAX0(I15+3*2*NGAUSS*NGAUSS,I12+NTOTAL)
NDREFAL=I16+MAX0(MMAX*NTWICE,9*2*NGAUSS*NGAUSS)
C MMAX=(MAX. NO. OF JTS IN ONE PARTITION)*6-(NO. OF FIXED D.O.F. IN
C THE SAME PARTITION). NTWICE=2*MMAX
J1=1
J2=J1+NJOINT
J3=J2+NPART
J4=J3+NPART
J5=J4+4*NELEM
J6=J5+NELEM
J7=J6+NTOTAL
J8=J7+NPOUN
J9=J8+NFREE
J10=J9+NLOAD
J11=J10+NELEM
J12=J11+NDISP
C NDIATE=J12+NLAYER*NGAUSS*NGAUSS
RETURN
END

```

```

EFFECT* NOTFRM.ID.EBCDIC.SOURCE.NOLIST.NODECK.LOAD.NOMAP.NOTEST
EFFECT* NAME = COUNT . LINECNT = 56
SOURCE STATEMENTS = 36 PROGRAM SIZE = 1742
NO DIAGNOSTICS GENERATED

```



RELEASE 2.0

INPUT

DATE = 77154

11/22/35

RELEASE 2.0

INPUT

DATE = 77154

11/22/35

```

SURROUTINE INPUT(NJOINT,NPART,NELEM,NBOUN,NLOAD,INIT,NOISP,
  NFREE,ELAS,V,SYIELD,NHARD,EXPON,SOT,ET,ITOTAL,
  MMAX,MTWICE,NTOTAL,
  COORD,THICK,XC,YC,PLDAD,UDISP,
  IPLNAR,NFIRST,NLAST,NOD,NTRANS,NREAC,NF,NB,LF,
  INDIC,NU)
  IMPLICIT REAL*8 (A-H,O-Z), INTEGER*2 (I-N)
  INTEGER NJOINT,NPART,NOISP,NELEM,NONCOP,NBOUN,NLOAD,NGAUSS,NLAYER,
  NIMPER,NFREE,NTOTAL,MMAX,MTWICE
  DIMENSION COORD(3,NJOINT),THICK(NELEM),XC(NELEM),YC(NELEM),
  NU(NOISP),PLDAD(NFREE,NLOAD),UDISP(NFREE,NOISP),
  NFIRST(NPART),NLAST(NPART),NOD(4,NELEM),NTRANS(NELEM),
  NREAC(NTOTAL),NF(NLOAD),NB(NFREE),LF(NLOAD),INDIC(NELEM),
  IPLNAR(NJOINT)
  READ IN INPUT DATA
  DO 12 I=1,NJOINT
  12 READ(5,14) K,(COORD(J,K),J=1,3),IPLNAR(K)
  DO 16 I=1,NPART
  16 READ(5,26) K,NFIRST(K),NLAST(K)
  DO 20 I=1,NFLEM
  20 READ(5,22) K,(NOD(J,K),J=1,4),NTRANS(K),THICK(K),XC(K),YC(K),
    INDIC(K)
  DO 21 I=1,NTOTAL
  21 NREAC(I)=1
  DO 23 I=1,NBOUN
  READ(5,26) NF(I),(NB(J),J=1,NFREE)
  K=(NF(I)-1)*NFREE
  DO 23 J=1,NFREE
  23 NREAC(K+J)=NB(J)
  ITOTAL=0
  MMAX=0
  DO 40 I=1,NPART
  J=(NFIRST(I)-1)*NFREE+1
  K=NLAST(I)*NFREE
  N=0
  DO 50 L=J,K
  IF(NREAC(L),EQ,0) GO TO 50
  N=N+1
  NREAC(L)=N
  50 CONTINUE
  IF(MMAX.LT,N) MMAX=N
  ITOTAL=ITOTAL+N
  40 CONTINUE
  MTWICE=2*MMAX
  DO 24 I=1,NLOAD
  24 READ(5,30) LF(I),(PLDAD(J,I),J=1,NFREE)
  DO 32 I=1,NOISP
  32 READ(5,30) NU(I),(UDISP(J,I),J=1,NFREE)
  READ(5,16) ELAS,V,SYIELD,NHARD,EXPON,SOT,ET
  IF(ET.NE,1) RETURN
  14 FORMAT(110,3F10.0,A2)
  22 FORMAT(15,3F10.0,15)

```

```

26 FORMAT(715,6F7.0)
30 FORMAT(110,6F10.0)
36 FORMAT(3F10.0,110,3F10.0)

```

ECHO INPUT DATA AT FIRST RUN ONLY

```

70 WRITE(6,82)
DO 84 I=1,NJOINT
84 WRITE(6,86) I,(COORD(J,I),J=1,3),IPLNAR(I)
WRITE(6,90)
DO 92 I=1,NPART
92 WRITE(6,94) I,NFIRST(I),NLAST(I)
WRITE(6,94)
DO 100 I=1,NELEM
100 WRITE(6,102) I,(NOD(J,I),J=1,4),NTRANS(I),THICK(I),XC(I),YC(I),
  INDIC(I)
WRITE(6,106)
DO 112 I=1,NBOUN
K=(NF(I)-1)*NFREE
DO 107 J=1,NFREE
NB(J)=NREAC(K+J)
IF(NB(J).NE,0) NR(J)=1
107 CONTINUE
112 WRITE(6,108) NF(I),IPLNAR(NF(I)),(NB(J),J=1,NFREE)
IF(NLOAD,EQ,1)AND(LF(NLOAD),EQ,0) GO TO 119
WRITE(6,116)
DO 118 I=1,NLOAD
118 WRITE(6,120) LF(I),IPLNAR(LF(I)),(PLDAD(J,I),J=1,NFREE)
119 IF(NOISP,EQ,1)AND(NU(NOISP),EQ,0) GO TO 121
WRITE(6,117)
DO 115 I=1,NOISP
115 WRITE(6,120) NU(I),IPLNAR(NU(I)),(UDISP(J,I),J=1,NFREE)
121 WRITE(6,130) ELAS,V,SYIELD,NHARD
IF(NHARD,EQ,2) WRITE(6,132) EXPON,SOT
IF(NHARD,EQ,1) WRITE(6,134) ET
82 FORMAT(11,10,'JOINT NO',T30,'X-ORDINATE',T50,'Y-ORDINATE',T70,'Z-ORDINATE',T90,'COPLANAR OR NON-COPLANAR JOINT',T110,'T35,11 IN,1'
  '1X,'GLOBAL',13X,'SYSTEM 1',T91,'L = COPLANAR JOINT',T93,'
  'G = NON-COPLANAR JOINT',T95)
86 FORMAT(' ',T10,15,T10,3F20.5,T100,A2)
90 FORMAT(' ',T10,'PARTITION LINE NO',T40,'FIRST JOINT IN THE LINE',T
  '70,'LAST JOINT IN THE LINE',T110)
94 FORMAT(' ',T15,15,T45,15,T75,15)
98 FORMAT(' ',T2,'ELEMENT NO',T15,' ',T21,'J',T26,'K',T31,'L',T36,'NO
  'NONCOPLANAR ELEMENT NO. ',T66,'THICKNESS',T86,'XC',T124,'YC',T115
  ' ',T1,'FIRST IN A ROW',T13,' ',T13,'L = COPLANAR JOINT',T115,'2=LAST
  'IN A ROW',T13,' ',T115,'0=INTERMEDIATE',T115)
102 FORMAT(' ',T7,T12,415,T46,12,T15,3F10.5,T120,T2)
106 FORMAT(' ',T10,'JOINT NO',T12,'COORDINATE',T47,'ORDINARY COORDINATE',T
  ' ',T12,'(L=LOCAL',T30,'10 = FIXED, 1 = FREE TO MOVE)',T13,
  'G=GLOBAL',T11)
108 FORMAT(' ',T15,T15,A2,A10)
116 FORMAT(' ',T5,'JOINT NO',T20,'COORDINATE',T60,'MAGNITUDE OF UNIT L
  'OAD',T20,'(L=LOCAL',T39,'X-LOAD',T53,'Y-LOAD',T67,'Z-LOAD',T

```

RELEASE 2.0

INPUT

DATE = 77154

11/22/75

RELEASE 2.0

TRANS

DATE = 77154

11/22/75

```

*53,'X-MOMENT',T98,'Y-MOMENT',T113,'Z-MOMENT',/,,'T22,'G=GLOBAL',
*,//)
117 FORMAT('---',T5,'JOINT NO',T20,'COORDINATE',T60,'MAGNITUDE OF UNIT D
ISP',/,,'T20,'(L=LOCAL',T39,'X-DISP',T53,'Y-DISP',T68,'Z-DISP',T
*43,'X-ROTATN',T98,'Y-ROTATN',T113,'Z-ROTATN',/,,'T22,'G=GLOBAL',
*,//)
120 FORMAT(' ',T5,T5,T25,A2,T30,6F15.5)
130 FORMAT('---',T5,'ELASTICITY MODULUS',T55,'=',F20.5,/,,'T5,'POISS
SON RATIO IN ELASTIC RANGE',T55,'=',F20.5,/,,'T5,'INITIAL UNIAXI
AL YIELD STRESS',T55,'=',F20.5,/,,'T5,'HARDENING PROPERTY OF STR
ESS-STRAIN CURVE',T55,'=',F110)
132 FORMAT(' ',T5,'EXPONENT USED FOR STRESS-STRAIN EQUATION',T55,'=',F
20.5,/,,'T5,'SECANT YIELD STRESS AT 0.7E',T55,'=',F20.5,/)
134 FORMAT(' ',T5,'TANGENT MODULUS FOR LINEAR HARDENING',T55,'=',F20.5
*,//)
146 RETURN
END

```

EFFECT\* NOTERM,ID,EBCDIC,SOURCE,NOLIST,NODECK,LOAD,NOMAP,NOTEST  
 EFFECT\* NAME = INPUT , LINECNT = 56

SOURCE STATEMENTS = 87, PROGRAM SIZE = 5764  
 NO DIAGNOSTICS GENERATED

```

SUBROUTINE TRANS(NJOINT,NELEM,NONCOP,NIMPER,COORD,XC,YC,H,NOD,
* NTRANS)
IMPLICIT REAL*8 (A-H,O-Z), INTEGER*2 (I-N)
INTEGER NJOINT,NELEM,NIMPER,NONCOP
DIMENSION COORD(3,NJOINT),XC(4,NELEM),YC(NELEM),H(3,3,NIMPER,4,NELEM),
* NOD(4,NELEM),NTRANS(NLEFM)

```

TRANSFORMATION MATRIX

```

DO 165 LK=1,NELEM
IF(NTRANS(LK).EQ.0) GO TO 165
LL=NTRANS(LK)
H(1,1,LL)=1.
H(1,2,LL)=0.
H(1,3,LL)=0.
H(2,1,LL)=0.
H(3,1,LL)=0.
YA=COORD(2,NOD(4,LK))-COORD(2,NOD(1,LK))
ZA=COORD(3,NOD(4,LK))-COORD(3,NOD(1,LK))
DENU=DSORT(YA*YA+ZA*ZA)
H(2,2,LL)=YA/DENU
H(2,3,LL)=ZA/DENU
H(3,2,LL)=H(2,3,LL)
H(3,3,LL)=H(2,2,LL)

```

```

165 CONTINUE
RETURN
END

```

EFFECT\* NOTERM,ID,EBCDIC,SOURCE,NOLIST,NODECK,LOAD,NOMAP,NOTEST  
 EFFECT\* NAME = TRANS , LINECNT = 56  
 SOURCE STATEMENTS = 22, PROGRAM SIZE = 1322  
 NO DIAGNOSTICS GENERATED

RELEASE 2.0

SET

DATE = 77154

11/22/35

RELEASE 2.0

READY

DATE = 77154

11/22/35

```

SUBROUTINE SET ( NELEM,NLAYER,NGAUSS,INIT,NTOTAL,
  ELAS,V,SYIELD,NHARD,EXPON,S07,ET,HPRIME,EXX,EXY,
  EYZ,P,PTINT,WGT,P,UTOTAL,STRES,PLATRN,TOTSRN,
  KEEP,NREAD)
  IMPLICIT REAL*8 (A-H,O-Z), INTEGER*2 (I-N)
  INTEGER NLAYER,NGAUSS,NTOTAL,NREAD,NELFM
  DIMENSION XYPT(4,4),XYWGT(4,4),PTINT(NGAUSS),WGT(NGAUSS),PT(NTOTAL),
    UTOTAL(NTOTAL),
  STRES(3,NLAYER,NGAUSS,NGAUSS),TOTSRN(3,2,NGAUSS,NGAUSS),
  PLATRN(NLAYER,NGAUSS,NGAUSS),KEEP(NLAYER,NGAUSS,NGAUSS)
  DATA XYPT / 0., 0., 0., 0., -0.5773502691896, 0.5773502691896,
    0., 0., -0.7745955592415, 0., 0.7745955592415, 0.,
    -0.8611363115941, -0.8611363115941, 0.3399910435848, 0.3399910435848,
    0.8611363115941 /
  DATA XYWGT / 2., 0., 0., 0., 1., 1., 0., 0., 0.5555555555556,
    0.5555555555556, 0., 0.3478548451375,
    0.6521451548625, 0.6521451548625, 0.3478548451375 /
159 DO 160 I=1,NGAUSS
  PTINT(I)=XYPT(I,NGAUSS)
160 WGT(I)=XYWGT(I,NGAUSS)
  IF(NHARD.EQ.0) HPRIME=0.
  IF(NHARD.EQ.1) HPRIME=ET*FLAS/(ELAS-ET)
  T=ELAS/(1.-V*V)
  EXX=T
  EXY=T*V
  EYZ=T
  EZZ=T*(1.-V)/2.
  IF(INIT.NE.1) RETURN
65 DO 57 I=1,NTOTAL
  PT(I)=0.
67 UTOTAL(I)=0.
  REWIND NREAD
  WRITE (NREAD) UTOTAL
  DO 180 J=1,NGAUSS
  DO 180 JJ=1,NGAUSS
  DO 149 KK=1,NLAYER
  PLATRN(KK,JJ,I)=0.
  KEEP(KK,JJ,I)=0
  DO 149 J=1,1
  IF(KK.GT.2) GO TO 149
  TOTSRN(J,KK,JJ,I)=0.
149 STRES(J,KK,JJ,I)=0.
149 CONTINUE
  DO 200 K=1,NELFM
200 WRITE (NREAD) STRES,PLATRN,TOTSRN,KEEP
  XLEVEL=0.
  WRITE (NREAD) P,XLEVEL
  RETURN
END

```

```

EFFECT* NOTERM, ID, EBCDIC, SOURCE, NOLIST, NODECK, LOAD, NOMAP, NOTEST
EFFECT* NAME = SET LINECNT = 56
SOURCE STATEMENTS = 3A, PROGRAM SIZE = 2476
NO DIAGNOSTICS GENERATED

```

```

SUBROUTINE READY(NJOINT,NELEM,NONCOP,NGAUSS,NLAYER,NFREE,LK,NIMPER,
  ISTEP,INIT,NTOTAL,NREAD,NWRITE,H,UTOTAL,STRES,
  PLATRN,TOTSRN,IPLNAR,NOD,LL,KEEP,ITERA)
  IMPLICIT REAL*8 (A-H,O-Z), INTEGER*2 (I-N)
  INTEGER NJOINT,NELFM,NONCOP,NIMPER,NGAUSS,NLAYER,NTOTAL,NFREE,
  NREAD,NWRITE
  DIMENSION UTOTAL(NTOTAL),H(3,3,NIMPER,NONCOP),NOD(4,NELFM),
  STRES(3,NLAYER,NGAUSS,NGAUSS),PLATRN(NLAYER,NGAUSS,NGAUSS),
  TOTSRN(3,2,NGAUSS,NGAUSS),KEEP(NLAYER,NGAUSS,NGAUSS)
  COMMON SKT(24,24),S(24),W(24),DG(9),SK1(9,24),S1(3)
  INTEGER*2 IPLNAR(NJOINT),LOCAL/* L*/
  DO 971 I=1,24
  S(I)=0.
  DO 971 J=1,26
971 SKT(I,J)=0.
  IF(ISTEP.EQ.1.AND.(IFRA.EQ.1) RETURN
  IF(LL.NE.1) GO TO 200
  IF(ISTEP.EQ.INIT.AND.(ITERA.EQ.1) GO TO 100
  READ (NREAD)
  WRITE (NWRITE) UTOTAL
  GO TO 200
100 READ (NREAD) UTOTAL
200 ID=1
  DO 70 I=1,4
  IF(NIMPER.EQ.4) ID=I
  L=(I-1)*NFREE
  K=(NOD(I,LK)-1)*NFREE
  IF(LL.EQ.0.OR.IPLNAR(NOD(I,LK)).FQ.LOCAL) GO TO 50
  DO 40 J=1,2
  M=L+(J-1)*3
  N=K+(J-1)*3
  DO 30 I1=1,3
  T1=0.
  DO 20 J1=1,3
20 T1=T1+H(I1,J1,ID,LL)*UTOTAL(N+J1)
30 W(N+I1)=T1
40 CONTINUE
  GO TO 70
50 DO 60 J=1,NFREE
60 W(L+J)=UTOTAL(K+J)
70 CONTINUE
  READ (NREAD) STRES,PLATRN,TOTSRN,KEEP
  RETURN
END

```

```

EFFECT* NOTERM, ID, EBCDIC, SOURCE, NOLIST, NODECK, LOAD, NOMAP, NOTEST
EFFECT* NAME = READY LINECNT = 56
SOURCE STATEMENTS = 39, PROGRAM SIZE = 2140
NO DIAGNOSTICS GENERATED

```

RELEASE 2.0

DISGRD

DATE = 77154

11/22/35

RELEASE 2.0

DISGRD

DATE = 77154

11/22/35

```

SUBROUTINE DISGRD(   NGAUSS,ISTEP,INIT,LK,PTINT,XC,YC,D,ITERA)
IMPLICIT REAL*8 (A-H,O-Z), INTEGER*2 (I-N)
INTEGER NGAUSS
DIMENSION PTINT(NGAUSS),D(9,24,NGAUSS,NGAUSS)
IF(ISTEP.EQ.INIT.AND.ITERA.EQ.1) GO TO 10
READ (4) D
RETURN
10 DO 15 L=1,NGAUSS
DO 15 K=1,NGAUSS
DO 15 J=1,24
DO 15 I=1,9
15 D(I,J,K,L)=0.
A=XC/2.
B=YC/2.
AB=A*B
A1=3.*A
A2=9.*A
A3=A*A
B1=4.*B
B2=4.*B
B3=3.*B
DO 500 II=1,NGAUSS
DO 500 JJ=1,NGAUSS
X=PTINT(JJ)
Y=PTINT(II)
X1=1.-X
X2=1.+X
X3=1.-3.*X
X4=1.+3.*X
X5=X1*X2
Y1=1.-Y
Y2=1.+Y
Y3=1.-3.*Y
Y4=1.+3.*Y
Y5=Y1*Y2
D(1,1,JJ,II)=-Y1/A1
D(1,7,JJ,II)=-D(1,1,JJ,II)
D(1,13,JJ,II)=Y2/A1
D(1,19,JJ,II)=-D(1,13,JJ,II)
D(2,1,JJ,II)=-X1/B1
D(2,7,JJ,II)=-X2/B1
D(2,13,JJ,II)=-D(2,7,JJ,II)
D(2,19,JJ,II)=-D(2,13,JJ,II)
D(3,2,JJ,II)=-0.375*X5*Y1/A
D(3,6,JJ,II)=-X1*X4*Y1/9.
D(3,4,JJ,II)=-D(3,2,JJ,II)
D(3,12,JJ,II)=-X2*X3*Y1/9.
D(3,14,JJ,II)=0.375*X5*Y2/A
D(3,16,JJ,II)=-X2*X3*Y2/9.
D(3,22,JJ,II)=-D(3,14,JJ,II)
D(3,24,JJ,II)=-X1*X4*Y2/9.
D(4,7,JJ,II)=-X1*X1*(2.+X1)/92
D(4,6,JJ,II)=-A0X1*Y5/H2
D(4,4,JJ,II)=-X2*X2*(2.-X1)/92

```

```

D(4,12,JJ,II)=A*X2*X5/H2
D(4,14,JJ,II)=-D(4,6,JJ,II)
D(4,18,JJ,II)=-D(4,12,JJ,II)
D(4,20,JJ,II)=-D(4,2,JJ,II)
D(4,24,JJ,II)=-D(4,6,JJ,II)
D(5,3,JJ,II)=-Y1*(3.*X5-Y*Y2)/A2
D(5,4,JJ,II)=-B*Y1*Y5/A2
D(5,5,JJ,II)=-D(3,6,JJ,II)
D(5,9,JJ,II)=-D(5,3,JJ,II)
D(5,10,JJ,II)=-D(5,4,JJ,II)
D(5,11,JJ,II)=-D(3,12,JJ,II)
D(5,15,JJ,II)=Y2*(3.*X5*Y*Y1)/A2
D(5,16,JJ,II)=-B*Y2*Y5/A2
D(5,17,JJ,II)=-D(3,19,JJ,II)
D(5,21,JJ,II)=-D(5,15,JJ,II)
D(5,22,JJ,II)=-D(5,16,JJ,II)
D(5,23,JJ,II)=-D(3,24,JJ,II)
D(6,3,JJ,II)=-X1*(-X*X2+3.*Y5)/92
D(6,4,JJ,II)=-X1*Y1*Y4/9.
D(6,5,JJ,II)=-D(4,6,JJ,II)
D(6,9,JJ,II)=-X2*(X*X1+3.*Y5)/32
D(6,10,JJ,II)=X2*Y1*Y4/(-8.)
D(6,11,JJ,II)=-D(4,12,JJ,II)
D(6,15,JJ,II)=-D(6,9,JJ,II)
D(6,16,JJ,II)=-X2*Y2*Y3/8.
D(6,17,JJ,II)=-D(6,11,JJ,II)
D(6,21,JJ,II)=-D(6,3,JJ,II)
D(6,22,JJ,II)=-X1*Y2*Y3/9.
D(6,23,JJ,II)=-D(6,5,JJ,II)
D(7,3,JJ,II)=0.75*X*Y1/A3
D(7,5,JJ,II)=2.*X3*Y1/A2
D(7,9,JJ,II)=-D(7,3,JJ,II)
D(7,11,JJ,II)=-7.*X4*Y1/A2
D(7,15,JJ,II)=0.75*X*Y2/A3
D(7,17,JJ,II)=-2.*X4*Y2/A2
D(7,21,JJ,II)=-D(7,15,JJ,II)
D(7,23,JJ,II)=2.*X3*Y2/A2
D(8,3,JJ,II)=0.75*X1*Y/H3
D(8,4,JJ,II)=-2.*X1*Y3/H2
D(8,9,JJ,II)=0.75*X2*Y/H3
D(8,10,JJ,II)=-2.*X2*Y3/H2
D(8,15,JJ,II)=-D(8,9,JJ,II)
D(8,16,JJ,II)=2.*X2*Y4/H2
D(8,21,JJ,II)=-D(8,3,JJ,II)
D(8,22,JJ,II)=7.*X1*Y4/H2
D(9,3,JJ,II)=[0.5-0.375*X*X-0.375*Y*Y]/A0
D(9,4,JJ,II)=Y1*Y4/A2
D(9,5,JJ,II)=-X1*X4/H2
D(9,9,JJ,II)=-D(9,3,JJ,II)
D(9,10,JJ,II)=-D(9,4,JJ,II)
D(9,11,JJ,II)=-X2*X3/H2
D(9,15,JJ,II)=D(9,3,JJ,II)
D(9,16,JJ,II)=-Y2*Y3/A2
D(9,17,JJ,II)=-D(9,11,JJ,II)

```

RELEASE 2.0

DISGRD

DATE = 77154

11/22/35

RELEASE 2.0

STRAIN

DATE = 77154

11/22/35

```

D(9.21,JJ,II)=D(9.3,JJ,II)
D(9.22,JJ,II)=D(9.16,JJ,II)
D(9.23,JJ,II)=D(9.5,JJ,II)
500 CONTINUE
WRITE (4) D
RETURN
END

```

```

EFFECT* NOTERM.ID.EMCDIC.SOURCE.NOLIST.NODECK.LOAD.NOMAP.NOTEST
EFFECT* NAME = DISGRD * LINECNT = 56
SOURCE STATEMENTS = 115 PROGRAM SIZE = 7280
NO DIAGNOSTICS GENERATED

```

```

SUBROUTINE STRAIN(NGAUSS,NLAYER,JJ,II,TH,STRAN,TOTSRN,O,ISTEP,INIT
,ITERA)
*
IMPLICIT REAL*8 (A-H,O-Z), INTEGER*2 (I-N)
INTEGER NGAUSS,NLAYER
DIMENSION STRAN(3,NLAYER),D(3,24,NGAUSS,NGAUSS),TOTSRN(3,2,NGAUSS,
NGAUSS),R0(3,24),R1(3,24),RT(3,24)
COMMON SKY(24,24),S(24),W(24),DG(9),SKI(9,24),SI(3)
EQUIVALENCE (SKI(1,1),R0(1,1)),(SKI(1,9),R1(1,1)),
(SKI(1,17),RT(1,1))
*
80 DO 100 I=1,9
DG(I)=0.
DO 100 J=1,24
100 DG(I)=DG(I)+D(I,J,JJ,II)*W(J)
IF(ISTEP.EQ.INIT.AND.ITERA.FO.1) RETURN
A=DG(5)/2.
B=DG(6)/2.
DO 200 J=1,24
B0(1,J)=D(1,J,JJ,II) + A*D(5,J,JJ,II)
B0(2,J)=D(4,J,JJ,II) + B*D(5,J,JJ,II)
B0(3,J)=D(2,J,JJ,II)+D(3,J,JJ,II)+B*D(5,J,JJ,II)+A*D(6,J,JJ,II)
B1(1,J)=D(7,J,JJ,II)
B1(2,J)=D(8,J,JJ,II)
200 B1(3,J)=2.*D(9,J,JJ,II)
DELTAH=TH/(NLAYER-1)
N=NLAYER-1
M=1
DO 500 I=1,NLAYER,N
IF(I.EQ.NLAYER) M=2
Z=-TH/2.+(I-1)*DELTAH
DO 400 K=1,3
A=TOTSRN(K,M,JJ,II)
TOTSRN(K,M,JJ,II)=0.
DO 300 J=1,24
BT(K,J)=R0(K,J)-Z*B1(K,J)
300 TOTSRN(K,M,JJ,II)=TOTSRN(K,M,JJ,II)+BT(K,J)*W(J)
400 STRAN(K,I)=TOTSRN(K,M,JJ,II)-A
500 CONTINUE
DO 600 I=2,N
Z=-TH/2.+(I-1)*DELTAH
DO 600 K=1,3
600 STRAN(K,I)=(STRAN(K,NLAYER)-STRAN(K,1))*((Z+TH/2.)/TH+STRAN(K,1)
DO 800 J=1,24
R0(1,J)=D(1,J,JJ,II)+DG(5)*D(5,J,JJ,II)
R0(2,J)=D(4,J,JJ,II)+DG(6)*D(6,J,JJ,II)
800 B0(3,J)=D(2,J,JJ,II)+D(3,J,JJ,II)+DG(6)*D(5,J,JJ,II)+DG(5)*D(6,J,JJ,II)
*
JJ,II)
RETURN
END

```

```

EFFECT* NOTERM.ID.EMCDIC.SOURCE.NOLIST.NODECK.LOAD.NOMAP.NOTEST
EFFECT* NAME = STRAIN * LINECNT = 56
SOURCE STATEMENTS = 44 PROGRAM SIZE = 1144
NO DIAGNOSTICS GENERATED

```

RELEASE 2-0

STRESS

DATE = 77154

11/22/35

RELEASE 2-0

STRESS

DATE = 77154

11/22/35

```

SUBROUTINE STRESS(NGAUSS,NLAYER,JJ,II,LK,ELAS,SYIELD,NHARD,EXPON,
  S07,EXX,EXY,EYY,EZZ,IYIELD,ISTEP,INIT,HPRIME,
  NWRITE,E,STRAN,STRES,PLATRN,TOTSRN,KEEP,NT,ITERA
  )
  IMPLICIT REAL*8 (A-H,O-Z), INTEGER*2 (I-N)
  INTEGER NGAUSS,NLAYER,NWRITE
  DIMENSION STRAN(3,NLAYER),STRES(3,NLAYER,NGAUSS,NGAUSS),E(3,3,NLAY
  ER),TFMP(3),SOLTA(3),X(3),PLATRN(NLAYER,NGAUSS,NGAU
  SS),KEEP(NLAYER,NGAUSS,NGAUSS),TOTSRN(3,2,NGAUSS,NGAUSS)
  C
  C FOR NHARD=0 (PERFECT PLASTIC MATERIAL)
  120 DO 1000 KK=1,NLAYER
    IF(KEEP(KK,JJ,II).EQ.0) IP=1
    IF(KEEP(KK,JJ,II).NE.0) IP=2
    DO 500 N=1,P,3
      400 CALL MODULI(STRES(1,KK,JJ,II),STRES(2,KK,JJ,II),STRES(3,KK,JJ,II),
        * KEEP(KK,JJ,II),SYIELD,HPRIME,EXX,EXY,EYY,EZZ,
        * E(1,1,KK),E(1,2,KK),E(1,3,KK),E(2,1,KK),E(2,2,KK),
        * E(2,3,KK),E(3,1,KK),E(3,2,KK),E(3,3,KK),SX,SY,DEN,
        * X(1),X(2),X(3))
      410 IF(ISTEP.EQ.INIT.AND.ITERA.EQ.1) GO TO 850
      IF(N.GE.3) GO TO 850
      SOLTA(1)=EXX*STRAN(1,KK)+EXY*STRAN(2,KK)
      SOLTA(2)=EXY*STRAN(1,KK)+EYY*STRAN(2,KK)
      SOLTA(3)=EZZ*STRAN(3,KK)
      IF(KEEP(KK,JJ,II).EQ.0) GO TO 550
      FDELTA=3.*(E(1,3)*SOLTA(1)+E(2,3)*SOLTA(2)+STRES(3,KK,JJ,II)*SOLTA
        (3))/SYIELD
      IF(FDELTA.LT.0.) GO TO 480
      450 DO 500 I=1,3
        SOLTA(I)=0.
        DO 500 J=1,3
          500 SOLTA(I)=SOLTA(I)+E(I,J,KK)*STRAN(J,KK)
          DO 400 I=1,3
            TFMP(I)=STRES(I,KK,JJ,II)*SOLTA(I)
          400 STRES(I,KK,JJ,II)=0.
          GO TO 450
        480 KEEP(KK,JJ,II)=0
        DO 400 I=1,3
          STMP(I)=STRES(I,KK,JJ,II)
        600 STRES(1,KK,JJ,II)=STRES(1,KK,JJ,II)+SOLTA(1)
          IF(N.EQ.2) GO TO 800
        650 SE=DSORT(STRES(1,KK,JJ,II)+STRES(1,KK,JJ,II)-STRES(1,KK,JJ,II)*STR
          * STRES(2,KK,JJ,II)+STRES(2,KK,JJ,II)*STRES(2,KK,JJ,II)+3.*STRES(3,
          * KK,JJ,II)*STRES(3,KK,JJ,II)
          IF(SE.LT.SYIELD) GO TO 950
        650 DO 660 I=1,3
          550 X(1)=STRES(1,KK,JJ,II)-TFMP(1)
            AX(X(1)+X(1)+X(2)+X(2)+3.*X(3)+X(3))
            H=2.*X(1)+TFMP(1)-X(1)+TFMP(2)-X(2)+TFMP(1)+2.*X(2)+TFMP(2)+6.*X(3
            )+TFMP(1)
            CT=TFMP(1)+TFMP(1)-TFMP(1)+TFMP(2)+TFMP(2)+TFMP(2)+1.*TFMP(3)+TFMP(
            3)+SYIELD*SYIELD

```

```

      T=B*B-4.*A*C
      IF(T.GE.0.) GO TO 670
      T=0.
      GO TO 675
    670 T=DSORT(T)
      T1=(-B+T)/(2.*A)
      T2=(-B-T)/(2.*A)
      IF(DABS(T1).LE.DABS(T2)) T=T1
      IF(DABS(T2).LE.DABS(T1)) T=T2
    675 DO 680 I=1,3
      680 STRES(I,KK,JJ,II)=TEMP(1)+X(1)*T
      IF(KEEP(KK,JJ,II).NE.0) GO TO 800
      DO 700 I=1,3
        790 STRAN(I,KK)=STRAN(I,KK)*(1.-DABS(T))
        KEEP(KK,JJ,II)=1
      800 CONTINUE
      950 IF(KEEP(KK,JJ,II).NE.0) IYIELD=1
    1000 CONTINUE
      IF(ISTEP.EQ.INIT.AND.ITERA.EQ.1) RETURN
      IF(JJ.EQ.INGAUSS.AND.II.EQ.INGAUSS) WRITE(NWRITE) STRES,PLATRN,
        TOTSRN,KEEP
      IF(ISTEP.NE.NT) RETURN
      IF(ITERA.NE.1) RETURN
      40 IF(LK.NE.1.OR.JJ.NE.1.OR.II.NE.1) GO TO 890
      WRITE(6,50)
      50 FORMAT('0',///,'0',T5,'ELEMENT NO',T20,'LOCATION ( INTERGRATION PT
        *INTS )',T55,'LAYER NO',T78,'CUMULATED STRESSES IN LOCAL COORDINATE
        *',T124,'0=ELASTIC',/,',',T27,'JJ(X)',T39,'II(Y)',T70,'K - NORMAL',
        RT90,'Y - NORMAL',T110,'SHEAR STRESS',T124,'1=PLASTIC',//)
      890 DO 1200 KK=1,NLAYER
        900 IF(KK.EQ.1) GO TO 930
        IF(KK.EQ.NLAYER.OR.KEEP(KK,JJ,II).NE.0) GO TO 905
        IF(KEEP(KK-1,JJ,II).EQ.0.AND.KEEP(KK+1,JJ,II).EQ.0) GO TO 1200
        905 WRITE(6,910) KK,(STRES(I,KK,JJ,II),I=1,3),KEEP(KK,JJ,II)
        910 FORMAT(' ',T55,T5,T62,3020.5,T127,T2)
        GO TO 1200
      930 IF(JJ.EQ.1.AND.II.EQ.1) GO TO 970
        WRITE(6,950) JJ,II,KK,(STRES(I,KK,JJ,II),I=1,3),KEEP(KK,JJ,II)
        950 FORMAT('0',T27,T3,T39,T3,T55,T5,T62,3020.5,T127,T2)
        GO TO 1200
      970 WRITE(6,980) LK,JJ,II,KK,(STRES(I,KK,JJ,II),I=1,3),KEEP(KK,JJ,II)
      980 FORMAT('0',T5,T5,T27,T3,T39,T3,T55,T5,T62,3020.5,T127,T2)
    1200 CONTINUE
      RETURN
      END

```

```

EFFECT* NOTERM,IO,EBCDIC,SOURCE,NOLIST,NODECK,LOAD,NOMAP,NOTES*
EFFECT* NAME = STRESS * LINECNT = 56
SOURCE STATEMENTS = 78,PROGRAM SIZE = 5916
NO DIAGNOSTICS GENERATED

```

RELEASE 2.0

MODUL1

DATE = 77154

11/22/35

RELEASE 2.0

TRUEPT

DATE = 77154

11/22/35

```

SUBROUTINE MODUL1(A,H,C,N,SHAR,MPRIME,EXX,EXY,EYY,EZZ,E11,F12,E13,
*      E21,E22,E23,E31,E32,E33,SK,SY,DEN,D1,D2,D3)
IMPLICIT REAL*8 (A-H,O-Z), INTEGER*2 (I-N)
IF(N.EQ.0) GO TO 200
G1=(A+B)/3.
SX=A-G1
SY=Y-G1
D1=1.5*(EXX*SH+EXY*SY)/SHAR
D2=1.5*(EXY*SK+EYY*SY)/SHAR
D3=1.5*(EZZ*C/SHAR
DEN=MPRIME+A.5*(0.5*EXX*SK+EXY*SK*SY+0.5*EYY*SY*SY+2.*EZZ*C*C)/
*(SHAR*SHAR)
E11=EXX-D1*D1/DEN
E12=EXY-D1*D2/DEN
E13=-D1*D3/DEN
E21=F12
E22=EYY-D2*D2/DEN
E23=-D2*D3/DEN
E31=E13
E32=E23
E33=EZZ-D3*D3/DEN
RET JDN
200 E11=EXX
F12=EXY
E13=0.
E21=EXY
E22=EYY
E23=0.
F11=0.
E32=0.
E33=EZZ
RETURN
END

```

EFFECT\* NOTERM,IO,EBCDIC,SOURCE,NOLIST,MODECK,LOAD,NOMAP,NOTEST  
 EFFECT\* NAME = MODUL1, LINECNT = 56  
 SOURCE STATEMENTS = 31, PROGRAM SIZE = 1462  
 NO DIAGNOSTICS GENERATED

```

SUBROUTINE TRUEPT(NGAUSS,NLAYER,JJ,II,WGT,TH,XC,YC,STRFS,ISTEP,
*      INIT,ITERA)
IMPLICIT REAL*8 (A-H,O-Z), INTEGER*2 (I-N)
INTEGER NGAUSS,NLAYER
DIMENSION STRES(3,NLAYER,NGAUSS,NGAUSS),S2(3),WGT(NGAUSS),
*      B0(3,24),B1(3,24)
COMMON SKT(24,24),S(24),W(24),DG(9),SK1(9,24),S1(3)
EQUIVALENCE (SK1(1,1),B0(1,1)),(SK1(1,9),B1(1,1))
DO 100 I=1,3
S1(I)=0.
100 S2(I)=0.
N=NLAYER-1
DELTAH=TH/N
Z1=-TH/2.
DO 400 KK=1,N,2
Z2=Z1+DELTAH
Z3=Z2+DELTAH
DO 200 I=1,3
S1(I)=S1(I)+STRES(I,KK,JJ,II)*4.*STRES(I,KK+1,JJ,II)+STRES(I,KK+2,
*      JJ,II)
IF(ISTEP.EQ.INIT.AND.ITERA.EQ.1) GO TO 200
S2(I)=S2(I)+Z1*STRES(I,KK,JJ,II)+Z2*4.*STRES(I,KK+1,JJ,II)+Z3*STRES
*      (I,KK+2,JJ,II)
200 CONTINUE
Z1=Z3
400 CONTINUE
DO 450 I=1,3
S1(I)=S1(I)*DELTAH/3.
450 S2(I)=S2(I)*DELTAH/3.
IF(ISTEP.EQ.INIT.AND.ITERA.EQ.1) RETURN
DO 600 I=1,24
T=0.
DO 500 J=1,3
500 T=T+B0(J,I)*S1(J)-B1(J,I)*S2(J)
600 S(I)=S(I)+WGT(JJ)*WGT(II)*T
IF(JJ.NE.INGAUSS.OR.II.NE.INGAUSS) RETURN
AB=XC*YC/4.
DO 700 I=1,24
S(I)=S(I)+AB
700 S(I)=S(I)+AB
800 RETURN
END

```

EFFECT\* NOTERM,IO,EBCDIC,SOURCE,NOLIST,MODECK,LOAD,NOMAP,NOTEST  
 EFFECT\* NAME = TRUEPT, LINECNT = 56  
 SOURCE STATEMENTS = 37, PROGRAM SIZE = 2060  
 NO DIAGNOSTICS GENERATED

RELEASE 2.0

STIFF

DATE = 77154

11/22/75

RELEASE 2.0

STIFF

DATE = 77154

11/22/75

```

SUBROUTINE STIFF(NGAUSS,NLAYER,JJ,II,ISTEP,IYIELD,EXX,EXY,EYY,EZ7,
  WGT,E,TH,XC,YC,D,ITERA)
  IMPLICIT REAL*8 (A-H,O-Z), INTEGER*2 (I-N)
  INTEGER NGAUSS,NLAYER
  DIMENSION WGT(NGAUSS),D(9,24),NGAUSS,NGAUSS),E(3,3,NLAYER),EE(3,3),
    EEZ(3,3),EEZZ(3,3),SK(9,9)
  COMMON SKT(24,24),S(24),W(24),DG(9),SK1(9,24),S1(3)
  IK(IYIELD,EQ,1) GO TO 300

```

```

  IYIELD=0      FULLY ELASTIC THRU THICKNESS

```

```

100 SK(1,1)=TH*EXX
  SK(1,2)=0.
  SK(1,3)=0.
  SK(1,4)=TH*EXY
  SK(2,2)=TH*EZZ
  SK(2,3)=SK(2,2)
  SK(2,4)=0.
  SK(3,3)=SK(2,2)
  SK(3,4)=0.
  SK(4,4)=TH*EYY
  E1=TH*TH/12.
  SK(7,7)=E1*EXX
  SK(7,8)=E1*EXY
  SK(8,7)=SK(7,8)
  SK(9,9)=E1*EYY
  SK(9,9)=4.*E1*EZZ
  IF(ISTEP.NE.1.OR.ITERA.NE.1) GO TO 240
  DO 150 I=1,6
  DO 150 J=5,8
150 SK(I,J)=0. D 0
  GO TO 280
240 SK(1,5)=TH*EXX*DG(5)
  SK(1,6)=TH*EXY*DG(6)
  SK(2,5)=TH*EZZ*DG(6)
  SK(2,6)=TH*EZZ*DG(5)
  SK(3,5)=SK(2,5)
  SK(3,6)=SK(2,6)
  SK(4,5)=TH*EXY*DG(5)
  SK(4,6)=TH*EYY*DG(6)
  SK(5,5)=TH*(EXX*DG(5)*DG(5)+EZZ*DG(6)*DG(6))+S1(1)
  SK(5,6)=TH*(EXY*EZZ*DG(5)*DG(6))+S1(3)
  SK(5,5)=TH*(EYY*DG(6)*DG(6)+EZZ*DG(5)*DG(5))+S1(2)
280 K=0
  GO TO 340

```

```

  IYIELD=1      YIELDING AT AT LEAST ONE INTEGRATING POINT THRU THICKNESS

```

```

300 DO 310 I=1,3
  DO 310 J=1,3
  -E(I,J)=0.
  EEZ(1,1)=0.
310 EEZ(I,J)=0.
  N=LAYER-1

```

```

  DELTAH=TH/N
  Z1=-TH/2.
  DO 340 KK=1,N,2
  Z2=Z1+DELTAH
  Z3=Z2+DELTAH
  DO 320 I=1,3
  DO 320 J=1,3
  EE(I,J)=EE(I,J)+E(I,J,KK)+4.*E(I,J,KK+1)+E(I,J,KK+2)
  EEZ(I,J)=EEZ(I,J)+Z1*E(I,J,KK)+Z2*4.*E(I,J,KK+1)+Z3*E(I,J,KK+2)
320 EEZ(I,J)=EEZ(I,J)+Z1*Z1*E(I,J,KY)+Z2*Z2*4.*E(I,J,KK+1)+Z3*Z3*E(I,J,KK+2)
  Z1=Z3
340 CONTINUE
  DO 345 I=1,3
  DO 345 J=1,3
  EE(I,J)=EE(I,J)*DELTAH/3.
  EEZ(I,J)=EEZ(I,J)*DELTAH/3.
345 EEZ(I,J)=EEZ(I,J)*DELTAH/3.
  SK(1,1)=EE(1,1)
  SK(1,2)=EE(1,3)
  SK(1,3)=EE(1,3)
  SK(1,4)=EE(1,2)
  SK(1,5)=EE(1,1)*DG(5)+EE(1,3)*DG(6)
  SK(1,6)=EE(1,2)*DG(6)+EE(1,3)*DG(5)
  SK(1,7)=EEZ(1,1)
  SK(1,8)=EEZ(1,2)
  SK(1,9)=2.*EEZ(1,3)
  SK(2,2)=EE(3,3)
  SK(2,3)=EE(3,3)
  SK(2,4)=EE(2,3)
  SK(2,5)=EE(3,3)*DG(6)+EE(1,3)*DG(5)
  SK(2,6)=EE(3,3)*DG(5)+EE(2,3)*DG(6)
  SK(2,7)=EEZ(1,3)
  SK(2,8)=EEZ(2,3)
  SK(2,9)=2.*EEZ(3,3)
  DO 350 J=3,9
350 SK(1,J)=SK(2,J)
  SK(4,4)=EE(2,2)
  SK(4,5)=EE(1,2)*DG(5)+EE(2,3)*DG(6)
  SK(4,6)=EE(2,2)*DG(6)+EE(2,3)*DG(5)
  SK(4,7)=EEZ(1,2)
  SK(4,8)=EEZ(2,2)
  SK(4,9)=2.*EEZ(2,3)
  SK(5,5)=EE(1,1)*DG(5)*DG(5)+EE(3,3)*DG(6)*DG(6)+2.*EE(1,3)*DG(5)*
    DG(6)+S1(1)
  SK(5,6)=(EE(1,2)+EE(3,3))*DG(5)*DG(6)+EE(1,3)*DG(5)*DG(5)+EE(2,3)*
    DG(6)*DG(6)+S1(3)
  SK(5,7)=EEZ(1,1)*DG(5)+EEZ(1,3)*DG(6)
  SK(5,8)=EEZ(1,2)*DG(5)+EEZ(2,3)*DG(6)
  SK(5,9)=2.*EEZ(1,3)*DG(5)+EEZ(1,3)*DG(6)
  SK(6,6)=FF(2,2)*DG(6)*DG(6)+FF(1,3)*DG(5)*DG(5)+2.*FF(2,3)*DG(6)*
    DG(6)+S1(2)
  SK(6,7)=EEZ(1,2)*DG(6)+EEZ(1,3)*DG(5)
  SK(6,8)=EEZ(2,2)*DG(6)+EEZ(2,3)*DG(5)

```



RELEASE 2.0

STIFF

DATE = 77154

11/22/35

RELEASE 2.0

STIFF

DATE = 77154

11/22/35

```

SK(6.9)=2.*EEZ(3.3)*DG(5)+EEZ(2.3)*DG(6))
SK(7.7)=EEZZ(1.1)
SK(7.8)=EEZZ(1.2)
SK(7.9)=2.*EEZZ(1.3)
SK(8.8)=EEZZ(2.2)
SK(8.9)=2.*EEZZ(2.3)
SK(9.9)=4.*EEZZ(3.3)
K=9
380 DO 390 I=7,K
L=I-1
DO 390 J=1,L
390 SK(I,J)=SK(J,I)
DO 420 I=1,9
M=1
DO 419 J=1,24
M=M+1
IF(M.GT.3) GO TO 404
IF(IYIELD.EQ.0.AND.I.GE.7) GO TO 418
IF(M.EQ.2) GO TO 402
K1=3
K2=4
GO TO 408
402 K1=1
K2=2
GO TO 408
404 K1=5
IF(IYIELD.EQ.0.AND.I.GE.7.AND.I.LE.8) K1=7
IF(IYIELD.EQ.0.AND.I.EQ.9) K1=9
K2=9
IF(IYIELD.EQ.0.AND.I.LE.6) K2=6
IF(IYIELD.EQ.0.AND.I.GE.7.AND.I.LE.8) K2=8
408 SK(I,J)=0.
DO 410 K=K1,K2
410 SK(I,J)=SK(I,J)+SK(I,K)*D(K,J,JJ,II)
IF(M.EQ.6) M=0
418 CONTINUE
420 CONTINUE
LL=7
DO 440 I=1,24
L=(I+1)-LL*6
M=M+LL
DO 439 J=1,24
M=(J+1)-M*6
IF(L.GT.3) GO TO 424
IF(L.EQ.2) GO TO 422
K1=3
K2=4
GO TO 428
422 K1=1
K2=2
GO TO 424
424 K1=5
K2=9
IF(IYIELD.EQ.0.AND.M.LE.3) K2=6

```

```

428 T=0.
DO 430 K=K1,K2
430 T=T+D(K,I,JJ,II)*SK1(K,J)
SKY(I,J)=SKY(I,J)+T*WGT(JJ)*WGT(II)
136 IF(M.EQ.6) MM=MM+1
438 CONTINUE
IF(L.EQ.6) LL=LL+1
440 CONTINUE
460 IF(JJ.NE.NGAUSS.OR.(I.NE.NGAUSS)) RETURN
AB=XC*YC/4.
DO 480 I=1,24
DO 480 J=1,24
480 SKY(I,J)=SKY(I,J)*AB
490 RETURN
END

```

```

EFFECT* NOTERM.ID.EBCDIC.SOURCE.NOLIST.NODECK.LOAD.NOMAP.NOTEST
EFFECT* NAME = STIFF , LINECNT = 56
SOURCE STATEMENTS = 165, PROGRAM SIZE = 5792
NO DIAGNOSTICS GENERATED

```

RELEASE 2.0

ROT

DATE = 77154

11/22/35

RELEASE 2.0

ROT

DATE = 77154

11/22/35

SUBROUTINE ROT(NJOINT,NELEM,ISTEP,NT,LK,H,IPLNAR,NOD,LL,NONCOP,  
NIMPER,INIT,ITERA)

IMPLICIT REAL\*8 (A-H,O-Z), INTEGER\*2 (I-N)

INTEGER NJOINT,NELEM,NONCOP,NIMPER

DIMENSION H(3,3,NIMPER,NONCOP),NOD(4,NELEM),C(3)

INTEGER\*2 IPLNAR(NJOINT),LOCAL/\* L\*/

COMMON SKT(24,24),S(24),W(24),DG(9),SKI(9,24),SI(3)

EQUIVALENCE (C(1),SI(1))

TRANSFORM ELEMENT STIFFNESS MATRIX AND RESDUE FORCE VECTOR FROM  
LOCAL TO GLOBAL COORDINATE FOR THOSE NON-COPLANAR JOINTS

DO 1

IF(ISTEP.EQ.0) GO TO 650

DO 600 I=1,4

DO 600 JJ=1,4

DO 500 I2=1,2

I1=6\*(I+3\*I2-8

DO 500 J2=1,2

IF(H(I,FQ,JJ,AND(I2.GT.J2) GO TO 500

J1=6\*(JJ+3\*J2-8

IF(IPLNAR(NOD(JJ,LK)).EQ.LOCAL) GO TO 250

IF(NIMPER.EQ.4) ID=JJ

IF(I1.NE.JJ.OR.I2.NE.J2) GO TO 50

DO 40 I=2,3

M=I+I1-1

KK=I-1

DO 40 K=1,KK

N=K+J1-1

40 SKT(M,N)=SKT(N,M)

50 DO 200 I=1,3

M=I+I1-1

DO 100 J=1,3

C(J)=0.

DO 100 K=1,3

N=K+J1-1

100 C(J)=C(J)+SKT(M,N)\*H(K,J,IO,LL)

DO 200 J=1,3

M=J+J1-1

200 SKT(M,N)=C(J)

250 IF(IPLNAR(NOD(I1,LK)).EQ.LOCAL) GO TO 500

IF(NIMPER.EQ.4) ID=I1

DO 400 J=1,3

N=J+J1-1

DO 300 I=1,3

C(I)=0.

DO 100 K=1,3

M=K+I1-1

300 C(I)=C(I)+H(K,I,IO,LL)\*SKT(M,N)

DO 400 I=1,3

M=I+I1-1

400 SKT(M,N)=C(I)

500 CONTINUE

500 CONTINUE

IF(ISTEP.EQ.0) GO TO 650

650 DO 900 I=1,4

IF(NIMPER.EQ.4) ID=I1

IF(IPLNAR(NOD(I1,LK)).EQ.LOCAL) GO TO 900

DO 900 I2=1,2

I1=6\*(I+3\*I2-8

DO 700 I=1,3

C(I)=0.

DO 700 K=1,3

M=K+I1-1

700 C(I)=C(I)+H(K,I,IO,LL)\*S(M)

DO 800 I=1,3

M=I+I1-1

800 S(M)=C(I)

900 CONTINUE

950 RETURN

END

EFFECT\* NOTERM,IO,EBCDIC,SOURCE,NOLIST,NODECK,LOAD,NOMAP,NOTEST

EFFECT\* NAME = ROT, LINECNT = 56

SOURCE STATEMENTS = 66, PROGRAM SIZE = 2752

NO DIAGNOSTICS GENERATED

RELEASE 2.0

STORE

DATE = 77154

11/22/35

RELEASE 2.0

STORE

DATE = 77154

11/22/35

```

SUBROUTINE STORE(IPART,NELEM,NFREE,LK,MMAX,MTWICE,ST,NFIRST,NLAST,
  MOD,NREAC,INDIC,NTOTAL)
  IMPLICIT REAL*8 (A-H,O-Z), INTEGER*2 (I-N)
  INTEGER NPART,NELEM,NFREE,NTOTAL,MMAX,MTWICE,KREAD,KWRITE
  DIMENSION INDEX(4), ST(MMAX,MTWICE),NFIRST(NPART),NLAST(NPART),
  MOD(4,NELEM),INDIC(NELEM),NREAC(NTOTAL)
  COMMON SKT(24,24),S(24),W(24),OG(9),SK1(9,24),S1(3)

  STORE STIFFNESS MATRIX INTO CORRESPONDING PARTITION ON DISK

  IF(INDIC(LK).NE.1.AND.INDIC(LK).NE.12) GO TO 450
  IF(LK.NE.1) GO TO 300
  IPART1=1
  IPART2=2
  KREAD=1
  KWRITE=2
  GO TO 450
300 IPART1=IPART1+1
  IPART2=IPART2+1
450 DO 505 KK=1,4
505 INDEX(KK)=0
  DO 530 JL=1,2
530 NJ=1
  DO 527 KK=1,4
  IF(INDEX(KK).EQ.1) GO TO 527
  DO 510 MM=IPART1,IPART2
  IF(MOD(KK,LK).GE.NFIRST(MM).AND.MOD(KK,LK).LE.NLAST(MM)) GO TO 515
510 CONTINUE
515 IF(NROUND.NE.1) GO TO 517
  IF(LK.EQ.1) GO TO 516
  IF(INDIC(LK).EQ.1.AND.JL.EQ.2) GO TO 516
  IF(INDIC(LK).EQ.12.AND.JL.EQ.2) GO TO 516
  READ (KREAD) M1,N1,((ST(K1,K2),K2=K1,N1),K1=1,M1)
  GO TO 519
516 NN=MM+1
  IF(MM.EQ.NPART) NN=MM
  DO 460 I=MM,NN
  K=NLAST(I)*NFREE
  DO 440 L=1,K
  KK=K-L+1
  IF(NREAC(KK).NE.0) GO TO 455
440 CONTINUE
455 IF(I1.EQ.MM) M1=NREAC(KK)
  IF(I1.EQ.NN) N1=NREAC(KK)+M1
460 CONTINUE
  IF(MM.EQ.NPART) N1=M1
  DO 175 K=1,M1
  DO 175 L=K,N1
175 ST(K,L)=0.
519 IPART=MM
517 IF(NROUND.NE.2.AND.MM.NE.IPART) GO TO 527
  I=KK-1)*NFREE
  DO 525 LL=1,4
  IF(MOD(KK,LK).GT.MOD(LL,LK)) GO TO 525

```

```

  J=(LL-1)*NFREE
  DO 523 M1=1,NFREE
  MM1=NREAC((MOD(KK,LK)-1)*NFREE+M1)
  IF(MM1.EQ.0) GO TO 523
  IM1=1+M1
  DO 520 NJ=1,NFREE
  NNJ=NREAC((MOD(LL,LK)-1)*NFREE+NJ)
  IF(NNJ.EQ.0) GO TO 520
  IF(IPART.EQ.IPART1.AND.MOD(LL,LK).GT.NLAST(IPART1)) NNJ=NNJ+M1
  IF(MM1.GT.NNJ) GO TO 520
  JNJ=J+NJ
  IF(IM1.GT.JNJ) SKT(IM1,JNJ)=SKT(JNJ,IM1)
  ST(MM1,NNJ)=ST(MM1,NNJ)+SKT(IM1,JNJ)
520 CONTINUE
523 CONTINUE
525 CONTINUE
  INDEX(KK)=1
  NROUND=NROUND+1
  IF(NROUND.GT.2) GO TO 534
527 CONTINUE
534 IF(INDIC(LK).NE.2.AND.INDIC(LK).NE.12) GO TO 524
  IF(LK.NE.NELEM.AND.JL.NE.1) GO TO 524
  WRITE (3) M1,N1,((ST(K1,K2),K2=K1,N1),K1=1,M1)
  GO TO 530
524 WRITE(KWRITE) M1,N1,((ST(K1,K2),K2=K1,N1),K1=1,M1)
530 CONTINUE
  IF(LK.EQ.1) GO TO 600
  IF(INDIC(LK).EQ.1.OR.INDIC(LK).EQ.12) GO TO 500
  IF(LK.EQ.NELEM) RETURN
  BACKSPACE KREAD
500 BACKSPACE KREAD
600 BACKSPACE KWRITE
  IF(INDIC(LK).EQ.2.OR.INDIC(LK).EQ.12) GO TO 700
  BACKSPACE KWRITE
700 KK=KREAD
  KREAD=KWRITE
  KWRITE=KK
  RETURN
  END

```

```

EFFECT= NOTERM, ID, ERCDIC, SOURCE, NOLIST, NOCHECK, LOAD, NOMAP, NOTEST
EFFECT= NAME = STORE, LINECNT = 56
SOURCE STATEMENTS = 88, PROGRAM SIZE = 3648
NO DIAGNOSTICS GENERATED

```

RELEASE 2.0

SUM

DATE = 77154

11/22/35

RELEASE 2.0

RES

DATE = 77154

11/22/35

```

SUBROUTINE SUM(NJOINT,NELEM,NFREE,NTOTAL,U,IPLNAR,NOD,LK)
  IMPLICIT REAL*8 (A-H,O-Z), INTEGER*2 (I-N)
  INTEGER NJOINT,NELEM,NFREE,NTOTAL
  DIMENSION U(NTOTAL),NOD(4,NELEM),IPLNAR(NJOINT)
  COMMON SKT(24,24),S(24),V(24),DG(9),SK1(9,24),S1(3)

```

```

C CALCULATE TRUE FORCE
C

```

```

  IF(LK.NE.1) GO TO 532
  100 DO 180 I=1,NTOTAL
  180 J(1)=0.
  532 DO 540 I=1,4
    K=(NOD(I,LK)-1)*NFREE
    DO 535 J=1,NFREE
  535 U(K+J)=U(K+J)+S((I-1)*NFREE+J)
  540 CONTINUE
  IF(LK.NE.NELEM) RETURN
  WRITE(6,505)
  505 FORMAT(' ',T5,' JOINT NO',T20,' COORDINATE',T60,' TRUE FORCES
    ' ',T20,' (L=LOCAL',T38,' X-LOAD',T53,' Y-LOAD',T68,' Z-LOAD',T
    '83,' X-MOMENT',T98,' Y-MOMENT',T113,' Z-MOMENT',T128,' ',T22,' G=GLOBAL)
    ' //)
  DO 507 I=1,NJOINT
    K=(I-1)*NFREE+1
    K1=1+NFREE
  507 WRITE(6,120) I,IPLNAR(I),(U(J),J=K,K1)
  120 FORMAT(' ',T5,' ',T25,' A2,T32,6D15.5)
  RETURN
END

```

```

EFFECT* NOTERM, ID, ERCDIC, SOURCE, NDLIST, NODECK, LOAD, NDMAP, NOTEST
EFFECT* NAME = SUM LINECNT = 56
STJRCF STATEMENTS = 23, PROGRAM SIZE = 1232
NO DIAGNOSTICS GENERATED

```

```

SUBROUTINE RES(NJOINT,NLOAD,NFREE,NDISP,ISTEP,INIT,NT,SIZE,PLOAD,
  * UDISP,U,P,IPLNAR,NREAC,LF,NU,NTOTAL,NWRITE,NREAD,NITER,
  * ITERA,TOLNCE,DISERR,ERROR,XLEVEL)
  IMPLICIT REAL*8 (A-H,O-Z), INTEGER*2 (I-N)
  INTEGER NJOINT,NLOAD,NFREE,NDISP,NTOTAL,NWRITE,NREAD
  DIMENSION PLOAD(NFREE,NLOAD),P(NTOTAL),U(NTOTAL),NREAC(NTOTAL),
    LF(NLOAD),NU(NDISP),UDISP(NFREE,NDISP),IPLNAR(NJOINT)

```

```

  160 DO 180 I=1,NTOTAL
  180 P(I)=0.
    FNORM=0.
    IF(NLOAD.EQ.1.AND.LF(NLOAD).EQ.0) GO TO 200
    WRITE(6,350)
  350 FORMAT(' ',T5,' JOINT NO',T20,' COORDINATE',T60,' CUMULATED APPLIED F
    *ORC',T20,' (L=LOCAL',T38,' X-LOAD',T53,' Y-LOAD',T68,' Z-LOAD',T
    *83,' X-MOMENT',T98,' Y-MOMENT',T113,' Z-MOMENT',T128,' ',T22,' G=GLOBAL)
    ' //)
    DO 185 I=1,NLOAD
      K=(LF(I)-1)*NFREE
      DO 182 J=1,NFREE
  182 FNORM=FNORM+P(K+J)*P(K+J)
      K=K+1
      K1=LF(I)*NFREE
  185 WRITE(6,120) LF(I),IPLNAR(LF(I)),(P(J),J=K,K1)
  200 IF(NDISP.EQ.1.AND.NU(NDISP).EQ.0) GO TO 300
  DO 250 I=1,NDISP
    K=(NU(I)-1)*NFREE
    DO 250 J=1,NFREE
  250 U(K+J)=0.
    IF(DABS(UDISP(J,1)).LT.0.0000001) GO TO 250
    FNORM=FNORM+U(K+J)*U(K+J)
    U(K+J)=0.
  300 CONTINUE
  300 RNORM=0.
  DO 588 I=1,NTOTAL
    IF(NREAC(I).EQ.0) GO TO 588
    P(I)=P(I)-U(I)
    RNORM=RNORM+P(I)*P(I)
  588 CONTINUE
  FNORM=DSQRT(FNORM)
  RNORM=DSQRT(RNORM)
  RESERR=RNORM/FNORM
  WRITE(6,605)
  605 FORMAT(' ',T5,' JOINT NO',T20,' COORDINATE',T60,' RESIDUAL FORCES
    ' ',T20,' (L=LOCAL',T38,' X-LOAD',T53,' Y-LOAD',T68,' Z-LOAD',T
    *83,' X-MOMENT',T98,' Y-MOMENT',T113,' Z-MOMENT',T128,' ',T22,' G=GLOBAL)
    ' //)
  DO 607 I=1,NJOINT
    K=(I-1)*NFREE+1
    K1=1+NFREE
  607 WRITE(6,120) I,IPLNAR(I),(P(J),J=K,K1)
  120 FORMAT(' ',T5,' ',T25,' A2,T32,6D15.5)
  WRITE(6,150) RNORM,FNORM,RESERR
  150 FORMAT(' ',RESIDUAL FORCE NORM =',D20.5,' ',APPLIED FORCE NORM =',D20.5,' ',RATIO OF RESIDUAL FORCE NORM TO APPLIED FORCE NORM =',D20.5,' ')

```

RELEASE 2.0

RES

DATE = 77154

11/22/35

RELEASE 2.0

NEW

DATE = 77154

11/22/35

```

*V = F10.5)
WRITE (NWRITE) P,XLEVEL
WRITE(6,140) NWRITE
140 FORMAT(' ', 'ALL DATA UP TO THIS STEP STORED ON DISK #', I2)
ERRJRD=DMAX((RESERR,DISERR)
IF(ITER.NE.1) GO TO 420
IF(ERROR.LT.10.*TOLNCE) GO TO 700
WRITE(6,410)
410 FORMAT(' ', 'PROGRAM TERMINATED DUE TO HIGH ERROR. REDUCE EITHER ST
EP SIZE OR TO BE ADDED RESIDUAL FORCES')
STOP
420 IF(ISTEP.LT.(NT-1).AND.ITERA.GT.2.AND.ERROR.LE.TOLNCE) GO TO 800
IF(ITERA.EQ.2) GO TO 450
IF(ITERA.EQ.2.AND.RESERR.LE.ERROLD) GO TO 450
IF(ERROR.LE.ERROLD) GO TO 450
WRITE(6,440)
440 FORMAT(' ', 'DIVERGENCE OR NON-MONOTONIC CONVERGENCE OCCUR. USE SMA
LLER STEP SIZE')
STOP
450 ERRJLD=ERROR
IF(ITERA.NE.1) RETURN
420 IF(ERROR.GF.5.*TOLNCE) SIZE=SIZE/2.
420 IF(ERROR.LE.5.*TOLNCE) SIZE=2.*SIZE
RETURN
END

```

EFFECT\* NOTFRM.ID.EBCDIC.SOURCE.NOLIST.NODECK.LOAD.NOMAP.NOTEST  
EFFECT\* NAME = RES LINECNT = 56  
SOURCE STATEMENTS = 66, PROGRAM SIZE = 3644  
NO DIAGNOSTICS GENERATED

```

SUBROUTINE NEW(NELEM,NLOAD,NGAUSS,NLAYER,NFREE,NTOTAL,ISTEP,INIT,
* NT,ITER,ITERA,NWRITE,SIZE,XLEVEL,PLOAD,UTOTAL,P,
* STRES,PLATRN,TOTSRN,LF,KEEP,NREAD,ERRCP,TOLNCE)
IMPLICIT REAL*8 (A-H,O-Z), INTEGER*2 (I-N)
INTEGER NELEM,NLOAD,NGAUSS,NLAYER,NFREE,NTOTAL,NWRITE,NREAD
DIMENSION PLOAD(NFREE,NLOAD),UTOTAL(NTOTAL),P(NTOTAL),STRES(3,NLAY
* ER,NGAUSS,NGAUSS),PLATRN(NLAYER,NGAUSS,NGAUSS),
* TOTSRN(3,2,NGAUSS,NGAUSS),LF(NLOAD),KEEP(NLAYER,NGA
* USS,NGAUSS)

```

STORE RESULTS TO INSURANCE DISK WHEN ERROR LESS THAN TOLERANCE

```

IF(ISTEP.EQ.INIT.AND.ITERA.EQ.1) GO TO 609
IF(ITERA.NE.1) GO TO 620
IF(ITERA.EQ.1.AND.ITERA.NE.NT) GO TO 601
IF(ERROR.GT.TOLNCE) GO TO 600
REWIND NWRITE
RFAIND 13
READ (NWRITE) UTOTAL
WRITE (13) UTOTAL
DO 100 I=1,NELEM
READ (NWRITE) STRES,PLATRN,TOTSRN,KEEP
WRITE (13) STRES,PLATRN,TOTSRN,KEEP
100 CONTINUE
READ (NWRITE) P,XLEVEL
WRITE (13) P,XLEVEL
WRITE(6,200)
200 FORMAT(' ', 'RESULTS STORED ON INSURANCE DISK #13')
600 IF(ISTEP.EQ.NT) STOP

```

SUM CURRENT LOAD INCREMENT AND RESIDUAL FORCES

```

609 IF(ISTEP.EQ.1.AND.ITERA.EQ.1) BACKSPACE NREAD
IF(ISTEP.EQ.INIT.AND.ITERA.EQ.1) READ (NREAD) P,XLEVEL
601 IF(NLOAD.EQ.1.AND.LF(NLOAD).EQ.0) GO TO 621
DO 999 I=1,NTOTAL
P(I)=0.1*P(I)
DO 610 J=1,NLOAD
K=(LF(I)-1)*NFREE
DO 610 J=1,NFREE
610 P(K+J)=P(K+J)+PLOAD(J,I)*SIZE
621 XLEVEL=XLEVEL+SIZE
620 WRITE(6,622) ISTEP,SIZE,XLEVEL,ITERA
622 FORMAT(' ', 'STEP =', I5, 'T30, 'CURRENT STEP SIZE =',
* F10.5, 'T30, 'CUMULATED STEP SIZE (XLEVEL) =', F10.5, 'T30, '
* ITERATION =', I5, 'T30')
RETURN
END

```

EFFECT\* NOTFRM.ID.EBCDIC.SOURCE.NOLIST.NODECK.LOAD.NOMAP.NOTEST  
EFFECT\* NAME = NEW LINECNT = 56  
SOURCE STATEMENTS = 75, PROGRAM SIZE = 2720  
NO DIAGNOSTICS GENERATED

RELEASE 2.0

FIX

DATE = 77154

11/22/75

RELEASE 2.0

SOLVE

DATE = 77154

11/22/75

```

SUBROUTINE FIX(NPART,NDISP,NFREE,NUMB,NTOTAL,MMAX,MTWICE,SIZE,
  UDISP,P,ST,NFIRST,NLAST,NREAC,NU,ITERA)
  IMPLICIT REAL*8 (A-H,O-Z), INTEGER*2 (I-N)
  INTEGER NPART,NDISP,NFREE,NTOTAL,MMAX,MTWICE
  DIMENSION P(NTOTAL),ST(MMAX,MTWICE),NFIRST(NPART),NLAST(NPART),
    NU(NDISP),UDISP(NFREE,NDISP),NREAC(NTOTAL)

```

```

C   INTRODUCE APPLIED DISPLACEMENTS
C

```

```

REWIND 1
PEWIND 3
NUMB=0
DO 670 KK=1,NPART
  READ (3) M1,N1,((ST(I,J),J=1,M1),I=1,M1)
  M1=(NFIRST(KK)-1)*NFREE+1
  NJ=NLAST(KK)*NFREE
  DO 620 I=1,NJ
    IF(NREAC(I).EQ.0) GO TO 620
    P(NREAC(I))=P(I)
620 CONTINUE
    IF(NDISP.EQ.1.AND.NJ(NDISP).EQ.0) GO TO 660
    IF(NU(NDISP).LT.NFIRST(KK)) GO TO 660
    DO 650 I=1,NDISP
      IF(NU(I).LT.NFIRST(KK).OR.NU(I).GT.NLAST(KK)) GO TO 650
      K=(NU(I)-1)*NFREE
      DO 640 J=1,NFREE
        IF(DABS(UDISP(J,I)).LT.0.0000001) GO TO 640
        NJ=NREAC(K+J)
        NUJ=NU+K+J
        ST(NJ,MJ)=ST(NJ,MJ)+1.00*12
        P(NJ)=ST(NJ,MJ)*UDISP(J,I)*SIZE
        IF(ITERA.NE.1) P(NJ)=0.0
640 CONTINUE
650 CONTINUE
660 VM=M1+1
        LL=NI-M1
        WRITE (1) M1,LL,((ST(I,J),J=1,M1),I=1,M1),P(I),I=1,M1)
        IF(KK.EQ.NPART) RETURN
        WRITE (1) ((ST(I,J),I=1,M1),J=MN,M1)
670 CONTINUE
        RETURN
        END

```

```

EFFECT= YTERN,IO,EMCOIC,SOURCE,NOLIST,NODECK,LOAD,NOMAP,NOTEST
EFFECT= NAME = FIX      LINECNT =      56
SOURCE STATEMENTS =      37,PROGRAM SIZE =      2190
NO DIAGNOSTICS GENERATED

```

```

SUBROUTINE SOLVE(NJOINT,NPART,NDISP,NFREE,MMAX,ITOTAL,NTOTAL,NJMB,
  U,UTOTAL,AM,3M,1PLNAR,NFIRST,NREAC,DISPFR,ITPRA)
  IMPLICIT REAL*8 (A-H,O-Z), INTEGER*2 (I-N)
  INTEGER NJOINT,NPART,NDISP,NFREE,MMAX,NTOTAL
  DIMENSION UTOTAL(NTOTAL),U(NTOTAL),AM(MMAX,MMAX),BM(MMAX,MMAX),
    NFIRST(NPART),NREAC(NTOTAL),1PLNAR(NJOINT),
    F(210),TF(210),DIS(210),C(216)
  COMMON SKT(24,24),S(24),W(24),DG(9),SK1(9,24),S1(3)
  EQUIVALENCE (SKT(1),F(1)),(SKT(211),TF(1)),(SKT(421),DIS(1)),
    (SKT(1),C(1))

```

```

REWIND 1
REWIND 2
DFT=0.
DO 300 LL=1,NPART
  READ (1) M,N,((AM(I,J),J=1,M),I=1,M),(F(1),I=1,M)
  IF(LL.EQ.1) GO TO 150
  DO 100 I=1,M
    F(I)=F(I)-TF(I)
  DO 100 J=1,M
100 AM(I,J)=AM(I,J)-BM(J,I)
150 CALL CHOLAS(M,AM,LL,DET,MMAX)
  DO 250 I=1,M
    DIS(I)=0.0
  DO 250 J=1,M
    IF(I.GT.J) AM(I,J)=AM(J,I)
250 DIS(I)=DIS(I) + AM(I,J) * F(J)
    IF(LL.FO.NPART) GO TO 350
    READ (1) ((BM(I,J),I=1,M),J=1,N)
    WRITE (2) M,N,((AM(I,J),J=1,M),I=1,M),(F(I),I=1,M),
      ((BM(I,J),I=1,M),J=1,N)
  DO 280 I=1,N
    TF(I)=0.0
  DO 280 J=1,M
280 TF(I)=TF(I) + BM(J,I) * DIS(J)
  DO 285 I=1,M
    DO 282 J=1,N
      C(J) = 0.0
    DO 282 K=1,M
282 C(J) = C(J) + AM(I,K)*BM(K,J)
  DO 285 J=1,N
285 AM(I,J) = C(J)
  DO 295 I=1,N
    DO 290 J=1,N
      C(J) = 0.0
    DO 290 K=1,M
290 C(J) = C(J) + BM(K,I)*AM(K,J)
  DO 295 J=1,N
295 BM(J,I)=C(J)
300 CONTINUE
350 M1=ITOTAL-M
  DO 400 I=1,M
400 U(M1+I)=DIS(I)
  NA=NPART-1
  DO 600 LL=1,NA

```

RELEASE 2.0

SOLVE

DATE = 77154

11/22/35

RELEASE 2.0

CHOLES

DATE = 77154

11/22/35

```

BACKSPACE 2
IF(ILL.FO.I) GO TO 420
BACKSPACE 2
420 READ (2) M,N,((AM(I,J),J=1,M),I=1,M),(F(I),I=1,M),
      ((BM(I,J),I=1,M),J=1,N)
      NI=M1-M
      DO 450 I=1,M
      DO 450 J=1,N
450 F(I)=F(I)-BM(I,J)*DIS(J)
      DO 550 J=1,M
      TEMP=0.0
      DO 500 J=1,M
      IF(I.GT.J) AM(I,J)=AM(J,I)
500 TEMP=TEMP+AM(I,J)*F(J)
      DIS(I)=TEMP
550 U(M1+I)=TEMP
500 CONTINUE
      IF(NDISP.NE.0) DET=DET*DFLOAT(NUMB*12)
      WRITE(6,650) DET
650 FORMAT(' *T5, *DETERMINANT LOG10(DET)=',T40,D25.13,///)
      DNORM=0.
      N=ITOTAL
      DO 700 J=1,ITOTAL
      J=NTOTAL+1-I
      IF(NREAC(J).EQ.0) GO TO 700
      UTOTAL(J)=UTOTAL(J)+0.1(K)
      DNORM=DNORM+UTOTAL(J)+UTOTAL(J)
      K=K+1
700 CONTINUE
      DNORM=DSORT(DNORM)
      WRITE(6,720)
720 FORMAT(' *T5, *JOINT NO',T20,'COORDINATE',T60,'CUMULATED(TOTAL) DI
      *SP',T20,'(L=LOCAL',T30,'X-DISP',T53,'Y-DISP',T68,'Z-DISP',T
      *83,'X-ROTA',T98,'Y-ROTA',T113,'Z-ROTA',T128,'X=GLOBAL)',
      *///)
      DO 730 I=1,NJOINT
730 WRITE(6,420) I,IPLNAR(I),UTOTAL(J),J=K,K1)
420 FORMAT(' *T5,I5,T25,A2,T32.6)I5.5)
      WRITE(6,450) DNORM
450 FORMAT(' *T5,DISPLACEMENT NORM =',D20.5)
      IF(ITERA.EQ.1) GO TO 870
      DISERR=DABS((DNORM-DISOLD)/DNORM)
      WRITE(6,460) DISERR
460 FORMAT(' *T5,Ratio of difference of disp. norm to norm of total dis
      *P',F10.5)
      GO TO 840
470 DISERR=0.
480 DISOLD=DNORM
      RETURN
      END

```

```

EFFECT* NAME=ID,ERCDIC,SOURCE,NOLIST,NODECK,LOAD,NOMAP,NOTEST
EFFECT* NAME= SOLVE LINECNT = 56
SOURCE STATEMENTS = 94,PROGRAM SIZE = 4670
DIAGNOSTICS GENERATED

```

```

SUBROUTINE CHOLES(N,A,LL,DET,MMAX)
IMPLICIT REAL*8 (A-H,O-Z), INTEGER*2 (I-N)
INTEGER MMAX
DIMENSION A(MMAX,MMAX)

```

DECOMPOSITION, DETERMINANT AND INVERSION

```

DO 20 I=2,N
DO 20 J=1,N
K1= I-1
DO 10 K=1,K1
10 A(I,J)=A(I,J)-A(K,I)*A(K,J)/A(K,K)
IF(I.EQ.J.AND.A(I,J).LE.0.) GO TO 30
20 CONTINUE
DO 25 I=1,N
25 DET=DET+DLOG10(A(I,I))
A(I,I)=1./A(I,I)
I1=N-1
DO 1 I1=1,I
J1=I+1
DO 1 J=J1,N
SUM=0.0
K1=J-1
DO 28 K=1,K1
28 SUM=SUM-A(K,I)*A(K,J)
1 A(J,I)=SUM+A(J,J)
DO 40 I=1,N
DO 40 J=1,N
SUM=0.
DO 65 K=J,N
65 SUM=SUM+A(K,I)*A(K,J)/A(K,K)
80 A(I,J)=SUM
RETURN
30 WRITE(6,40) LL,I,J,A(I,J)
40 FORMAT(' *O, ///, *STIFFNESS MATRIX IS NOT POSITIVE DEFINITE, SUB
ROUTINE CHOLES FAIL AT PARTITION',I5,/, ' *ROW',I5,IOX,'COL',I5,
*OX,'A(I,J)=' ,D20.5)
STOP
END

```

```

EFFECT* NAME=ID,ERCDIC,SOURCE,NOLIST,NODECK,LOAD,NOMAP,NOTEST
EFFECT* NAME= CHOLES LINECNT = 56
SOURCE STATEMENTS = 34,PROGRAM SIZE = 1899
NO DIAGNOSTICS GENERATED

```

RELEASE 2.0

TRANS

DATE = 77154

11/22/35

RELEASE 2.0

TRANS

DATE = 77154

11/22/35

```

SUBROUTINE TRANS(NJOINT,NELEM,NONCOP,NIMPER,COORD,XC,YC,H,NOD,
  * NTRANS)
  IMPLICIT REAL*8 (A-H,O-Z), INTEGER*2 (I-N)
  INTEGER NJOINT,NELEM,NIMPER,NONCOP
  DIMENSION COORD(3,NJOINT),XC(NELEM),YC(NELEM),H(3,3,NIMPER,NONCOP),
  * NOD(4,NELEM),NTRANS(NELEM),XE(3,3)

```

## FOUR NODES TRANSFORMATION MATRIX

```

DO 165 LK=1,NELEM
  IF(NTRANS(LK).EQ.0) GO TO 165
  LL=NTRANS(LK)
  XC(LK)=0.
  DO 1 I=1,4
    IF(I.NE. 1) GO TO 2
    DO 5 J=1,3
      XE(1,J) = COORD(J,NOD(1,LK))
      XE(2,J) = COORD(J,NOD(2,LK))
      XE(3,J) = COORD(J,NOD(4,LK))
    GO TO 10
  2 IF(I.NE. 2) GO TO 4
    DO 3 J=1,3
      DO 3 K=1,3
        XE(K,J) = COORD(J,NOD(K,LK))
      GO TO 10
    4 IF(I.NE. 3) GO TO 8
      DO 6 J=1,3
        XE(1,J) = COORD(J,NOD(4,LK))
        XE(2,J) = COORD(J,NOD(3,LK))
        XE(3,J) = COORD(J,NOD(2,LK))
      GO TO 10
    6 DO 7 J=1,3
      XE(1,J) = COORD(J,NOD(4,LK))
      XE(2,J) = COORD(J,NOD(3,LK))
      XE(3,J) = COORD(J,NOD(1,LK))
    7 10 A1 = (XE(2,2)-XE(1,2))*(XE(3,3)-XE(1,3))-(XE(3,2)-XE(1,2))*(XE(2,3)
  * -XE(1,3))
    B1 = -(XE(2,1)-XE(1,1))*(XE(3,3)-XE(1,3))
  * +(XE(3,1)-XE(1,1))*(XE(2,3)-XE(1,3))
    C1 = (XE(2,1)-XE(1,1))*(XE(3,2)-XE(1,2))
  * -(XE(3,1)-XE(1,1))*(XE(2,2)-XE(1,2))
    IF(I.LE. 2) GO TO 9
    A1 = - A1
    B1 = - B1
    C1 = - C1
  9 D1 = XE(2,1) - XE(1,1)
    FE = XE(2,2) - XE(1,2)
    FI = XE(2,3) - XE(1,3)
    D1 = DSORT((D1**2) + (FE**2) + (FI**2))
    XC(LK)=XC(LK)+D1/4.0
    Z1 = D1*FE - C1*FE
    S1 = C1*D1 - A1*FI
    T1 = A1*FE - H1*D1
    Z1 = DSORT((Z1**2) + (S1**2) + (T1**2))

```

```

11 P1 = DSORT((A1**2) + (B1**2) + (C1**2))
  H(1,1,1,LL) = D1/O1
  H(1,2,1,LL) = EE/O1
  H(1,3,1,LL) = F1/O1
  H(2,1,1,LL) = R1 / Z1
  H(2,2,1,LL) = S1 / Z1
  H(2,3,1,LL) = T1 / Z1
  H(3,1,1,LL) = A1 / P1
  H(3,2,1,LL) = B1 / P1
  H(3,3,1,LL) = C1 / P1
  D1 = COORD(1,NOD(2,LK))-COORD(1,NOD(3,LK))
  EE = COORD(2,NOD(2,LK))-COORD(2,NOD(3,LK))
  F1 = COORD(3,NOD(2,LK))-COORD(3,NOD(3,LK))
  O1 = DSORT((D1**2) + (EE**2) + (F1**2))
  D1 = COORD(1,NOD(1,LK))-COORD(1,NOD(4,LK))
  EE = COORD(2,NOD(1,LK))-COORD(2,NOD(4,LK))
  F1 = COORD(3,NOD(1,LK))-COORD(3,NOD(4,LK))
  O2 = DSORT((D1**2) + (EE**2) + (F1**2))
  YC(LK)=(O1+O2)/2.0

```

```

165 CONTINUE
RETURN
END

```

```

EFFECT* NOTERM, ID, EBCDIC, SOURCE, NOLIST, NODCK, LOAD, NODAP, NOTEST
EFFECT* NAME = TRANS, LINECNT = 56
SOURCE STATEMENTS = 68, PROGRAM SIZE = 3612
NO DIAGNOSTICS GENERATED

```





RELEASE 2.0

STRESS

DATE = 77154

11/22/35

RELEASE 2.0

STRESS

DATE = 77154

11/22/35

SOURCE STATEMENTS =  
NO DIAGNOSTICS GENERATED

03, PROGRAM SIZE = 7304

```

SUBROUTINE STRESS(NGAUSS,NLAYER,JJ,II,LK,ELAS,SYIELD,NHARD,EXPON,
* SPL,EXX,EXY,EYY,EZZ,IYIELD,ISTEP,INIT,HPRIME,
* NWRITE,E,STRAN,STRES,PLATRN,TOTSPN,XFEP,NT,ITERA
* ,INDEX)
IMPLICIT REAL*8 (A-H,O-Z), INTEGER*2 (I-N)
INTEGER NGAUSS,NLAYER,NWRITE
DIMENSION STRAN(3,NLAYER),STRES(3,NLAYER,NGAUSS),E(3,3,NLAY
* ER),TEMP(3),SDNOW(3),SOLAST(3),PLATRN(NLAYER,NGAUSS,NGAU
* SS),KEEP(NLAYER,NGAUSS,NGAUSS),TOTERN(3,2,NGAUSS,NGAUSS)
* ,X(3)
C
C
C   FOR NHARD=2 (NON-LINEAR HARDENING MATERIAL)
FTR=(SYIELD-SPL)**EXPON/0.002
120 DO 1000 KK=1,NLAYER
130 DO 150 I=1,3
150 SOLAST(I)=0.
    PDLAST=0.
    IF(KEEP(KK,JJ,II),EQ.0) IP=1
    IF(KEEP(KK,JJ,II),NE.0) IP=2
    DO 500 N=IP,3
    IF(N,EQ.3) GO TO 360
    IF(PLATRN(KK,JJ,II),NF.0.0.OR.(KEEP(KK,JJ,II),NE.0)) GO TO 160
    SRAR=SPL
    GO TO 400
160 IF(PLATRN(KK,JJ,II),NE.0.0) GO TO 190
    SBAR=1.001*SPL
    GO TO 360
180 T=DABS(PLATRN(KK,JJ,II))*FTR
    SBAR=DEXP(DLOG(T)/EXPON)*SPL
350 IF(KEEP(KK,JJ,II),EQ.0) GO TO 400
360 HPRIME=FTR/(EXPON*(SBAR-SPL)**(EXPON-1.))
400 CALL MODUL1(STRES(1,KK,JJ,II),STRES(2,KK,JJ,II),STRES(3,KK,JJ,II),
* KEEP(KK,JJ,II),SRAR,HPRIME,EXX,EXY,EYY,EZZ,F(1,1,KK),
* E(1,2,KK),F(1,3,KK),F(2,1,KK),F(2,2,KK),E(2,1,KK),
* E(3,1,KK),E(3,2,KK),F(3,3,KK),EX,SY,DETX,X(1),X(2),X(3))
    IF(ISTEP,EQ.1,AND,ITERA,EQ.1) GO TO 450
    IF(N,EQ.3,AND,KEEP(KK,JJ,II),EQ.0) GO TO 450
    IF(N,EQ.3,AND,KEEP(KK,JJ,II),NF.0) GO TO 450
    SDNOW(1)=EXX*STRAN(1,KK)+EXY*STRAN(2,KK)
    SDNOW(2)=EXY*STRAN(1,KK)+EYY*STRAN(2,KK)
    SDNOW(3)=EZZ*STRAN(3,KK)
    IF(KEEP(KK,JJ,II),EQ.0) GO TO 550
    FDELTA=3.*(0.5*SY*SDNOW(1)+0.5*SY*SDNOW(2)+STRES(1,KK,JJ,II)*SDNOW
    (1))/SRAR
    IF(FDELTA,LT.0.) GO TO 480
450 DO 500 I=1,3
    SDNOW(I)=0.
    DO 500 J=1,3
500 SDNOW(I)=SDNOW(I)+E(I,J,KK)*STRAN(J,KK)
    DO 510 I=1,3
    STRES(1,KK,JJ,II)=STRES(1,KK,JJ,II)+SDNOW(I)-SOLAST(I)
510 SOLAST(I)=SDNOW(I)

```

RELEASE 2.0

STRESS

DATE = 77154

11/22/35

RELEASE 2.0

STRESS

DATE = 77154

11/22/35

```

T=0.
DO 700 I=1,3
700 T=X(I)*STRAN(I,KK)
PONDW= T/DEN
PLATRN(KK,JJ,I)=PLATRN(KK,JJ,I)+PONDW-PDLAST
PDLAST=PONDW
SBAR=SE
GO TO 800
800 KEEP(KK,JJ,I)=0
550 DO 600 I=1,3
600 YEMP(I)=STRES(I,KK,JJ,I)
650 STRES(I,KK,JJ,I)=STRES(I,KK,JJ,I)+SDNDW(I)
IF(N.EQ.2) GO TO 800
650 SE=DSORT(STRES(I,KK,JJ,I)+STRES(I,KK,JJ,I)-STRES(I,KK,JJ,I)*STR
* ES(2,KK,JJ,I)+STRES(2,KK,JJ,I)+STRES(2,KK,JJ,I)+3.*STRES(3,
* KK,JJ,I)+STRES(3,KK,JJ,I))
700 IF(S.LT.SBAR) GO TO 850
850 DO 660 I=1,3
660 X(I)=STRES(I,KK,JJ,I)-TEMP(I)
A=X(1)*X(1)-X(1)*X(2)+X(2)*X(2)+3.*X(1)*X(3)
B=2.*X(1)*TEMP(1)-X(1)*TEMP(2)-X(2)*TEMP(1)+2.*X(2)*TEMP(2)+6.*X(3
)*TEMP(1)
C=TEMP(1)*TEMP(1)-TEMP(1)*TEMP(2)+TEMP(2)*TEMP(2)+3.*TEMP(3)*TEMP(
*3)-SBAR*SBAR
T=B*B-4.*A*C
IF(T.GE.C.) GO TO 670
T=0.
GO TO 670
670 T=DSORT(T)
T1=(-B+T)/(2.*A)
T2=(-B-T)/(2.*A)
IF(DABS(T1).LE.DABS(T2)) T=T1
IF(DABS(T2).LE.DABS(T1)) T=T2
675 DO 500 I=1,3
500 STRES(I,KK,JJ,I)=TEMP(I)+X(I)*T
DO 700 I=1,3
700 STRAN(I,KK)=STRAN(I,KK)*(1.-DABS(T))
KEEP(KK,JJ,I)=1
800 CONTINUE
850 IF(KEEP(KK,JJ,I).NE.0) IYIELD=1
1700 CONTINUE
IF(ISTEP.EQ.INIT.AND.ITERA.EQ.1) RETURN
IF(JJ.EQ.NGAUSS.AND.II.EQ.NGAUSS) WRITE(NWRITE) STRES,PLATRN,
* YOTSRN,KEEP
IF(ISTEP.NE.NTI) RETURN
IF(ITERA.NE.1) RETURN
40 IF(LK.NE.1.OR.JJ.NE.1.OR.II.NE.1) GO TO 890
WRITE(6,50)
50 FORMAT('0',///,'0',T5,'ELEMENT NO',T20,'LOCATION ( INTERGRATION PO
* INTS )',P55,'LAYER NO',T78,'CUMULATED STRESSES IN LOCAL COORDINATE
* ',T124,'CELASTIC',/,,'0',T27,'JJ(X)',T38,'II(Y)',T70,'K - NORMAL',
* T70,'Y - NORMAL',T110,'SHEAR STRESS',T124,'I=PLASTIC',/)
400 DO 1700 KK=1,MAYER
1700 IF(KK.EQ.1) GO TO 930

```

```

IF(KK.EQ.MAYER.OR.KEEP(KK,JJ,I).NE.0) GO TO 905
IF(KEEP(KK=1,JJ,I).EQ.0.AND.KEEP(KK=1,JJ,I).EQ.0) GO TO 1200
905 WRITE(6,910) KK,(STRES(I,KK,JJ,I),I=1,3),KEEP(KK,JJ,I)
910 FORMAT(' ',T55,'I5,T62,3E20.5,T127,12)
GO TO 1200
930 IF(JJ.EQ.1.AND.II.EQ.1) GO TO 970
WRITE(6,950) JJ,II,KK,(STRES(I,KK,JJ,I),I=1,3),KEEP(KK,JJ,I)
950 FORMAT('0',T27,'I3,T38,'I3,T55,'I5,T62,3F20.5,T127,12)
GO TO 1200
970 WRITE(6,980) LK,JJ,II,KK,(STRES(I,KK,JJ,I),I=1,3),KEEP(KK,JJ,I)
980 FORMAT('0',T5,'I5,T27,'I3,T38,'I3,T55,'I5,T62,3F20.5,T127,12)
1200 CONTINUE
RETURN
END

```

```

EFFECT* NOTERM,IO,EBCDIC,SOURCE,NOLIST,NODECK,LOAD,NOMAP,NOTEST
EFFECT* NAME * STRESS * LINECNT * 56
SOURCE STATEMENTS * 100,PROGRAM SIZE = 8052
NO DIAGNOSTICS GENERATED

```

NO DIAGNOSTICS THIS STEP